CATALYTIC ASPECTS OF IMMOBILIZED METAL COMPLEXES

A THESIS

*Submitted in partial fulfilment of the
requirements for the award of the degree
of*
DOCTOR OF PHILOSOPHY
in
CHEMISTRY

by

AARTI

DEPARTMENT OF CHEMISTRY
INDIAN INSTITUTE OF TECHNOLOGY ROORKEE
ROORKEE - 247 667 (INDIA)
JUNE, 2009

INDIAN INSTITUTE OF TECHNOLOGY ROORKEE
ROORKEE

CANDIDATE'S DECLARATION

I hereby certify that the work which is being presented in the thesis entitled **CATALYTIC ASPECTS OF IMMOBILIZED METAL COMPLEXES** in partial fulfilment of the requirements for the award of the degree of *Doctor of Philosophy* and submitted in the Department of Chemistry of the Indian Institute of Technology Roorkee, Roorkee is an authentic record of my own work carried out during a period from July, 2005 to June, 2009 under the supervision of Dr. Kamaluddin and Dr. M. R. Maurya, Professors, Department of Chemistry, Indian Institute of Technology Roorkee, Roorkee.

The matter presented in this thesis has not been submitted by me for the award of any other degree of this or any other Institute.

(AARTI)

This is to certify that the above statement made by the candidate is correct to the best of our knowledge.

(M. R. Maurya)
Supervisor

(Kamaluddin)
Supervisor

Dated: 02 June 2009

The Ph.D. Viva-Voce Examination of **Ms. Aarti**, Research Scholar, has been held on 4. 9. 2009

Signature of Supervisor(s)

Signature of External Examiner.

ABSTRACT

The word catalysis has origin from Greek which means "decomposition" or "dissolution". The catalyst decreases the activation energy of a reaction by altering the reaction path but itself remains unchanged. From the beginning the catalysis is an important area of research and continuous efforts have been made to understand and utilize the phenomenon for practical purposes. Nowadays catalysts are playing a vital role in petrochemicals, fine chemicals, pharmaceuticals, fertilizers and food industries. The biochemically significant processes are also based on catalysis. They activate the chemical reaction at milder conditions through the bonding of reactant molecules with definite functional groups called 'active sites', where they react and finally detach from the catalyst for the next cycle. Most of the catalytic processes, which are widely engaged in the manufacture of bulk as well as fine chemicals, are homogeneous in nature. A large amount of waste materials have been produced during these processes which imposed a hazardous impact on the environment. Homogeneous catalysts also face the problem of separation from the substrate and products, and very often decompose or polymerize during catalytic action. Therefore, there is a necessity to create new highly effective industrial processes, which are selective, ecologically safe and consume minimum energy. In this direction, immobilization of homogeneous catalysts facilitates the easy product separation, catalysts recovery and recycle ability is the major concerns of industries as well as researchers. Alumina and silica gels are readily available inorganic compounds and have been modified to immobilize various catalysts by direct reaction of surface hydroxyl groups with reactive species. Even, mesoporous molecular sieves such as MCM-41 and SBA-15 have also been used for the immobilization of homogeneous catalysts. Transition metal complexes having good catalytic properties have also been encapsulated in the super cages of zeolites to give them solid support.

Discovery of Merrifield resin i.e. chloromethylated polystyrene cross-linked with divinylbenzene, has attracted researchers to use functionalised polymers for the

heterogenisation of homogeneous materials. Immobilisation of homogeneous catalysts through covalent bonding with chloromethylated polystyrene cross-linked with divinylbenzene have developed them as environmentally safe heterogeneous catalysts for various catalytic reactions and attracted attention in recent years. This method has the advantages of both homogeneous as well heterogeneous catalysts, as this enhances the thermal stability, selectivity, and recycles ability of the catalyst and ease separation of catalyst from the reaction mixture. Polymer immobilised (also called polymer-anchored) complexes have provided opportunity to develop catalytic process in the synthesis of fine chemicals and being used in various types of oxidation as well as hydrogenation reactions. Though, different types of ligands and various transition metal ions have been used to develop polymer-anchored catalysts. Discovery of vanadium(V) in the active site of vanadate-dependent haloperoxidases and its importance in various catalytic reactions has stimulated research on the catalytic potentials of vanadium complexes. Many vanadium complexes have been reported to show potential catalytic activity towards the oxidative halogenation and sulfoxidation along with other oxidation reactions. All these encouraged us to design polymer-anchored vanadium based catalysts and use them for various oxidation reactions.

The thesis entitled "Catalytic Aspects of immobilized metal complexes" mainly deals with the syntheses of vanadium, molybdenum and copper complexes of Schiff bases immobilised onto chloromethylated polystyrene (cross-linked with 5 % divinylbenzene) and their characterization by various physico-chemical techniques. Catalytic activities towards oxidation and hydroamination of various substrates have also been carried out under optimized reaction conditions to achieve maximum oxidation products. For convenience the work present in the thesis has been divided in the following five chapters:

First chapter is the introductory one and describes various types of solid inert support that have been used for immobilisation of homogeneous catalysts. A brief introduction on functionalised polymers and different modes to use them for immobilisation of catalysts has been described. Literature on polymer-immobilised

metal complexes and their catalytic applications for various reactions have also been reviewed.

Second chapter describes the anchoring of the Schiff base derived from salicylaldehyde and histamine (Hsal-his) to the chloromethylated polystyrene cross-linked with 5 % divinylbenzene (abbreviated as PS-Hsal-his, **2.II**). Treatment of [VO(acac)$_2$] with PS-Hsal-his in dimethylformamide (DMF) gave oxovanadium(IV) complex, PS-[VO(sal-his)(acac)] (**2.1**). Complex **2.1** can be oxidised to dioxovanadium(V) species, PS-[VO$_2$(sal-his)] (**2.2**) on aerial oxidation in presence of H$_2$O$_2$. All these complexes have been characterised by various techniques. All these complexes catalyse the oxidation of methyl phenyl sulfide, diphenyl sulfide and benzoin efficiently. Under the optimised reaction conditions, a maximum of 93.8% conversion of methyl phenyl sulfide with 63.7% selectivity towards methyl phenyl sulfoxide and 36.3% towards methyl phenyl sulfone has been achieved in 2 h with PS-[VO$_2$(sal-his)]. Under similar conditions, diphenyl sulfide gave 83.4% conversion where selectivity of reaction products varied in the order: diphenyl sulfoxide (71.8%) > diphenyl sulfone (28.2%). A maximum of 91.2% conversion of benzoin has been achieved within 6 h, and the selectivity of reaction products are: methylbenzoate (37.0%) > benzil (30.5%) > benzaldehyde-dimethylacetal (22.5%) > benzoic acid (8.1%). The PS–bound complex, PS–[V^{IV}O(sal–his)(acac)] exhibits very comparable catalytic potential. Their corresponding neat complexes have also been prepared and catalytic activities have been compared.

Syntheses of polymer-anchored ligands PS-S-tmbmz (**3.II**), from the Htmbmz (**3.I**) (Htmbmz = 2-thiomethylbenzimidazole) and their oxovanadium(IV), dioxomolybdenum(VI) and copper(II) complexes have been described in **Chapter third**. The polymer-anchored ligands PS-S-tmbmz (**3.II**), on treatment with [VO(acac)$_2$], [MoO$_2$(acac)$_2$] and Cu(CH$_3$COO)$_2$ in dimethylformamide (DMF) gave oxovanadium(IV), dioxomolybdenum(VI) and copper(II) complexes, PS-[VO(S-tmbmz)$_2$] (**3.1**), PS-[MoO$_2$(S-tmbmz)$_2$] (**3.2**) and PS-[Cu(S-tmbmz)$_2$] (**3.3**), respectively. The corresponding neat complexes, [VO(tmbmz)$_2$] (**3.4**), [MoO$_2$(tmbmz)$_2$] (**3.5**) and [Cu(tmbmz)$_2$] (**3.6**) have also been prepared. EPR was

particularly useful to characterise the binding modes in PS-[VO(S-tmbmz)$_2$] (**3.1**) and PS-[Cu(S-tmbmz)$_2$] (**3.3**), confirming that the vanadium and copper centers are well dispersed in the polymer matrix and supporting the presence of N$_2$O$_2$ binding modes in both cases and the preservation of the binding mode at the end of the catalytic reactions carried out. The catalytic potential of these complexes was tested for the oxidation of styrene, cyclohexene and ethylbenzene using 30 % H$_2$O$_2$ as an oxidant. Styrene gave three products with the selectivity order: benzaldehyde > 1-phenylethane-1,2-diol > styrene oxide. Oxidation of cyclohexene gave three products, the order of selectivity being: cyclohexane-1,2-diol > 2-cyclohexene-1-one > cyclohexeneoxide. At least four reaction products with the selectivity order: benzaldehyde > phenylacetic acid > acetophenone > 1-phenylethane-1,2-diol have been obtained on oxidation of ethylbenzene. The recycle ability of polymer-anchored metal complexes was checked; the results confirm that the polymer-bound complexes were not leached during the reaction/recovery procedures. Catalytic activities of the PS-supported complexes were higher than those of the corresponding non-polymer-bound complexes.

The monobasic tridentate ligand H$_2$fsal-dmen (**4.I**) derived from 3-formyl salicylic acid and N,N-dimethylethylene diamine has been covalently bonded to the chloromethylated polystyrene cross-linked with 5 % divinylbenzene through carboxylic group. Synthesis of oxovanadium(IV) and dioxo-vanadium(V) complexes, PS-[VO(fsal-dmen)(acac)] (**4.1**) and PS-[VO$_2$(fsal-dmen)] (**4.2**) from the resulting ligand PS-Hfsal-dmen (**4.II**) has been reported in **Chapter fourth**. The corresponding neat complexes, [VO(sal-dmen)(acac)] (**4.3**) and [VO$_2$(sal-dmen)] (**4.4**) have been prepared by the reaction of [VO(acac)$_2$] with Hsal-dmen (**4.III**) in methanol. These complexes have been characterised by IR, and electronic spectroscopic studies, magnetic susceptibility measurements, and thermal as well as scanning electronic micrographs. The catalytic oxidative desulfurization of model organosulfur compounds like thiophene (T), dibenzothiophene (DBT), benzothiophene (BT), 2-methyl thiophene (MT) and diesel has been carried out using complexes PS-[VO(fsal-dmen)(acac)] (**4.1**) and PS-[VO$_2$(fsal-dmen)] (**4.2**). The sulfur in model organosulfur

compounds and diesel has been oxidised to the corresponding sulfones in presence of H_2O_2. The polymer-bound heterogeneous catalysts were free from leaching during catalytic action and recyclable.

The tridentate Schiff base ligand derived from 3-formylsalicylic acid and 2-(2-aminoethyl)pyridine (H_2fsal-aepy, **5.I**) has been covalently bonded to chloromethylated polystyrene cross-linkined with 5 % divinylbenzene (abbreviated as PS-Hfsal-aepy, **5.II**). Reaction between PS-Hfsal-aepy and [VO(acac)$_2$] (Hacac = acetylacetone) gave polymer-anchored complex, PS-[VO(fsal-aepy)(acac)] (**5.1**). Complex PS-[VO(fsal-aepy)(acac)] (**5.1**) has been oxidised to the dioxidovanadium(V) species, PS-[VO$_2$(fsal-aepy)] (**5.2**) on aerial oxidation in the presence of H_2O_2 in MeOH. Characterisation of the catalyst using scanning electron micrographs, spectroscopic (infrared and electronic), thermogravimetric and elemental analyses studies and its catalytic activities has been included in the **fifth Chapter**. Corresponding neat complexes, [VO(sal-aepy)(acac)] (**5.3**) and [VO$_2$(sal-aepy)] (**5.4**) with the ligand Hsal-his has also been prepared to compare the spectral properties and catalytic activities. Complexes PS-[VO(fsal-aepy)(acac)] (**5.1**) and PS-[VO$_2$(fsal-aepy)] (**5.2**) catalyse the hydroamination of styrene and vinyl pyridine with amines (aniline and diethylamine) and gave a mixture of two hydroaminated products in good yields. Amongst the two hydroaminated products, the anti-Markovnikov product is favoured over the Markovnikov product. The polymer-anchored heterogeneous catalyst is recyclable. Catalytic activity of neat analogue has been found to be lower than that of the anchored one.

Acknowledgements

I am on the brink of giving a final shape to my dream. It is very cheerful and pulsating moment of my life to acknowledge the persons who are directly or indirectly associated with this thrashing task.

*First and foremost thanks to God for his all Devin blessing he showered on me for my success. It gives me immense pleasure in expressing deep sense of gratitude and admire to my mentors **Prof. Kamaluddin** & **Prof. M.R. Maurya** for their valuable and scrupulous guidance, enthusiastic interest throughout my research work with affectionate treatment. Especially the experience of **Prof M.R. Maurya** has accelerated me to bring my present work to conclusion. I am highly indebt for his gentle and benign behavior, patient correcting my mistakes during my research work. I am highly grateful to him for articulating this path and being a constant source of inspiration.*

*I am highly thankful to **Prof. & Head Kamaluddin** and **Prof. Ravi Bhushan** former Head, Department of Chemistry, Indian Institute of Technology Roorkee, Roorkee for providing me all the facilities required for my work.*

My special thanks to the Head, Institute Instrumentation Centre of our institute for providing me necessary instrumentation facilities. My sincere thanks to Mr. Anil Saini, Mr. Deepak and Mrs. Rekha for recording the TGA-DTA, NMR and SEM of my samples. I also acknowledge the technical and non-technical staffs Mr. Abdul Haque, Mr. V.P. Saxena, Mr. Hem Singh Panwar, Mr. Madan Pa, and Mr. Tilak Ram for their altruistic help. I am also grateful to all the members of Chemistry Department for their cooperation and timely help for my research work.

I am also thankful to Prof. Joao Costa-Pessoa and Dr. Amit Kumar, Instituto Superior Tecnico, Portugal for carrying out the EPR studies and ^{51}V NMR spectra of some of my samples. I am also thankful to Prof. Fernando Avecilla, Departamento de Química Fundamental, Facultad de Ciencias, Universidade da Coruña, Spain for carrying out Single crystal data of some of my samples.

I own my special thanks to Dr. Umesh Kumar, senior lab mate, for his selfless

LIST OF PUBLICATIONS

1. M.R. Maurya, M. Kumar and **A. Arya**
   Model dioxovanadium(V) complexes through direct immobilization on polymer support, their characterization and catalytic activities, *Catalysis Comm.*, 2008, **10**, 187 – 191.

2. M.R. Maurya, **A. Arya**, P. Adão and J.C. Pessoa
   Immobilisation of oxovanadium(IV), dioxomolybdenum(VI) and copper(II) complexes on polymer for the oxidation of styrene, cyclohexene and ethylbenzene, *Applied Catalysis A: Gen.*, 2008, **351**, 239 – 252.

3. M.R. Maurya, **A. Arya**, A. Kumar and J.C. Pessoa
   Polystyrene bound oxovanadium(IV) and dioxovanadium(V) complexes of histamine derived ligand for the oxidation of methyl phenyl sulfide, diphenyl sulfide and benzoin, *Dalton Trans.*, 2009, 2185 – 2195.

4. M. R. Maurya, **A. Arya**, U. Kumar, A. Kumar and J.C. Pessoa
   Polymer-bound oxidovanadium(IV) and dioxidovanadium(V) complexes: synthesis, characterization and catalytic application for the hydroamination of styrene and vinyl pyridine, Submitted.

5. M. R. Maurya, **A. Arya**, A. Kumar, J.C. Pessoa and F. Avecilla
   Polymer-bound oxovanadium(IV) and dioxovanadium(V) complexes as catalyst for the oxidative desulfurization of model organosulfur compounds in diesel, Under preparation.

*****

PAPERS PRESENTED IN SYMPOSIA / CONFERENCES

1. M.R. Maurya and **Aarti**
   Polymer anchored metal complexes of VO(IV), Mo(VI) and Cu(II) for the liquid phase oxidation of styrene and cyclohexene, *National Symposium in Chemistry on Modern Trends in Chemical Sciences*, PP-25 (2006), Krukshetra University, Krukshetra.

2. M.R. Maurya and **Aarti**
   Polystyrene bound dioxovanadium(V) complex of histamine derived ligand for the oxidation of benzoin, methyl phenyl sulfide and diphenyl sulfide, *26th Annual Conference of Indian Council of Chemists*, IO-CYSA-08 (2008), Dr. H.S. Gour University, Sagar (M. P.).

3. M.R. Maurya and **Aarti**
   Modification of polymer through covalent bonding of oxovanadium(IV), dioxomolybdenum(VI) and copper(II) complexes for the liquid phase oxidation of styrene, cyclohexene and ethylbenzene, *International Conference on Advances in Polymer Science & Technology*, PMFN-PO-139 (2008), Indian Institute of Technology New Delhi & India Habitat Centre New Delhi, India.

4. M.R. Maurya and **Aarti**
   Oxovanadium(IV), dioxomolybdenum(VI) and copper(II) complexes supported on polymer for the liquid phase oxidation of styrene, cyclohexene and ethyl benzene, *27th Annual Conference of Indian Council of Chemists*, IO-CYSA-11 (2008), Gurukul Kangri Vishwavidyalaya, Haridwar.

5. M.R. Maurya and **Aarti**
   Polymer-bound oxo- and dioxo-vanadium complexes prepared from 2-(2-aminoethyl)pyridine derived ligand for the hydroamination of styrene and vinyl pyridine, *19th National symposium on catalysis titled "Catalysis for Sustainable Energy and Chemicals"*, National Chemical Laboratory, Pune.

*****

INDIAN COUNCIL OF CHEMISTS

INDIAN COUNCIL OF CHEMISTS · ESTD. 1981

YOUNG SCIENTIST AWARD

$\mathcal{T}$his is to certify that Dr/Sri/Ms. ...... **Aarti** ......
of ...Deptt. of Chemistry, Indian Instt. of Tech. Roorkee, Roorkee...
has been awarded the **Young Scientist Award** *for the best* **ORAL** *presentation*
of his/her paper in Inorganic Chemistry Section *in the* **27th Annual Conference**
of the Indian Council of Chemists held at Gurukul Kangri Vishwavidyalaya, Haridwar on
$26^{th}, 27^{th}$ & 28th December, 2008.

Prof. Rajesh Dhakarey
Secretary

Haridwar
28th December, 2008

Dr. G. C. Saxena
President

The Catalysis Society of India

Regd. Office - Indian Institute of Technology, Madras
Chennai-600 036.
(Reg. No. 163/1974)

Hindustan Platinum Award for the Best Poster Presentation

Certified that _Aarti & Coworkers_ . has been awarded the best poster presentation

award for the paper entitled, "_Polymer-bound----- Styrene and vinyl pyridine_",

and presented during the CATSYMP - 19 held at the National Chemical Laboratory, Pune, India during

January 18-21, 2009.

Dated _21.01.2009_
Pune

Director
Hindustan Platinum

President
Catalysis Society of India

Convener
Organizing Committee
NCL, Pune

CONTENTS

CHAPTER 1

General introduction: History of catalytic development, solid supports for catalysts and polymer anchored catalysts

CHAPTER 2

Polystyrene bound oxidovanadium(IV) and dioxidovanadium(V) complexes of histamine derived ligand for the oxidation of methyl phenyl sulfide, diphenyl sulfide and benzoin

CHAPTER 3

Immobilisation of oxidovanadium(IV), dioxidomolybdenum(VI) and copper(II) complexes on polymers for the oxidation of styrene, cyclohexene and ethylbenzene

CHAPTER 4

Polymer-bound oxidovanadium(IV) and dioxidovanadium(V) complexes as catalyst for the oxidative desulfurization of model organosulfur compounds in diesel

CHAPTER 5

Polymer-bound oxidovanadium(IV) and dioxidovanadium(V) complexes: syntheses, characterisation and catalytic application for the hydroamination of styrene and vinyl pyridine

LIST OF FIGURES

benzoin (a) using PS–[V^{V}O$_2$(sal–his)] as a catalyst. (b) benzil, (c) benzoic acid, (d) benzaldehyde-dimethylacetal, (e) methyl benzoate and (f) others (non-identified).

eq. H_2O_2; (c) 1.0 eq. H_2O_2; (d,e) 1.5 eq. H_2O_2; (f) 2.0 eq. H_2O_2; (g) 2.5 eq. H_2O_2; (h) 1.0 eq. methyl phenyl sulfide; (i) 2.0 eq. methyl phenyl sulfide; (j) 3.0 eq. methyl phenyl sulfide (k) 3.0 eq. methyl phenyl sulfide (after 24 hr). All spectra were recorded including an external reference of aqueous vanadate at pH ~12 (peak at ca. -536 ppm).

solution);. The corresponding visible spectra follow the evolution shown in the inset of Fig. 3.12. The arrows indicate the position of the high field A∥ lines in spectra (a)-(c). Upon addition of H_2O_2 a 2nd species is detected and its relative amount increases from (b) to (f).

LIST OF TABLES

Chapter-1

General introduction: History of catalytic development, solid supports for catalysts and polymer anchored catalysts

1.1. HISTORY

Chemical reactions generally proceed through the breaking and formation of bonds between atoms in molecules to produce new compounds. The catalyst decreases the activation energy of a reaction by altering the reaction path but it itself remains unchanged. The period of catalysis started with the dawn of civilisation when the production of alcohol and vinegar was done by fermentation process. The word "Catalysis" was probably used first time in the sixteenth century by the chemist A. Libavious in his book Alchemia [1]. In 1793, Clement and Desormes used the nitre as a catalyst for the syntheses of sulfuric acid in presence of air. In 1835 Jöns Jakob Berzelius used the term catalysis for some compounds / chemicals which can fasten the reaction. The word catalysis has origin from Greek which means "decomposition" or "dissolution". Syntheses of sulfuric acid by burning sulfur with nitric acid in humid air are one of the examples for the catalysis in the middle age. This was followed by the discovery of Ammonia syntheses by Nernst and Haber. Horiuti and Polanyi, in 1930s, suggested a catalytic reaction mechanism for ethylene hydrogenation [2]. Langmuir in the same period derived the Langmuir adsorption isotherm, suggesting the heterogeneous surface [3] which has different sites and these different sites have different rates for reaction. Langmuir used the heterogeneous nickel surface for the nickel carbonyl formation. The first significant use of solid catalyst was made in the cracking of hydrocarbons during 1935–1940 in the petroleum industry [4-6]. The catalytic naphtha reforming, dehydrogenation of cyclohexene to benzene and isomerisation of straight chain alkenes were developed in 1950. In around 1960, hydro treating catalyst was introduced in catalyst technology at refineries for the removal of sulfur, nitrogen and metals from petroleum products [7-10]. Ziegler and Natta in 1955 discovered the use of $AlCl_3$ as a catalyst for the production of polypropylene at low pressure [11]. In the Wacker process in 1960, catalyst $[PdCl_4]^{2-}$ enabled the reduction of temperature from 500 to 100 °C at 7 atm during the formation of acetaldehyde from ethylene [12, 13]. In 1960, Weisz and Frilette used

the unique property of zeolites in shape selective catalysis for cracking of n-alkanes to exclusively straight chain products [14, 15]. In early 1970s, catalytic reaction was classified by Boudart in two groups: (i) structure sensitive and (ii) structure insensitive [16]. According to Boudart, the rate of reaction of structure sensitive reactions changes as a function of particle size, while on increasing the particle size the structure insensitive reactions kept reaction rate unchanged [17]. Haensel in same period proposed the concept of bifunctional catalysis to obtain a desired product using two catalysts, in the dual catalytic system initially one catalyst produces one reaction intermediate and afterwards this shifts to other catalyst for the formation of other reaction intermediate or products and finally reaction products separate out from the catalyst. Noble metal catalysts were developed in the late 1970 and early 1980's for the control of CO, hydrocarbon and NO emission from automobiles [18, 19]. During 1980–1990, the vanadia, titania and zeolite catalysts were developed for the selective reduction of nitrogen oxides with ammonia or light hydrocarbons [20, 21]. Catalysts for the removal of volatile hazardous organic hydrocarbons such as chlorohydrocarbons were also developed during this period [22, 23]. Now a day's catalysts are playing a vital role in petrochemicals, fine chemicals, pharmaceuticals, fertilizers and food industries. The biochemically significant processes are also based on catalysts.

Researches in catalysis involve many areas of chemistry, notably organic chemistry, organometallic chemistry and materials science. Catalysis is relevant to many aspects of environmental science, e.g. the catalytic converter in automobiles and the dynamics of the ozone hole. Catalytic reactions are preferred in environment friendly green chemistry due to the reduced amount of waste generated [24], as opposed to stoichiometric reactions in which all reactants are consumed and more side products are formed. The most common catalyst is the proton (H^+). Many transition metals and transition metal complexes are used as catalyst as well. A group of catalysts called enzymes are important in biological systems.

1.2. HETEROGENEOUS CATALYSIS

In today's world catalysis has become an important part of life due to its wide application in various fields like, production of materials such as plastics, fuel and food. Catalyst can be homogeneous or heterogeneous in nature and can be of any form starting from atoms and molecules to an extent of enzymes and zeolites. Sabatier gave the concept of the use of metals as heterogeneous catalysts for the hydrogenation of oils [25] and postulated the formation of unstable intermediates during catalytic reaction. Metal such as nickel showed good activity for the hydrogenation, as it forms intermediate nickel hydride which decomposes to regenerate the free metal. Sabatier also demonstrated the importance of the introduction of solid supports in the enhancement of activity and selectivity of the catalysts. Since the catalytic action occurs at specific sites on the solid surface, often called as 'active sites', the uniform dispersion of the supported metal catalysts is desirable for significant improvement in the catalytic action [25].

1.3. VARIOUS HETEROGENEOUS SUPPORTS FOR CATALYSTS

With the extensive use of catalysts in various industrial processes, a lot of research has been done to develop highly efficient catalysts. But a long way is remaining to achieve more efficient heterogeneous catalysts. Most of the homogenous catalysts are expensive but very active and selective. However, due to their homogeneous nature it is difficult to recover them from the reaction mixture. Heterogenisation of homogeneous catalysts can be accomplished by immobilising, grafting, anchoring or encapsulating them with inert solid like organic polymer or inorganic support and materials having thermal stability and chemical inertness can also be used for the support. Alumina, clays, aluminosilicates, activated carbon and silica are the most common support. For the preparation of supported catalyst co-precipitation of the catalytically active component is one of the oldest methods to prepare supported catalysts and the support to give a mixture which is subsequently dried, calcined and reduced to give a porous material with a high surface area. Another but most preferred method is loading pre-existing material supports in the

form of shaped bodies with the catalytically active phase by means of impregnation or precipitation from solution [26].

Heterogenisation of homogenous catalyst gives advantageous features like easy product separation and easy recovery of catalyst. Alumina and silica have been used for the immobilisation of various catalysts by direct reaction of surface hydroxyl groups with reactive species (catalyst); Scheme 1.1 [27-30].
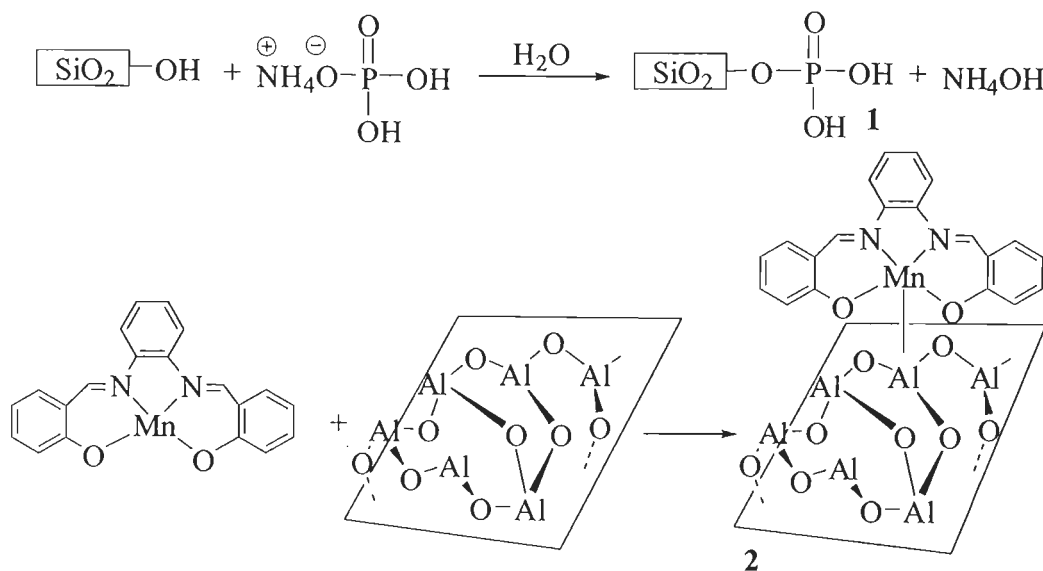
Scheme 1.1. Immobilisation of catalysts on silica and alumina

Other examples of immobilised catalysts supported on silica and other supports are given in Scheme 1.2 [31, 32].

The mesoporous MCM-41 was discovered by Mobil group in 1992 [33]. After that it has attracted various researchers as a solid support for heterogenisation of various catalysts. The molecular sieves such as Si-MCM-41 and Si-SBA-15, have free hydroxyl group on the surface and therefore these materials are suitable aspirants for immobilisation of catalyst. The dioxomolybdenum(VI) has been immobilised to MCM-41 surface according to the procedure shown in Scheme 1.3 [34, 35].

Scheme 1.2

Scheme 1.3

pypr = [N,N'-bis(2-pyrrolmethylidenaminopropyl)amine]

$Ti(OIPr)_4 + H_2O + (S)\text{-}Binol + ILSBA\text{-}15 \xrightarrow[\text{1h}]{\substack{[BMIM]PF_6, \\ CCl_4, DCM}} TiILSBA\text{-}15$

6
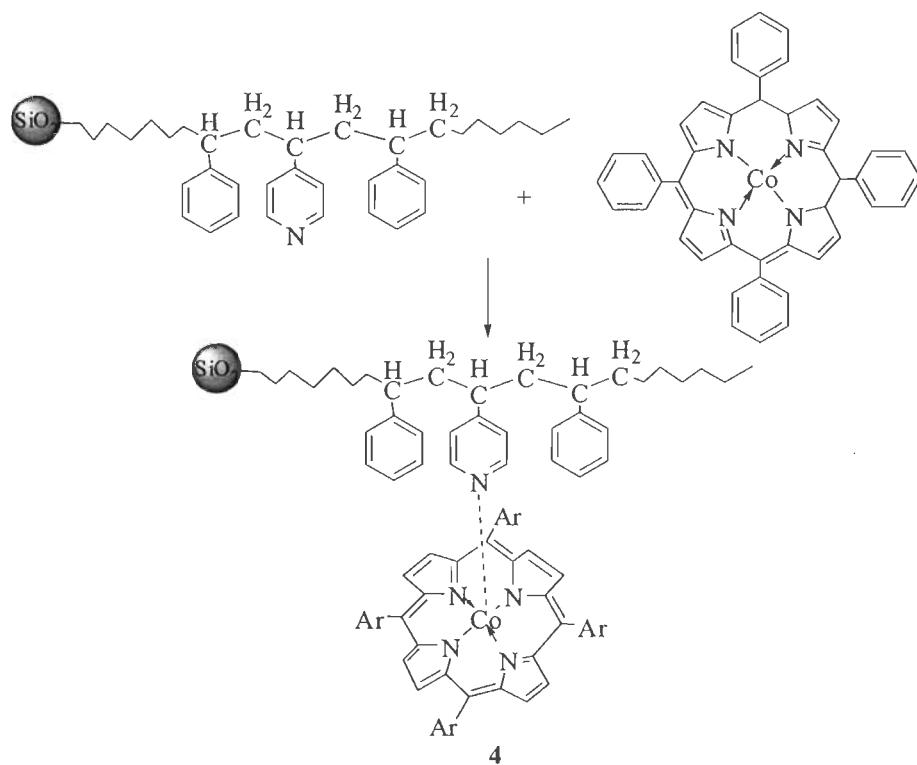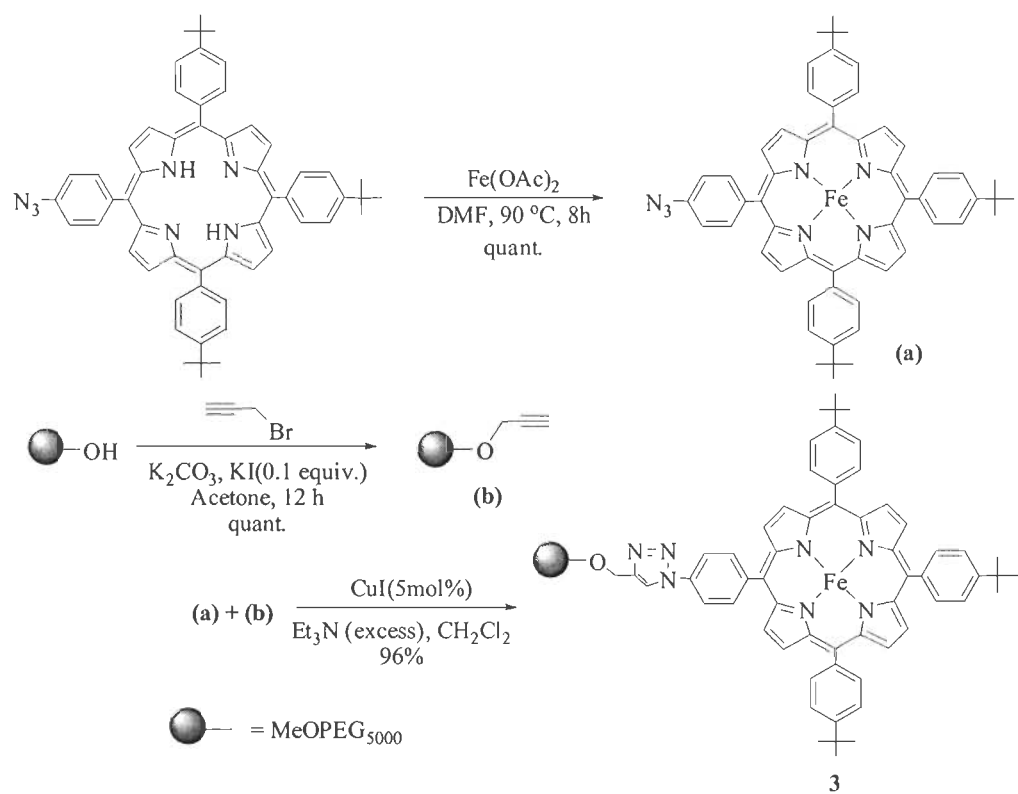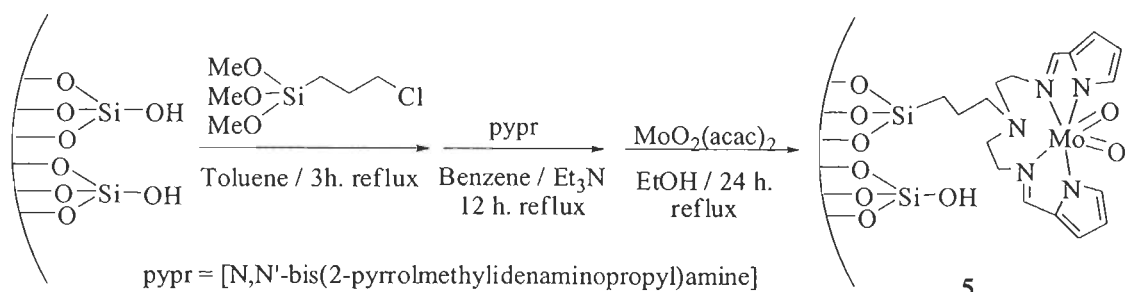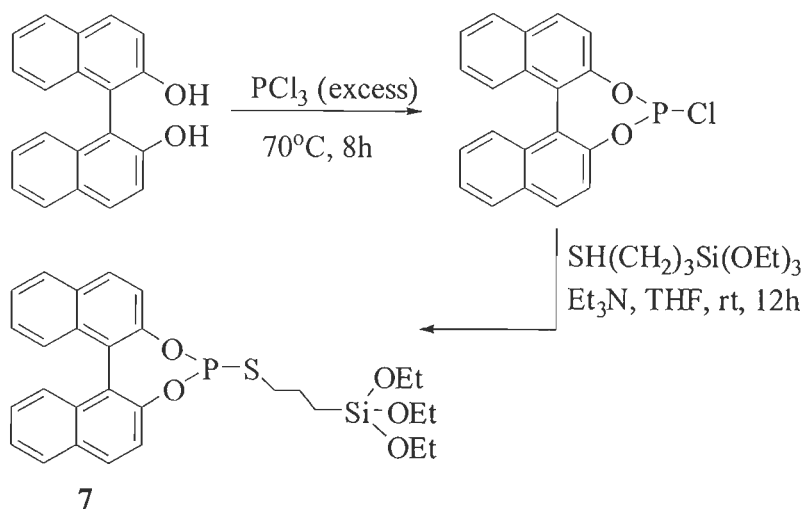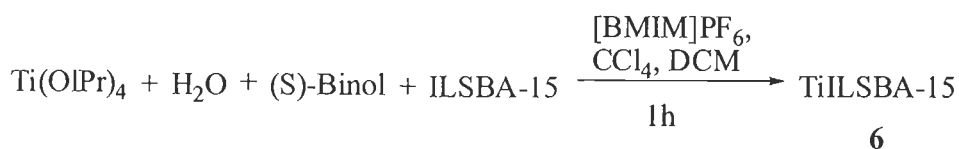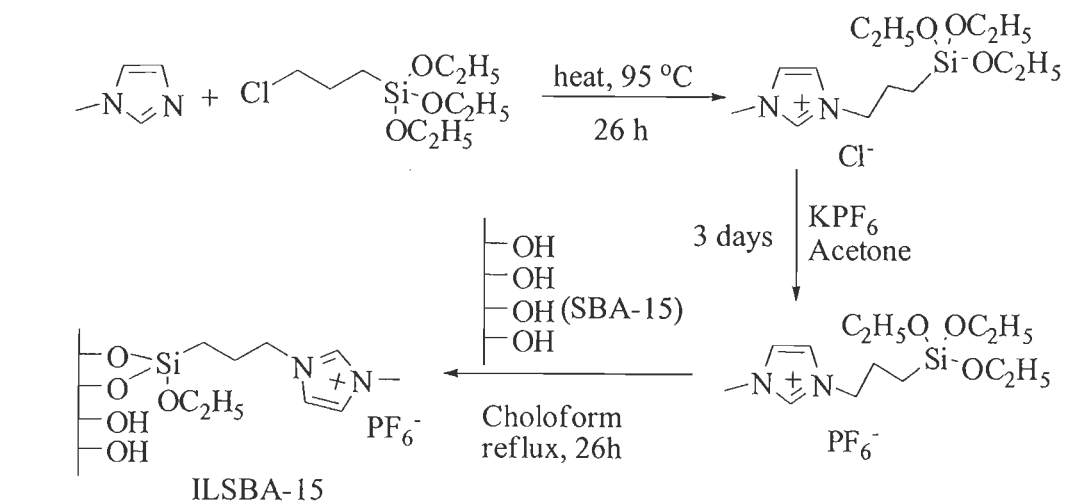
Scheme 1.4

Halligudi *et al.* have reported the immobilisation of chiral Ti-binol complex onto ionic liquid modified SBA-15 [36-38]. Similarly BINAP (2,2'-bis(diphenylphosphino)-1,1'-binaphthyl)-ruthenium and -rhodium complexes have been immobilised on silica [39] by functionalising it as shown in Schemes 1.4 and 1.5.
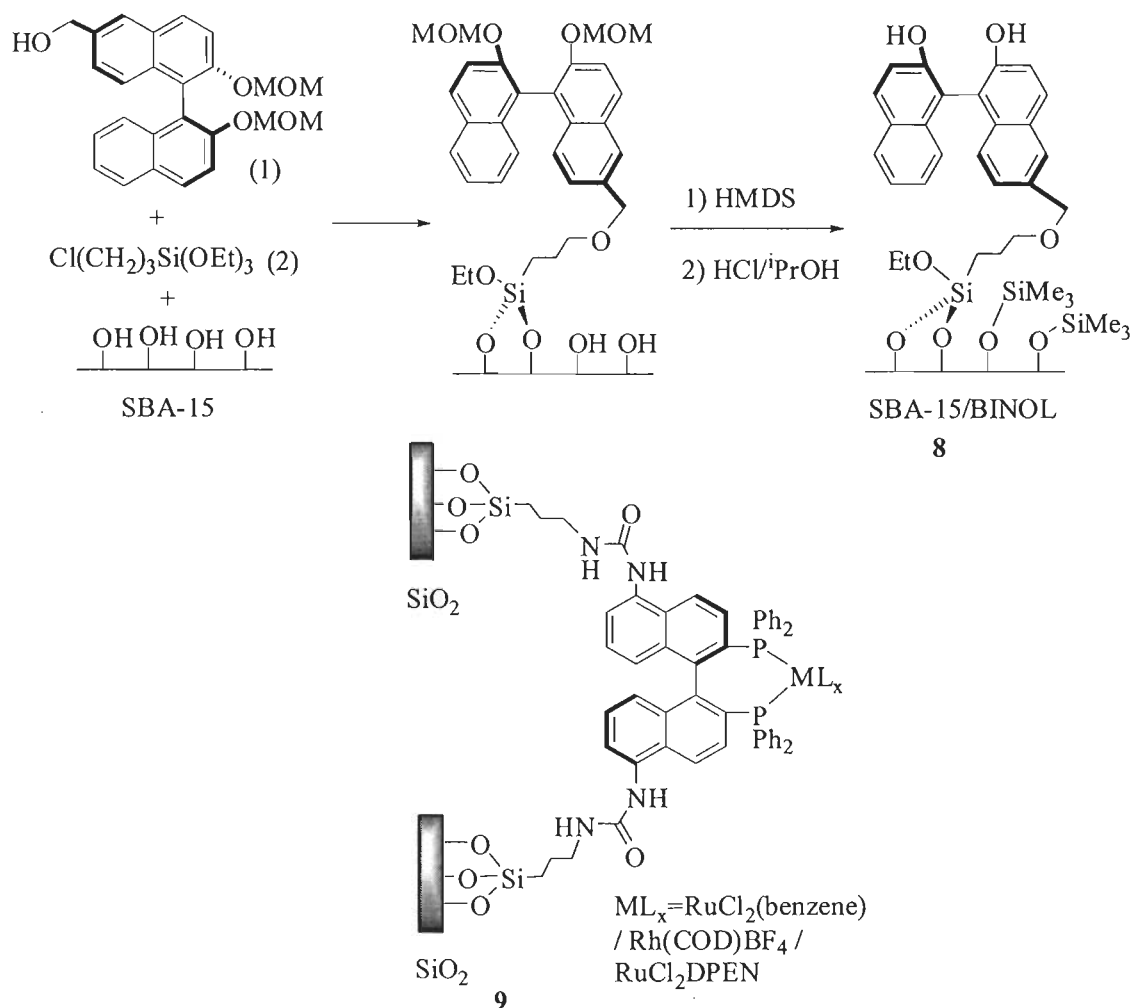
Scheme1.5

The super cages of zeolites have attracted researcher for the encapsulation of transition metal complexes (Fig. 1.1). This new class of catalysts is called Zeolite Encapsulated Metal Complexes (ZEMC) or ship-in-bottle complexes. As

the metal complex is not bonded to the host zeolite cavity, it shares advantageous features of homogeneous catalysts as well. The pore size of zeolite makes the catalyst shape and size selective.

(a)　　　　　　　　　(b)　　　　　　　　　(c)
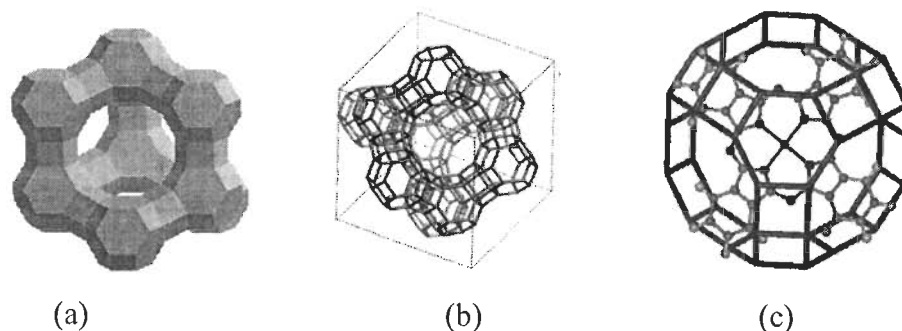
Fig. 1.1. Structure of zeolite-Y (a and b) and metal complex encapsulated in zeolite-Y (c).

Romanovsky *et al.* first reported the metal phthalocynines encapsulated in the super cages of the zeolite-Y [40]. Jacobson's catalyst encapsulated in Na-Y has emerged as an important catalyst for the oxidation of olefins [41]. Metal complexes encapsulated in zeolite have been used for hydrogenation, arylation and nitration reaction [42-44]. Transition metal complexes such as [VO_2(sal-ambmz)]-Y, [Cu(sal-ambmz)Cl]-Y, [VO(sal-dach)]-Y, [Cu(sal-dach)]-Y, [VO(sal-oaba)(H_2O)]-Y, [Cu(sal-oaba)(H_2O)]-Y, [Ni(sal-oaba)(H_2O)$_3$]-Y, [VO(tmbmz)$_2$]-Y, [Cu(tmbmz)$_2$]-Y have been encapsulated in Na-Y for the oxidation of styrene, phenol, cyclohexene, cyclohexane, ethylbenzene, methyl phenyl sulfide and diphenyl sulfide [45-48].

Recently Serrano *et al.* have synthesised the n-ZSM-5, Al-MCM-41 and hybrid zeolitic-mesostructured materials, HZM(0) for the Friedel-Craft acylation of anisole [49]. Supported complexes, [Co(N^O)$_2$]-Y, [Cu(N^O)$_2$]-Y, [Co(N^O)$_2$]–Al_2O_3, [Cu(N^O)$_2$]–Al_2O_3, [Co(N^O)$_2$]–AMPS and [Cu(N^O)$_2$]–AMPS (where, N^O = η^2-(N,O) coordinated 2-pyrazinecarboxylic acid; AMPS = aminopropyl silica) complexes have also been synthesised and used for the oxidation of cyclohexene; Scheme 1.6 [50].
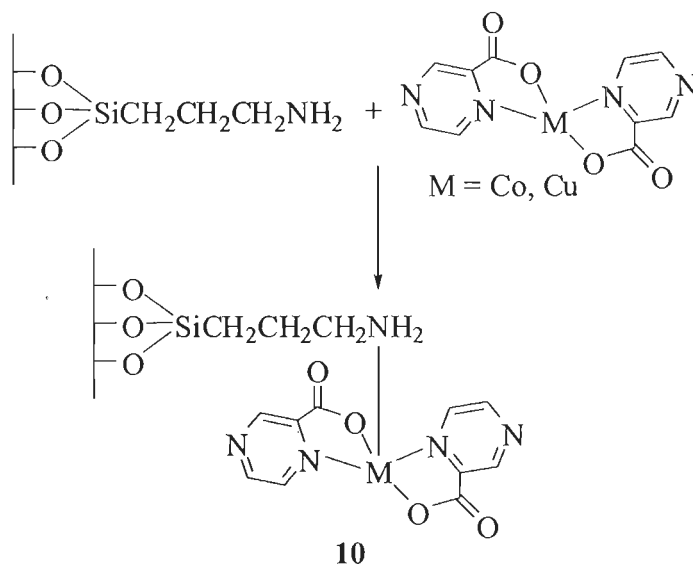
Scheme 1.6

Niasari *et al.* have encapsulated transition metals Mn(II), Co(II), Ni(II) and Cu(II) in zeolite cavity for the syntheses of [Mn(salophen)]-NaY, [Mn(H$_4$salophen)]-NaY, [Co(salophen)]-NaY, [Co(H$_4$salophen)]-NaY, [Ni(salophen)]-NaY, [Ni(H$_4$salophen)]-NaY, [Cu(salophen)]-NaY, [Cu(H$_4$salophen)]-NaY, [Ni([12]aneN$_4$)]$^{2+}$–NaY, [Ni([14]aneN$_4$)]$^{2+}$–NaY, [Ni(Bzo$_2$[12]aneN$_4$)]$^{2+}$–NaY, [Ni(Bzo$_2$[14]aneN$_4$)]$^{2+}$–NaY complexes and studied their catalytic potentials for the cyclohexane and cyclohexene oxidation [51, 52].

1.4. FUNCTIONALISED POLYMERS AS SOLID SUPPORT FOR HOMOGENEOUS CATALYSTS

The polymer-bound heterogeneous catalysts offer many advantageous features such as environment friendly and easy recovery from the reaction mixtures, better thermal stability and reduced possibility of contamination of catalyst with products. These valuable properties have attracted many researchers to develop new polymer-bound catalysts having high activity and selectivity [53-55]. In these catalysts, every active site is isolated from other with high surface area therefore they are

commercially beneficial for industrial processes. A historical background for the syntheses of polystyrene support has been summarised in Table 1.1.

Table 1.1. Historical background for the syntheses of polymer support

Author(s)	Polymer Support	Bead size	Results
R. Merrifield (1963)	Polystyrene-Divinylbenzene (PS-DVB)	-	First time introduced the concept of polymers in solid phase peptide syntheses
Kunin *et al.* (1968)	Polystyrene-Divinylbenzene (PS-DVB)	-	Explained the experimental basis for the formation of macroreticular structure by suspension polymerisation involving phase transfer.
Balakrishnan *et al.* (1982)	Polystyrene-Divinylbenzene (PS-DVB)	-	Used styrene, chloromethylstyrene and divinylbenzene for syntheses of resin to avoid the use of carcinogenic agent chloromethyl methyl ether.
Kolarz *et al.* (1986)	Acrylonitrile-Divinylbenzene (AN-DVB)	1-2 mm	Styrene unit was replaced by acrylonitrile and effect of porous structure was studied.
Gramain *et al.* (1993)	Polystyrene-Divinylbenzene (PS-DVB)	2-20 mm	Described two stages suspension polymerisation for the formation of PS-DVB microspheres.
Hu Xizhang *et al.* (1998)	Polystyrene-Divinylbenzene (PS-DVB)	0.3-1 mm	Anion exchangers were prepared by first acetylation and then reductive amination by Leuckart reaction.
Hamid *et al.* (1999)	N-Vinylcarbazole Divinylbenzene (NVC-DVB)	2 mm	Porous beads were synthesised in non solvating diluents by suspension technique and subsequently cation exchangers were prepared by sulfonation reaction.

Fernanda *et al.* (2001)	Acrylonitrile-Divinylbenzene (AN-DVB)	0.25-4mm	Beads were prepared by suspension technique and chemical modified by hydroxylamine
Kumar *et al.* (2001)	Polystyrene-Divinylbenzene (PS-DVB	16-25 mm	Beads were prepared by suspension technique and subsequently nitrated by NO and NO_2 (called NO_x).
Maria *et al.* (2003)	Methacrylamide-Styrene-Divinylbenzene	_	Beads were synthesised in the presence of diluents to act as a precipitant.
Singh *et al.* (2005)	Phenol-Formaldehyde	0.2-1.8mm	Cross-linked beads were prepared by suspension technique and various effects were studied on bead morphology.
Nahas *et al.* (2006)	Polyester-styrene	0.5-2mm	Polymer beads were prepared by gamma irradiation and chemical suspension polymerisation technique.
Chenet *et al.* (2007)	Polymethyl metha acrylate-Divinylbenzene (PMMA-DVB)	1.8-2.5 mm	Beads of magnetic PMMA microspheres were synthesised by modified suspension polymerisation technique.
Schubert *et al.* (2007)	Polystyrene-Divinylbenzene (PS-DVB)	0.5-2.7 mm	First time used ionic liquids as reaction media or stabilising agent in the syntheses of resin by suspension technique.
Gong *et al.* (2008)	Polystyrene-Divinylbenzene (PS-DVB)	0.2-1 mm	Developed new route to synthesise PS-DVB of uniform size by membrane emulsification, suspension polymerisation and post cross-linking of remaining vinyl groups.

The polymers are non-reactive in nature, but they can be made reactive by imparting the functionality. Thus, polymers bearing the reactive functional groups are called functionalised polymers. The syntheses of polypeptide chain over chloromethylated polystyrene by Robert Bruce Merrifield in 1963 has inspired a number of researchers [56, 57] to develop new polymer-supported catalyst. Various polymers such as polystyrene, polyvinylchloride, polyvinylpyridine, polyaniline, polyallyl, polyaminoacid, acrylic polymer, cellulose, silicate can be functionalised easily. They are capable of undergoing a variety of chemical reactions. Merrifield resin (chloromethylated polystyrene cross-linked with divinyl benzene) is the most widely used functional resin. The functionality to the polystyrene resin beads can be introduced by direct copolymerisation of a mixture of styrene, divinyl benzene and *p*-(chloromethyl)styrene in the desired ratio [58], by chemical modification of the preformed unfunctionalised polymer [59] and also by combining two previous procedures [60]. The syntheses of chloromethylated polystyrene, having –CH$_2$Cl group, by co-polymerisation method is shown in Scheme 1.7.
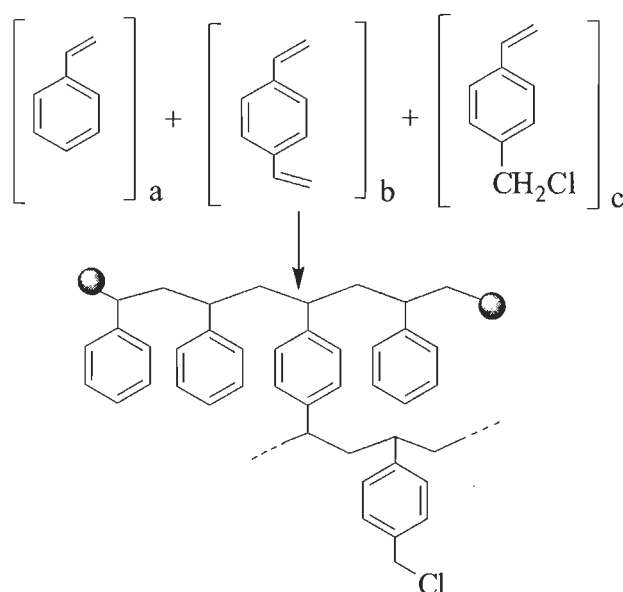
Scheme 1.7. Chloromethylated polystyrene cross-linked with divinylbenzene.

Functionalised polymers may be classified into two forms, (i) straight chain polymers e.g. linear polymerisation of styrene monomer units with chloromethylated

styrene and (ii) cross-linked functionalised polymers e.g. chloromethylated polystyrene where network of polymeric chains joined together at some points due to cross-linking agents. Generally, straight chain polymers have lesser strength than cross-linked polymers. The chloromethylated polystyrene cross-linked with 1–2 % divinylbenzene finds wide applications in combinatorial syntheses and solid-state catalysis. Higher cross-linked chloromethylated polystyrene has been used for other purposes. Several other cross-linkers such as divinylsulfide, S_2Cl_2, CCl_3CHO, biphenols, diamines [61], ethyleneglycol dimethacrylate (EGDMA) [62], N,N-methylenebis(acrylamide) (MBA) [63], trimethylpropanetrimethyacrylate (TRIM), 1,4-bis (vinylphenoxy)butane [64] and bis(vinylphenoxy)polyethylene glycol (PEG) [65, 66] have also been reported in the literature. In chloromethylated polystyrene, one of the important cross-linker is divinylbenzene.

Depends on the extent of cross-linking, the cross-linked polymer may further be classified as macro porous or micro porous polymers. The macro porous polymeric resins have generally less than 5 % cross-linking while resins having cross-linking more than 5 % are referred to as micro porous polymeric resins. The permanent pores may be seen in the macro porous polymeric resins in dry state and due to their interconnection, they have large surface area. However, the functional groups present in them are not always easily accessible as they are located on the internal surface of the micro pores. In macro porous polymeric resins, the functionalised groups are accessible easily by swelling the resins in the suitable solvent. Fig. 1.2 presents the scanning electron micrographs (SEM) of chloromethylated polystyrene (an example of micro porous resin) where micro pores are not visible (a) and with fine visible pores after swelling in DMF (b).

These functionalised polymers (cross-linked as well as straight chain) have widely been used as support for homogeneous catalysts through covalent bonding. Metal complexes as such may form covalent bond if suitable coordinating site is present on the functional group or functionalised group of polymer may react with organic molecule having suitable coordinating site(s) followed by its coordination with metal ion to give polymer-supported metal complex. The polymer-bound organic

molecules having suitable coordinating sites are also called polymer-anchored ligands and their complexes are called polymer-anchored complexes. Practical convenience and operational flexibility due to their insolubility, polymer-anchored catalysts (metal complexes) enjoy the advantageous features of heterogeneous catalyst while retain the nature of homogeneous catalyst. Complete recoveries of the catalytic reaction products are thus possible. Besides, regeneration and recycle ability make them commercially beneficial.

(a)   (b)
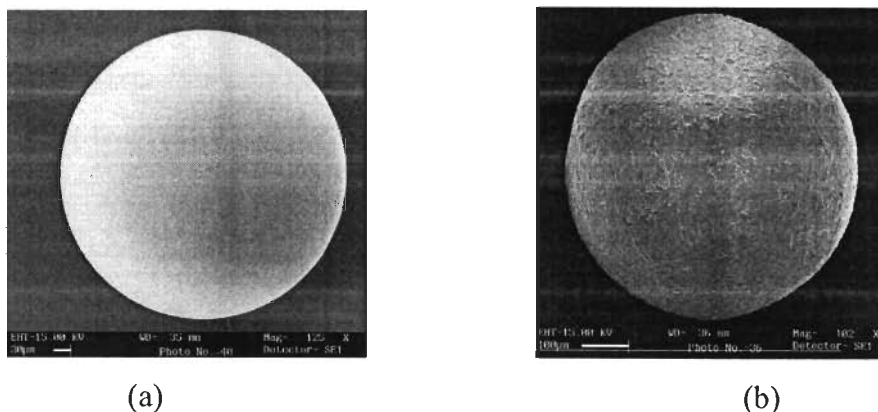
Fig. 1.2. SEM of chloromethylated polystyrene having coordinating functional group before swelling (a) and after swelling in DMF (b).

1.4.1. Preparation of polymer-anchored ligands and complexes

As mentioned above functionalised cross-linked polymer may further be modified with organic molecules having suitable coordinating sites to give polymer-anchored ligands. Chloromethylated polystyrene has widely been used for such modifications. Different synthetic approaches described below are based on such modifications.

One of the most straightforward methods is the reaction of $-CH_2Cl$ group of chloromethylated polystyrene with organic molecules bearing functional groups such as carboxylic, sulfonic, hydroxyl and amine groups [67-71]. Scheme 1.8 represents the synthetic approach **(11-17)**.
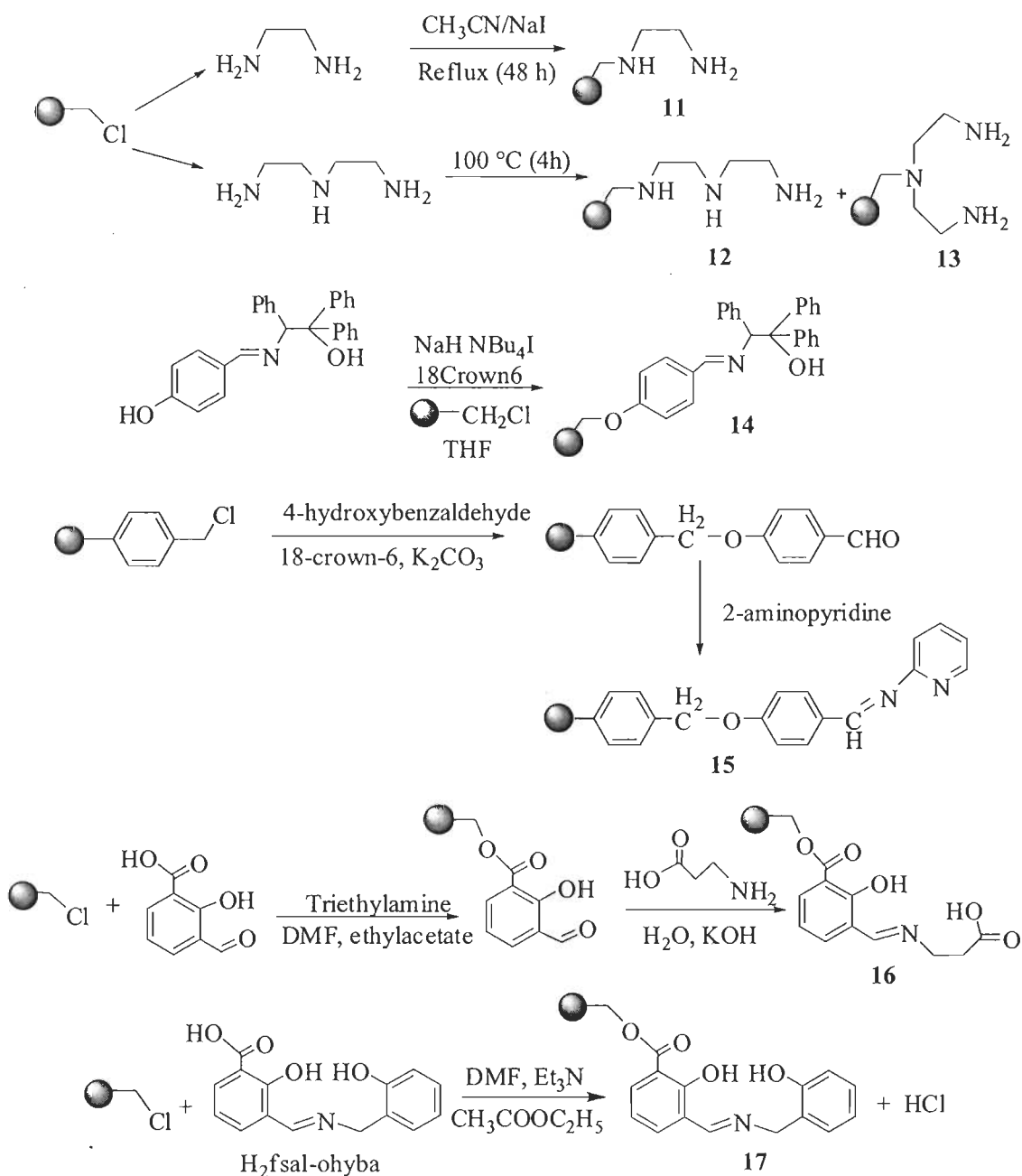
Scheme 1.8

Carboxylic acid and sulfonic acid generally reacts with $-CH_2Cl$ in mild basic conditions. Triethyl amine in ethylacetate has been used to abstract HCl produced in the reaction (**18 – 23**) [72, 73]. Phenolic hydroxyl group requires alkali carbonate along with triethyl amine (**24 – 32**) [74]. Porphyrins such as 5,10,15-tris(4-R-phenyl)-20-(4-hydroxyphenyl)porphyrins (**26**) bearing peripheral hydroxyl group have been

covalently linked with chloromethylated polystyrene by carrying out reaction in DMF at 80 °C in presence of K_2CO_3 [75]. Some of the polymer-anchored ligands (**18 – 32**) synthesised by this method are presented in Scheme 1.9 [76-78].
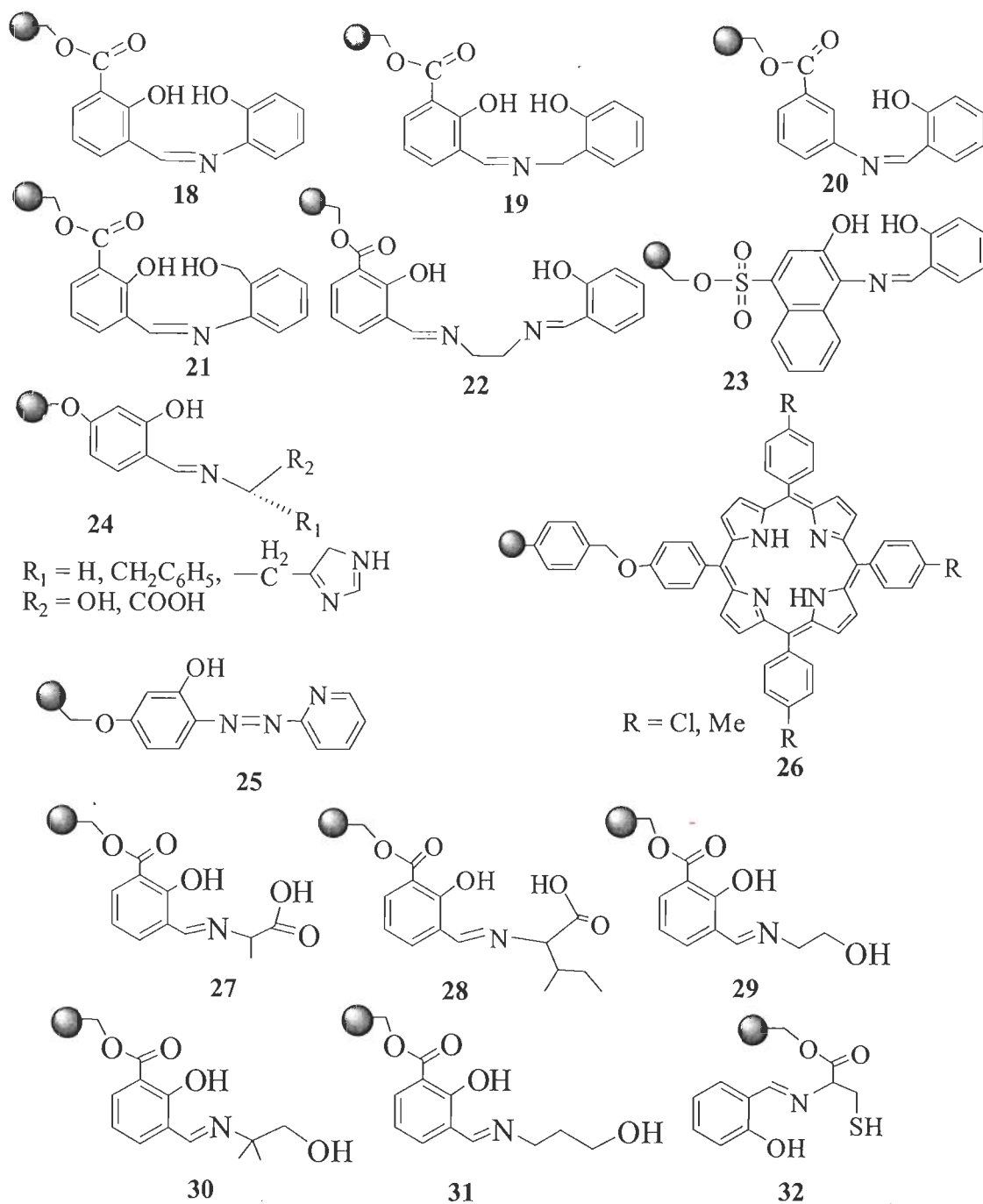
Scheme 1.9. Structure of polymer-anchored ligands

16

Carboxybenzimidazole can be attached to the polymer via its sodium salt; Scheme 1.10 [79, 80].

33
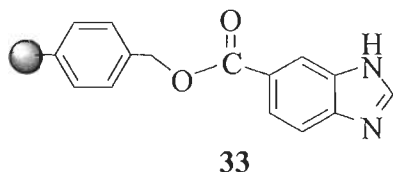
Scheme 1.10

The polymer-bound salicylaldehyde on reaction with 1,2-cyclohexyldiamine gives mono condensed ligand leaving one amino group free. Further reaction of this compound with di-*tert*-butylsalicylaldehyde gives polymer-anchored dibasic tetradentate ligand **34**; Scheme 1.11 [81]. Using similar approach, several such ligands have been covalently bonded to porous styrene based resin, gel-type styrene based resin and porous methylacrylate based resin [82, 83].

34
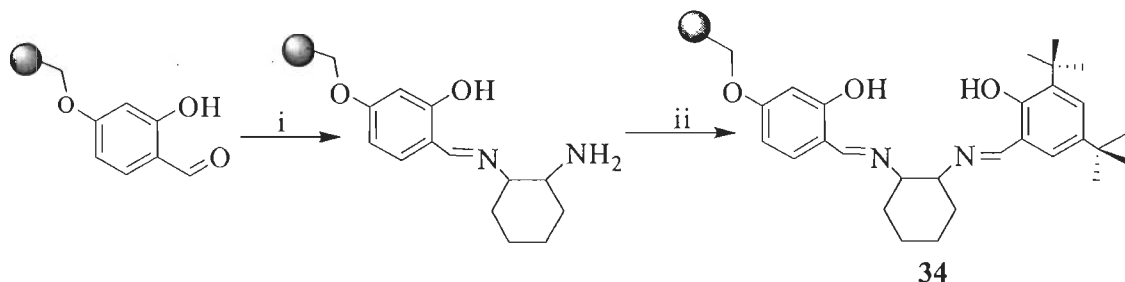
(i) (S, S)-1, 2-diaminocyclohexene, dioxane, 18-Crown-6, K_2CO_3, 85 °C, 3 days.

(ii) Salicylaldehyde derivatives, 18-Crown-6, K_2CO_3, 85 °C, 3 days.

Scheme 1.11

Chloromethylated polystyrene also reacts with –NH group present in the ring e.g. imidazole under the reaction conditions prescribed for carboxylic acid group to give polymer-anchored ligand; Scheme 1.12 [84, 85].

Under the above reaction conditions 2-(2-pyridyl)benzimidazole reacts with chloromethylated polystyrene to give the corresponding polymer-anchored ligand; Scheme 1.13 [86]. Sherrington *et al.* have reported that 2-(2-pyridyl)imidazole can be anchored onto polystyrene, through covalent attachment of imine nitrogen, by the

reaction of ligand and chloromethylated polystyrene in refluxing toluene [87]. Ligands presented in Scheme 1.13 are based on such type of reactions [88-94].
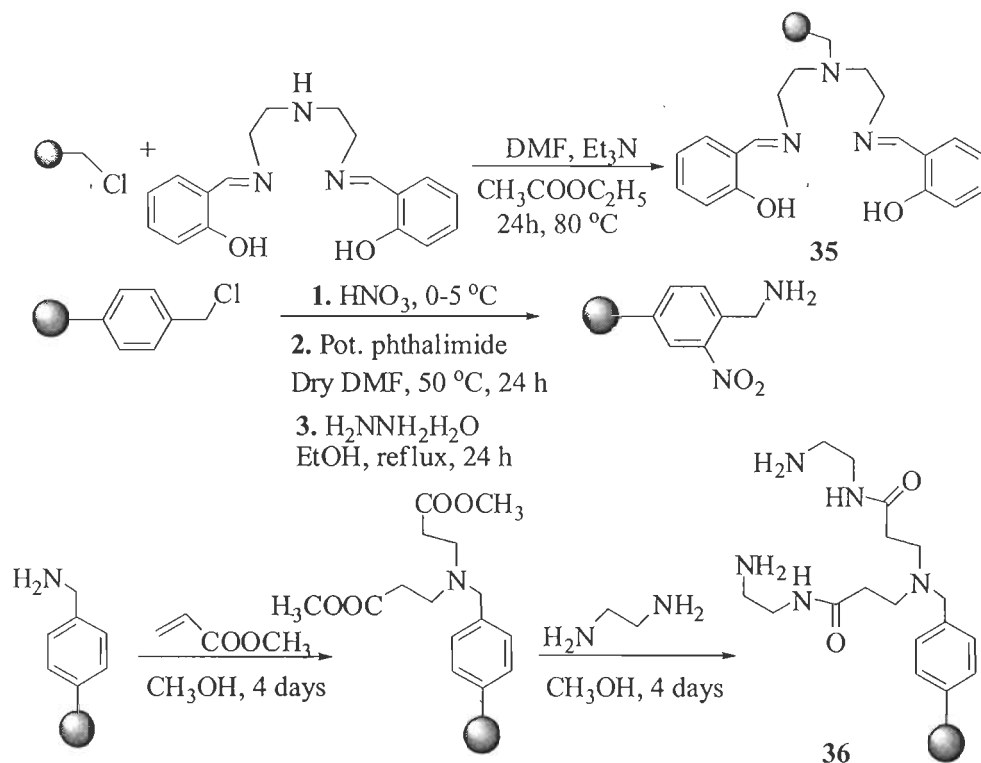
Scheme 1.12

Scheme 1.13

18
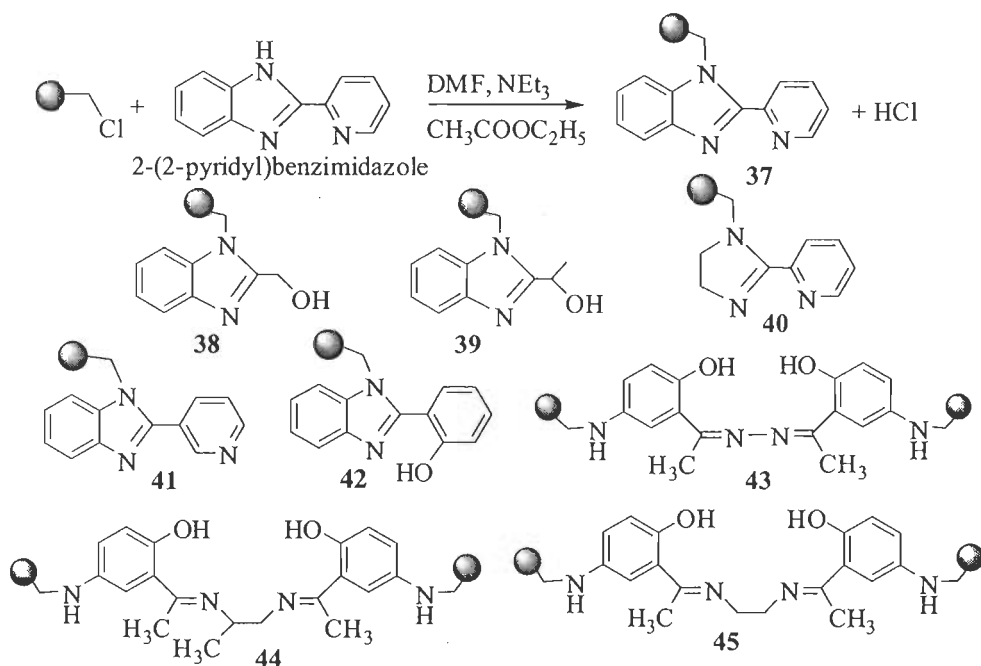
Amino group can also react with chloromethylated polystyrene in refluxing toluene. For example, condensation of aminomethylpyridine with chloromethylated polystyrene gives aminomethylpyridine containing polymer. Another group may further replace the hydrogen of the imine moiety by suitable reagents. Scheme 1.14 presents some of such examples [79, 80].

46   **47**   **48**
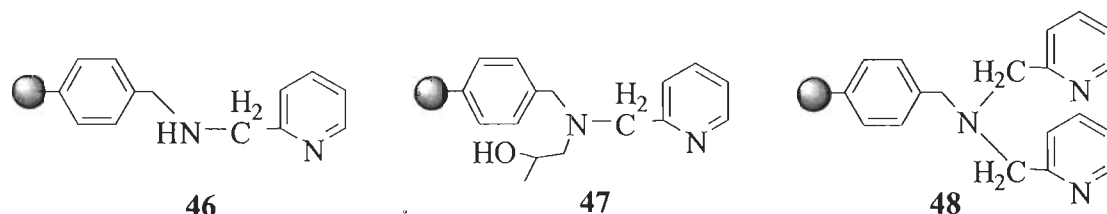
Scheme 1.14

The chloromethylated polystyrene can be modified to some other functionalised resins like aldehydo and amino analogues. Aldehyde group has been obtained by the reaction of chloromethylated polystyrene with $NaHCO_3$ in DMSO (Scheme 1.15) while amino appended resin has been obtained by refluxing chloromethylated polystyrene in HCl in the presence of hexamine; Scheme 1.15 [95-98].

49

50
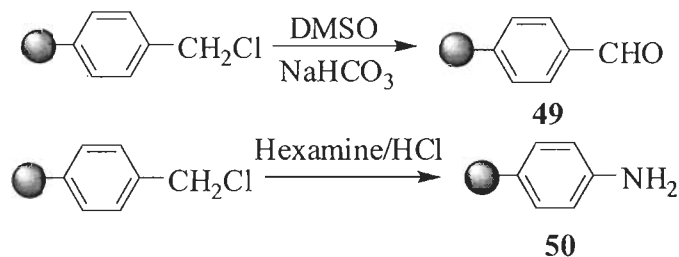
Scheme 1.15

Variety of ligands can be attached to these groups via simple condensation. Some examples are given in Scheme 1.16.

51   **52**   **53**

Scheme 1.16

19
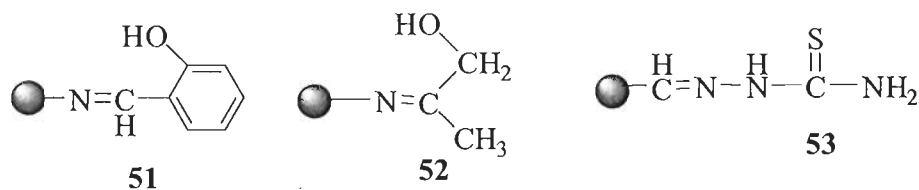
Small organic molecules having suitable coordinating atoms can also be attached with the polymer; Scheme 1.17. The coordinating atom(s) of polymer then directly interact with metal center of complexes to give polymer-anchored complexes [99]. Similarly polymer supported ligands, **55, 56, 57** and **58** (Scheme 1.17) are able to coordinate to the metal centre of the complexes [80].
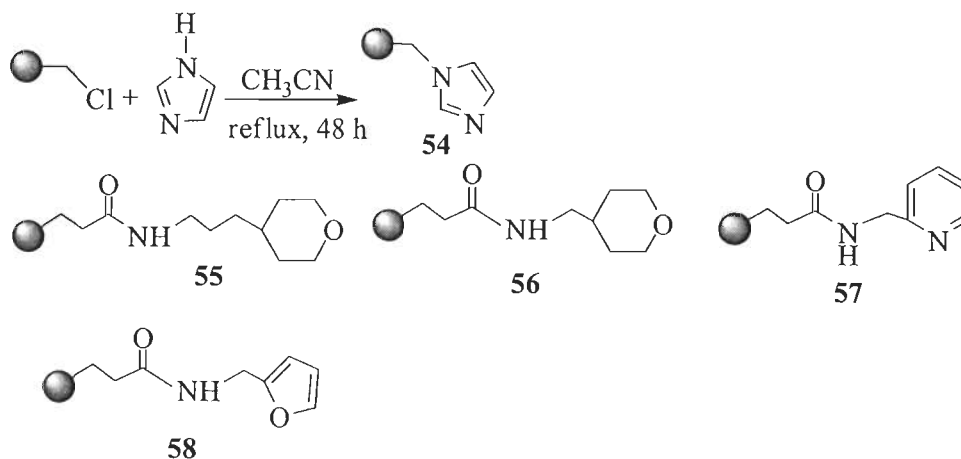
Scheme 1.17

Polymer-anchored metal complexes may also be obtained by co-polymerisation of metal complexes having suitable binding site such as vinyl group on ligand with styrene and divinylbenzene (**59**); Scheme 1.18 [100].
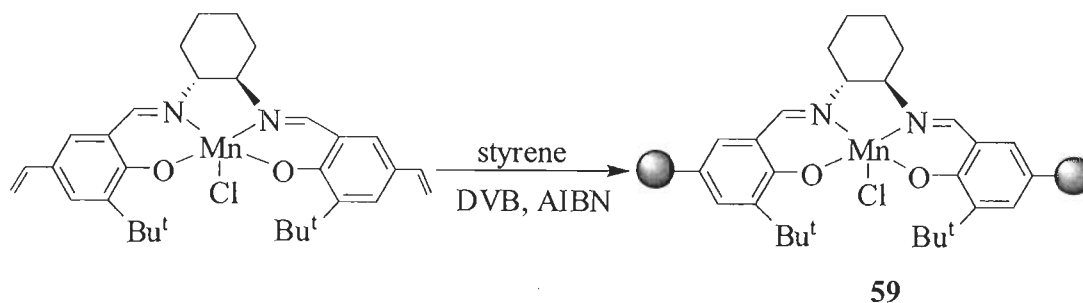
Scheme 1.18

The polymer-anchored ligands on reactions with suitable metal precursors give polymer-anchored metal complexes. A brief literature survey considering only selected metal complexes prepared via above methods or other specified methods are presented here.

Syamal *et al.* have prepared several series of polymer-anchored Cu(II), Ni(II), Co(II), Zn(II), Cd(II), Zr(IV), MoO$_2$(VI) and UO$_2$(VI) complexes with polymer-anchored ligands, **18, 19, 20, 21, 22** and **23** presented in Scheme 1.9. Except molybdenum complexes where [MoO$_2$(acac)$_2$] was used as precursor, all complexes were prepared by reacting corresponding metal acetates with appropriate ligands. Complexes of Cu(II), Zn(II), Cd(II) and UO$_2$(VI) are of the types PS-[ML·DMF] (PS represents polymeric back bone, M = metal ions and LH$_2$ = dibasic tridentate ligands) whereas molybdenum complexes have general formula PS-[MoO$_2$L·DMF] and zirconium complexes have PS-[Zr(OH)$_2$L·2DMF]. (NH$_4$)$_2$[MoOCl$_5$] reacts with some of these ligands to give oxomolybdenum(V) complexes of the type [MoOCl(L)·DMF] under nitrogen atmosphere. The complexes of the type PS-[FeCl(L)·2DMF] have been obtained from FeCl$_3$. Bidentate ligands **51, 52** and **53** of Scheme 1.16 have also been used to prepare polymer-anchored metal complexes [95-99]. Same group of authors have also prepared several polymer-anchored ligands derived from 3-formylsalicylic acid and nicotinic acid hydrazide, 2-aminobenzylalcohol, 4-amino-5-mercapto-3-methyl-1,2,4-triazole, 2-aminopyridine, 2-hydroxybenzylamine, semicarbazide, 2-amino-3-hydroxypyridine, ethanolamine etc. Polymer-anchored complexes of all these metal ions mentioned above have also been prepared and characterised [101-107]. Syntheses of unsymmetrical Schiff bases N,N'-ethylenemono(salicylideneimine) mono(3-carboxysalicylideneimine) and N,N'-propylenemono(salicylideneimine) mono(3-carboxysalicylideneimine) and their anchoring with chloromethylated polystyrene followed by metallation have also been reported [72, 108].

Treatment of Amino acids e.g. glycine and L-valine with chloromethylated polystyrene in THF-acetone-water at 60 °C resulted in the formation of polymer-bound amino acids. Ruthenium complexes of these ligands have been prepared by treating RuCl$_3$ with ligands in ethanol. Similarly, Cu(II) and Pd(II) complexes of L-valine have also been prepared. Chloromethylated polystyrene-divinylbenzene co-polymer beads with variable cross-linking have been used to prepare these complexes. In most cases two possible structures (**60, 61** and **62**) have been proposed. All

structures have been grouped together in Scheme 1.19 [109-112].
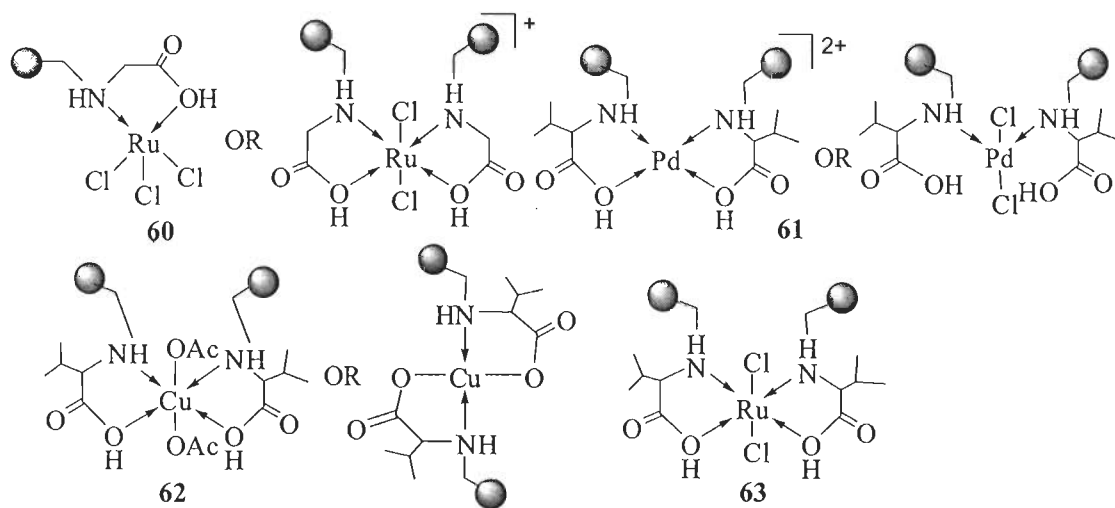
Scheme 1.19

Simple diamines such as ethylenediamine and *o*-phenylenediamine have also been covalently bonded to polystyrene and their Pd(II) and Ni(II) complexes have been prepared and characterised [113, 114]. The polymer-anchored ethylenediamine has further been reacted with salicylaldehyde to give Schiff base type of ligand. Ru(III) and Pd(II) complexes of the obtained Schiff base ligands have also been prepared and characterised. Proposed structures of these complexes are presented in Scheme 1.20.
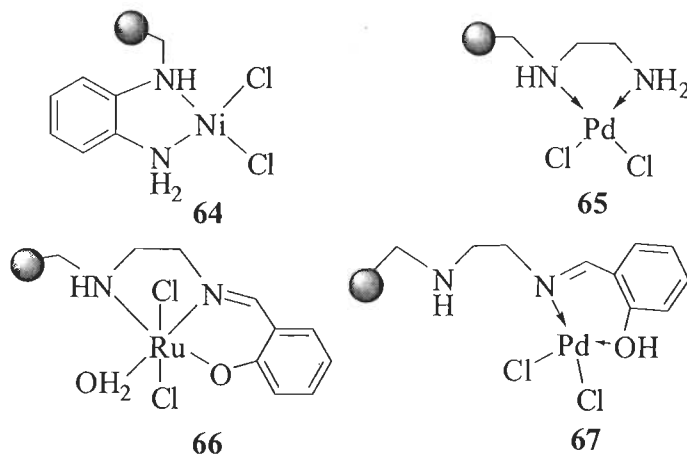
Scheme 1.20

N,N'-bis(*o*-hydroxyacetophenone)ethylenediamine were reacted with cross-linked chloromethylated polystyrene beads to give polymer supported ligand. This ligand on further reaction with ferric chloride, copper nitrate and zinc chloride gives polymer supported metal complexes [92-94, 115] as presented in Scheme 1.21.
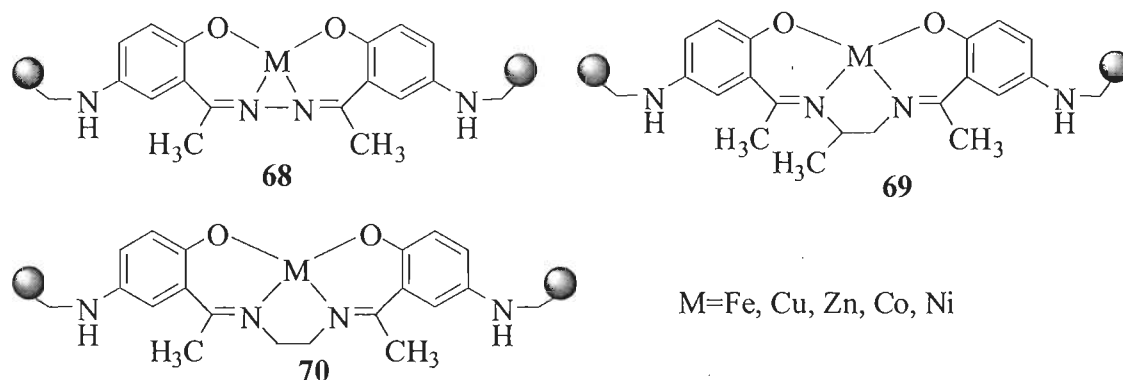
Scheme 1.21

1.4.2. The catalytic activities of polymer-anchored complexes

As polymer-anchored metal complexes have the advantageous features of homogeneous catalyst, various catalytic reaction such as oxidation of benzene, phenol, ethylbenzene, oxidative halogenations of various organic substrates like salicylaldehyde, oxidation of various organic sulfides, oxidative amination and hydroamination have been carried out.

Hydroamination is the direct addition of amine to an unsaturated C-C bond. The amine addition is regioselective in nature and gives Markovnikov and anti-Markovnikov type of products [116]. During recent years hydroamination became a widely explored reaction for the syntheses of nitrogen heterocyclic and complex molecules [117-120]. Various Ti complexes [121, 122] and zeolite encapsulated compounds [123] were found highly active catalyst for hydroamination reaction.

Organo-sulfur compounds are one of the ubiquitous impurities present in crude oil and also present in diesel fuel which on combustion emit SO_2 and suspended particulate matter (SPM). These are harmful for the environment as they contribute to

air pollution, and acid rain. Thus, removal of these organo-sulfur compounds from liquid fuel is the necessity for environment concern. Various methods are in use for removing sulfur compounds from petroleum products such as hydrodesulfurization, oxidative desulfurization, selective adsorption, biodesulfurization etc.. Hydrodesulfurization process is the catalytic treatment of various sulfur compounds with hydrogen to convert them into hydrogen sulfide [124, 125] and sulfur hydrocarbons at high temperature and pressure [126]. As hydrodesulfurization requires harsh reaction conditions and large hydrogen consumption leads to decrease of catalyst life, more emphasis has been made on oxidative desulfurization [127-134]. In this process, sulfur compounds have been oxidised to sulfones using an oxidant *viz.* molecular oxygen [135], H_2O_2 [136-139], nitric acid/NO_2 [140], ozone [141], *tert*-butyl hydroperoxide (t-BuOOH) [142], and potassium superoxide [143]. Then sulfones from fuel have been removed by extraction, adsorption, distillation or decomposition. The unreacted sulfur compounds can be removed by an adsorbent at low temperatures and at ambient pressure. Various types of adsorbents such as carbon aerogels [144, 145], zeolites (Cu (I)-Y [146], Na-Y [147], etc.), activated carbon [148], organic waste derived carbons [149] etc., have been used. For the selective adsorption of thiophenic compounds, activated carbons $PdCl_2$/AC [146] or metal-loaded polystyrene based activated carbons [150] have also been used. Various solid catalysts such as polymolybdates supported on alumina [151], V_2O_5/Al_2O_3, V_2O_5/TiO_2 [152], Co-Mo/Al_2O_3 [153], Ti-MCM-41 [129] and MoO_3/Al_2O_3 [133] have also been found useful for oxidative desulfurization.

The catalytic oxidation of cyclohexane and toluene by *tert*-butyl hydroperoxide using ruthenium complexes as catalyst at 45 °C was studied by Valodkar *et al.* [154]. These complexes are also active for the epoxidation of olefins like cyclohexene, cis-cyclooctene, styrene and norbornylene. Catalytic oxidation of benzyl alcohol, cyclohexanol and styrene has been tested using Cu(II) complexes. Pd(II) complexes have been used for the hydrogenation of 1-octene, cyclohexene, acetophenone and nitrobenzene.

Polymer-anchored complex PS-[Cu(hebmz)$_2$] catalyses the oxidative coupling of 2-aminophenol to 2-aminophenoxazine-3-one (APX) as shown by Scheme 1.22. Kinetics of the above reaction indicated that the rate of oxidative coupling have first order dependence with respect to substrate, catalyst and air (dissolved O$_2$) concentrations [88].

2-aminophenoxazine-3-one
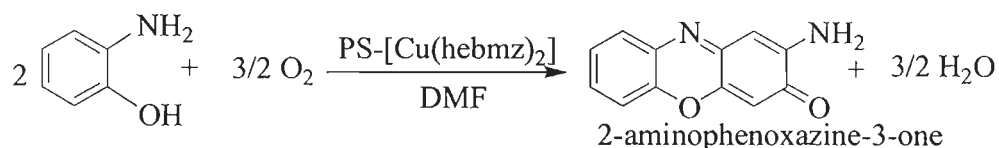
Scheme 1.22

Unsymmetrical polymer-supported Pd(II) complex **71** has been isolated by reacting neat complex with chloromethylated polystyrene in presence of sodium hydride in DMF / THF at ambient temperature; Scheme 1.23. This catalyst has been used for the Suzuki cross-coupling reaction of a variety of aryl bromides with phenylboronic acid to give different derivatives of biphenyls [155].

71
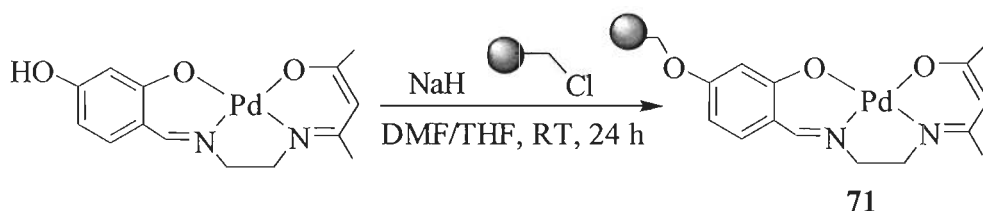
Scheme 1.23

Suzuki coupling is very useful method to prepare polystyrene bearing chiral 1,1'-bi-(2-naphthol) (BINOL) (**72**) by reaction between 6-bromo-1,1'-bi-(2-naphthol) and cross-linked polystyrene resin bearing phenylboronic acid group; Scheme 1.24. These polymer-supported BINOLs catalyse the selective oxidation of (prochiral) thioethers to sulfoxides [156]. Polymer-anchored zirconium(IV) complexes (**73**) with very similar BINOLs have been reported by Kobayashi *et al.* and used for the Diels-Elder reaction [157].
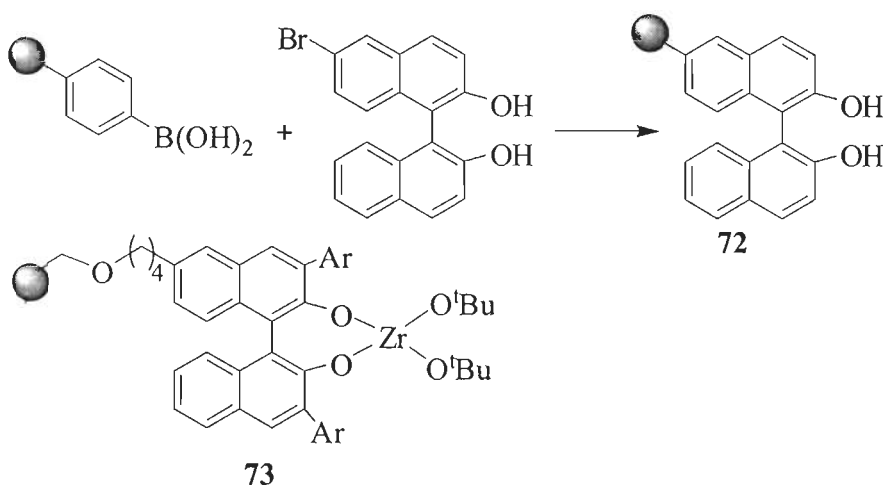
Scheme 1.24

Jacobson's group has synthesised polymer-anchored chiral Co(III) complex **74** with the ligand derived from *trans*-1,2-diaminocyclohexane and di-*tert*-butylsalicylaldehyde [158]. Isolation of polymer-supported Jacobson's catalyst by co-polymerisation method has also been attempted [159]. The monocondensation of *trans*-1,2-diaminocyclohexane with salicylaldehyde bound polymer followed by reaction with di-*tert*-butylsalicylaldehyde gave polymer-anchored ligand. Polymer-anchored Mn(III) complex **75** was synthesised by the reaction of manganese acetate with above ligand [81]. Similarly complexes, **76** supported on *p*-acetoxystyrene functionalised polystyrene, porous styrene based, gel-type styrene based and porous methylacrylate based resins have been synthesised and characterised [83, 160]. Angelino *et al.* have used 2,4,6-trihydroxybenzaldehyde bound polymer and adopted the above approach to prepare Mn(III) complex **77** [161]. Reger and Janda have reported complex **78** supported on different polymers, namely poly(ethyleneglycol)monoethylether, non-cross linked polystyrene (both are soluble in nature), chloromethylated polystyrene and a resin synthesised by them (both insoluble in nature) [162]. Polymer-anchored Mn(III) complex **79** has been synthesised by functionalisation of pyrrolidine moiety, followed by anchoring with polymer and reaction with suitable metal precursor as reported by Jacobson [163]. All these complexes are grouped together in Scheme 1.25. These complexes have

extensively been used for the asymmetric epoxidation of various simple and substituted olefins such as styrene, *trans*-stilbene, 1-indene, dihydronaphthalene and allylic alcohols.

= Poly(ethyleneglycol)monoethylether
= Non-cross linked polystyrene
= Chloromethylated polystyrene
= Resin synthesized by Zanda et al. (*J*anda *J*el resin)
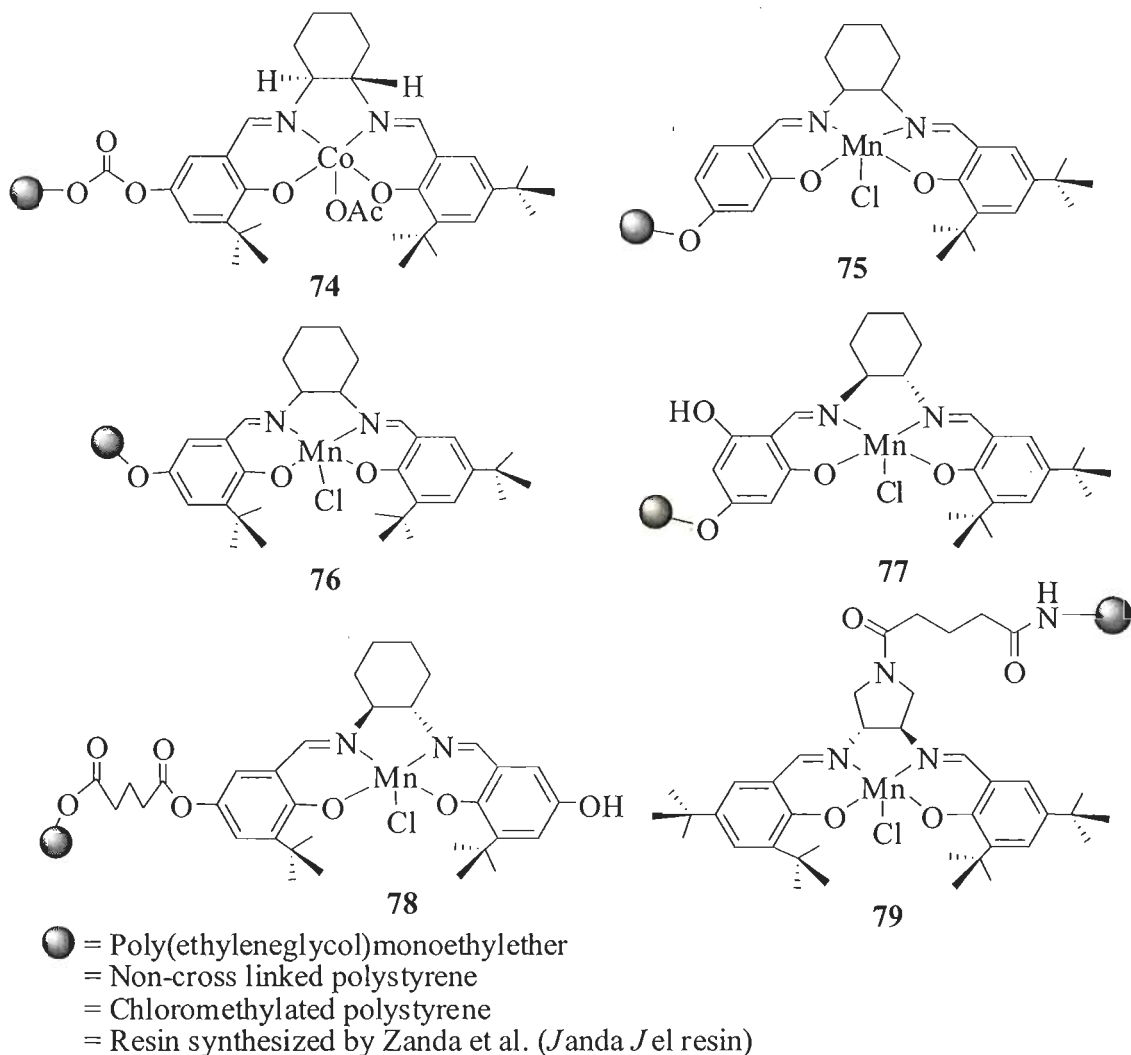
Scheme 1.25

Using the procedure as mentioned in Scheme 1.18 i.e. condensation of metal complex having 5-vinyl substitution at ligand with styrene and divinylbenzene resulted in the formation of polymer-anchored complexes. Complexes **80, 81, 82** and **83** [164-166] have also been prepared by very similar procedure. Complexes **81** and **83** have ethyleneglycol dimethylacrylate derived polymer backbone. Ligands derived

from 2,4-dihydroxybenzaldehyde and (R,R)-*trans*-1,2-diaminocyclohexane on co-polymerisation with styrene and divinylbenzene gave the corresponding polymer-anchored ligand. Metallation of the ligand with $Mn(II)(CH_3COO)_2$ / LiCl in air yield complex **84** [167]. Mn(III) complex having alkyl carboxylic acid group at sixth position of 2-hydroxy-1-naphthaldehyde derivative also interacts easily with chloromethylated polystyrene to produce polymer-anchored Mn(III) complex **85** [168]. Complex **85** has been reported to be highly enantioselective catalyst. Structures of these complexes are presented in Scheme 1.26. Complexes as mentioned above have good catalytic activity for the asymmetric epoxidation of olefins.
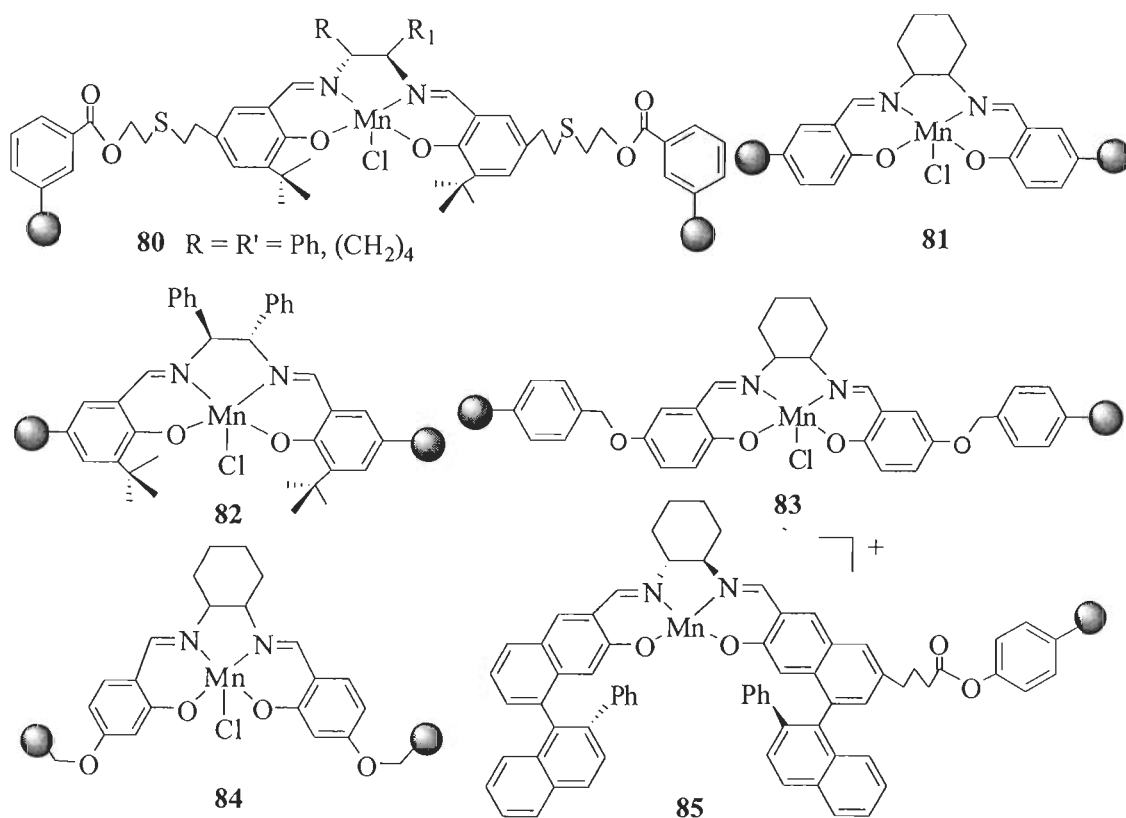
Scheme 1.26

Kureshi *et al.* have selected polymer bound pyridine that coordinates to the metal centre of complex (**86**) through pyridine for enantioselective epoxidation of styrene [169]. Using similar approach Zhang *et al.* have prepared a series of polymer-

bound Mn(III) complexes (**87**) with hydroxyl or sulfonic acid bound polystyrene. Structures of these complexes are presented in Scheme 1.27 [170].

86 R$'$ = R$''$ = (CH$_2$)$_4$
R$'$ = H, R$''$ = CH$_3$
R$'$ = R$''$ = C$_6$H$_5$

87 R$'$ = ^{t}Bu, R$''$= R$'''$ = -(CH$_2$)$_4$-
R$'$ = ^{t}Bu, R$''$ = R$'''$ = Ph
R$'$ = ^{t}Pn, R$''$= R$'''$ = -(CH$_2$)$_4$-
X = -O$^-$, -SO$_3^-$
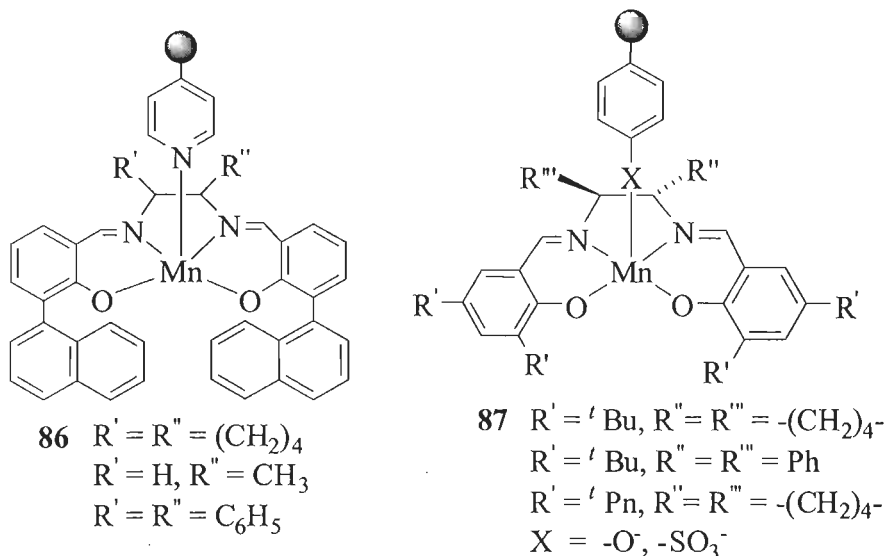
Scheme 1.27

Tangestaninejad's group have reported the molybdenum and tungsten hexacarbonyls attached to polymer-pendent coordinating groups (**88**) for the oxidation of styrene, *cis*-cyclooctene, α-methylstyrene, indene, *trans*- and *cis*-stilbene in the presence of H$_2$O$_2$ or *tert*-butylhydroperoxide [171, 172]. They have also reported polymer-supported metalloporphyrins (e.g. **89** and **90**) for the oxidation of olefins and aromatic hydrocarbons. Complexes reported by these groups are presented in Scheme 1.28 [173-178].

88   **89** (Tetraphenylporphyrin)   **90** (Octabromotetraphenylporphyrin)

Scheme 1.28

29
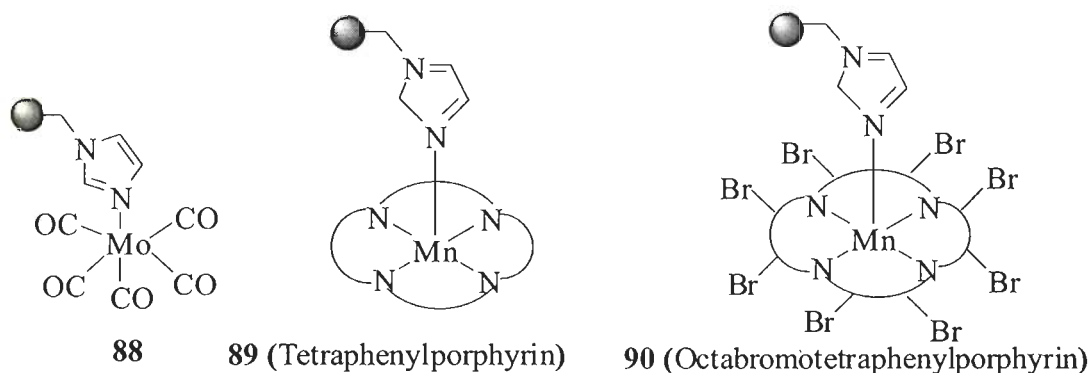
Other types of porphyrins have also been supported on polymer through covalent bonding and have been used for the oxidation of various alkenes and hydrocarbons. Scheme 1.29 presents the substrates tested for the oxidations using polymer-anchored metalloporphyrins [75, 179, 180].

Cyclohexane   Styrene   Ethylbenzene   1-Propylbenzene

Limonene Admantane   Cyclooctane 1,2,3,4-Tetrahydronaphthalene

Cinnamyl alcohol Benzyl alcohol   Benzoin
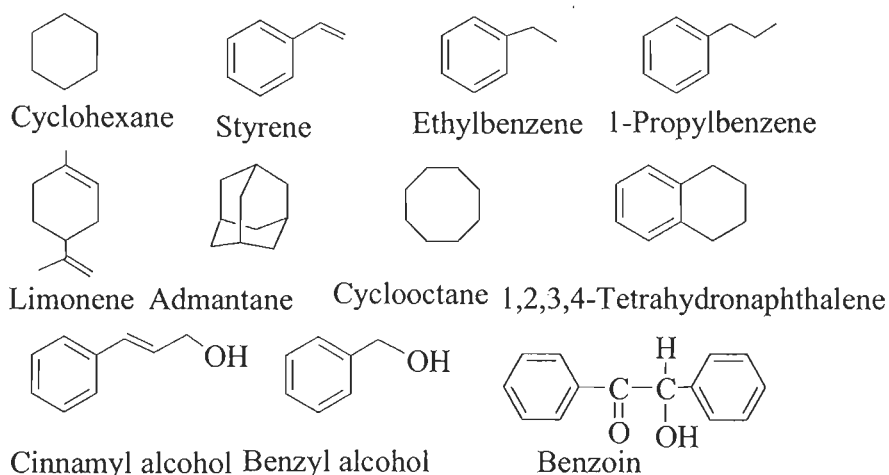
Scheme 1.29

Microwave assisted cyanation of aryl halides in presence of $Zn(CN)_2$ has been catalysed by palladium acetate and polymer-anchored triphenylphosphine [181]. Dichloro bis(diphenylphosphine)palladium(II) complex supported on polymer has been used for the cross-coupling of chloroarenes and chloropyridines with arylboronic acids [182].

Leadbeater *et al.* have reviewed polymer-supported metal complexes of phosphorous containing ligands and their catalytic activities for hydroformylation and hydrogenation reactions [183]. Hydrogenation of alkenes by **91**, nitrobenzene by **92**, 1-benzothiophene by **93**, quinoline and benzylideneacetone by **94**, enamide by **95** and many more reactions have been reported. Structures of some of these catalysts are presented in Scheme 1.30.
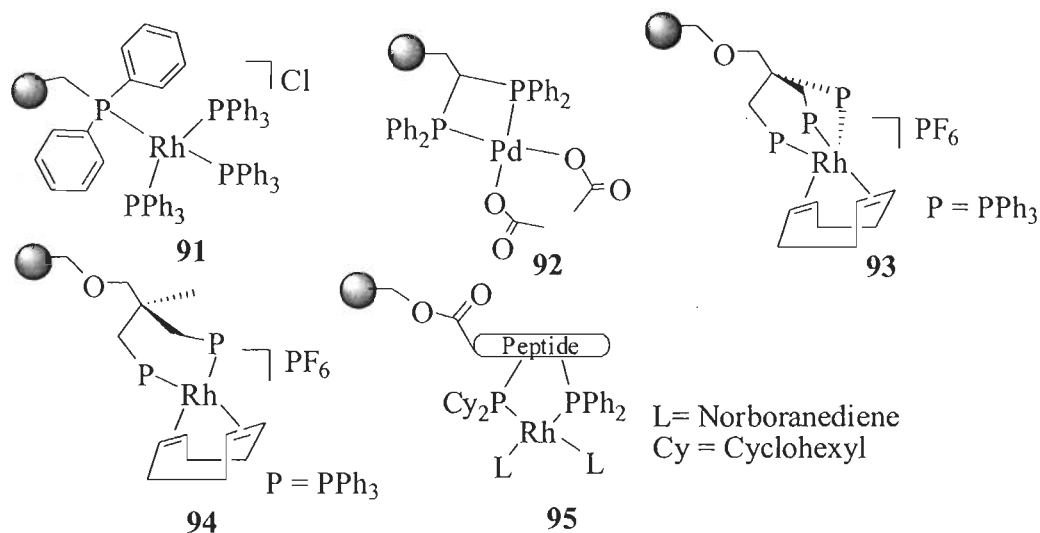
Scheme 1.30

1.4.3. Catalytic activities of polymer-anchored vanadium complexes

VO(acac)$_2$ on reaction with polymer supported 3-formyl salicylaldehyde-*o*-hydroxybenzylamine, PS-[Hfsal-ohyba] gives PS-[VO(fsal-ohyba).DMF] (**96**) [184]. Similarly, PS-[VO(fsal-ea).DMF] (**97**), PS-[VO(fsal-pa).DMF] (**98**), PS-[VO(fsal-amp).DMF] (**99**), PS-[VO(hpbmz)$_2$] (**100**) and PS-[VO(sal-cys).DMF] (**101**) were synthesised by the reaction of VO(acac)$_2$ with PS-[H$_2$fsal-ea], PS-[H$_2$fsal-pa], PS-[H$_2$fsal-amp], PS-[Hhpbmz], PS-[H$_2$sal-cys] respectively; Scheme 1.31 [77, 78, 91].
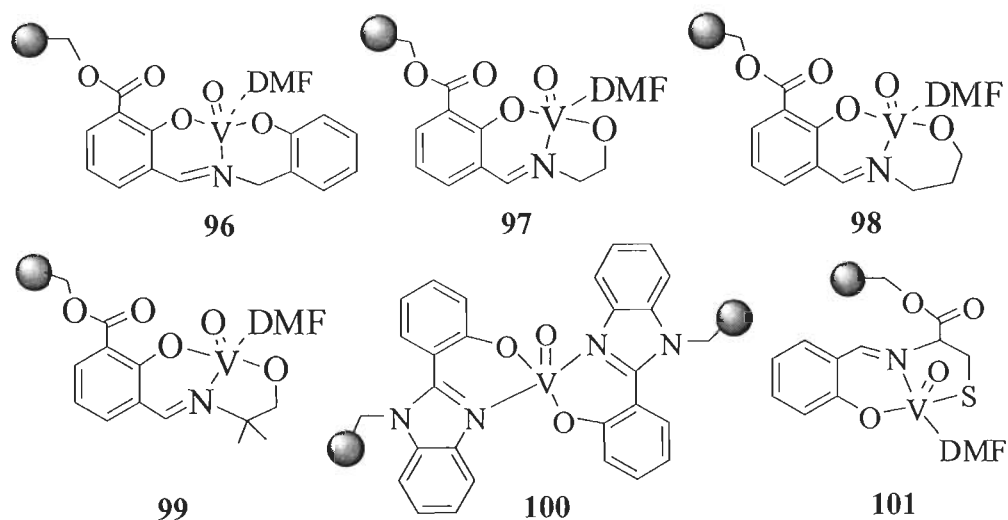
Scheme 1.31

Oxoperoxovanadium(V) complexes of 2-(2-pyridyl)benzimidazole (2-pybmz) and 2-(3-pyridyl)benzimidazole (3-pybmz) have been covalently bonded to the chloromethylated polystyrene cross-linked with 5 % divinylbenzene. The isolated complexes have been represented by the formula PS-K[VO(O$_2$)$_2$(2-pybmz)] (**102**) and PS-K[VO(O$_2$)$_2$(3-pybmz)] [86]. Similarly, polymer-bound oxido-vanadium(IV) complexes, PS-[VO(fsal-DL-ala)(H$_2$O)] (**103**) and PS-[VO(fsal-L-ile)(H$_2$O)] (**104**) have been prepared using similar reaction conditions [76]. The polymer-bound imidazole ligands were used to synthesise PS-K[VO$_2$(sal-inh)(im)] (**105**), PS-K[VO$_2$(sal-bhz)(im)] (**106**) dioxido-vanadium complexes; Scheme 1.32 [185].

102   **103**   **104**

105   **106**
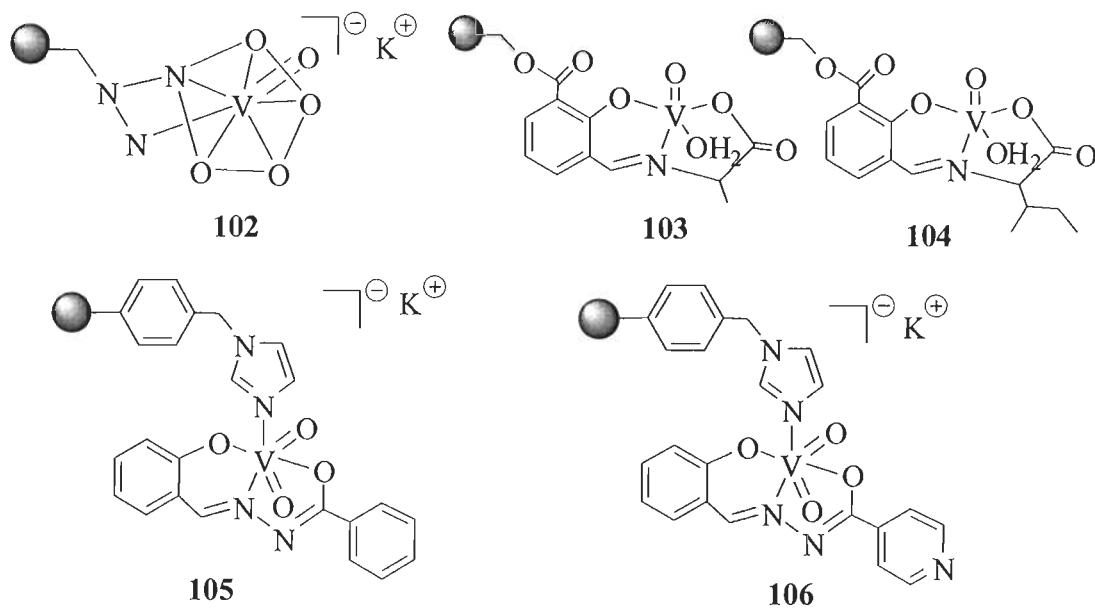
Scheme 1.32

Vanadyl sulphate on reaction with 2-(α-hydroxymethyl)benzimidazole and 2-(α-hydroxyethyl)benzimidazole covalently bonded to chloromethylated polystyrene cross-linked with 5% divinylbenzene gives PS–[VO(hmbmz)$_2$] (**107**) and PS–[VO(hebmz)$_2$] (**108**) (where, PS–hmbmz and PS–hebmz are deprotonated ligand; Scheme 1.33 [89, 186].

Oxidation of styrene catalysed by different vanadium complexes such as PS-[VO(fsal-ohyba)·DMF] (**96**), PS-K[VO$_2$(fsal-ohyba)], PS-[VO(fsal-ea)·DMF] (**97**),

PS-[VO(fsal-pa)·DMF] (**98**), PS-[VO(fsal-amp)·DMF] (**99**), PS-[VO(hpbmz)$_2$] (**100**), PS-K[VO(O$_2$)(2-pybmz)] (**102**), PS-K[VO(O$_2$)(3-pybmz)] and PS-[VO(hmbmz)$_2$] (**107**) in presence of H$_2$O$_2$ / *tert*-butyl hydroperoxide gave three major products styrene oxide, benzaldehyde and benzoic acid; Scheme 1.34 [77, 86, 89, 91,184]. Some of these complexes PS-[VO(fsal-ea)·DMF] (**97**), PS-[VO(fsal-pa)·DMF] (**98**), PS-[VO(fsal-amp)·DMF] (**99**), PS-K[VO$_2$(sal-inh)(im)] (**105**) and PS-K[VO$_2$(sal-bhz)(im)] (**106**) used for benzene oxidation while PS-[VO(fsal-β-ala)·DMF] has been used for the oxidation of cyclohexane, benzene, cumene, cyclohexene, *trans*-stilbene and naphthalene [70, 77, 185]. PS-[VO(fsal-DL-ala)(H$_2$O)] (**103**) and PS-[VO(fsal-L-ile)(H$_2$O)] (**104**) also catalyse the oxidation of cyclohexene and *p*-chlorotoluene [76].

107   108

Scheme 1.33

Styrene → Styreneoxide (so) + Benzaldehyde (bza) + Benzoic acid (bzac) + other

Catalyst / H$_2$O$_2$/ TBHP
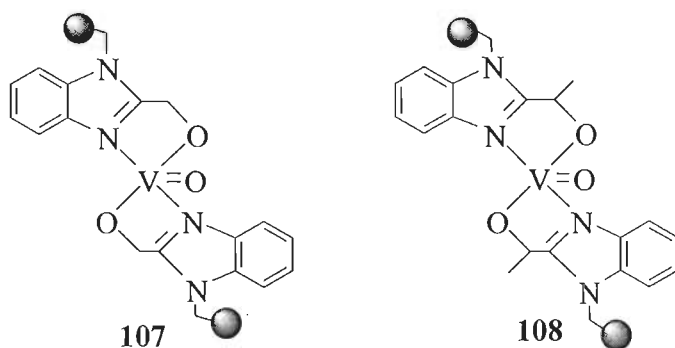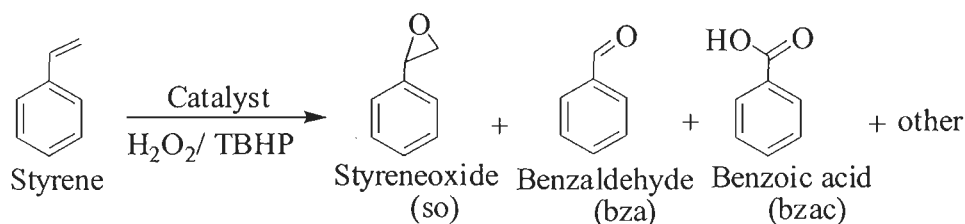
Scheme 1.34. Oxidation products of styrene

The complexes PS-[VO(fsal-ohyba).DMF] (**96**), PS-[VO(hpbmz)$_2$] (**100**), PS-[VO(hmbmz)$_2$] (**107**) catalyse the oxidation of ethylbenzene to acetophenone as the major product [89, 91, 184]. Oxidative bromination of salicylaldehyde in presence of H$_2$O$_2$ / KBr using PS-[VO(fsal-ohyba).DMF] (**96**), PS-K[VO$_2$(sal-inh)(im)] (**105**),

PS-K[VO₂(sal-bhz)(im)] $\quad$ **(106)** $\quad$ and $\quad$ PS-[VO(hmbmz)₂] $\quad$ **(107)** $\quad$ gave $\quad$ 5-bromosalicylaldehyde selectively in quantitative yield; Scheme 1.35[89, 184, 185].
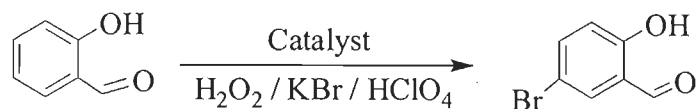
Scheme 1.35

Catalytic potential of PS–[VO(hebmz)₂] **(108)** has been tested for the oxidation of benzoin using *tert*-butyl hydroperoxide as an oxidant in methanol; Scheme 1.36. Various parameters such as different solvents and concentration of the substrate as well as oxidant amount have been taken into consideration for the maximum oxidation of benzoin. Under the optimised reaction conditions, a maximum 98.9 % conversion was achieved with 48.5 % selectivity for methylbenzoate [186].
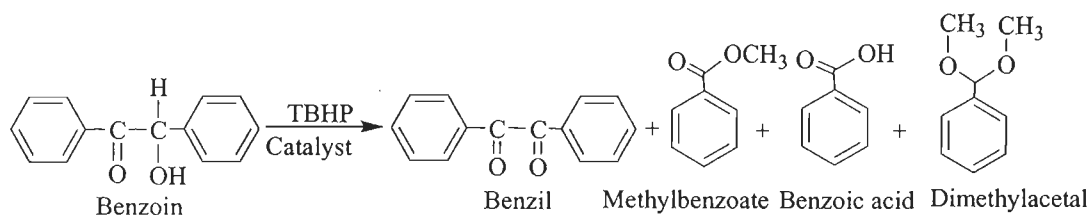
Scheme 1.36

Polymer-anchored PS-[VO(fsal-ohyba).DMF] **(96)**, PS-K[VO(O₂)(2-pybmz)] **(103)**, PS-K[VO(O₂)(3-pybmz)] and PS-[VO(sal-dien)] have been used for the catalytic oxidation of phenol [84, 86, 184]. It has been demonstrated that solvent plays an important role in altering the selectivity of reaction products. In acetonitrile, the catalyst is more selective towards the catechol and hydroquinone formation. However, in water selectivity goes towards catechol and *p*-benzoquinone formation. At higher temperature (ca. 80 °C), the conversion speeds up while lower temperature (ca. 70 °C) is good to keep *p*-benzoquinone in solution for longer time.

Recently reported oxidovanadium complex, [VO(3,5-^{t}Bu$_2$-salophen)] (H$_2$[3,5-^{t}Bu$_2$-salophen] = Schiff base derived from 3,5-di-tert-butylsalicylaldehyde and *o*-phenylenediamine) should exhibit a good catalytic activity but only characterisation of the complex has been reported [187]. This complex should be immobilised onto polymer support and various catalytic activities should be explored. Similarly complexes, chloro[hydrotris(pyrazol-1-yl)borato]oxo(1-*H*-pyrazole)vanadium(IV) and chloro(N,N-dimethylformamide)[hydrotris(pyrazol-1-yl)borato]oxovanadium(IV) can be covalently bonded with polymer through boron for the evaluation of their catalytic activities [188, 189].

Vanadium complexes are known to catalyse the oxidation of organic sulfides (thioethers) by H$_2$O$_2$ to sulfoxides. The sulfur atom in methyl phenyl sulfide is electron rich species and facilitates the electrophilic oxidation to give sulfoxide and further to sulfones. The oxidation of methyl phenyl sulfide has been carried out using PS-[VO(hpbmz)$_2$] **(100)**, PS-K[VO$_2$(sal-inh)(im)] **(105)**, PS-K[VO$_2$(sal-bhz)(im)] **(106)** and PS-[VO(sal-paba)$_2$] [91, 185, 190]. Oxidation of methyl phenyl sulfide gave a mixture of methyl phenyl sulfoxide and methyl phenyl sulfone in acetonitrile at ambient temperature as shown in Scheme 1.37.
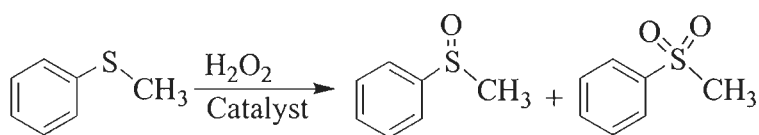
Scheme 1.37

Metal-catalysed addition of nucleophilic amines to alkenes, called amination, has been considered as one of the important routes to synthesise nitrogen based organic molecules [191]. Efficient catalytic intramolecular hydroamination of alkenes have been developed [191-197]. Normally, catalysts based on late transition metal (e.g. of Pd, Pt, Ru, Rh etc.) complexes or lanthanides have been used for amination reaction. Since late transition metal complexes are less sensitive towards air, they

favour hydroamination. However, literature cites several reports on the hydroamination [191-197] as well as oxidative amination of alkenes [198-212]. As complexes of early transition metals e.g. vanadium is sensitive toward amines and alkenes [78], this may proved to be potential candidate for the hydroamination. Polymer-anchored complex PS-[VO(sal-cys)·DMF] **(101)** have been used for the oxidative amination of styrene with diethylamine, imidazole and benzimidazole in mild basic conditions to give the mixture of two aminated products in very good yield; Scheme 1.38.
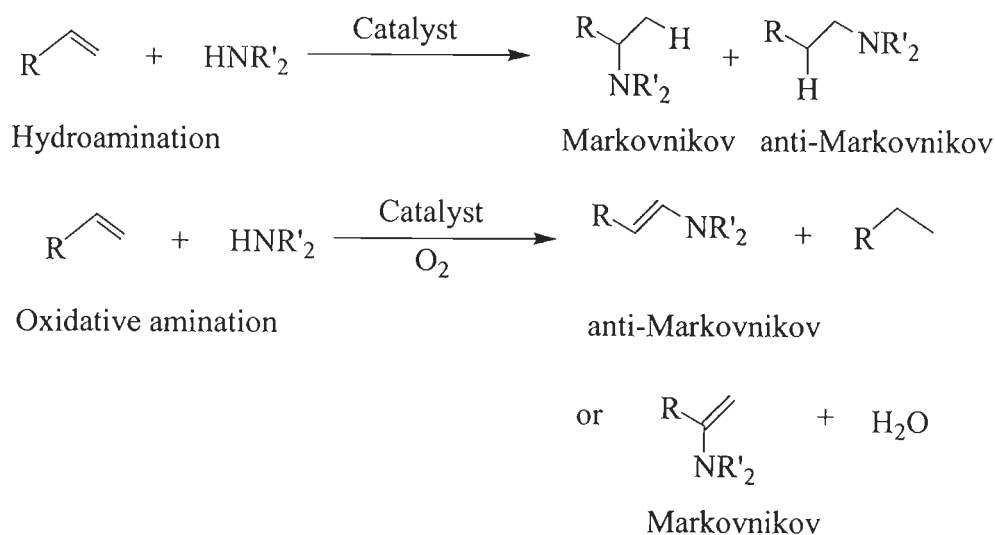
Scheme 1.38

1.5. OBJECTIVE OF THE PRESENT INVESTIGATION

The literature reviewed clearly indicates that polymer-anchored catalysts are good option to explore the industrial processes for the syntheses of new molecules along with the oxidation as well as reduction of various organic substrates. However, very limited literature deals with the catalytic potentials of immobilised vanadium complexes. It was, therefore, reasonable to undertake systematic study on the syntheses and characterisation of new polymer-supported vanadium complexes, and to explore their catalytic potentialities under optimised reaction conditions.

Present study is aimed to describe the syntheses of oxidovanadium(IV) and dioxidovanadium(V) complexes of the following ligands covalently bonded to the chloromethylated polystyrene. In some chapters, polymer-anchored copper(II) and dioxidomolybdenum(VI) complexes have also been prepared to compare their catalytic properties.

(i) Monobasic tridentate ONN donor ligand derived from salicylaldehyde and histamine (Hsal-his):
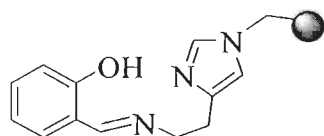
PS- [Hsal-his],**I**

(ii) Monobasic bidentate NS donor 2-thiometyl benzimidazole (Htmbmz):
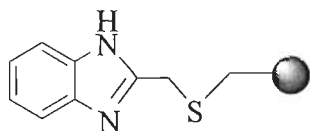
PS-S-tmbmz,**II**

(iii) Monobasic tridentate ONN donor ligand derived from 3-formyl salicylic acid and N,N-dimethylethylenediamine (H_2fsal-dmen):
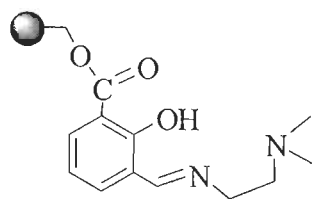
PS-Hfsal-dmen, **III**

(iv) Schiff base derived from 3-formyl salicylic acid and 2-(2-aminoethyl)pyridine (H_2fal-aepy):
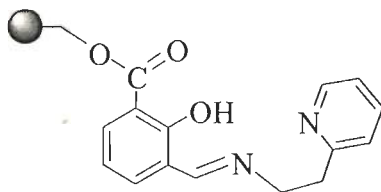
PS-Hfsal-aepy, **IV**

All synthesised complexes have been characterised by chemical, spectral (IR, electronic, EPR and NMR) and thermal studies, and scanning electron micrographs. Respective non-polymer bound complexes have also been prepared and characterised. Structures of some of the non-polymer bound complexes have been confirmed by single crystal X-ray study. Catalytic potentials of these complexes have been explored for the following oxidation reactions:

(a) Oxidation of methyl phenyl sulfide

(b) Oxidation of diphenyl sulfide

(c) Oxidation of benzoin

(d) Oxidation of styrene

(e) Oxidation of ethylbenzene

(f) Oxidation of cyclohexene

(g) Oxidative desulfurization

(h) Hydroamination of styrene and vinyl pyridine

Reaction conditions for all these catalytic reactions have been optimised considering various parameters to obtain best performance of the catalysts. Their recycle abilities have also been tested. Catalytic activities of these complexes have also been compared with the respective non-polymer bound complexes.

Chapter-2

Polystyrene bound oxidovanadium(IV) and dioxidovanadium(V) complexes of histamine derived ligand for the oxidation of methyl phenyl sulfide, diphenyl sulfide and benzoin

2.1. INTRODUCTION

The coordination chemistry of vanadium has received increasing attention of researchers, particularly after the discovery of vanadate dependent enzymes, vanadium haloperoxidases [213–219] from various sea algae and terrestrial fungi [220]. They are very active for the oxidative halogenation and oxidation of organic substrates in the presence of H_2O_2 [221, 222]. Various structural and functional models have been developed to understand the role of enzyme and mechanism of the reaction [223]. Generally these functional models are homogeneous in nature and decompose during the catalytic reaction and thus are not suitable for industrial applications. Encapsulation of monomeric complexes in microporous materials such as zeolites [224], and mesoporous materials e.g. MCM-41 [225–228], or their immobilisation onto polymer supports through covalent attachment are means to overcome this problem. Heterogenisations through encapsulation or immobilisation of homogeneous catalysts have advantages over their homogeneous counterparts due to the easy separation from the reaction mixture, leading to operational flexibility and their facile regenarability. Recently we have used chloromethylated polystyrene cross-linked with divinylbenzene, one of the most widely employed macromolecular supports [229–232], for immobilisation of model vanadium complexes and have tested their catalytic potential for a variety of oxidation reactions [76–78].

Herein we report the preparation and characterisation of chloromethylated polystyrene bound oxidovanadium(IV) and dioxidovanadium(V) complexes of Hsal–his (**2.I**), Scheme 2.1. The corresponding non-polymer-bound complexes of **2.I**, which are considered as structural models of haloperoxidases, have also been prepared. Spectral evidence is presented for peroxide binding, in the presence of H_2O_2, to the vanadium centre. Catalytic potential of these complexes has been demonstrated by studying the oxidation of methyl phenyl sulfide, diphenyl sulfide and benzoin.

Hsal-his (**2.I**)
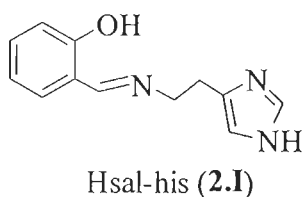
Scheme 2.1.

2.2. EXPERIMENTAL

2.2.1. Materials and methods

Chloromethylated polystyrene [18.9 % Cl (5.3 mmol Cl per gram of resin)] cross-linked with 5 % divinylbenzene was obtained as a gift from Thermax Limited, Pune, India. Analytical reagent grade V_2O_5, (Loba Chemie, India), 30 % H_2O_2, salicylaldehyde (Ranbaxy, India), histamine hydrochloride, methyl phenyl sulfide, diphenyl sulfide (Himedia, India, or Acros, UK), benzoin (SRL, India) and other chemicals were used as purchased. [VO(acac)$_2$] [233] and Hsal–his [234] were prepared according to the methods reported in the literature.

Elemental analyses of the ligands and complexes were obtained by an Elementar model Vario-EL-III. IR spectra were recorded as KBr pellets on a Nicolet NEXUS Aligent 1100 FT-IR spectrometer. Electronic spectra of the polymer-bound complexes were recorded in Nujol on a Shimadzu 1601 UV-Vis spectrophotometer by layering a mull of the sample on the inside of one of the cuvettes while keeping the other one layered with Nujol as reference. Spectra of non-polymer bound ligand and complexes were recorded in methanol. The EPR spectra were recorded with a Bruker ESP 300E X-band spectrometer. For the polymer-anchored complex samples the spectra were measured at room temperature and also at 77K after swelling in DMF; for the neat complexes the samples either in MeOH or DMF were frozen in liquid nitrogen, and the EPR spectra were measured at 77 K. The spin Hamiltonian parameters were obtained by simulation of the spectra with the computer program of Rockenbauer and Korecz [235]. The ^{51}V NMR spectra were recorded on a Bruker Avance II+ 400 Mhz (Ultrashield Magnet) instrument. Thermo gravimetric analyses of the complexes were carried out using Perkin Elmer (Pyris Diamond) under oxygen

atmosphere. The energy dispersive X-ray analyses (EDX) of anchored ligand and complexes were recorded on a FEI Quanta 200 FEG. The samples were coated with a thin film of gold to prevent surface charging, to protect the surface material from thermal damage by the electron beam and to make the sample conductive. The identity of the products was confirmed using a GC-MS Perkin-Elmer Clarus 500, and comparing the fragments of each product with the library available. A Thermax Nicolet gas chromatograph with a HP–1 capillary column (30 m × 0.25 μm × 0.25 μm) was used to analyse the reaction products, and their quantifications were made on the basis of the relative peak area of the respective product.

2.2.2. Syntheses of ligand and complexes

2.2.2.1. Polymer-anchored ligand, PS–Hsal–his (2.II)

Chloromethylated polystyrene (3.0 g) was allowed to swell in DMF (40 ml) for 2 h. A solution of Hsal–his (4.60 g, 25 mmol) in DMF (30 ml) was added to the above suspension followed by triethylamine (4.50 g) in ethylacetate (40 ml). The reaction mixture was heated at 90 °C for 15 h with slow mechanical stirring. After cooling to room temperature, the yellow resins were separated by filtration, washed thoroughly with hot DMF followed by hot methanol and dried in an air oven at 120 °C. Found: C, 74.40; H, 11.61; N, 9.41 %.

2.2.2.2. PS–[$V^{IV}O$(sal–his)(acac)] (2.1)

Polymer-anchored ligand PS–Hsal–his (2.00 g) was allowed to swell in DMF (25 ml) for 2 h. A solution of [VO(acac)$_2$] (5.30 g, 20 mmol) in 20 ml DMF was added to the above suspension and the reaction mixture was heated at 90 °C for 14 h with slow mechanical stirring. After cooling to room temperature, the dark black polymer-anchored complex was separated by filtration, washed with hot DMF followed by hot methanol and dried at 120 °C in an air oven. Found: C, 68.56; H, 10.24; N, 7.45; V, 8.89 %.

2.2.2.3. PS–[$V^{V}O_2$(sal–his)] (2.2)

Method A. A solution of KVO$_3$ was generated in situ by dissolving V$_2$O$_5$ (5.46 g,

30 mmol) in aqueous KOH (3.36 g, 60 mmol in 50 ml H_2O). PS–Hsal–his (2 g) was suspended in the above solution and stirred mechanically for ca. 48 h where colour of beads changed to orange. They were separated by filtration, washed with water followed by methanol and dried in desiccator. Found: C, 67.13; H, 9.12; N, 6.96; V, 8.41 %.

Method B. Complex, PS–[V^{IV}O(sal–his)(acac)] (**2.1**) (1.5 g) was suspended in methanol (40 ml) and air was bubbled through the suspension for *ca.* 4 days. During this period the colour of the beads slowly changed to orange. They were separated by filtration, washed with water followed by methanol and dried in a desiccator. Found: C, 67.10; H, 9.14; N, 6.94; V, 8.43 %.

2.2.2.4. [V^{IV}O(sal–his)(acac)] (2.3)

Complex **2.3** was prepared according to the reported procedure [234]. Yield 65 %. Found: C, 53.21; H, 5.54; N, 10.85; V, 12.83 %. Calcd. for $C_{18}H_{23}N_3O_5V$: C, 53.27; H, 5.78; N, 10.96; V, 13.29 %.

2.2.2.5. [V^{V}O$_2$(sal–his)] (2.4)

Complex **2.3** (0.383 g, 1 mmol) was dissolved in 50 ml of methanol and after addition of aqueous 30 % H_2O_2 (0.2 ml) air was gently passed through the solution for 4 days. During this period the V^{IV} in **2.3** completely oxidised and the solution became yellow. The yellow solid of **2.4** was obtained after reducing the solvent volume to ca. 5 ml, which was filtered and dried *in vacuo*. Yield 63 %. Found: C, 48.24; H, 3.96; N, 13.93; V, 16.42 %. Calcd. for $C_{12}H_{12}N_3O_3V$: C, 48.50; H, 4.07; N, 14.14; V, 17.14 %. ^{1}H NMR(DMSO-d$_6$, δ/ppm): 12.82 (s, 1H, -NH), 8.70 (s, 1H, -CH=N-), 8.07(s, 1H), 7.47(s, 1H), 7.37(s, 1H), 7.12(s, 1H), 6.74 (s, 1H), 6.72(d, 1H) (aromatic), 3.91(b, 4H, -CH$_2$). ^{51}V NMR (MeOD-d$_4$, δ/ppm): –547.

2.2.3. Catalytic activity studies

Oxidation of methyl phenyl sulfide, diphenyl sulfide and benzoin was carried out in 50 ml reaction flasks.

2.2.3.1.   Oxidation of methyl phenyl sulfide and diphenyl sulfide

Polymer-anchored catalyst, after swelling in methanol for 2 h, was used for the oxidation of methyl phenyl sulfide and diphenyl sulfide. Methyl phenyl sulfide (1.24 g, 10 mmol) or diphenyl sulfide (1.86 g, 10 mmol), 30 % aqueous H_2O_2 (1.71 g, 15 mmol), and catalyst (0.045 g) in 10 ml acetonitrile were stirred at room temperature and the reaction was monitored by withdrawing samples at different time intervals and analysing them quantitatively by gas chromatography. The identities of the products were confirmed by GC-MS. Various parameters such as amount of oxidant and catalyst were considered in order to study their effect on the reaction products.

2.2.3.2.   Oxidation of benzoin

In a typical oxidation reaction, benzoin (1.06 g, 5 mmol), aqueous 30 % H_2O_2 (1.71 g, 15 mmol) and catalyst (0.030 g) were mixed in 25 ml methanol. The reaction mixture was heated under reflux with stirring for 6 h. The progress of the reaction was monitored as mentioned above. The effect of various parameters such as temperature, amount of oxidant and catalyst were checked to optimise the conditions for the best performance of catalyst.

2.3. RESULTS AND DISCUSSION

2.3.1. Syntheses, reactivity and solid state characteristics

Reaction of Hsal–his with chloromethylated polystyrene, cross-linked with 5 % divinylbenzene in DMF in the presence of triethylamine gave the polymer-anchored ligand, PS–Hsal–his. The reaction was carried out at 90 °C. At this temperature the ligand did not decompose. Miller and Sherrington have used refluxing toluene to carry out the anchoring of 2-(2-pyridyl)imidazole through covalent attachment of imine nitrogen to chloromethylated polystyrene [87]. During this process the –NH group of histamine reacts with the –CH$_2$Cl group as shown in Scheme 2.2. The remaining chlorine content of 1.5 % (0.42 mmol Cl per gram of resin) in the PS-bound ligand suggests ~92 % loading of the ligand.

Hsal-his (**2.I**)   PS- [Hsal-his] (**2.II**)
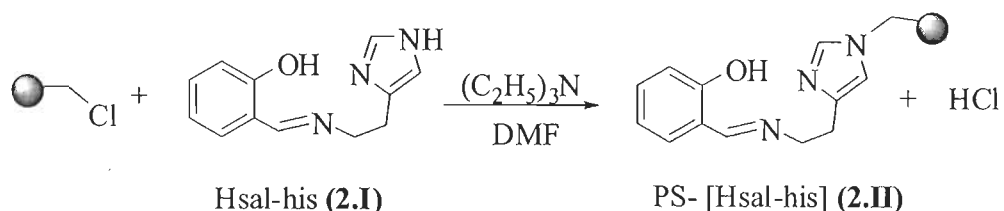
Scheme 2.2. Reaction of Hsal-his with chloromethylated polystyrene.

The anchored ligand on reaction with $[V^{IV}O(acac)_2]$ in DMF resulted in the formation of the oxidovanadium(IV) complex PS–$[V^{IV}O(sal–his)(acac)]$ (**2.1**). The chloromethylated group does not coordinate with vanadium precursor. Aerial oxidation of **2.1** in methanol is very slow but gave the dioxidovanadium(V) complex PS–$[V^{V}O_2(sal–his)]$ (**2.2**). Eqns. 1 and 2 summarise the synthetic procedures.

$$PS–Hsal–his + [V^{IV}O(acac)_2] \quad \rightarrow \quad PS–[V^{IV}O(sal–his)(acac)] \quad + Hacac \qquad (1)$$

$$2\ PS–[V^{IV}O(sal–his)(acac)] + \tfrac{1}{2}O_2 + H_2O \rightarrow 2\ PS–[V^{V}O_2(sal–his)] + 2Hacac \qquad (2)$$
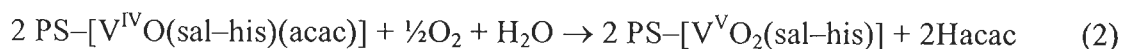
Table 2.1 provides data of metal and ligand loading in polymer-anchored complexes assuming the formation of PS–Hsal–his. The data show that metal to ligand ratio in polymer-bound complexes is close to 1 : 1.

Table 2.1. Ligand and metal loadings in polymer-bound complexes, and ligand-to-metal ratio data.

Compound	Ligand loading (mmol g^{-1} of resin)	Metal ion loading[a] (mmol g^{-1} of resin)	Ligand : Metal ratio
PS–[Hsal–his] (**2.I**)	2.24		
PS–[V^{IV}O(sal–his)(acac)](**2.1**)	1.66	1.74	1 : 0.95
PS–[V^{V}O$_2$(sal–his)] (**2.2**)	1.77	1.65	1 : 1.07

[a] Metal ion loading = $\dfrac{\text{Observed metal \%} \times 10}{\text{Atomic mass of metal}}$

44

The structure of non-polymer bound oxidovanadium(IV) complex **2.3** (refer to Scheme 2.5) has already been established by an X-ray single crystal study by Pecoraro and coworkers [234]. Aerial oxidation of **2.3** in the presence of a few drops of aqueous 30% H_2O_2 results in the formation of dioxidovanadium(V) complex **2.4**, which is now characterised by elemental and spectroscopic (IR, UV-vis, ^1H and ^{51}V NMR) studies. The corresponding polymer-bound complex **2.2** is proposed to have a similar binding mode.

2.3.2. Field emission-scanning electron microscope (FE-SEM) and energy dispersive X-ray aalyses (EDX) studies

Field emission scanning electron micrographs (FE-SEM) and energy dispersive X-ray aalyses (EDX) profiles for a single bead of polymer-bound ligand and the vanadium complexes were recorded to observe the morphological changes. Some of these images along with the energy dispersive X-ray aalyses (EDX) profile are reproduced in Fig. 2.1. As expected, the pure polystyrene bead has a smooth and flat surface while the polymer-bound ligand and complexes show a very slight roughening of the top layer. This roughening is more noticeable in complexes **2.1** and **2.2** possibly due to the interaction of vanadium with the polymer-bound ligand which results in the formation of complex with a fixed geometry. Accurate information on the morphological changes in terms of exact orientation of ligands coordinated to the metal ion has not been possible due to poor loading of the metal complex. However, pure polymer beads show mainly two components carbon (80.7 %) and chlorine (18.3 %) on the surface, as evaluated semi-quantitatively by energy dispersive X-ray aalyses. A considerable amount of N (ca. 8.1 %) and small amount of Cl (ca. 2.1 %), was determined on the surface of the beads containing bound ligand. The polystyrene beads of immobilised metal complexes PS–[V^{IV}O(sal–his)(acac)] and PS–[V^{V}O$_2$(sal–his)] also contain significant amount of metal along with nitrogen, suggesting the formation of metal complex with the anchored ligand at various sites.

(a)

PS–Hsal–his (2.II)

(b)
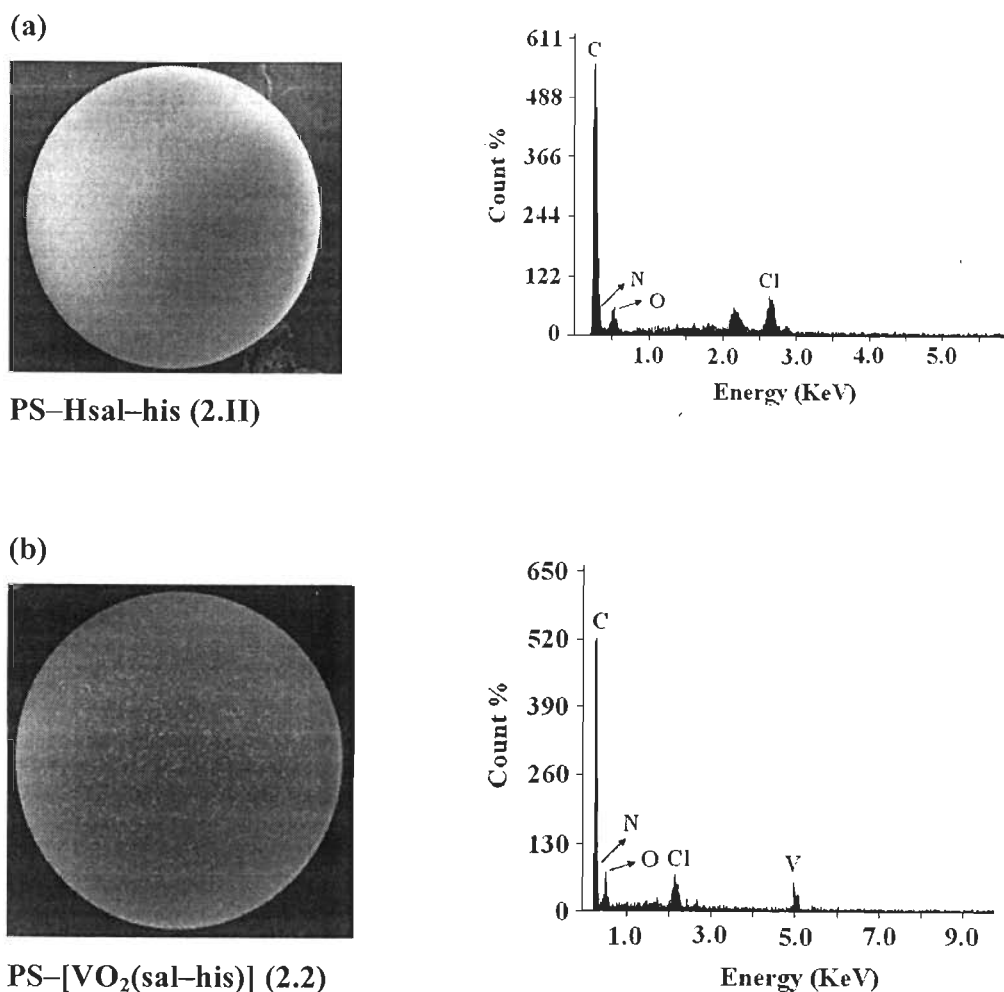
PS–[VO₂(sal–his)] (2.2)

Fig. 2.1. FE-SEM (left) and Energy dispersive X-ray aalyses (EDX) profile (right) of (a) PS–Hsal–his (**2.II**) and (b) PS–[V^{V}O$_2$(sal–his)] (**2.2**).

2.3.3. TGA study

Thermo gravimetric aalyses under an oxygen atmosphere shows the good stability of polymer-anchored complexes **2.1** and **2.2** up to *ca.* 200 °C and thereafter they decompose exothermically in several steps. Quantitative measurement of weight loss at various stages was not possible due to their overlapping nature. However, the residues due to the metal oxides obtained as the end product at ca. 850 °C (in **2.1**) and at ca. 500 °C (in **2.2**) indicate that the metal complexes are covalently bound to the

polymer. The decomposition of **2.1** is completed in four steps. Two overlapping steps occur in the temperature range 200 – 395 °C. At this stage the decomposed product is quite stable. The next weight loss starts at 725 °C and continues till the formation of end product. The observed residue of 29.8 % is close to the calculated value of 29.2 % for V_2O_5 at 850 °C. The first weight loss step in non-polymer bound complex **2.3** starts at ca. 200 °C and is completed at 290 °C with a weight loss of 42 %. The second weight loss step amounting to 7.6 % starts at ca. 290 °C and is completed at 375 °C. The final step starts at 375 °C and is completed at ca. 450 °C with a total weight loss of 68.7 %. The final residue of 31.3 % (Cal. 30.6 %) suggests the formation of V_2O_5 as the end product.

2.3.4. IR spectral study

A partial list of IR spectral data of the polymer-anchored ligand and complexes along with non-polymer bound ones are listed in Table 2.2. The Hsal–his (**2.I**) ligand exhibits a sharp band at 1632 cm^{-1} due to ν(C=N) (azomethine), and this band shifts to lower wavenumbers by 32 cm^{-1} (in **2.3**) and 21 cm^{-1} in **2.4** suggesting the coordination of azomethine nitrogen to the metal ion. The polymer-anchored ligand PS–Hsal–his (**2.II**) exhibits a sharp band at 1639 cm^{-1} due to the ν(C=N) stretch, and in the polymer-anchored complexes this band shows up at 1612–1617 cm^{-1}. This observation suggests the coordination of the azomethine nitrogen atom to the metal ion. The additional band observed at ca. 1630 cm^{-1} in all complexes is possibly due to coordination of the imidazole nitrogen atom.

The polymer-bound complex **2.1** exhibits a sharp band at 986 cm^{-1} due to ν(V=O) while **2.2** exhibits two such bands at 960 and 931 cm^{-1} corresponding to ν_{asym}(O=V=O) and ν_{sym}(O=V=O) modes, respectively [234]. As shown in Table 2.2, the corresponding non-polymer bound vanadium complexes display these bands at 945 cm^{-1} (in **2.3**), and at 927 and 895 cm^{-1} (in **2.4**) similarly to other examples reported in the literature [236].

Table 2.2.   IR spectral data of ligands and complexes

Compound	(C=N)	(V=O)
Hsal–his (**2.I**)	1632	-
[VO(acac)(sal–his)] (**2.3**)	1600	945
[VO$_2$(sal–his)] (**2.4**)	1611	927, 895
PS-Hsal–his (**2.II**)	1639	-
PS–[VO(acac)(sal–his)] (**2.1**)	1612	986
PS–[VO$_2$(sal–his)] (**2.2**)	1617	960, 931

2.3.5.   Electronic spectral study

The electronic spectral studies of Hsal–his and [V^{IV}O(sal–his)(acac)] have been described earlier in detail [234]. The electronic spectra of anchored and neat complexes are reproduced in Figs. 2.2 and 2.3, respectively. The electronic spectral patterns exhibited by the polymer-bound ligand and metal complexes are similar (Table 2.3) to those obtained for the corresponding non-polymer bound analogues, except for the low intensity of bands. The lower energy (less intense) bands appearing at 532 and 776 nm due to d – d transitions in [V^{IV}O(sal–his)(acac)] could not be located in the polymer-bound complex due to its poor loading in the polymer matrix. A band appearing at 394 nm in [V^{V}O$_2$(sal–his)] is assigned to a ligand-to-metal charge transfer (lmct) transition. Only a weak shoulder band could be observed in the polymer-bound dioxidovandium(V) complex in this region.

Table 2.3.   Electronic spectral data of ligands and complexes

Compounds	Solvent	λ_{max} / nm
Hsal–his (**2.I**)	Methanol	214, 254, 314, 402
[V^{IV}O(acac)(sal–his)] (**2.3**)	Methanol	215, 257, 277, 319, 384, 532, 776
[V^{V}O$_2$(sal–his)] (**2.4**)	Methanol	213, 253, 279, 322, 394
PS-Hsal–his (**2.II**)	Nujol	211, 229, 286, 330, 414
PS–[V^{IV}O(acac)(sal–his)] (**2.1**)	Nujol	209, 280, 329, 416
PS–[V^{V}O$_2$(sal–his)] (**2.2**)	Nujol	206, 276, 340, 390
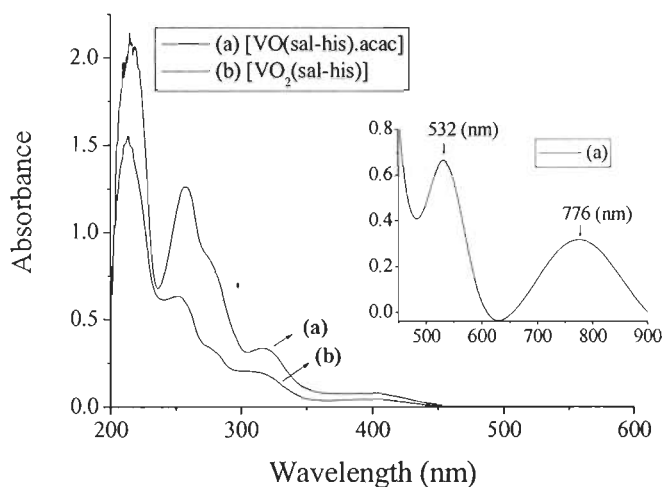
Fig. 2.2. Electronic spectra of neat metal complexes **2.3** and **2.4** in MeOH solution (ca. 10^{-4} M). The inset shows the spectrum of **2.3** in the visible range, recorded with a higher concentration of complex (ca. 10^{-3} M).
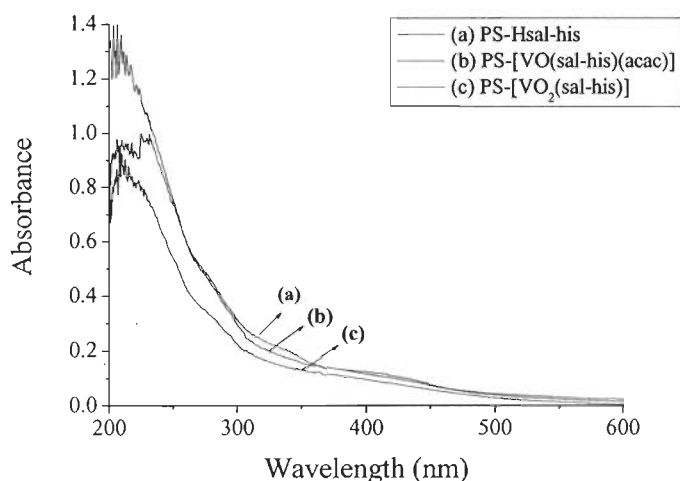
Fig. 2.3. Electronic spectra of polymer-anchored ligand and metal complexes dispersed in nujol mulls.

2.3.6. EPR Spectroscopy study

The 1st derivative EPR spectra have been recorded for "frozen" MeOH and DMF solutions of complex **2.3** and for **2.1** in the solid state at room temperature. The EPR spectra of **2.1** and **2.3** are shown in Fig. 2.4. The spectrum of **2.1** is characteristic

of magnetically diluted $V^{IV}O$-complex and the well resolved EPR hyperfine features indicate that the vanadium(IV) centers are well dispersed in the polymer matrix. Comparison with the spectra of **2.3** in MeOH and DMF indicates that the coordination environment of **2.1** and **2.3** are the same and as reported by Cornman *et al* [234]. The value of $A_\parallel$ can be estimated using the additivity relationship proposed by Wuethrich [237] and Chasteen [238], with estimated accuracy of $\pm 3 \times 10^{-4}$ cm^{-1}, and we do not expect any significant influence from the axial ligand [239]. The spectra were simulated and the spin Hamiltonian parameters obtained [235] are included in Table 2.4. By using the following partial contributions (O_{acac}, 37.6, $O_{phenolate}$, 38.9, N_{imine}, 41.6, N_{imid}, 45×10^{-4} cm^{-1})$_{equatorial}$, $(O_{acac})_{axial}$ [240], an estimated A$\parallel$ of 163.1 $\times 10^{-4}$ cm^{-1} is obtained. We can therefore conclude that the spectra are consistent with such a binding mode. The contribution of imidazole (N_{imid}) may depend on its orientation in respect to the V=O bond, ranges from 40 (parallel, best orbital overlap) to 45×10^{-4} (perpendicular) [240]. For the N_{imid} of ligand sal–his, taking into account the known molecular structure in the solid state [234]. We expect the imidazole ring to be positioned perpendicular to the V=O group, that a so a contribution close to 45×10^{-4} is predicted.
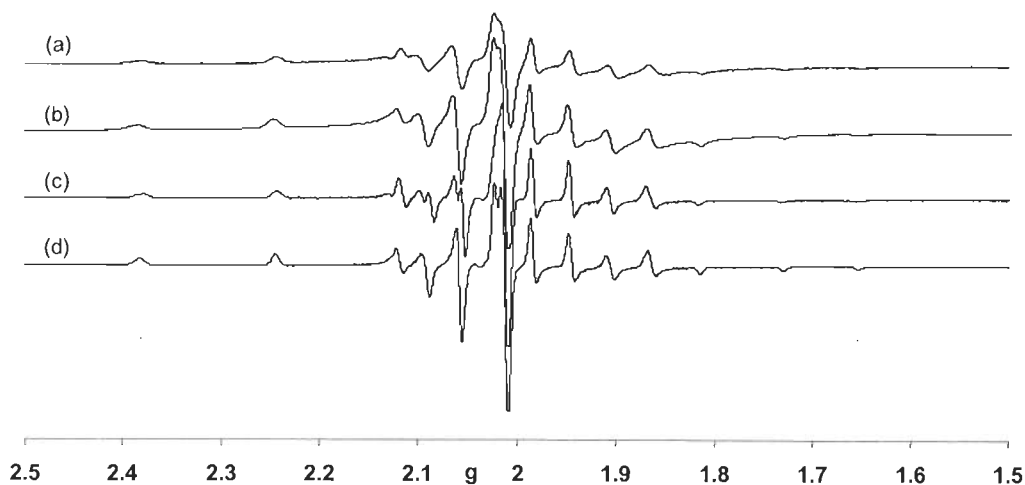
Fig. 2.4. 1st derivative EPR spectra of PS–[V^{IV}O(sal–his)(acac)]: (a) solid at room temperature, (b) in contact with DMF at 77K; and [VO^{IV}(sal–his)(acac)]: (c) in MeOH at 77K, (d) in DMF at 77K.

Table 2.4. Spin Hamiltonian parameters obtained from the experimental EPR spectra recorded the corresponding complexes dissolved in DMF

Complex	Solvent	$g_\parallel$	$A_\parallel$ $(\times 10^4 cm^{-1})$	$g_\perp$	$A_\perp$ $(\times 10^4 cm^{-1})$
PS–[V^{IV}O(sal–his)(acac)]	Solid	1.949	163.8	1.980	58.6
	DMF	1.952	164.8	1.980	57.5
[V^{IV}O(sal–his)(acac)]	MeOH	1.953	161.5	1.981	56.0
	DMF	1.954	161.5	1.980	55.7

2.3.7. Catalytic activity studies

The catalytic potential of the polymer-bound complexes **2.1** and **2.2** as well as their non-polymer bound analogues were explored for the oxidation of methyl phenyl sulfide, diphenyl sulfide and benzoin.

2.3.7.1. Oxidation of methyl phenyl sulfide and diphenyl sulfide

The oxidation of sulfides is catalysed by a variety of vanadyl [241–246], manganese [247, 248] and titanium complexes [249, 250]. Methyl phenyl sulfide and diphenyl sulfide have electron rich sulfur atoms which on electrophilic oxidation give sulfoxide, and upon further oxidation sulfone (see Scheme 2.3).
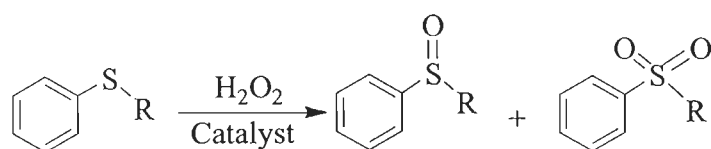
R = CH$_3$: Methyl phenyl sulfide
R = C$_6$H$_5$: Diphenyl sulfide

Scheme 2.3. Oxidation of Organic sulfides

Complexes PS–[V^{IV}O(sal–his)(acac)] (**2.1**) and PS–[V^{V}O$_2$(sal–his)] (**2.2**) have been used as catalysts for the oxidation of these sulfides by using aqueous 30 % H$_2$O$_2$. Reaction conditions have been optimised for the maximum oxidation of methyl

phenyl sulfide and diphenyl sulfide considering **2.2** as a representative catalyst while varying the amount of oxidant and catalyst.

The effect of the H_2O_2 concentration on the oxidation of methyl phenyl sulfide is illustrated in Fig. 2.5. Using three different concentrations of aqueous 30 % H_2O_2, *viz.* 10 mmol (1.14 g), 15 mmol (1.71 g) and 20 mmol (2.27 g) for fixed amounts of methyl phenyl sulfide (1.24 g, 10 mmol) and PS–[V^VO_2(sal–his)] (0.025 g) in CH_3CN (15 ml). The obtained conversions of methyl phenyl sulfide were 63.8, 93.8 and 96.3 %, respectively in 2 h of reaction time at room temperature. No appreciable improvement in the conversion is noted on increasing the oxidant to substrate molar ratios. Thus, the oxidant to substrate ratio of 1.5 : 1 may be considered as the most suitable at the expense of oxidant for the maximum oxidation of methyl phenyl sulfide.
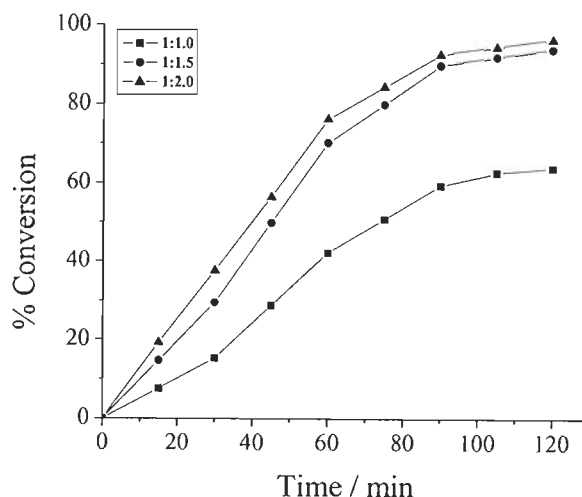
Fig. 2.5. Effect of amount of H_2O_2 on the oxidation of methyl phenyl sulfide. Reaction conditions: methyl phenyl sulfide (1.24 g, 10 mmol), PS-[VO_2(sal-his)] (0.025 g) in CH_3CN (15 ml).

For three different amounts *viz.* 0.015, 0.025 and 0.035 g of catalyst and methyl phenyl sulfide to H_2O_2 molar ratio of 1 : 1.5 under above reaction conditions, 0.015 g of catalyst gave only 75.0 % conversion. Increasing this amount to 0.025 g gave a conversion of 93.8 % while 0.035 g of catalyst has shown only slight

improvement in the conversion (Fig. 2.6). Thus, 0.025 g of catalyst was considered adequate to run the reaction under above conditions.
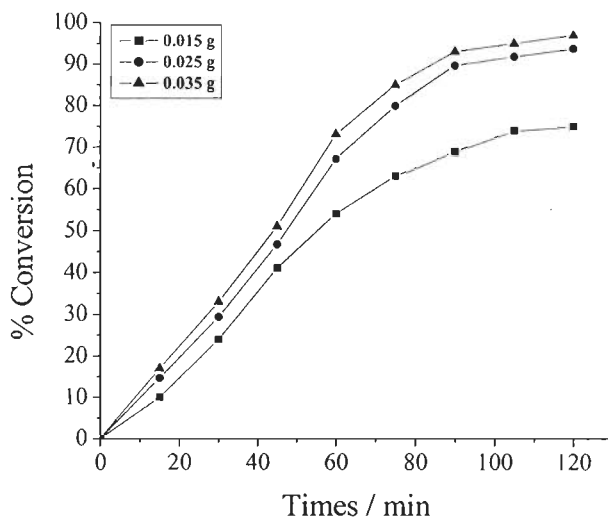
Fig. 2.6. Effect of amount of catalyst PS-[VO$_2$(sal-his)] on the oxidation of methyl phenyl sulfide. Reaction conditions: methyl phenyl sulfide (1.24 g, 10 mmol), H$_2$O$_2$ (1.71 g, 15 mmol) in CH$_3$CN (15 ml).

Thus, the optimised reaction conditions obtained for the maximum oxidation of 10 mmol of methyl phenyl sulfide are: catalyst (0.025 g), H$_2$O$_2$ (1.71 g, 15 mmol) and CH$_3$CN (15 ml). At least 2 h are required to complete the reaction. Similarly for 10 mmol of diphenyl sulfide, 0.045 g of catalyst and H$_2$O$_2$: diphenyl sulfide molar ratio of 3 : 1 in 15 ml of acetonitrile was found to be the best to give a maximum of 83.4 % conversion of diphenyl sulfide in 3 h of reaction time at room temperature. Catalyst, PS–[V^{IV}O(sal–his)(acac)] (**2.1**), under the above reaction conditions gave lower conversion (Table 2.5) for methyl phenyl sulfide as well as for diphenyl sulfide. Selectivity details for the products obtained for the oxidation of methyl phenyl sulfide and diphenyl sulfide are presented in Table 2.5. It is clear from the table that catalyst PS–[V^{V}O$_2$(sal–his)] has good catalytic potential for both substrates with high turn over frequency. But the selectivity for the formation of methyl phenyl sulfoxide is better (71.8 %) than for diphenyl sulfoxide (63.7 %).

Table 2.5. Conversion of sulfides, TOF and product selectivity data

Substrate[a]	Catalyst	Conv. (%)	TOF[b] (h⁻¹)	% Selectivity	
				Sulfoxide	Sulfone
Mps	PS–[V^{V}O$_2$(sal–his)	93.8	113.8	63.7	36.3
	[V^{V}O$_2$(sal–his)]	84.8	96.4	61.0	39.0
	PS–[V^{IV}O(sal–his)(acac)]	79.5	91.2	64.8	35.2
	[V^{IV}O(sal–his)(acac)]	72.1	83.3	62.9	37.1
Dps	PS–[V^{V}O$_2$(sal–his)]	83.4	37.5	71.8	28.2
	[V^{V}O$_2$(sal–his)]	70.7	30.2	67.8	32.2
	PS–[V^{IV}O(sal–his)(acac)]	67.4	28.7	73.1	26.9
	[V^{IV}O(sal–his)(acac)]	60.3	19.8	68.9	31.1

[a] Mps = methyl phenyl sulfide; Dps = diphenyl sulfide.

[b] TOF values in moles of product per mole of catalyst.

The catalytic activity of non-polymer bound complexes [V^{V}O$_2$(sal–his)] and [V^{IV}O(sal–his)(acac)] using the same mole concentration as used for the polymer-anchored complexes under reaction conditions established above has also been tested for comparison. Comparative profiles for the conversion of methyl phenyl sulfide and diphenyl sulfide using neat as well as polymer-bound complexes are also presented in Table 2.5 and Fig. 2.7. As shown in figure, conversions of both sulfides using neat complex are also very good, but always lower than their polymer-bound analogues. The selectivity of the formation of the corresponding sulfoxide is also lower with neat complex (Table 2.5). Blank reactions taking methyl phenyl sulfide (1.24 g, 10 mmol), aqueous 30 % H$_2$O$_2$ (1.71 g, 15 mmol) and acetonitrile (15 ml) resulted in 15.2 % conversion with selectivity sulfoxide : sulfone of 68 : 32. Blank reactions for diphenyl sulfide under above reaction conditions gave only 5.5 % conversion with selectivity sulfoxide : sulfone of 57 : 43.
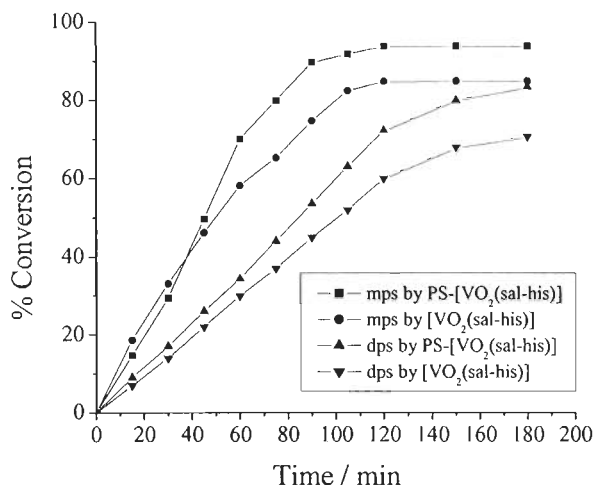
Fig. 2.7. Catalytic comparison of catalysts for the oxidation of methyl phenyl sulfide (mps) and diphenyl sulfide (dps).

2.3.7.2. Oxidation of Benzoin

The selective oxidation of α-hydroxyketones to α-diketones is one of the important reactions in fine chemical syntheses [251–255]. The oxidation of benzoin has attracted attention of researchers because one of its oxidised products, benzil, is a very useful intermediate for the syntheses of heterocyclic compounds and benzylic acid rearrangement [256]. Here, the oxidation of benzoin was successfully achieved with the catalyst PS–[V^VO_2(sal–his)] **(2.2)** using 30 % aqueous H_2O_2 as oxidant. Before starting the catalytic run, the catalyst was allowed to swell in methanol for 2 h, so that the substrate and oxidant can easily approach to the active sites of the catalyst in polymer cavity. The products mainly obtained were benzil, methylbenzoate, benzoic acid and benzaldehyde-dimethylacetal (Scheme 2.4).
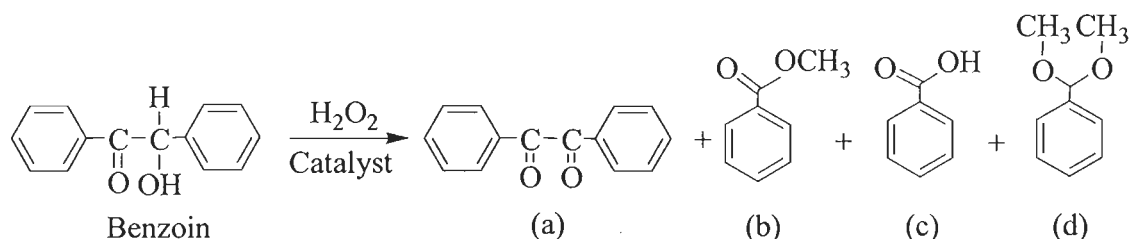
Scheme 2.4. Oxidised products of benzoin; (a) benzyl, (b) methyl benzoate, (c) benzoic acid and (d) benzaldehyde-dimethylacetal.

To optimise the reaction conditions for the maximum oxidation of benzoin, the effect of oxidant was studied by considering oxidant to substrate ratios of 2 : 1, 3 : 1 and 4 : 1for the fixed amount of catalyst (0.030 g) and substrate (1.06 g, 5 mmol) in 25 ml of refluxing methanol. Fig. 2.8 presents the conversion obtained as a function of time in each case. As shown in Fig. the conversion increases from 70.4 % to 91.2 % on increasing the oxidant to substrate ratios from 2 : 1 to 3 : 1in 6 h of reaction time. Further increment of H_2O_2 marginally affects on the net oxidation of benzoin. At the substrate to oxidant ratio of 1:3, where maximum conversion of benzoin was achieved, the selectivity of the formation of cleavage product methyl benzoate decreased from 38.2 % to 35.6 % and that of benzaldehyde-dimethylacetal reduced from 24 % to 18 %. Excess oxidant has also increased the selectivity of benzoic acid from 7.6 % to 17.9 %, while the formation of benzil decreased from 28.6 % to 26.3 %.
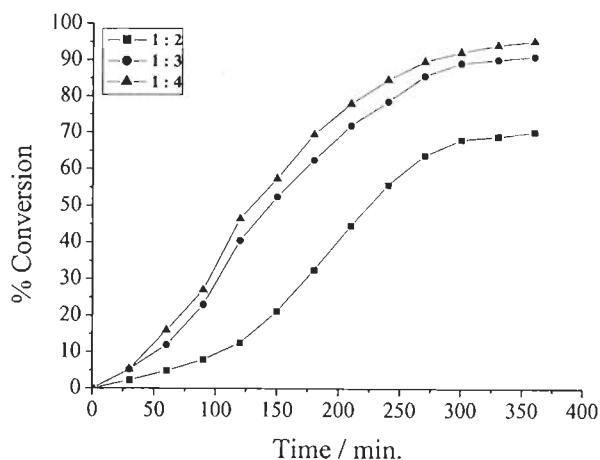
Fig. 2.8. Effect of H_2O_2 on the oxidation of benzoin. Reaction conditions: benzoin (1.06 g, 5 mmol), catalyst (0.03 g) in methanol (25 ml).

Fig. 2.9 illustrates the effect of the amount of catalyst on the rate of oxidation as a function of time. Similarly, among four different amounts of catalysts e.g. 0.015, 0.030, 0.050 and 0.070 g for the fixed amount of benzoin (1.06 g, 5 mmol) and 30 % H_2O_2 (1.7 g, 15 mmol) in 25 ml of methanol at the reflux temperature, the oxidation of benzoin was slow for the first 1.5 h with 0.015 g of catalyst, then reached 71.8 % in

ca. 6 h. Increasing the catalyst amount to 0.030 g resulted in significant improvement; here the conversion reached 91.2 % within 6 h of reaction time, followed by no further improvement with time. Further increment of catalyst amount to 0.050 or 0.070 g did not show considerable improvement either in the oxidation of benzoin or in the reduction in time to reach the steady state in the reaction processes.
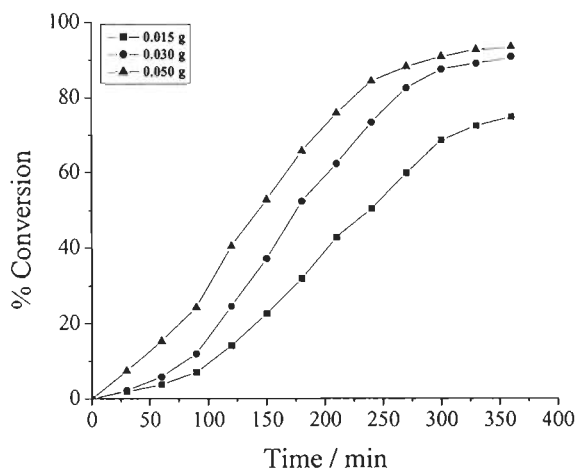
Fig. 2.9. Effect of catalyst amount on the oxidation of benzoin. Reaction conditions: benzoin (1.06 g, 5 mmol), H_2O_2 (1.71 g, 15 mmol) in methanol (25 ml).

Fig. 2.10 presents the selectivity of products along with the conversion of benzoin as a function of time (6 h) under the best suited experimental conditions as concluded above, i.e. benzoin (1.10 g, 5 mmol), 30 % H_2O_2 (1.7 g, 15 mmol), PS–[V^VO_2(sal–his)] (0.030 g, 0.014 mmol) and methanol (25 ml). It is clear from the plot that all products (four identified and one unidentified) form from the conversion of benzoin. With the highest selectivity of benzil (ca. 50 %) at the beginning, a continuous but slow decrease with time of its selectivity has been observed which finally reaches 30.5 % after 6 h. The selectivity of benzoic acid and benzaldehyde-dimethylacetal only marginally increases while that of methyl benzoate increases considerably from 15 to 37 %. Thus, with the maximum benzoin oxidation of 91.2 % after 6 h of reaction time, the selectivity of the reaction products varies in the order: methyl benzoate (37.0 %) > benzil (30.5 %) > benzaldehyde-dimethylacetal (22.5 %) > benzoic acid (8.1 %).

The catalytic activity of PS–[$V^{IV}O$(sal–his)(acac)] (**2.1**) is not so good giving 83.4 % conversion of benzoin, the selectivity of the different products being nearly the same. The performance of neat complexes using the same mole concentrations as used for polymer-anchored complexes has also been studied under the above optimised conditions. Thus, 0.0048 g (0.01615 mmol) of catalyst [V^VO_2(sal–his)] (**2.4**) was added to a mixture of benzoin (1.10 g, 5 mmol) and 30 % H_2O_2 (1.7 g, 15 mmol) in 25 ml of methanol, and the reaction products were analysed as a function of time. It was observed that the neat catalyst is also very active and gave 76.4 % conversion in 6 h of reaction time. Here, selectivity of the various products varies in the order: methylbenzoate (36.8 %) > benzil (27.8 %) > benzaldehyde-dimethylacetal (19.6 %) > benzoic acid (13.2 %) i.e. the same order as obtained for the polymer-bound catalyst. A maximum of 70.7 % conversion has been obtained with [$V^{IV}O$(sal–his)(acac)] (**2.3**) with similar selectivity under above conditions. The turns over frequencies for the polymer-anchored complexes are 14.1 (for **2.1**) and 15.4 (for **2.2**) and are higher than those obtained for the non-polymer-bound complexes. Moreover, the easy removal of the polymer-bound catalysts makes them better compared with their non-polymer-bound analogues.
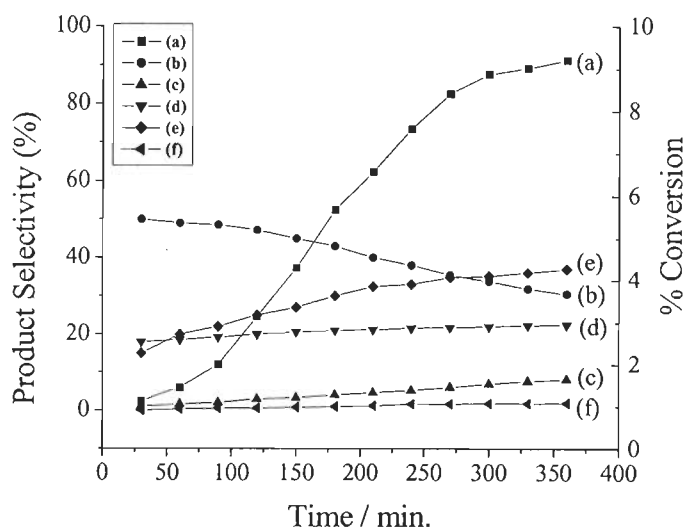
Fig. 2.10. Time vs. Product selectivity distribution plot for the conversion of benzoin (a) using PS–[V^VO_2(sal–his)] as a catalyst. (b) benzil, (c) benzoic acid, (d) benzaldehyde-dimethylacetal, (e) methyl benzoate and (f) others (non-identified).

Table 2.6. Percent conversion of benzoin and selectivity of various oxidation products.

Catalyst	Conv. (%)	Product selectivity (%)[a]					TOF/ h^{-1}
		a	b	c	d	Others	
PS–[V^{V}O$_2$(sal–his)]	91.2	30.5	8.1	22.5	37.0	1.9	15.4
[V^{V}O$_2$(sal–his)]	76.4	27.8	13.2	19.6	36.8	2.6	12.2
PS–[V^{IV}O(sal–his)(acac)]	83.4	31.2	5.8	23.4	37.5	2.1	14.1
[V^{IV}O(sal–his)(acac)]	70.7	29.5	12.2	20.2	35.2	2.3	11.3

[a] For details of abbreviations see Scheme 2.4.

2.3.8. Reactivity of non-polymer bound complexes with H$_2$O$_2$

Solutions of [V^{IV}O(sal–his)(acac)] (**2.3**) in methanol are sensitive towards addition of H$_2$O$_2$, as monitored by electronic absorption spectroscopy, yielding oxoperoxo species. Fig. 2.11 presents the spectral changes observed for **2.3**. Thus, the progressive addition of a dilute H$_2$O$_2$ solution in methanol to a solution of [V^{IV}O(sal–his)(acac)] in methanol results first in flattening of the band appearing at 776 nm; upon further addition of one drop portions of the H$_2$O$_2$ solution this band disappears. The intensity of the 532 nm band slowly increases, while the band at 382 nm gradually shifts to 394. At the same time new bands appear at 319 and 257 nm, while the intensity of the 265 nm band also increases. These changes indicate the interaction of [V^{IV}O(sal–his)(acac)] with H$_2$O$_2$ in methanol. The disappearance of d–d bands is in accordance with the oxidation of the V^{IV}O-complex to an oxoperoxovanadium(V), and the band appearing at ca. 425 nm is probably due to a LMCT band of the monoperoxo complex.

The spectral changes during a similar titration of **2.4** with H$_2$O$_2$ (diluted in methanol) in methanol is shown in Fig. 2.12. With low amounts of H$_2$O$_2$ added no appreciable changes in band positions were observed, but further additions of H$_2$O$_2$ yielded a final spectrum which is very similar to that obtained in the titration of [V^{IV}O (sal–his)(acac)] (**2.3**) with H$_2$O$_2$, thus demonstrating that the same oxoperoxovanadium(V) species form upon addition of H$_2$O$_2$ to methanolic solutions

of either **2.3** or **2.4**. Upon further additions of H_2O_2 (2 mmol of 30 % H_2O_2 dissolved in 5 ml of methanol), the band appearing at 322 nm slowly disappears with band tailing, this possibly being due to the formation of a diperoxo species.
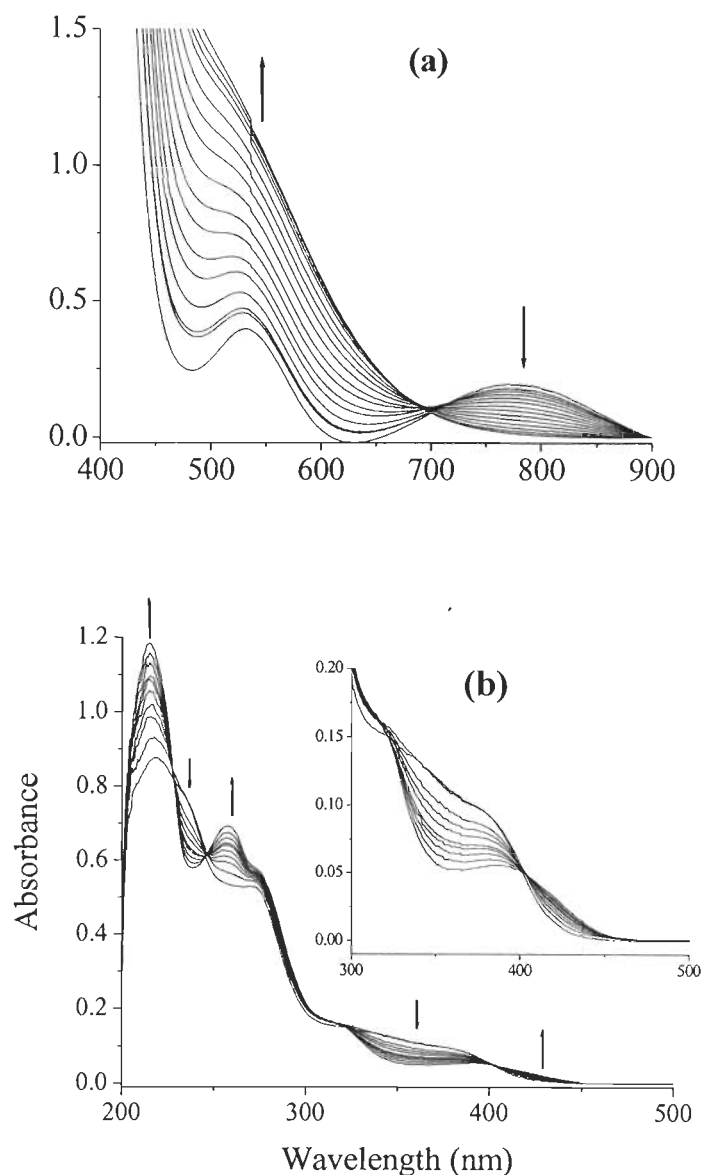
Fig. 2.11. UV-Vis spectral changes observed during titration of [VO(sal–his)(acac)] **(2.3)** with H_2O_2. (a) The spectra were recorded after successive additions of one drop portions of H_2O_2 (6.6×10^{-4} mmol of 30 % H_2O_2 dissolved in 10 ml of methanol) to 50 ml of ca. 10^{-3} M solution of **2.3** in methanol. (b) The equivalent titration, but with lower concentrations of a [$V^{IV}O$(sal–his)(acac)] **(2.3)** solution (ca. 10^{-4} M); the inset

60

shows an enlargement of the 300 – 500 nm region.
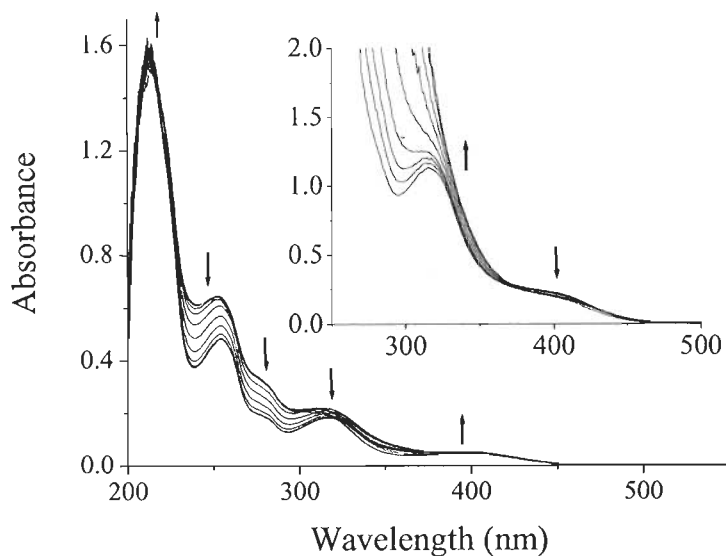
Fig. 2.12. Spectral changes observed during titration of [V^{V}O$_2$(sal–his)] (**2.4**) with H$_2$O$_2$. The spectra were recorded after successive additions of one drop portions of H$_2$O$_2$ (6.6×10^{-4} mmol of 30 % H$_2$O$_2$ dissolved in 10 ml of methanol) to 50 ml of ca. 10^{-4} M solution of **2.4** in methanol. The inset shows the equivalent titration, but with higher concentration of [V^{V}O$_2$(sal–his)] (ca. 10^{-3} M) with one drop portions of H$_2$O$_2$ (2 mmol of 30% H$_2$O$_2$ dissolved in 5 ml of methanol).

Stepwise addition of 2 equiv H$_2$O$_2$ (0.5, 1, 1.5 and 2 equiv) to a methanolic solution of **2.3** leads to slight increments of $A_\parallel$ from 161.8 to 164 ×10^4 cm^{-1}, suggesting some change in the coordination/ solvation environment of **2.3** (Fig. 2.13). Simultaneously the intensity of the spectrum decreases, and after the addition of the 2 equiv of H$_2$O$_2$ the EPR intensity becomes ca. 1/5th of that of the initial solution. The ^{51}V NMR of these solutions confirmed the presence of compound **2.4** (and also **2.5**, see below) Subsequent addition of 2 equiv methyl phenyl sulfide originated spectra with the same values of g and A parameters, the EPR signal increasing to ~50 % of that of the initial solution, indicating the reversibility of the redox process occurring

during the catalytic reaction.
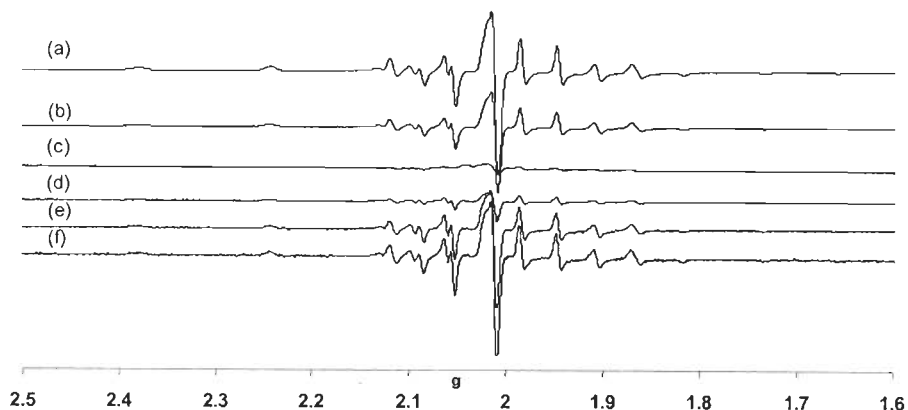
Fig. 2.13. Treatment of compound **2.3** with 30 % H_2O_2 followed by the addition of methyl phenyl sulfide; (a) in MeOH; (b) 0.5 eq. H_2O_2; (c) 2.0 eq. H_2O_2; (d) 1.0 eq. methyl phenyl sulfoxide; (e) 2.0 eq. methyl phenyl sulfoxide; (f) 2.0 eq. methyl phenyl sulfoxide (after 20 h) at 77K.

The V^V-system was also investigated by using ^{51}V NMR spectroscopy to detect intermediate species formed during the catalytic cycle with both **2.3** and **2.4**, choosing the oxidation of methyl phenyl sulfide as a model reaction. Complex **2.4** in methanolic solution (3 mM) shows one strong resonance at $\delta = -547$ ppm which we assign to $[V^VO_2(sal–his)]$ (**2.4**). This solution displays another minor (2.3 %) signal at $\delta = -558$ ppm (Fig. 2.14a). Both values are expected for V^VO_2-complexes having a O/N donor set [257]. We tentatively assign the -558 ppm peak to the dioxidovanadium(V) species $[V^VO_2(sal–his)(MeOH$ or $H_2O)]$ (**2.5**).

Upon successive additions of 30 % H_2O_2 (0.5 equiv steps) the relative intensity of the $\delta = -547$ ppm resonance decreases, and after the addition of 1.5 equiv of H_2O_2, a peak is detected at $\delta = -579$ ppm, which we assign to $[V^VO(O)_2(sal–his)]$ (**2.6**). These observations are in agreement with the UV-Vis data discussed above.

This reaction mixture was divided into two portions. In the first portion, upon addition of methyl phenyl sulfide, the peroxovanadium(V) species **2.6** is disappeared immediately, with concomitant production of **2.4** (Fig. 2.14e), indicating that **2.6** is one of the relevant species in the reaction with the sulfide. The final ^{51}V NMR spectrum was identical to the initial spectrum of **2.4**, but the global intensity of the

^{51}V NMR signals decreased.
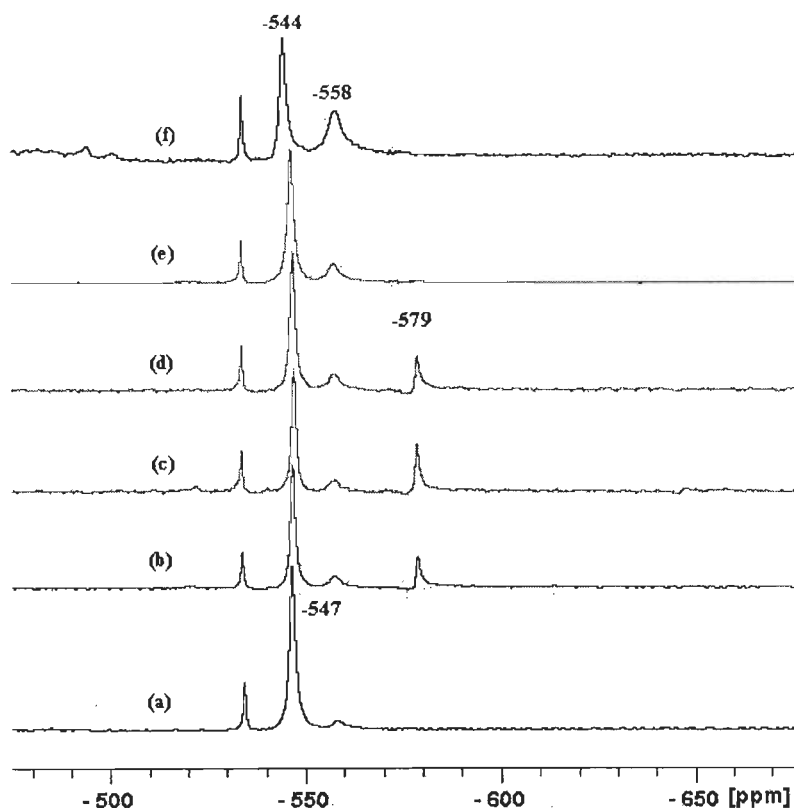
Fig. 2.14. ^{51}V NMR spectra for [V^{V}O$_2$(sal–his)] **(2.4)**: (a) in MeOH, (b) 0.5 equiv H$_2$O$_2$; (c) 1.5 equiv H$_2$O$_2$; (d) 1.0 equiv methyl phenyl sulfide; (e) 2.0 equiv methyl phenyl sulfide; (f) after 20 h. All spectra were recorded including an external reference of aqueous vanadate at pH ~12 (peak at ca. –536 ppm).

The second portion of the reaction mixture (Fig. 2.15e) after ca. 20 h gave only one intense signal corresponding to **2.4**, indicating that formation of monoperoxovanadium(V) was reversible. Addition of 0.5 equiv H$_2$O$_2$ generated again the signal corresponding to [V^{V}O(O)$_2$(sal–his)] **(2.6)**, along with a new signal at δ = –729 ppm (spectrum f in Fig. 2.15). We tentatively assign this signal as due to the formation of bisperoxovanadium imidazole mono anion, [V^{V}O(O$_2$)$_2$(sal–his)]$^-$ **(2.10)** (see Scheme 2.5), with the sp^2 nitrogen atom of imidazole coordinated to the vanadium center, which is consistent with previously reported chemical shifts for similar coordination modes [257, 258–261, 262].

63

Another possibility for this peak is the formation of $H_xVO_2(O_2)_2^{(3-x)-}$[263]. On further addition of 0.5 equiv H_2O_2 three new signals at $\delta = -715$ ppm (**2.11**), -668 ppm (**2.12**) and -648 ppm (**2.13**) are detected (spectrum g in Fig. 2.15), which increase intensity upon new additions of 0.5 equiv H_2O_2 (spectra h and i in Fig. 2.15) and correspond to various types of peroxo complexes (tentative assignments are presented in Scheme 2.5).

The addition of methyl phenyl sulfide to the same reaction mixture resulted in the disappearance of the peaks of **2.6**, **2.10**, **2.11**, **2.12** and **2.13** (spectrum l in Fig. 2.15 and Scheme 2.5). The fact that a ^{51}V NMR spectrum similar to the initial one (the solution of **2.4** in MeOH) is now obtained, confirms the reversibility of the processes involving complex **2.4**, namely the regeneration of **2.4** after the addition of H_2O_2 , formation of an oxoperoxo complex and its reaction with the sulfide.
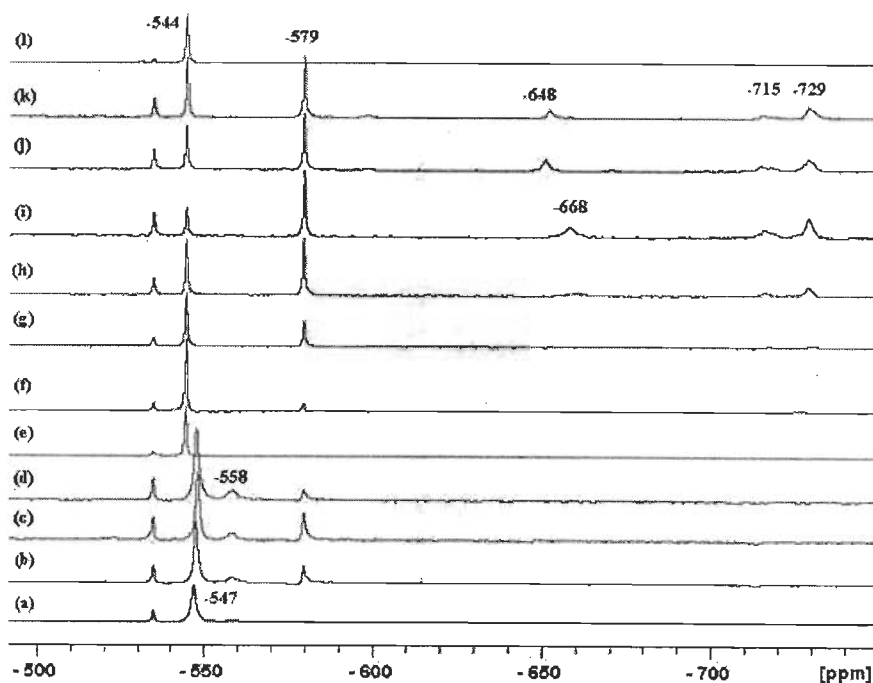
Fig. 2.15. ^{51}V NMR spectra for [V^VO_2(sal–his)] (**2.4**): (a) in MeOH; (b) 0.5 eq. H_2O_2; (c) 1.0 eq. H_2O_2; (d) 1.5 eq. H_2O_2; (e) after 20 hr; (f) 0.5 eq. H_2O_2; (g) 1.0 eq. H_2O_2; (h) 1.5 eq. H_2O_2; (i) 2.0 eq. H_2O_2; (j) 1.0 eq. methyl phenyl sulfide; (k) 2.0 eq. methyl phenyl sulfide; (l) 2.0 eq. methyl phenyl sulfide (after 24 hr). All spectra were recorded including an external reference of aqueous vanadate at pH ~12 (peak at ca. −536 ppm).

Solutions of **2.4** in methanol are also sensitive to pH changes, and were also monitored by ^{51}V NMR spectroscopy. Addition of 1 equiv HCl to a methanolic solution of **2.4** resulted in a reduction in intensity of the $\delta = -547$ ppm and $\delta = -558$ ppm peaks, while a new signal at $\delta = -524$ ppm was detected (Fig. 2.16). Further addition of 1 equiv of HCl gave a spectrum with only one intense signal at $\delta = -524$ ppm. We assign this to the protonation of the imidazole N atom, the sal–his ligand becoming bidentate and the solvent also coordinating [V^VO_2(sal-Hhis)(MeOH)] ($\delta = -524$ ppm) **2.7** (see Scheme 2.5). A rather similar explanation was given by Pecoraro and coworkers [234] for the $V^{IV}O$ with the same ligand system.

As compound **2.3** is paramagnetic, no signal was observed by ^{51}V NMR spectroscopy when dissolved in methanol. However, after addition of 0.5 equiv H_2O_2, three signals ($\delta = -494, -547$ and -558 ppm) appear (Fig. 2.17), and we tentatively assign them to [$V^VO(OH)$(sal-Hhis)(MeOH)] ($\delta = -494$ ppm) **(2.8)**, [V^VO_2(sal–his)] ($\delta = -547$ ppm) **(2.4)** and {[V^VO_2(sal–his)(MeOH)] ($\delta = -558$ ppm) **(2.5)**. Upon further addition of 0.5 equiv of H_2O_2 another three signals at: $\delta = -579, -524$ and -572 ppm were detected, which we tentatively assign as [$V^VO(O_2)$(sal–his)] ($\delta = -579$ ppm) **(2.6)**, {[V^VO_2(sal-Hhis)(MeOH)] ($\delta = -524$ ppm) **(2.7)** and [$V^VO(O_2)$(sal-Hhis)]$^+$ ($\delta = -572$ ppm) **(2.9)**. Further addition of 0.5 equiv H_2O_2 originated the formation of the peak at -729 ppm (see above), and [$VO(O_2)_2(H_2O)$(MeOH)]$^-$ ($\delta = -648$ ppm) **(2.13)**.

Upon addition of methyl phenyl sulfide (spectra h-j in Fig. 2.17), the monoperoxovanadium(V) and bisperoxovanadium(V) species are consumed, and the final ^{51}V NMR spectrum showed only two major signals identical to the initial spectrum of methanolic solutions of **2.4**, showing that the V^V-catalyst is regenerated after the consumption of H_2O_2. Besides having an easily measurable ^{51}V NMR spectrum, for this solution a reasonably intense EPR spectrum was also recorded. This confirmed the formation of **2.3**, and even after 5 days a similar EPR spectra could be obtained.

In Scheme 2.5, we summarise our observations regarding the reaction processes involving **2.3** and **2.4** in MeOH solutions, as measured by ^{51}V NMR and EPR spectroscopy.
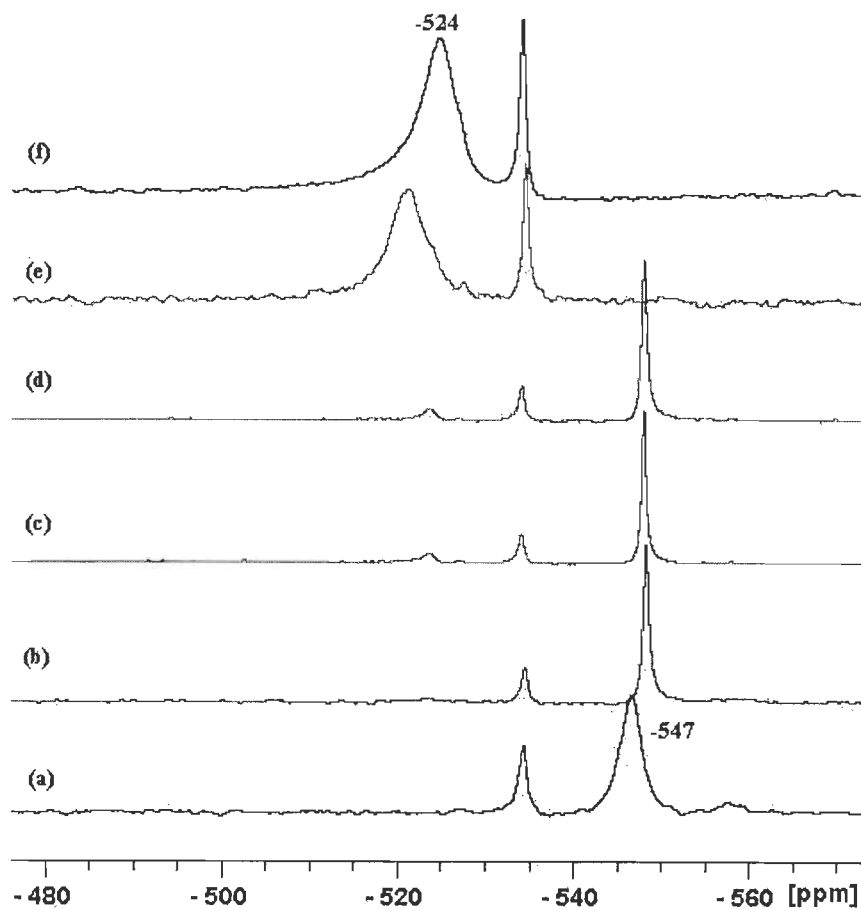
Fig. 2.16. ^{51}V NMR spectra for [V^{V}O$_2$(sal–his)]: (a) in MeOH, (b) 0.5 equiv HCl; (c) 1.0 equiv HCl; (d) 1.5 equiv HCl; (e) 2.0 equiv HCl; (f) 2.5 equiv HCl. All spectra were recorded including an external reference of aqueous vanadate at pH ~12 (peak at ca. −536 ppm).
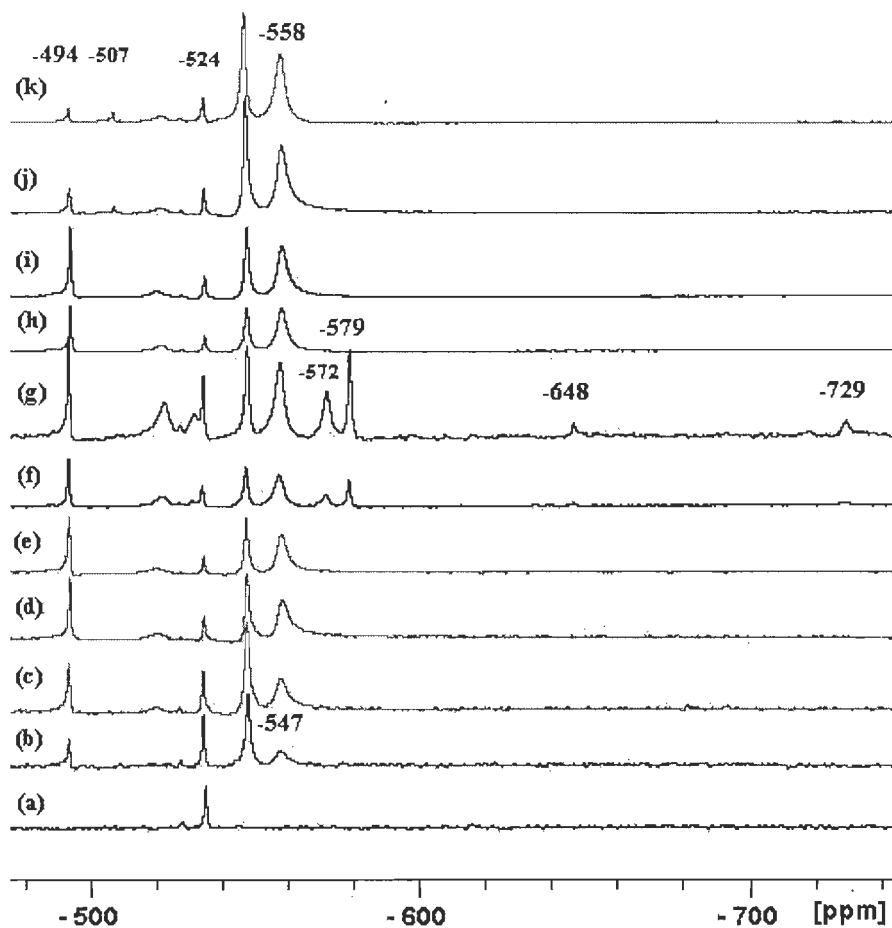
Fig. 2.17. ^{51}V NMR spectra for [V^{IV}O(sal–his)(acac)] (**2.3**): (a) in MeOH, (b) 0.5 eq. H$_2$O$_2$; (c) 1.0 eq. H$_2$O$_2$; (d,e) 1.5 eq. H$_2$O$_2$; (f) 2.0 eq. H$_2$O$_2$; (g) 2.5 eq. H$_2$O$_2$; (h) 1.0 eq. methyl phenyl sulfide; (i) 2.0 eq. methyl phenyl sulfide; (j) 3.0 eq. methyl phenyl sulfide (k) 3.0 eq. methyl phenyl sulfide (after 24 hr). All spectra were recorded including an external reference of aqueous vanadate at pH ~12 (peak at ca. -536 ppm).
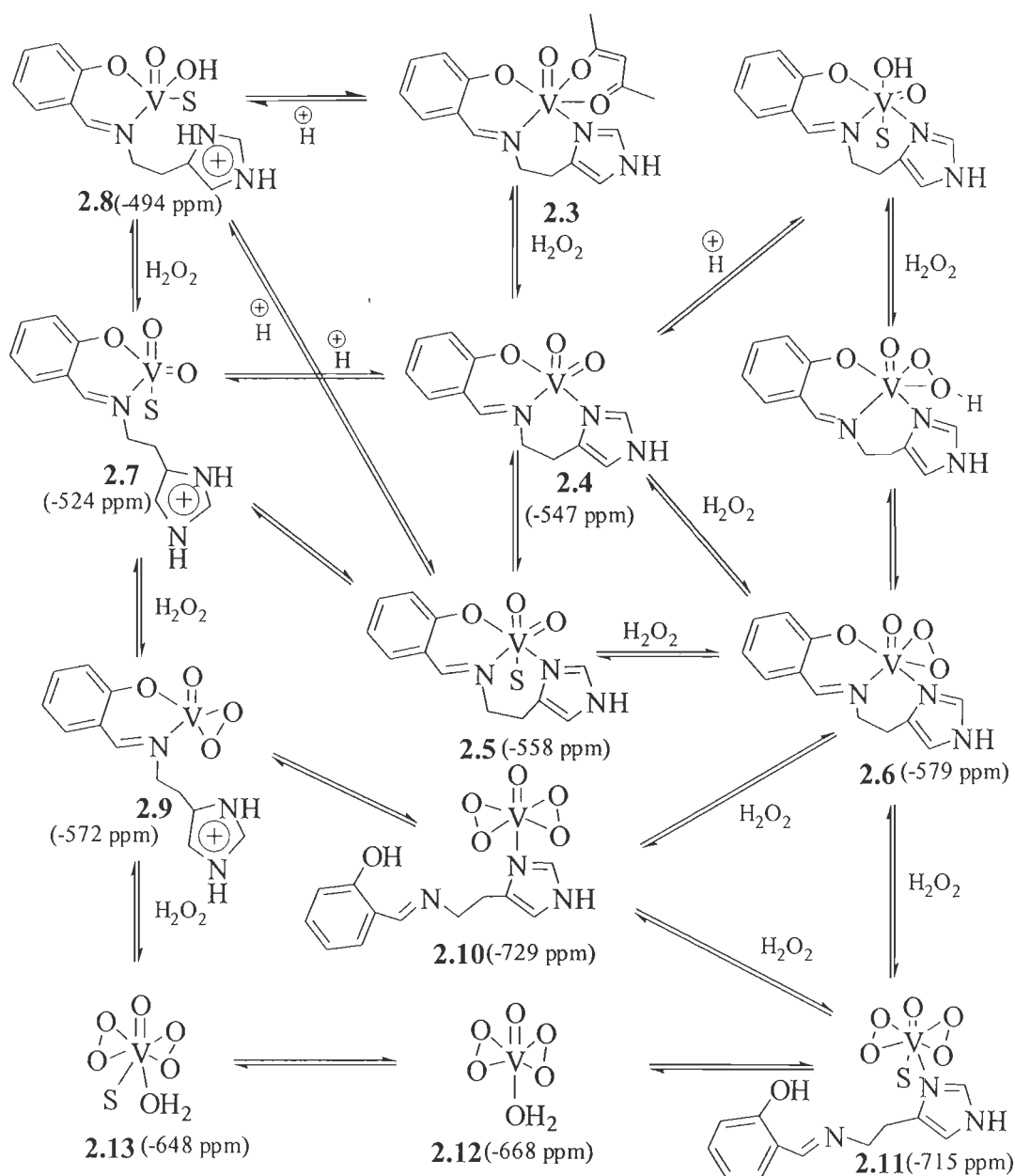
Scheme 2.5. Proposed reaction scheme (see text) and tentative assignments of the ^{51}V NMR chemical shifts involving oxidovanadium(V)-, dioxidovanadium(V)-, monoperoxovanadium(V)- and bisperoxovanadium(V)-species formed in methanolic solutions of **2.3** and **2.4** based on ^{51}V NMR spectroscopy, on addition of aqueous H_2O_2, HCl and methyl phenyl sulfide (this may originate reduction to **2.3**). S indicates solvent.

2.3.9. Mechanism of sulfide oxidation

It is well known that V^V-peroxo compounds mediate oxygenations reactions including the oxidation of sulfides to sulfoxides and sulfones and the epoxidation of alkenes and allylic alcohols [264–271].

The sulfur atom of methyl phenyl sulfide is electron rich and undergoes electrophilic oxidation giving the sulfoxide. We clearly demonstrated that complexes 2.3 and 2.4 are able to generate monoperoxo and even bis-peroxovanadium(V) species on treatment with H_2O_2. The peroxo-complexes being stable and detectable, it is likely that hydroperoxovanadium(V) complexes also form as aqueous H_2O_2 is being added and the pH decreases, enhancing the electrophilicity of the coordinated peroxo ligand and facilitating the nucleophilic attack by the sulfide. An outline of the catalytic cycle for oxidation of methyl phenyl sulfide, which has also been proposed by other authors [234, 240, 272–277] is given in Scheme 2.6.
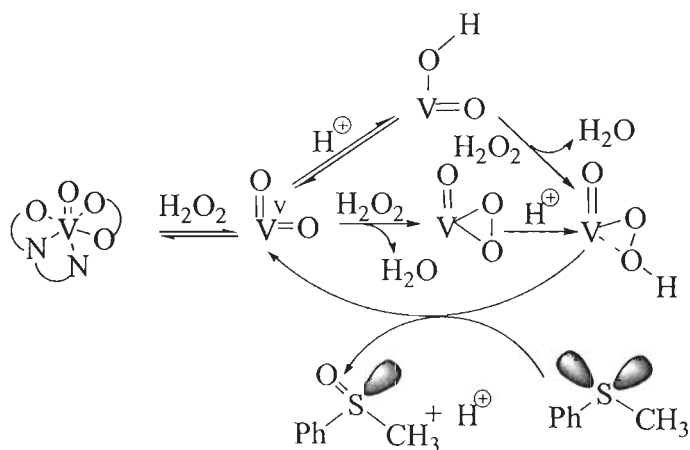
Scheme 2.6. Reaction mechanism of oxidation of methyl phenyl sulfide as a model substrate for sulfoxidations.

2.4. CONCLUSIONS

The compound Hsal–his (2.I) derived from salicylaldehyde and histamine has been covalently bonded to chloromethylated polystyrene cross-linked with 5% divinylbenzene. Upon reaction with $[V^{IV}O(acac)_2]$ the complex PS–$[V^{IV}O(sal–his)(acac)]$ (2.1) was obtained, which upon oxidation yielded the dioxidovanadium(V)

PS–[$V^{V}O_2$(sal–his)] **(2.2)**. The corresponding non-polymer bound complexes [$V^{IV}O$(sal–his)(acac)] **(2.3)** and [$V^{V}O_2$(sal–his)] **(2.4)** have also been prepared and characterised. Complexes **2.1** and **2.2** have been used as catalyst for the oxidation of methyl phenyl sulfide, diphenyl sulfide and benzoin with aqueous H_2O_2 as an oxidant. Under the optimised reaction conditions, a maximum of ca. 94 % conversion of methyl phenyl sulfide and ca. 83 % of diphenyl sulfide has been achieved in 2 h, with significant amounts of the corresponding sulfones. A maximum of 91.2 % conversion of benzoin has been achieved within 6 h. The corresponding neat complexes gave slightly lower conversions and selectivity, but significantly lower turn-over frequencies. Moreover, the polymer-bound catalysts did not leach during catalytic action and are recyclable, further emphasising their advantage over the neat complexes.

UV-Vis, EPR and ^{51}V NMR spectroscopy were used to characterise methanolic solutions of **2.3** and **2.4**, and to identify species formed upon addition of H_2O_2 and/or acid, similar oxo or peroxo species being detected by ^{51}V NMR spectroscopy starting either with solutions of **2.3** or of **2.4**. Addition of methyl phenyl sulfide to solutions containing peroxo species promoted the oxidation of the sulfide and regenerated the formation of the V^{IV}-species formed upon dissolution of **2.4** or oxidation of **2.3**. The EPR spectra also confirm that [$V^{IV}O$(sal–his)(acac)] **(2.3)** is also present in these solutions if the starting product is complex **2.3**. These studies confirm that most of these reactions involving complexes **2.3** or **2.4** are reversible, therefore supporting the catalytic nature of the sulfide oxidation processes.

*****

Chapter-3

Immobilisation of oxovanadium(IV), dioxomolybdenum(VI) and copper(II) complexes on polymers for the oxidation of styrene, cyclohexene and ethylbenzene

3.1. INTRODUCTION

Immobilisation of homogeneous catalysts on solid supports has become one of the important areas of research because this allows the design of more environment-friendly catalysts. The heterogeneous catalysts thus obtained not only become thermally more stable, they introduce certain new features to catalysts such as easy separation and recyclability, which in turn improve the turn over rates of the catalysts [278, 279]. The advantages of immobilised catalysts have prompted several groups to introduce various types of solid supports. Among various inorganic supports, alumina and silica are the most common. A review article by Jacobs *et al.* provides detailed accounts of such immobilised complexes [280]. The exchangeable properties of extra-framework cations and suitable cavity sizes of zeolites allowed their modifications by inclusion of homogeneous catalysts [281–284]. Recently, we started using chloromethylated polystyrene cross linked with divinylbenzene as a solid support to immobilise metal complexes, and we explored their catalytic potential for various oxidation reactions [77, 78, 184, 186].

We report herein the preparation and partial characterisation of the polymer supported/ anchored oxidovanadium(IV), dioxidomolybdenum(VI) and copper(II) complexes obtained from the reaction of chloromethylated polystyrene with 2-thiomethylbenzimidazole (Htmbmz, **3.I**), Scheme 3.1, followed by the introduction of the metal ions. The catalytic potentials of these complexes have been demonstrated by studying the oxidation of styrene, cyclohexene and ethylbenzene. Styrene oxide, an oxidation product of styrene, is an important intermediate in organic synthese and in the manufacture of the perfumery chemical, phenylethyl alcohol. Epoxidation of styrene has been reported using homogeneous catalysts [224, 285], titanosilicate zeolites [286, 287], hetero-polytungstates [288] and zeolite-encapsulated metal complexes [45, 226]. Amongst the various oxidation products of cyclohexene, cyclohexeneoxide is a highly reactive and selective organic intermediate widely used in the synthese of enantioselective drugs, epoxy paints and rubber promoters.

Acetophenone, the valuable product of the selective oxidation of ethylbenzene, has also attracted interest [289–294]. This is an useful intermediate in pharmaceuticals, resins, alcohols, esters, aldehydes and tear gas and is also used as a component in perfumery, in a drug to induce sleep, and as a solvent for cellulose ethers. Acetophenone is manufactured by the oxidation of ethylbenzene with molecular oxygen using cobalt cycloalkanecarboxylate or cobalt acetate as catalyst in acetic acid solvent [293]. This method is corrosive in nature and unfriendly to the environment. The oxidovanadium(IV), dioxidomolybdenum(VI) and copper(II) complexes reported in this paper exhibit good catalytic activity and selectivity in the catalytic oxidation of ethylbenzene to acetophenone.
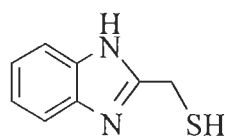
Htmbmz (**3.I**)

Scheme 3.1.

Among the important steps in the preparation of supported or anchored catalysts is their correct characterisation and, in the case of metal-complex catalysts, the understanding of their coordination geometry. The usual characterisation procedures, e.g. elemental analyses, electronic spectroscopy, energy dispersive X-ray analyses, XPS, FTIR, TG afford important information, but do not give much data to establish the coordination environment of the metal ions.

In this work, two of the metal centers used, $V^{IV}O^{2+}$ and Cu^{2+} have one unpaired electron, and EPR can be used to obtain important information that cannot be accessed for many other supported complexes such as the MoO_2^{2+} catalysts also studied here. The present work provides good examples of how useful and important the information obtained by EPR may be to understand the nature of the catalysts prepared.

3.2. EXPERIMENTAL

3.2.1. Materials and methods

Chloromethylated polystyrene (18.9 % Cl, i.e. 5.3 mmol Cl per gram of resin) and cross-linked with 5 % divinylbenzene) was obtained as a gift from Thermax Limited, Pune, India. Analytical reagent grade vanadium pentaoxide, ethylacetate, cupric acetate monohydrate, cyclohexene, ethylbenzene (Loba Chemie, India), DMF (S.D. fine chemicals, India), *o*-phenylenediamine, mercaptoacetic acid, ammonium heptamolybdate, acetylacetone (E. Merck, India), benzyl chloride, triethylamine (Ranbaxy, India), aqueous 30% H_2O_2 (Acros USA or Qualigens, India) and styrene (Acros, USA) were used as obtained. [VO(acac)$_2$] [233], [MoO$_2$(acac)$_2$] [295] and 2-thiomethylbenzimidazole (Htmbmz, **3.I**) [296] were prepared according to the methods reported in the literature.

Instrumentation and analyses details are reported in Chapter 2.

3.2.2. Syntheses of ligand and complexes

3.2.2.1. Reaction of 2-thiomethylbenzimidazole with benzylchloride

Sodium metal (0.428 g, 21 mmol) was added to a solution of Htmbmz (3.28 g, 20 mmol) in dry THF (75 ml) (dried over molecular sieve) with stirring where sodium slowly reacted with dissolution. Upon complete dissolution of sodium, a solution of benzyl chloride (2.78 g, 22 mmol) in dry THF (20 ml) was added and the reaction mixture was refluxed in an oil bath for 16 h under nitrogen atmosphere. After cooling to room temperature, water was added to the reaction mixture and the organic product was extracted with CHCl$_3$. On evaporating the solvent, purification by column chromatography using CHCl$_3$: MeOH (9 : 1) yielded a white solid in 45 % yield. Found: C, 70.6; H, 5.6; N, 10.9; S, 12.5 %. Calcd. for C$_{15}$H$_{14}$N$_2$S (254.03): C, 70.8; H, 5.6; N, 11.0; S, 12.6 %. ^{1}H NMR (DMSO-d$_6$): 6.95 (m, 2H), 6.59 – 6.71(m, 7H) (aromatic), 4.36(s, 4H, CH$_2$) ppm. ^{13}C (DMSO-d$_6$): 101.4, 123.0, 127.5, 128.9, 138.5, 153.0 (aromatic), 30.2, 36.6 (CH$_2$) ppm. All data indicate the condensation of thiol groups with benzyl chloride.

3.2.2.2. Polymer-anchored ligand, PS-ligand (3.II)

Chloromethylated polystyrene (5.0 g) was allowed to swell in DMF (30 ml) for 2 h. A solution of 2-thiomethylbenzimidazole (9.84 g, 60 mmol) in DMF (40 ml) was added to the above suspension followed by triethylamine (5.0 g) in ethylacetate (40 mL) and the reaction mixture was heated at 90 °C for 12 h with continuous mechanical stirring. After cooling to ambient temperature, the golden resin beads were filtered off, washed thoroughly with hot DMF (3 × 5 ml) followed by hot methanol and dried in an air oven at ca. 120 °C. Found: C, 74.0; H, 8.3; N, 6.4; S, 9.1 %.

3.2.2.3. PS-[VO(ligand)$_n$] (3.1)

The polymer-anchored ligand, PS-ligand (2 g), was allowed to swell in methanol (20 ml) for 2 h. A solution of [VO(acac)$_2$] (5.30 g, 20 mmol) in methanol (50 ml) was added to the above suspension and the reaction mixture was heated at reflux for 12 h with mechanical stirring. After cooling to room temperature, the dark green PS-[VO(ligand)$_n$] was separated by filtration, washed thoroughly with hot methanol and dried in an air oven at 100 °C to constant weight. Found: C, 67.2; H, 8.1; N, 6.3; S, 8.8; V, 5.2 %.

3.2.2.4. PS-[MoO$_2$(ligand)$_n$] (3.2) and PS-[Cu(ligand)$_n$] (3.3)

Polymer-anchored complexes, PS-[MoO$_2$(ligand)$_n$] (3.2) and PS-[Cu(ligand)$_n$] (3.3) were prepared as outlined for 3.1 by reacting the PS-ligand with [MoO$_2$(acac)$_2$] and Cu (CH$_3$COO)$_2$.H$_2$O respectively in methanol.

Data for 3.2: Found: C, 61.4; H, 5.9; N, 6.1; S, 8.9; Mo, 8.9 %.

Data for 3.3: Found: C, 66.1; H, 6.2; N, 6.1; S, 8.7; Cu, 6.4 %.

3.2.2.5. [VO(tmbmz)$_2$] (3.4)

A methanolic solution of Htmbmz (0.656 g, 4 mmol in 15 ml) was added to a solution of [VO(acac)$_2$] (0.53 g, 2 mmol) in methanol (10 ml) and the reaction mixture was stirred for 2 h at room temperature. The precipitated violet solid was filtered, washed with methanol and dried in vacuum. Yield: 83 %. The same complex can also

be prepared by treating the ligands with $VOSO_4.5H_2O$ (2:1 molar ratio) in methanol / aqueous solution in 65 % yield. Found: C, 48.7; H, 3.7; N, 14.1; S, 16.1; V, 12.6 %. Calcd. for $C_{16}H_{14}N_4S_2OV$ (393.4): C, 48.7; H, 3.6; N, 14.2; S, 16.3; V, 12.9 %.

3.2.2.6. [MoO₂(tmbmz)₂] (3.5)

Complex $[MoO_2(tmbmz)_2]$ was prepared as mentioned above using Htmbmz (0.328 g, 2 mmol) dissolved in methanol (30 ml) and $[MoO_2(acac)_2]$ (0.328 g, 1 mmol) in methanol (15 ml). An orange solid of $[MoO_2(tmbmz)_2]$ that had formed was filtered, washed with methanol and dried in vacuum. Yield: 74 %. Found: C, 42.0; H, 3.3; N, 12.2; S, 13.9; Mo, 20.8 %. Calcd. for $C_{16}H_{14}N_4S_2O_2Mo$(454.3): C, 42.3; H, 3.1; N, 12.3; S, 14.1; Mo, 21.1 %. ^1H NMR (DMSO-d_6): 6.60 – 7.90 (m, 8H, aromatic), 4.46(s, 4H, CH_2) ppm.

3.2.2.7. [Cu(tmbmz)₂](3.6)

A solution of $Cu(CH_3COO)_2 .H_2O$ (1.0 g, 5 mmol) dissolved in 50 ml of methanol was added to a methanolic solution of Htmbmz (1.63, 10 mmol in 20 ml) with stirring. After addition of KOH (0.28 g, 5 mmol) dissolved in 5 ml of water with stirring, the reaction mixture was further stirred for 2 h. During this period, $[Cu(tmbmz)_2]$ slowly separated out; it was filtered, washed with the minimum amount of methanol and dried in vacuum over silica gel. Yield: 70 %. Found: C, 48.9; H, 3.8; N, 14.0; S, 16.3; Cu, 15.8 %. Calcd. for $C_{16}H_{14}N_4S_2Cu$ (389.9): C, 49.3; H, 3.6; N, 14.4; S, 16.4; Cu, 16.3 %.

3.2.3. Catalytic Reactions

Catalysts PS-[VO(ligand)$_n$], PS-[MoO$_2$(ligand)$_n$] and PS-[Cu(ligand)$_n$] were used to carry out the oxidation of styrene, cyclohexene and ethylbenzene. Each catalyst was allowed to swell in acetonitrile for 2 h prior to its use.

3.2.3.1. Oxidation of styrene

In a typical oxidation reaction, styrene (1.04 g, 10 mmol), aqueous 30 % H_2O_2 (2.27 g, 20 mmol) and an appropriate catalyst (0.040 g) were mixed in 10 ml of

acetonitrile and the reaction mixture was heated at 80 °C in an oil bath with stirring. The progress of the reaction was monitored by withdrawing samples at different time intervals and analysing them quantitatively by gas chromatography. The identities of the products were confirmed by GC-MS.

3.2.3.2. Oxidation of cyclohexene

Cyclohexene (0.82 g, 10 mmol), aqueous 30 % H_2O_2 (2.27 g, 20 mmol) and catalyst (0.035 g) were taken in acetonitrile (20 ml). The reaction mixture was allowed to heat at 80 °C for 6 h with continuous stirring. The analyses and identification of the reaction products were done as mentioned above.

3.2.3.3. Oxidation of ethylbenzene

Oxidation of ethylbenzene and analyses of the reaction products were carried out as mentioned above.

3.3. RESULTS AND DISCUSSION

3.3.1. Syntheses, reactivity and solid state characteristics

The reaction of chloromethylated polystyrene, cross linked with 5% divinylbenzene, with 2-thiomethylbenzimidazole in DMF in the presence of triethylamine would be expected to lead to the formation of the polymer-anchored species indicated in Scheme 3.2. The product formed in the reaction of Htmbmz with benzyl chloride (see experimental section), where the sulphur atom acts as the nucleophile in the reaction, confirms this.

Htmbmz (**3.I**)   PS-S-tmbmz (**3.II**)
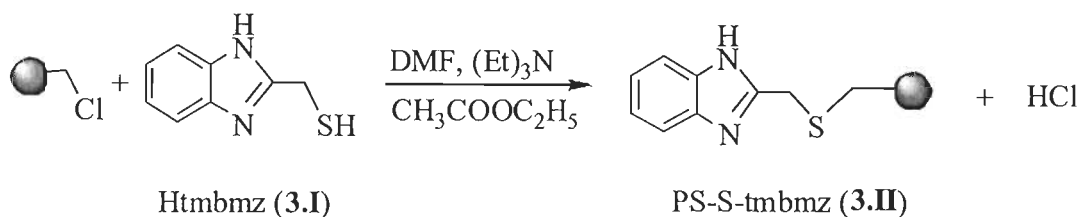
Scheme 3.2. Reaction of Htmbmz with chloromethylated polystyrene; the ball represents the polymer backbone.

However, the analytical results obtained, namely the S/N ratio, do not fully agree with the formation of PS-S-tmbmz, and products corresponding to a higher relative % of sulfur also form. It is possible that, before and after the Htmbmz binds to the solid, the thiol group oxidizes to disulphide, other oxidation products possibly also being formed. At this stage we will designate the products of reaction of Htmbmz with chloromethylated polystyrene by PS-ligand (**3.II**).

The remaining chlorine content of 1.5 % (0.42 mmol Cl per gram of resin) in PS-ligand (**3.II**) would suggest roughly 92 % loading of the ligand if only PS-S-tmbmz had formed. The anchored ligands, on reaction with [VO(acac)$_2$], gave an oxidovanadium(IV) complex which we designate as PS-[VO(ligand)$_n$] (**3.1**). Complexes PS-[MoO$_2$(ligand)$_n$] (**3.2**) and PS-[Cu(ligand)$_n$] (**3.3**) were prepared similarly from [MoO$_2$(acac)$_2$] and cupric acetate, respectively. Elemental analyses data of the isolated complexes are presented in the experimental section and the nature of the species bound to the polystyrene matrix will be discussed below in Section 3.3.8.

Table 3.1 provides data of metal and ligand loading in polymer-anchored complexes, assuming the formation of PS-S-tmbmz. The data show that the metal-to-ligand ratio in polymer-anchored complexes is close to 1 : 2.

Table 3.1. Ligand and metal loadings in polymer anchored complexes, and ligand-to-metal ratio data, assuming bonding in PS-ligand (**3.II**) as in Scheme 3.2

Compound	Ligand loading (mmol g^{-1} of resin)	Metal ion loading[a] (mmol g^{-1} of resin)	Ligand : Metal ratio
PS-ligand	2.65		
PS-[VO(ligand)$_n$]	2.24	1.03	1 : 2.17
PS-[MoO$_2$(ligand)$_n$]	2.17	0.93	1 : 2.33
PS-[Cu(ligand)$_n$]	2.18	1.02	1 : 2.12

[a] Metal ion loading = $\dfrac{\text{Observed metal } \% \times 10}{\text{Atomic weight of metal}}$

3.3.2. Thermo gravimetric studies

All polymer-anchored complexes are stable up to ca. 180 °C and thereafter they decompose in two major steps. It has not been possible to separate the observed mass loss due to the decomposition of complexes from polymer backbone because of their overlapping nature. However, the residues due to the metal oxides obtained as the end products at ca. 800 °C indicate the presence of the metal complexes covalently bonded to the polymer. Non-polymer-bound complexes are stable up to ca. 200 °C. They decompose in two major steps, giving the corresponding metal oxides as end products at ca. 600 °C. The amounts of V_2O_5, MoO_3 and CuO match with the expected values within experimental error.

3.3.3. Field-emission-scanning electron micrographs (FE-SEM) and energy dispersive X-ray analyses (EDX)

Field emission-scanning electron micrographs for single beads of pure chloromethylated polystyrene, polymer-anchored ligand and complexes were recorded to understand the morphological changes occurring on the polystyrene beads at various stages of the synthese. As expected, the pure polystyrene bead has a smooth surface. Introduction of ligands into polystyrene beads through covalent bonding causes the light roughening of the top layer of polymer-anchored beads. Images of metal complex beads show further roughening of the top layer, probably due to the changes that occur during the rearrangement of the chains to adapt the bound ligand to the fixed geometry of the complex. Energy dispersive X-ray analyses (EDX) supports this conclusion in that ca. 19 % chlorine content has been found in the pure polystyrene beads, while beads having anchored ligand show only ca. 1 % Cl along with ca. 6.5 % nitrogen and ca. 9.2 % sulfur. The polystyrene beads of immobilised metal complexes contain metal along with nitrogen and sulfur, suggesting the formation of metal complexes with the anchored ligand at various sites.

3.3.4. IR spectral studies

Table 3.2 presents a partial list of IR spectral data of ligands and non-polymer-bound as well as anchored complexes. The NH stretching band of Htmbmz occurs at 2650–2800 cm^{-1} as a broad feature, which indicates the presence of strong hydrogen bonding. Upon anchoring with polystyrene, the broad feature of NH disappears. Bands of medium intensity appear at 2800–2990 cm^{-1} due to the presence of CH_2 group of polystyrene. In addition, most characteristic bands observed in the free ligand also appear. The ν(C–S) (thioalcoholic) stretch in Htmbmz appearing at 747 cm^{-1}, shifts to lower wave numbers in non-polymer-bound complexes, indicating the involvement of sulfur in bonding [297]. The Htmbmz ligand exhibits a sharp band at 1638 cm^{-1} due to ν(C=N) (azomethine) and this band shifts to lower wave numbers (1618 – 1628 cm^{-1}) in non-polymer-bound complexes suggesting the coordination of azomethine nitrogen to the metal ion. PS-ligand (3.II) exhibits ν(C=N) (azomethine) at 1640 cm^{-1} and in polymer-anchored complexes this band appears at 1619–1634 cm^{-1}. Other characteristic bands are also observed, e.g.: ν(V=O) at 997 cm^{-1} in PS-[VO(ligand)$_n$] [236], ν_{sym}(O=Mo=O) and ν_{asym}(O=Mo=O) at 910 and 947 cm^{-1}, respectively in PS-[MoO$_2$(tmbmz)$_2$] [298], confirming the presence of vanadium and molybdenum in the solid. The corresponding non-polymer-bound complexes also exhibit these characteristic bands at slightly lower energies.

3.3.5. Electronic spectral studies

Electronic spectra of Htmbmz and its non-polymer-bound complexes were recorded in ethanol, while spectra of polymer-anchored ligands and their corresponding complexes were recorded in nujol. The electronic spectrum of ligand Htmbmz exhibits four intense bands at 205, 252, 278, 284 and 327 nm (Table 3.3). The bands at 278 and 284 nm are characteristic of the presence of benzimidazole group [299]. The other three bands are assignable to ϕ - ϕ^*, π - π^* and n - π^* transitions, respectively. The characteristic benzimidazole bands have also been observed in non-polymer-bound complexes. Other ligand bands appear within the expected region. In addition, if we used higher concentrations, two weak shoulder-bands at 524 and 665 nm in [VO(tmbmz)$_2$] and one band at 695 nm in [Cu(tmbmz)$_2$]

were also observed; these may be considered to be due to d – d transition(s). Complex [MoO$_2$(tmbmz)$_2$] exhibits only a ligand to metal charge transfer band at 375 nm in the visible region in addition to regular ligand bands. The electronic spectra of polymer-anchored ligands as well as complexes exhibit characteristic ligand bands in the expected range. However, the band due to d-d transition in polymer-bound complexes (see Fig. 3.1) could not be obtained due to poor loading of complexes and less favorable experimental conditions to record these bands when using nujol mulls.
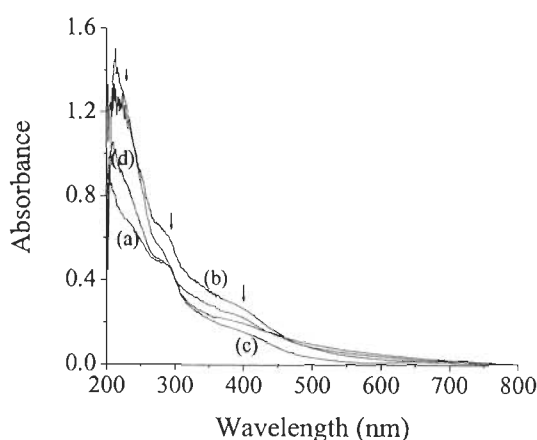
Fig. 3.1. Electronic spectra of polymer-anchored ligand and metal complexes dispersed in nujol mulls: PS-ligand (a), PS-[VO(ligand)$_n$] (b), PS-[MoO$_2$(ligand)$_n$] (c) and PS-[Cu(ligand)$_n$] (d).

Table 3.2. IR spectra of ligand, pure and bound complexes

Compound	ν(C=N)	ν(M=O)(M = V, Mo)
Htmbmz	1638	-
PS-ligand	1640	-
PS-[VO(ligand)$_n$]	1634	997
PS-[MoO$_2$(ligand)$_n$]	1619	947, 910
PS-[Cu(ligand)$_n$]	1632	-
[VO(tmbmz)$_2$]	1628	979
[MoO$_2$(tmbmz)$_2$]	1618	900, 848
[Cu(tmbmz)$_2$]	1621	-

Table 3.3. Electronic spectral data of ligands and complexes

Compound	Solvent	λ_{max} / nm[a]
Htmbmz	Ethanol	205, 252, 278, 284, 327(s)
PS-ligand	Nujol	205, 237, 283(s), 387(s)
PS-[VO(ligand)$_n$]	Nujol	211, 285(s), 391(s)
PS-[MoO$_2$(ligand)$_n$]	Nujol	213, 280(s), 398(s)
PS-[Cu(ligand)$_n$]	Nujol	209, 285(s), 382(s)
[VO(tmbmz)$_2$]	Ethanol	210, 240, 274, 280, 289, 396(s), 524, 665
[MoO$_2$(tmbmz)$_2$]	Ethanol	210, 245, 274, 279, 298(s), 375
[Cu(tmbmz)$_2$]	Ethanol	209, 230, 274, 280, 297, 382, 695(w)

[a] s = shoulder, w = weak

3.3.6. Catalytic activity studies

Catalytic activities of the polymer-anchored complexes are demonstrated by studying the oxidation of styrene, cyclohexene and ethylbenzene.

3.3.6.1. Oxidation of styrene

Oxidation of styrene, catalysed by PS-[VO(ligand)$_n$], PS-[MoO$_2$(ligand)$_n$] and PS-[Cu(ligand)$_n$], using H$_2$O$_2$ as an oxidant gave styrene oxide, benzaldehyde and 1-phenylethane-1,2-diol as main products, as shown in Scheme 3.3. The formation of at least five products has been observed when the polymer-supported catalyst PS-[VO(sal-ohyba)(DMF)] (H$_2$sal-ohyba = Schiff base derived from salicylaldehyde and *o*-hydroxybenzylamine) was applied as catalyst [184]. Others have also identified some of these products [226, 300, 301].

Preliminary experiments showed the good activity of PS-[VO(ligand)$_n$] amongst these catalysts, it was, therefore, taken as a representative, and the different parameters *viz.* amount of oxidant (moles of H$_2$O$_2$ per mole of styrene), catalyst, and temperature of the reaction mixture were checked to get optimised reaction conditions for the maximum oxidation of styrene.
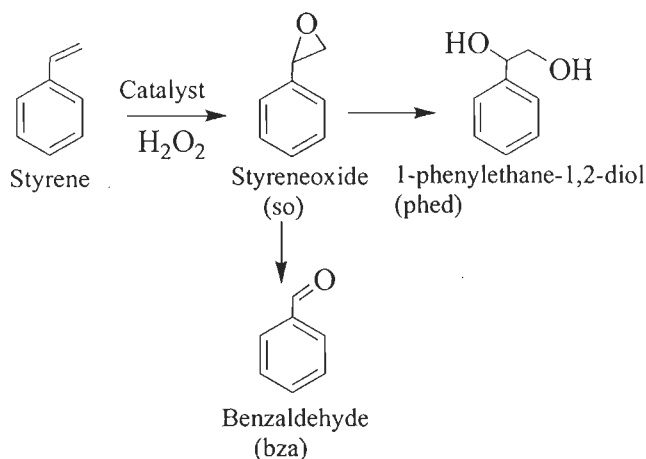
Scheme 3.3. Reaction products on oxidation of styrene, and abbreviations used

Thus, for three different styrene to aqueous 30 % H_2O_2 molar ratios, *viz.* 1 : 1, 1 : 2 and 1 : 3, the amount of styrene (1.04 g, 10 mmol) and catalyst (0.035 g) were taken in CH_3CN (10 ml), and the reaction was carried out at 80 °C. The formation of products was regularly analysed at time intervals. As illustrated in Fig. 3.2, the oxidation of styrene improved from 47.8 % to 81 % upon increasing the styrene to aqueous 30 % H_2O_2 molar ratio from 1 : 1 to 1 : 2. The oxidation remained nearly constant upon further increasing this ratio to 1 : 3, which suggested that a large amount of oxidant is not an essential condition to improve the oxidation of styrene.

Similarly, for three different amounts *viz.* 0.025, 0.035 and 0.045 g of catalyst under the above reaction conditions, 0.025 g catalyst gave only 40.5 % conversion while 0.035 and 0.045 g catalyst have shown maximum conversions of 81.0 and 85 %, respectively; Fig. 3.3. However, at the expense of H_2O_2, 0.035 g catalyst can be considered sufficient enough to carry out the reaction. Further, the turnover rate (TOF h^{-1} = moles of substrate converted per mole of catalyst per hour) is also higher for 0.035 g catalyst to achieve 81 % conversion of styrene. The temperature of the reaction mixture has also influenced the performance of the catalyst; running the reaction at 80 °C gave much better conversion. Moreover, the time required to achieve the maximum conversion was also reduced on carrying out the reaction at 80 °C.
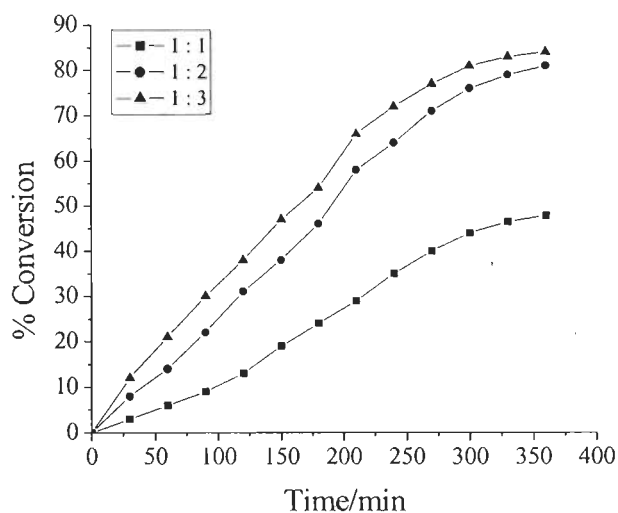
Fig. 3.2. Effect of amount of H_2O_2 on the oxidation of styrene as a function of time. Reaction conditions: styrene (1.04 g, 10 mmol), PS-[VO(ligand)$_n$] (0.035 g), CH_3CN (10 ml) and 80 °C.
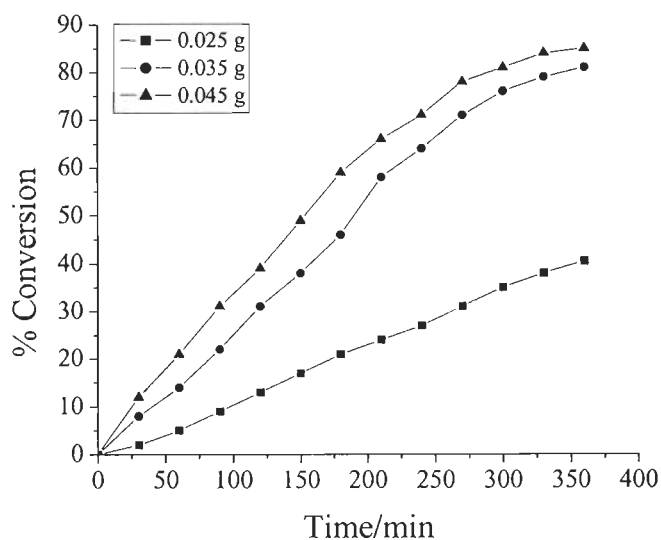
Fig. 3.3. Effect of amount of catalyst PS-[VO(ligand)$_n$] on the oxidation of styrene as a function of time. Reaction conditions: styrene (1.04 g, 10 mmol), H_2O_2 (2.27 g, 20 mmol), CH_3CN (10 ml) and 80 °C.

Thus, for the maximum oxidation of 10 mmol of styrene other required parameters were: catalyst (0.035 g), H_2O_2 (2.27 g, 20 mmol), CH_3CN (10 ml) and reaction temperature (80 °C). Other catalysts, PS-[MoO$_2$(ligand)$_n$] and PS-[Cu(ligand)$_n$] were also tested under the above optimised reaction conditions and the results are presented in Table 3.4. It is clear from the data that PS-[VO(ligand)$_n$] exhibits better catalytic activity with 81 % conversion, followed by PS-[MoO$_2$(ligand)$_n$] with 68 %. Catalyst PS-[Cu(ligand)$_n$] has shown only 57 % conversion after 6 h of reaction time.

The catalytic activities of these polymer-anchored complexes were compared with those of their "corresponding" non-polymer-bound ones. The conversion percentage of styrene for each catalyst as a function of time is presented in Fig. 3.4. Table 3.4 presents the selectivity details of various products obtained after 6 h of reaction time. The catalytic performances of the non-polymer-bound complexes are also good. However, the TOF values are much lower in comparison to the respective polymeric ones. Moreover, easy recovery of the anchored catalyst, no leaching and recycle ability (vide infra) make them better than the non-polymer-bound complexes.
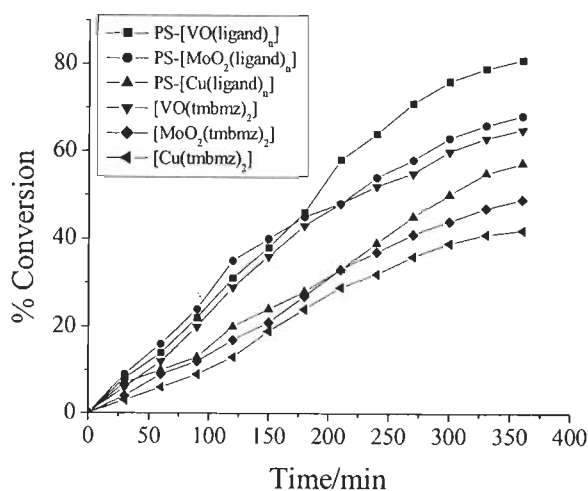
Fig. 3.4. Comparison of catalysts for the oxidation of styrene as a function of time. Reaction conditions: styrene (1.04 g, 10 mmol), catalyst (0.035 g), H_2O_2 (2.27 g, 20 mmol), CH_3CN (10 ml) and 80 °C.

It is clear from the Table 3.4 that the selectivity of the different oxidation products formed varies in the order: benzaldehyde > 1-phenylethane-1,2-diol > styrene oxide. The formation of benzaldehyde has been obtained in highest yield in all cases; this may be due to the nucleophilic attack of H_2O_2 on the styrene oxide formed in the first step, followed by the cleavage of the intermediate hydroperoxy styrene. Benzaldehyde formation may also be facilitated by direct oxidative cleavage of the styrene side chain double bond *via* a radical mechanism [301]. The formation of 1-phenylethane-1,2-diol formation is possible through hydrolysis of styrene oxide by the water present in H_2O_2.

Table 3.4. Percentage conversion of styrene, product selectivity and turn over frequency (TOF)

Catalyst	Conv. (%)	TOF (h^{-1})	Product selectivity (%)[a]			
			So	bza	phed	Others
[VO(tmbmz)$_2$]	65.0	22.0	3.6	66.3	28.6	1.5
PS-[VO(ligand)$_n$]	81.0	37.5	4.9	62.6	31.3	1.2
PS-[VO(ligand)$_n$][b]	80.4	-	3.8	62.5	31.6	1.1
PS-[VO(ligand)$_n$][c]	80.2	-	3.6	62.7	31.5	1.2
[MoO$_2$(tmbmz)$_2$]	49.0	18.8	3.0	68.8	27.0	1.2
PS-[MoO$_2$(ligand)$_n$]	68.0	14.1	3.1	66.0	29.5	1.4
PS-[MoO$_2$(ligand)$_n$][b]	67.5	-	2.9	66.4	29.4	1.3
PS-[MoO$_2$(ligand)$_n$][c]	67.2	-	3.0	66.4	29.4	1.2
[Cu(tmbmz)$_2$]	42.0	34.7	3.7	61.5	32.9	1.9
PS-[Cu(ligand)$_n$]	57.0	31.3	3.6	63.7	31.4	1.3
PS-[Cu(ligand)$_n$][b]	56.6	-	3.4	63.2	32.3	1.1
PS-[Cu(ligand)$_n$][c]	56.1	-	3.2	63.1	32.5	1.2

[a] For details of abbreviations see Scheme 3.3. [b] First cycle of used catalyst. [c] Second cycle of used catalyst.

The conversion of styrene and the selectivity of different reaction products using PS-[VO(ligand)$_n$] as catalyst under the optimised reaction conditions have been analysed as a function of time and are presented in Fig. 3.5. It is clear from the plot that the formation of styrene oxide is good in the beginning but it decreases considerably with time, while the selectivities of benzaldehyde and 1-phenylethane-1,2-diol increase slowly with the conversion of styrene. Almost identical trends have also been obtained with the two other catalysts. After 6 h only minor changes have been observed in the selectivity of the different reaction products.
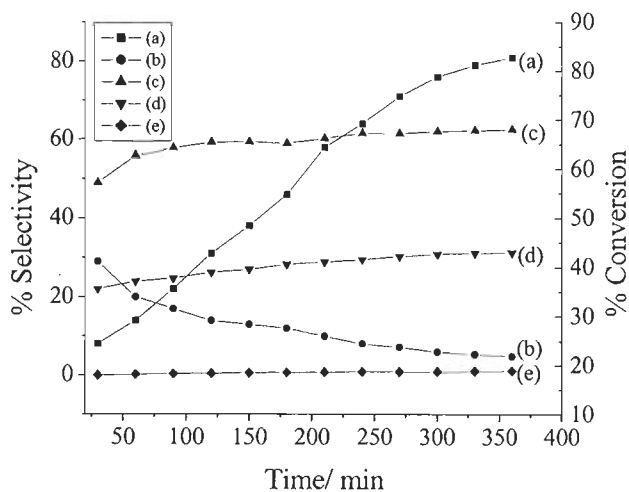
Fig. 3.5. Conversion of styrene and variation in the selectivity of different reaction products as a function of time using PS-[VO(ligand)$_n$] as catalyst: (a) conversion of styrene, (b) selectivity of styrene oxide, (c) benzaldehyde and (d) 1-phenylethane-1,2-diol.

3.3.6.2. Oxidation of cyclohexene

These complexes: PS-[VO(ligand)$_n$], PS-[MoO$_2$(ligand)$_n$] and PS-[Cu(ligand)$_n$], have also been used for the oxidation of cyclohexene by H$_2$O$_2$; they gave three products, namely cyclohexeneoxide, 2-cyclohexene-1-one and cyclohexane-1,2-diol, as represented by Scheme 3.4. Again, PS-[VO(ligand)$_n$] is the most efficient catalyst and the various parameters were varied to optimise the reaction conditions to get the maximum oxidation of cyclohexene.

86

cyclohexene → Cyclohexeneoxide + 2-cyclohexene-1-one + Cyclohexane-1,2-diol
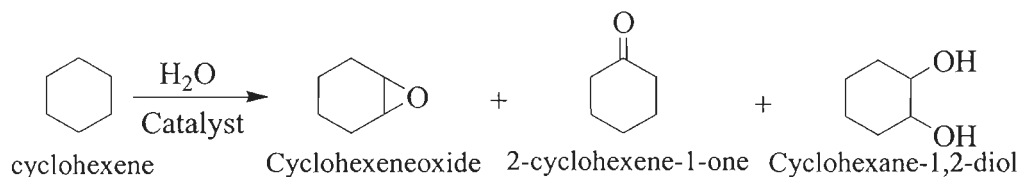
Scheme 3.4. Reaction products on oxidation of cyclohexene.

Three different cyclohexene : aqueous 30 % H_2O_2 molar ratios *viz.* 1 : 1, 1 : 2 and 1 : 3 were considered. Other reagents such as cyclohexene (0.82 g, 10 mmol) and catalyst (0.045 g) were taken in acetonitrile (10 ml) and the reaction was carried out at 80 °C. Fig. 3.6 presents the percentage conversion obtained as a function of time. A maximum of 53 % conversion was obtained at a cyclohexene to H_2O_2 molar ratio of 1 : 1 in 6 h of reaction time. This conversion improved to 86 % at a cyclohexene to H_2O_2 molar ratio of 1 : 2. No important improvement in the conversion was observed upon further increasing this ratio. Thus, a cyclohexene to H_2O_2 molar ratio of 1 : 2 can be considered as an optimum ratio.

The effect of amount of catalyst on the oxidation of cyclohexene was also studied. Three different amounts of PS-[VO(ligand)$_n$] *viz.* 0.025, 0.045 and 0.060 g were taken while keeping other conditions as above. The results obtained as a function of time are presented in Fig. 3.7. It is clear from the figure that 0.025 g of catalyst exhibited poor conversion, while a maximum of 86 % conversion was achieved with 0.045 g of catalyst. A further improvement in conversion of ca. 2 % could only be obtained upon increasing the catalyst amount to 0.060 g. As turn over frequency would be higher for 0.045 g of catalyst compared to 0.060 g, an amount of 0.045 g of catalyst may be considered enough to obtain maximum oxidation of cyclohexene.
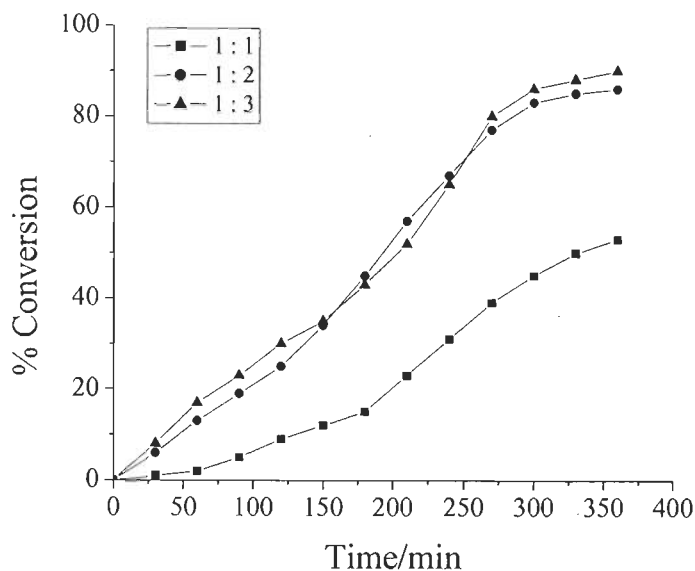
Fig. 3.6. Effect of amount of H_2O_2 on the oxidation of cyclohexene. Reaction conditions: cyclohexene (0.82 g, 10 mmol), PS-[VO(ligand)$_n$] (0.045 g), CH$_3$CN (10 ml) and 80 °C.
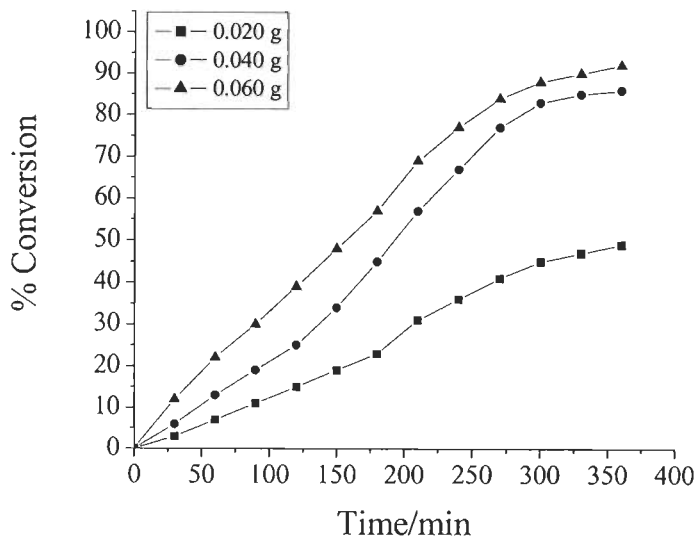
Fig. 3.7. Effect of amount of catalyst PS-[VO(ligand)$_n$] on the oxidation of cyclohexene. Reaction conditions: cyclohexene (0.82 g, 10 mmol), H$_2$O$_2$ (2.27 g, 20 mmol), CH$_3$CN (10 ml) and 80 °C.

As observed in Section 3.3.6.1, running the reaction at 80 °C gave a maximum conversion under the given conditions. Thus, the optimised conditions for the oxidation of 10 mmol of cyclohexene were fixed as follows: catalyst (0.045 g), 30 % aqueous H_2O_2 (2.27 g, 20 mmol), CH_3CN (20 ml) and reaction temperature (80 °C). Other catalysts: PS-[MoO_2(ligand)$_n$] and PS-[Cu(ligand)$_n$], tested under the above optimised reaction conditions gave maxima of 66 % and 51 % conversion, respectively. Thus, amongst the three anchored catalysts, the catalytic efficiency vary in the order: PS-[VO(ligand)$_n$] > PS-[MoO_2(ligand)$_n$] > PS-[Cu(ligand)$_n$]. Fig. 3.8 presents the conversion profile as a function of time, while the selectivity of different products along with the conversion and turn over frequency for these catalysts are presented in Table 3.5. It is clear from the table that the selectivity of the various products obtained vary in the order: cyclohexane-1, 2-diol > 2-cyclohexene-1-one > cyclohexeneoxide.

Table 3.5. Percentage conversion of cyclohexene, product selectivity and TOF

Catalyst	Conv. (%)	TOF (h^{-1})	Product selectivity (%)[a]			
			a	b	c	Others
[VO(tmbmz)$_2$]	64.0	14.7	2.4	12.4	84.7	0.5
PS-[VO(ligand)$_n$]	86.0	31.0	3.2	14.8	81.3	0.7
PS-[VO(ligand)$_n$][b]	85.5	-	3.0	14.9	81.2	0.9
PS-[VO(ligand)$_n$][c]	84.8	-	3.1	14.8	81.2	0.9
[MoO$_2$(tmbmz)$_2$]	55.0	14.1	2.2	11.1	85.7	1.0
PS-[MoO$_2$(ligand)$_n$]	66.0	26.2	2.3	13.2	83.4	1.1
PS-[MoO$_2$(ligand)$_n$][b]	65.0	-	2.1	13.4	83,1	1.4
PS-[MoO$_2$(ligand)$_n$][c]	64.4	-	2.2	13.4	83.2	1.2
[Cu(tmbmz)$_2$]	39.0	8.7	2.1	12.4	84.4	1.1
PS-[Cu(ligand)$_n$]	51.0	18.5	2.8	12.9	83.3	1.0
PS-[Cu(ligand)$_n$][b]	49.0	-	3.0	12.8	83.4	0.8
PS-[Cu(ligand)$_n$][c]	48.0	-	2.9	12.7	83.5	0.9

[a] For details of abbreviations see Scheme 3.4. [b] First cycle of used catalyst. [c] Second cycle of used catalyst.

Non-polymer-bound complexes: $[VO(tmbmz)_2]$, $[MoO_2(tmbmz)_2]$ and $[Cu(tmbmz)_2]$ exhibited at 64, 55 and 39 % conversion, respectively (Fig. 3.8), and thus show good catalytic activity as well. The order of the selectivity of reaction products is also the same as that observed for their polymer-anchored analogues. Again, the formation of cyclohexeneoxide in these cases is very low. Table 3.5 also presents the relevant data for non-polymer-bound complexes. The calculated turn over frequencies in these cases are low (14.7 for $[VO(tmbmz)_2]$, 14.1 for $[MoO_2(tmbmz)_2]$ and 8.7 for $[Cu(tmbmz)_2]$). Thus, turn over frequency as well as other characteristics such as stability, recycle ability and operational flexibility make the polymer-anchored catalysts better than the non-polymer-bound complexes.
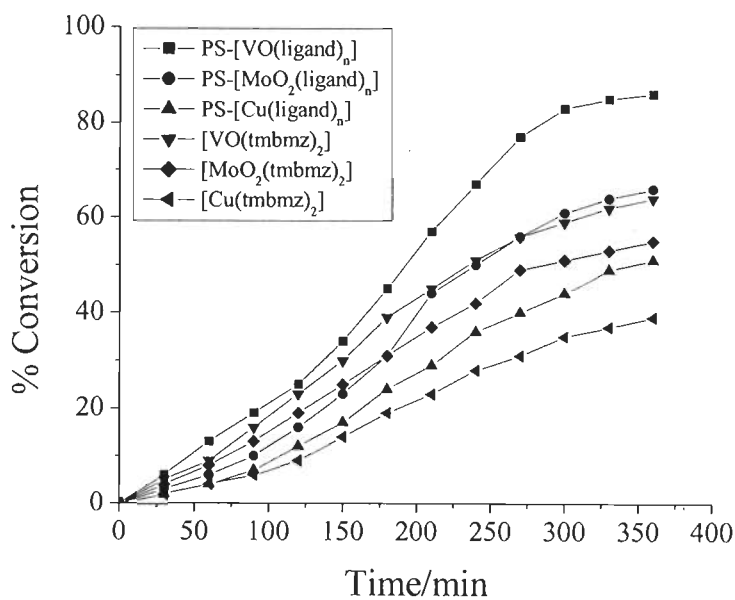
Fig. 3.8. Comparison of catalysts for the oxidation of cyclohexene. Reaction conditions: cyclohexene (0.82 g, 10 mmol), catalyst (0.045 g), H_2O_2 (2.27 g, 20 mmol), CH_3CN (10 ml) and 80 °C.

3.3.6.3. Oxidation of ethylbenzene

Oxidation of ethylbenzene catalysed by PS-[VO(ligand)$_n$], PS-[MoO$_2$(ligand)$_n$] and PS-[Cu(ligand)$_n$] using H$_2$O$_2$ as oxidant gave benzaldehyde, phenylacetic acid, acetophenone and 1-phenylethane-1,2-diol, as shown in Scheme 3.5.
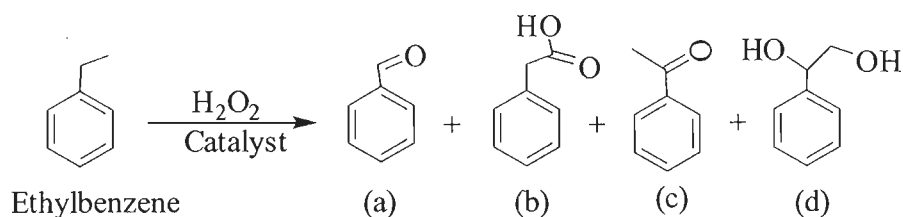
Ethylbenzene   (a)   (b)   (c)   (d)

Scheme 3.5. Reaction products on oxidation of ethylbenzene: (a) benzaldehyde, (b) phenylacetic acid, (c) acetophenone and (d) 1-phenylethane-1,2-diol

Again, we have checked the influence of the amount of oxidant (moles of H$_2$O$_2$ per mole of ethylbenzene), catalyst and temperature of the reaction using PS-[VO(ligand)$_n$] as a representative catalyst. The effect of temperature on the oxidation of ethylbenzene was studied at three different temperatures (*viz.* 55, 70 and 80 °C) while keeping ethylbenzene (1.06 g, 10 mmol), aqueous 30 % H$_2$O$_2$ (3.34 g, 30 mmol), and catalyst (0.060 g) in 10 ml of CH$_3$CN. As observed earlier, the performance of the catalyst is much better at 80 °C than at to 55 and 70 °C, along with achieving the maximum conversion in considerably less time.

The influence of H$_2$O$_2$ concentration on the oxidation of ethylbenzene was studied considering ethylbenzene : aqueous 30 % H$_2$O$_2$ molar ratios of 1 : 1.5, 1 : 3 and 1 : 4 while keeping ethylbenzene (1.06 g, 10 mmol), catalyst (0.060 g), CH$_3$CN (10 ml) and temperature (80 °C) constant. As illustrated in Fig. 3.9, the conversion improved from 12 % at 1 : 1.5 mole ratio to 26 % at 1 : 3 and finally to 29 % at 1 : 4 mole ratio in 8 h of reaction time. However, at the expense of oxidant a minimum of 1 : 3 molar ratio may be considered necessary to observe maximum oxidation. Further, the turn over rates for substrate-to-oxidant ratio of 1 : 3 with 26 % conversion would be higher than that calculated at 1 : 4 ratio with 29 % conversion.

The effect of amount of catalyst on the oxidation of ethylbenzene is illustrated in Fig. 3.10. It is clear from the plot that the reaction proceeded slowly and gave only

11 % conversion with 0.040 g of catalyst under the above reaction conditions. Increasing the catalyst amount to 0.060 g improved this conversion to 26 % within 8 h of reaction time. Further increment of catalyst amount showed no further improvement in the oxidation of ethylbenzene.
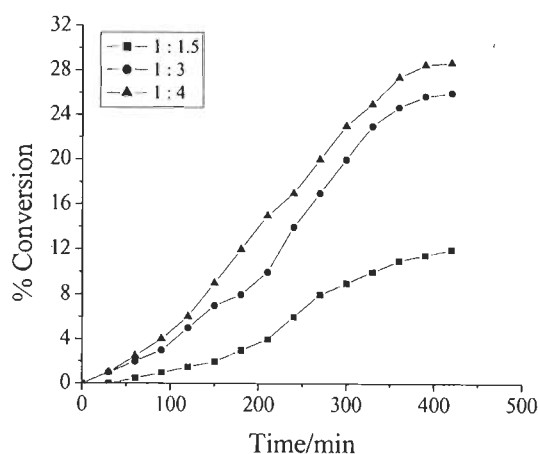
Fig. 3.9. Effect of amount of H_2O_2 on the oxidation of ethylbenzene. Reaction conditions: ethylbenzene (1.06 g, 10 mmol), PS-[VO(ligand)$_n$] (0.060 g), CH$_3$CN (10 ml) and 80 °C.
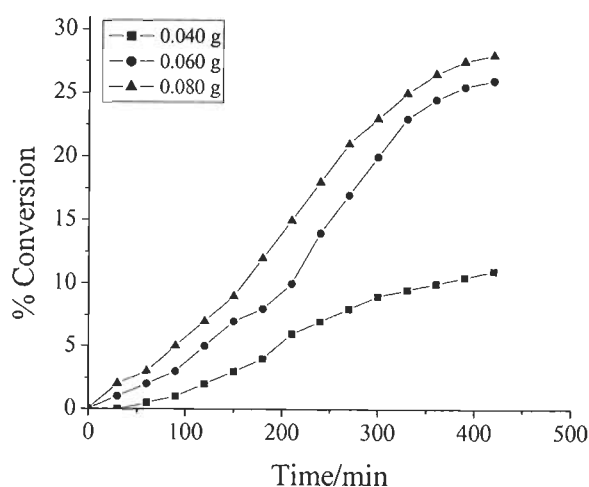
Fig. 3.10. Effect of amount of catalyst on the oxidation of ethylbenzene. Reaction conditions: ethylbenzene (1.06 g, 10 mmol), H_2O_2 (3.34 g, 30 mmol), CH$_3$CN (10 ml) and 80 °C.

Table 3.6 presents the results of ethylbenzene oxidation under the optimised reaction conditions after 8 h of reaction time, while Fig. 3.11 presents the conversion as a function of time. Catalyst PS-[VO(ligand)$_n$] exhibits a maximum of 26 % conversion while PS-[MoO$_2$(ligand)$_n$] and PS-[Cu(ligand)$_n$] gave lower but similar conversions of 17 % and 15 %, respectively. The products formed are independent of catalyst and follow the order: benzaldehyde > phenylacetic acid > acetophenone > 1-phenylethane- 1,2-diol (see Table 3.6). A very small amount of an unidentified product was also noticed. No significant improvement in the oxidation of ethylbenzene was observed beyond 8 h of reaction time. The non-polymer-bound complexes [VO(tmbmz)$_2$], [MoO$_2$(tmbmz)$_2$] and [Cu(tmbmz)$_2$] showed 14, 11 and 9 % conversion of ethylbenzene, respectively, when their 0.030 g amount was used under the above optimised conditions. However, the turnover rates are very low compared to those of their respective polymer-anchored complexes.

Table 3.6. Percentage conversion of ethylbenzene, product selectivity and TOF

Catalyst	Conv. (%)	TOF (h^{-1})	Product selectivity (%)[a]			
			a	b	c	d
[VO(tmbmz)$_2$]	14.0	2.7	69.6	21.1	5.7	3.6
PS-[VO(ligand)$_n$]	26.0	6.0	66.7	23.3	6.2	3.8
PS-[VO(ligand)$_n$][b]	25.4	-	66.7	23.3	6.2	3.8
PS-[VO(ligand)$_n$][c]	24.0	-	66.5	23.4	6.4	3.7
[MoO$_2$(tmbmz)$_2$]	11.0	2.4	71.6	20.2	5.2	3.0
PS-[MoO$_2$((ligand)$_n$]	17.0	4.3	69.7	22.2	4.6	3.5
PS-[MoO$_2$((ligand)$_n$][b]	16.7	-	69.7	22.2	4.6	3.5
PS-[MoO$_2$((ligand)$_n$][c]	15.3	-	69.9	21.9	4.5	3.7
[Cu(tmbmz)$_2$]	9.0	1.7	72.6	20.2	4.2	3.0
PS-[Cu(ligand)$_n$]	15.0	3.5	70.5	21.7	4.5	3.3
PS-[Cu(ligand)$_n$][b]	14.0	-	70.3	21.6	4.7	3.4
PS-[Cu(ligand)$_n$][c]	13.6	-	71.0	20.9	4.6	3.5

[a] For details of abbreviations see Scheme 3.5. [b] First cycle of used catalyst. [c] Second cycle of used catalyst.
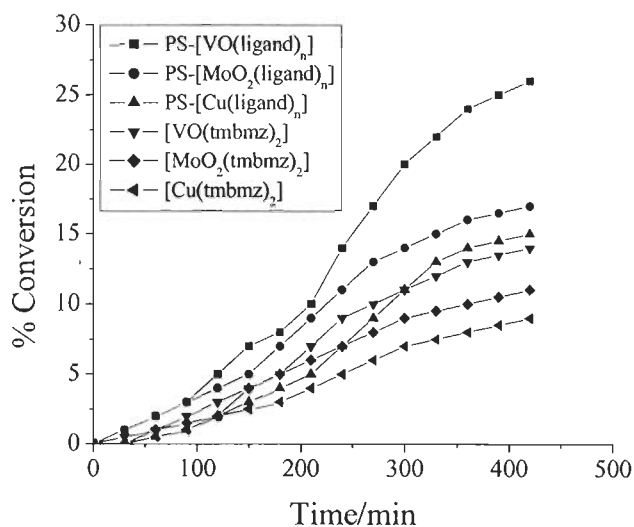
Fig. 3.11. Comparison of catalytic potential of the catalysts on the oxidation of ethylbenzene under optimised conditions. Reaction conditions: ethylbenzene (1.06 g, 10 mmol), H_2O_2 (3.34 g, 30 mmol), catalyst (0.060 g), CH_3CN (10 ml) and 80 °C.

3.3.7. Test for recyclability and heterogeneity of the reaction

The recycle ability of the polymer-anchored catalysts **3.1**, **3.2** and **3.3** were tested for the oxidation of styrene, cyclohexene and ethylbenzene. The reaction mixture after a contact time of 6 h was filtered and the separated catalysts were washed with acetonitrile, dried and subjected to further catalytic reactions under similar conditions. No appreciable loss in the activities (see Tables 3.4, 3.5 and 3.6) were found in all cases, indicating that whatever the actual structures of the metal complexes, these remain unchanged, and the catalysts were active even after the second cycle. The product distributions with time and selectivity of the reaction products are nearly preserved as obtained for fresh catalyst within the experimental error. During catalytic oxidation of styrene, cyclohexene and ethylbenzene, the filtrates collected after separating the solid catalysts were placed into the reaction flasks, and the reaction was continued after adding fresh oxidant for another 2 h. The gas chromatographic analyses showed no further increment in the conversion. This confirms that the reaction did not proceed upon removal of the solid catalyst and hence the catalysis is heterogeneous in nature.

3.3.8. Studies concerning the elucidation of the possible reaction pathway

3.3.8.1. UV-Vis studies

The non-polymer-bound complexes dissolved in methanol were treated with methanolic solutions of H_2O_2 and the progress of each reaction was monitored by electronic absorption spectroscopy. Thus, the titration of $[V^{IV}O(tmbmz)_2]$ dissolved in methanol (ca. 10^{-4} M solution) with two-drop portions of 30 % H_2O_2 dissolved in methanol resulted in the slow weakening of the 240 nm band with decrease in intensity, while the 210 nm band experienced a slight increase in intensity. The bands appearing at 274, 280 and 289(s) nm experienced a slight decrease in intensity. At the same time, the weak shoulder band appearing at 396 nm shifted to 370 nm with increase in intensity. The bands appearing at 524 and 665 nm due to d – d transitions at higher concentration of $[V^{IV}O(tmbmz)_2]$ (ca. 10^{-3} M), slowly disappeared upon addition of H_2O_2. These spectral changes and the presence of an isobestic point at 325 nm suggest the oxidation of V^{IV} and the interaction of the vanadium(V) complex formed with H_2O_2, to give oxoperoxovanadium(V) species [299]. The spectral changes are presented in Fig. 3.12.
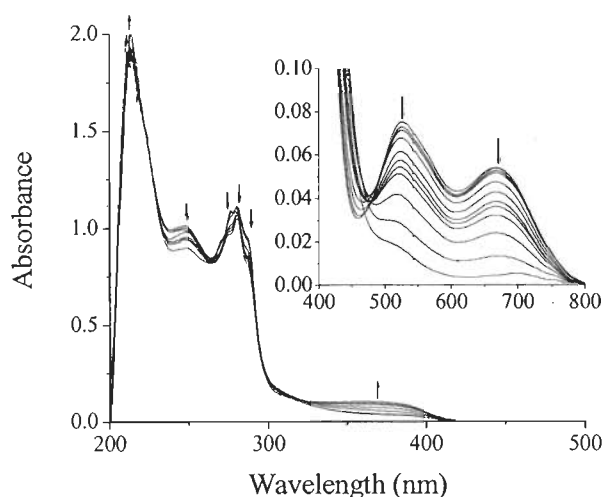
Fig. 3.12. Spectral changes observed during titration of $[V^{IV}O(tmbmz)_2]$ with H_2O_2. The spectra were recorded after successive additions of two-drop portions of H_2O_2 (5 $\times 10^{-4}$ mol of 30 % H_2O_2 dissolved in 10 ml of methanol) to 10 ml of a ca. 10^{-4} M solution of $[VO(tmbmz)_2]$ in methanol. The inset displays equivalent titrations, but with a higher concentration of $[V^{IV}O(tmbmz)_2]$ (ca. 10^{-3} M) dissolved in methanol.

The addition of one-drop portions of 5×10^{-3} mol of 30 % H_2O_2 dissolved in 10 ml of ethanol to a ethanolic solution of [Cu(tmbmz)$_2$] (ca. 10^{-4} M solution) resulted in the gradual increment of the intensity of bands appearing at 274 and 280 nm (see Fig. 3.13). The band appearing at 230 nm slowly shifts to 236 nm with an increase in band maximum, while the band at 297 nm slowly broadens with a slight increase in intensity. The very weak shoulder appearing at 382 nm slowly disappears. At higher concentration (ca. 10^{-3} M in dimethylsulfoxide) [Cu(tmbmz)$_2$)] exhibits a band at 695 nm. This band slowly shifts to 722 nm with a slight decrease in intensity upon treatment with H_2O_2. But further addition of H_2O_2 did not reduce its intensity further as shown in the inset of Fig. 3.13. The spectral changes in the UV region on treatment with H_2O_2 suggest structural changes due to the formation of intermediate peroxo species.
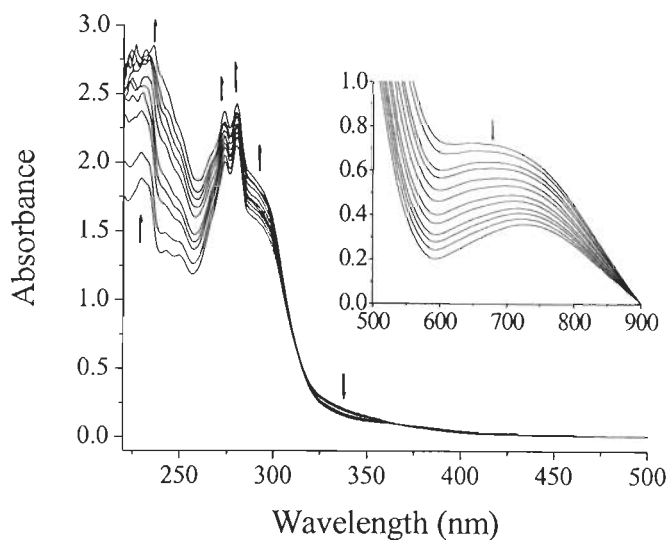
Fig. 3.13. Spectral changes observed during titration of [Cu(tmbmz)$_2$] with H_2O_2. The spectra were recorded after successive additions of two-drop portions of H_2O_2 (5×10^{-3} mol of 30 % H_2O_2 dissolved in 10 ml of ethanol) to 10 ml of ca. 10^{-4} M solution of [Cu(tmbmz)$_2$] in ethanol. The inset displays equivalent titration, but with a higher concentration of [Cu(tmbmz)$_2$] (ca. 10^{-3} M) dissolved in DMSO.

The molybdenum complex [MoO$_2$(tmbmz)$_2$] follows similar spectral changes in the UV region during titration; see Fig. 3.14. The weak shoulder band appearing at 375 nm slowly shifts to 370 nm with a slight increase in intensity (see inset of Fig. 3.14). This shift is interpreted as due to the formation of an oxomonoperoxomolybdenum(VI) species. Formations of such peroxomolybdenum(VI) species by the reaction of dioxidomolybdenum(VI) complexes with H$_2$O$_2$ are well known [298].
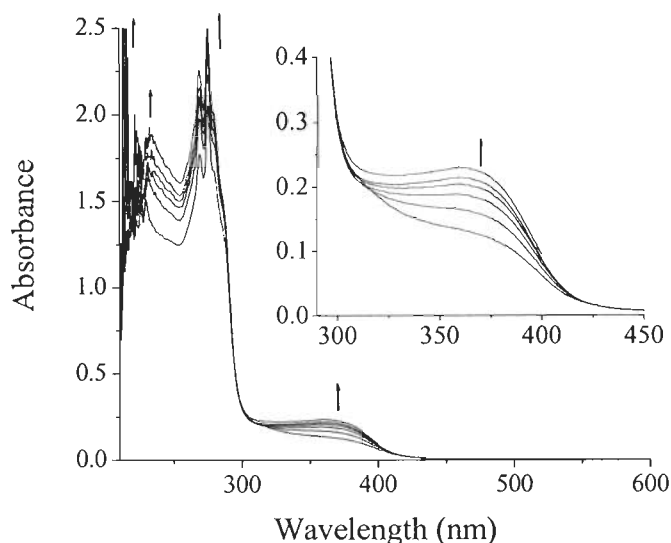
Fig. 3.14. Spectral changes observed during titration of [MoO$_2$(tmbmz)$_2$] with 30 % H$_2$O$_2$; the spectra were recorded after successive additions of 1 drop portions of H$_2$O$_2$ (5 × 10^{-4} mol of 30 % H$_2$O$_2$ dissolved in 10 ml of methanol) to 10 ml of ca. 1×10^{-4} M solution of [MoO$_2$(tmbmz)$_2$] in methanol.

3.3.8.2. EPR Spectral studies

The EPR spectra of powdered samples of the polymer-anchored V^{IV}O- and Cu^{II}-complexes were recorded at room temperature and those of the non-polymer-bound complexes were obtained from "frozen" solutions (77 K). The spectra obtained for the polymer-anchored V^{IV}O-complex and that of [V^{IV}O(tmbmz)$_2$] in DMF are presented in Fig. 3.15. The spectrum of [V^{IV}O(tmbmz)$_2$] in MeOH/DMSO solution is almost identical to the one in DMF.
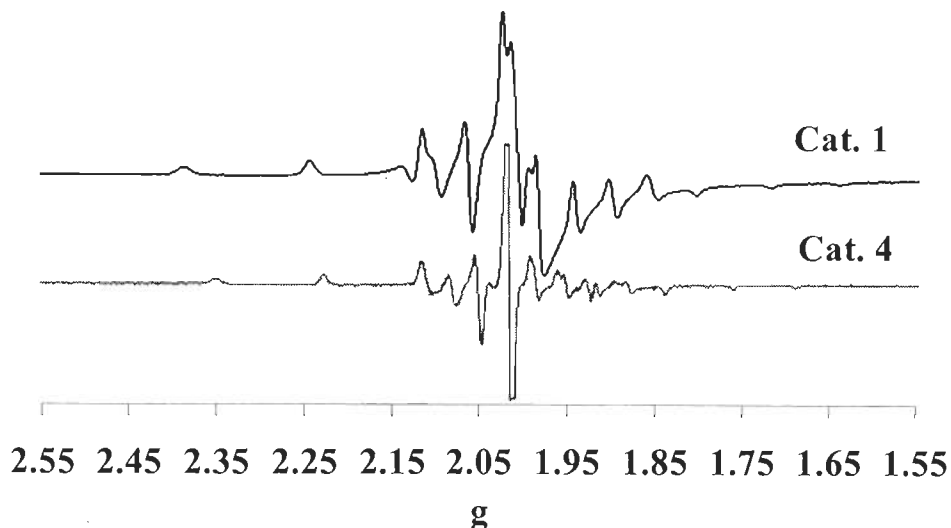
Fig. 3.15. Powder EPR spectrum of fresh catalyst **3.1** at room temperature and of $[V^{IV}O(tmbmz)_2]$ (**3.4**) in DMF at 77K.

The spectrum of **3.1** is characteristic of magnetically diluted $V^{IV}O$-complexes; the resolved EPR pattern indicates that the vanadium centers are well dispersed in the polymer matrix. The EPR spectrum of a powdered sample of **3.1** after being used for catalytic reactions is equal to that of the fresh catalyst. The spectra were simulated and the spin Hamiltonian parameters obtained [235] for **3.1** are $g_\perp = 1.978$, $g_\parallel = 1.942$, $A_\perp = 61.8\times10^{-4}$ cm^{-1} and $A_\parallel = 167.9\times10^{-4}$ cm^{-1}, and for $[V^{IV}O(tmbmz)_2]$ in DMF: $g_\perp = 1.986$, $g_\parallel = 1.966$, $A_\perp = 48.7\times10^{-4}$ cm^{-1} and $A_\parallel = 147.6\times10^{-4}$ cm^{-1} (in MeOH/DMSO the parameters obtained are very similar: $g_\perp = 1.987$, $g_\parallel = 1.967$, $A_\perp = 48.4\times10^{-4}$ cm^{-1} and $A_\parallel = 146.6\times10^{-4}$ cm^{-1}). While the EPR spectrum of $[V^{IV}O(tmbmz)_2]$ (**3.4**) is in agreement with a N_2S_2 binding mode, the spectrum for the $V^{IV}O$-supported complex **3.1** clearly indicates that there is no thiolate donor coordinated in equatorial position.

If any oxidisable sulfur atom existed in catalyst **3.1**, we would expect it would be oxidised during the catalytic reactions performed. If this indeed occurs, it does not affect the EPR spectra recorded and, as mentioned, the EPR of fresh and used catalyst **3.1** are equal. For catalyst **3.3** also, no differences were detected in the EPR spectra

obtained at room temperature for powdered samples of the fresh polymer-anchored Cu^{II}-complex **3.3** and those of the corresponding spent catalyst.

After swelling with DMF, and freezing down to 77 K, the features of the powder EPR spectrum of the polymer-bound Cu^{II}-complex **3.3** are the same but the spectrum shows slightly better resolution, due to a slight decrease in the dipolar interactions. The spectra were simulated and the spin Hamiltonian parameters obtained [235] for **3.3** are $g_{\parallel} \approx 2.286$, and $A_{\parallel} \approx 150 \times 10^{-4}$ cm^{-1}. Assuming a planar structure as a reference, this is in agreement with a N_2O_2 donor set and/or with a significant distortion toward the tetrahedron. It does not agree with a N_2S_2 donor set (at least in a first consideration). It may be consistent with a N_3O or even N_4 donor set assuming a tetrahedral distortion [302].

Figure 3.16 shows spectra of catalyst **3.3** and of solutions of $[Cu^{II}(tmbmz)_2]$ in DMF before and after the addition of increasing amounts of H_2O_2. At least two distinct components are detected, one with $g_{\parallel} = 2.335$ and $A_{\parallel} \approx 155 \times 10^{-4}$ cm^{-1}, and other one with $g_{\parallel} \approx 2.40$ and $A_{\parallel} \approx 130 \times 10^{-4}$ cm^{-1}. Assuming a planar structure as a reference, this is in agreement with a NO_3 donor set in the first complex, and a N_3O or N_4 donor set in the 2nd complex. Upon further addition of H_2O_2 few relevant differences are seen in the positions of the lines; apparently only a change in the relative intensities of some lines may be seen. It is possible that upon addition of H_2O_2 some of the sulfur atoms present experience further oxidation, producing additional S=O groups (eg. R-SO_2^- or R-SO_3^-) that may participate in the bonding to the metal centre. If this indeed occurs, it does not affect significantly the catalytic activity of **3.3** (see above).

Addition of styrene to the solution, corresponding to spectrum (f) of Fig. 3.16, where 3 eq. of H_2O_2 have been added, yields a different EPR spectrum; from the features of this spectrum the following spin Hamiltonian parameters were obtained: $g_{\parallel} \approx 2.34$ and $A_{\parallel} \approx 158 \times 10^{-4}$ cm^{-1}, not much different from the values of one of the components detected in the absence of styrene.
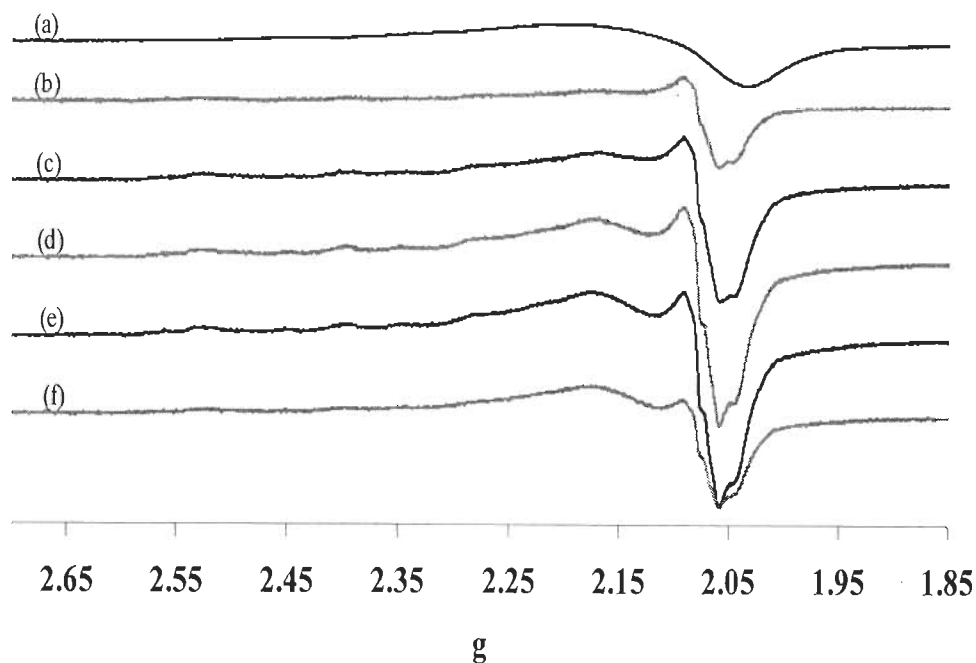
Fig. 3.16. Powder EPR spectrum of fresh catalyst **3.3** at room temperature (a) and of $[Cu^{II}(tmbmz)_2]$ **(3.6)** in DMF at 77K before (b) and after addition of increasing amounts of H_2O_2: (c) 1 eq.; (d) 2 eq. and (e) 3 eq. of H_2O_2. Spectrum (f) was recorded with the same solution of (e) after adding 100 equivalents of styrene.

Figure 3.17 includes spectra of $[Cu^{II}(tmbmz)_2]$ **(3.6)** in DMF before and after addition of 100 equivalents of styrene. In the presence of styrene the EPR spectrum shows clear changes, possibly due to the coordination of styrene to the Cu^{II} centre. From the features of this spectrum the following spin Hamiltonian parameters were obtained: $g_{\parallel} = 2.313$ and $A_{\parallel} = 161\times10^{-4}$ cm^{-1} for the major species present. Assuming a planar structure as a reference, this is in agreement with a higher extent of electron delocalisation from the d orbitals to the ligands (as compared with $[Cu^{II}(tmbmz)_2]$ **(3.6)** in the absence of styrene). These values are also consistent with a significant tetrahedral distortion.

Figure 3.18 includes the EPR spectrum of $[V^{IV}O(tmbmz)_2]$ (**3.4**) in a MeOH/DMSO solution (a), and the spectra obtained after successive additions of a diluted MeOH solution of H_2O_2. Spectrum (a) ($g_{\parallel} = 1.967$ and $A_{\parallel} = 146.6 \times 10^{-4}$ cm^{-1}), and the corresponding $V^{IV}O$-species spectra (b-e) are consistent with a N_2S_2 binding mode in equatorial position. Upon addition of H_2O_2 portions, a second complex species progressively forms with EPR parameters ($g_{\parallel} = 1.939$ and $A_{\parallel} = 176.4 \times 10^{-4}$ cm^{-1}); the $V^{IV}O$ is also progressively oxidised to V^V, and the intensity of the EPR spectra progressively decreases. According to the $g_{\parallel}$ and $A_{\parallel}$ values obtained, in this latter complex the binding mode appears to be either NO_3 or O_4.

6 in DMF

6 + styrene

| 2.65 | 2.45 | 2.25 | **g** | 2.05 | 1.85 |
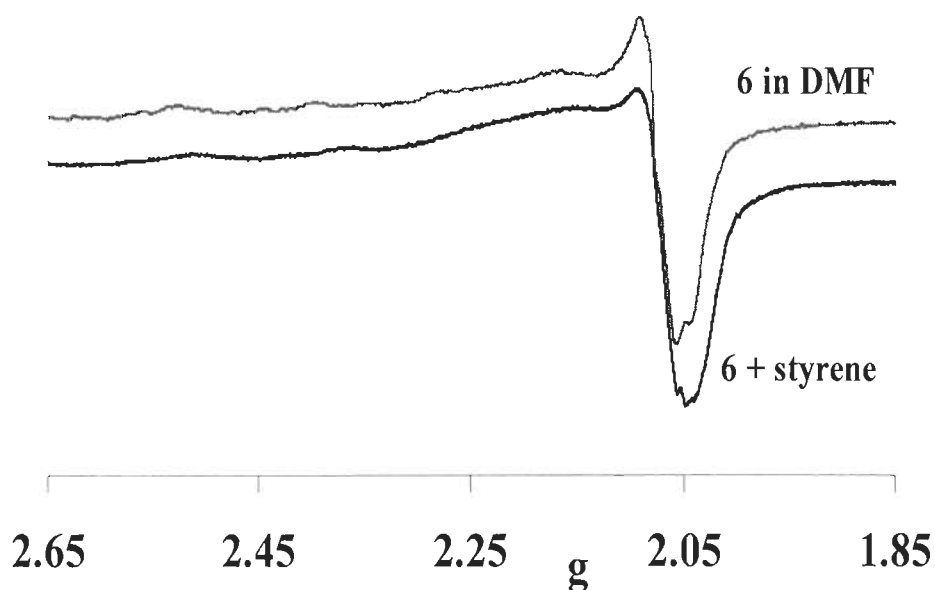
Fig. 3.17. EPR spectra of solutions of $[Cu^{II}(tmbmz)_2]$ (**3.6**) in DMF before and after addition of 100 equivalents of styrene.
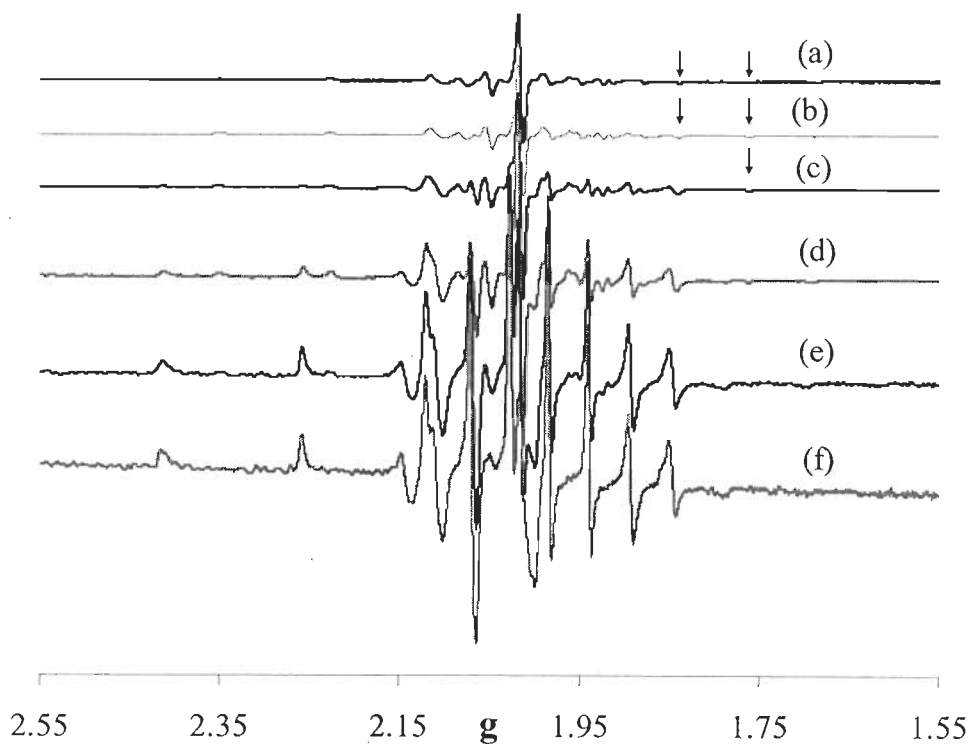
Fig. 3.18. EPR spectra of frozen (77 K) solutions of (a) [$V^{IV}O(tmbmz)_2$] (**3.4**) in MeOH/DMSO (violet solution) and after addition of increasing amounts of a methanolic solution of H_2O_2: (b) 0.25 eq.; (c) 0.75 eq.; (d) 1.0 eq.; (e) 1.25 eq.; (f) 1.75 eq. of H_2O_2 (greenish-orange solution);. The corresponding visible spectra follow the evolution shown in the inset of Fig. 3.12. The arrows indicate the position of the high field A∥ lines in spectra (a)-(c). Upon addition of H_2O_2 a 2nd species is detected and its relative amount increases from (b) to (f).

3.3.8.3. ^{51}V NMR studies

We have also recorded, see e.g. Fig. 3.19, the ^{51}V NMR spectra of some of these solutions, and a peak at ca. −546 ppm is clearly observed even upon adding only 0.75 eq. H_2O_2. In these solutions both V^{IV} and V^V species exist, and both the EPR and the ^{51}V NMR could be recorded.

Gradually adding H_2O_2 to a ca. 5 mM solution of [$V^{IV}O(tmbmz)_2$] (**3.4**) in DMF progressively oxidises the vanadium centre. After the addition of ~2 and 3 eq. of H_2O_2 two peaks could be clearly detected in the ^{51}V NMR spectra at −520 and −566

ppm, which may be tentatively assigned to V^V-ligand and V^V-(O-O)-ligand species, respectively, possibly also containing coordinated DMF.
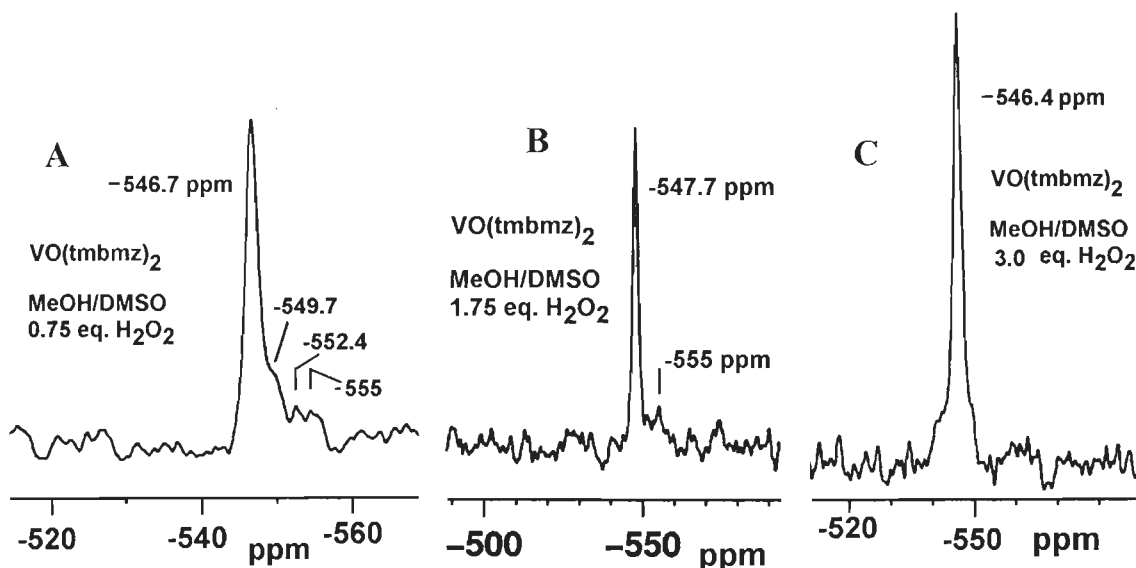
Fig. 3.19. ^{51}V NMR spectra of solutions (c) and (f) of Fig. 3.18 (spectra **A** and **B**, respectively), and of the same solution after adding up to 3 eq. of H_2O_2, i.e. 3 moles of H_2O_2 per mole of complex (spectrum **C**). The solution of spectrum **C** has a greenish colour.

ESI-MS spectra were also recorded for the solution of $[V^{IV}O(tmbmz)_2]$ (**3.4**) in MeOH/DMSO after addition of 3.0 eq. of H_2O_2 both in the positive and in the negative modes. In the positive mode peaks are seen at m/z of 165 (tmbmz.H^+ = L.H^+) and m/z = 327.1. This latter peak is one of the most intense peaks in the ESI-MS in the positive mode and possibly corresponds to the disulphide of tmbmz (L-L.H^+). A peak at m/z = 409 may correspond to the $V^VO_2(L-L)^+$ species.

In the negative mode there are several peaks between m/z = 363.8 and m/z = 440.9 that approximately correspond to a difference in MW of an O atom. We can suggest the following assignments: m/z = 363.8 (very intense): $V^{IV}O(L)_2^-$; m/z = 409.8 (very intense): $V^VO_2(L)_2^-$; m/z = 424.9 (medium intensity): $V^VO(O-O)(L)_2^-$; m/z 440.9 (medium/weak intensity): $V^VO_2(O-O)(L-L)^-$. Alternative assignments involving the

production of the corresponding complexes of oxidised products of tmbmz: tmbmz-SO_2^- and tmbmz-SO_3^-, could also be plausible.

These experiments confirm the oxidation of V^{IV} to V^V upon addition of H_2O_2 to a solution of $[V^{IV}O(tmbmz)_2]$ (**3.4**) (decrease of the EPR signal and detection of ^{51}V NMR spectra), and the oxidation of the thiol group with the formation of the corresponding disulfide. It is possible that other oxidation products have formed. The peak of the ^{51}VNMR spectra at ca. –547 ppm in Fig. 3.19 possibly corresponds to $V^VO_2(L-L)^+$. The peak at –555 ppm could correspond to $V^VO_2(O-O)(L-L)^-$.

Addition of an excess of styrene to the solution of spectrum **C** of Fig. 3.19 results in a slow reduction of the V(V)-centre, an increase of intensity of the corresponding EPR spectra, and a spectrum distinct from those of (a)-(f) shown in Fig. 3.18, where only the species with EPR parameters $g_{||} \sim 1.939$ and $A_{||} \sim 176 \times 10^{-4}$ cm^{-1} is detected. Therefore, the tmbmz$^-$ ligand is no longer present in this solution. After several hours the solution was blue but the EPR spectrum was identical. No clear ^{51}V NMR spectrum could be recorded for these solutions containing styrene. However, as mentioned above, after addition of 3 eq. of H_2O_2 to a solution of $[V^{IV}O(tmbmz)_2]$ (**3.4**) in DMF, two peaks could be detected in the ^{51}V NMR spectrum at –520 and –566 ppm; after addition of an excess of styrene to this solution no new peaks were detected.

Addition of a ~100-fold excess of styrene to a solution of $[V^{IV}O(tmbmz)_2]$ (**3.4**) in DMF yielded only a slightly different EPR spectrum. By simulation of this spectrum the $g_{||} = 1.966$ and $A_{||} = 149 \times 10^{-4}$ cm^{-1}, very close to those of (**3.4**) in DMF: $g_{||} = 1.966$ and $A_{||} = 147.6 \times 10^{-4}$ cm^{-1}. This means that, even if some coordination of styrene occurs forming $[V^{IV}O(tmbmz)_2(styrene)]$, it forms a very weak bond, possibly *trans* to the V=O.

3.3.8.4. Nature of complex species in catalysts 3.1 - 3.3

The reaction of chloromethylated polystyrene with 2-thiomethylbenzimidazole did not yield clean PS-S-tmbmz, according to Scheme 3.2. The analytical results

obtained (see experimental section), namely the S/N ratio of the PS-ligand (**3.II**) obtained, does not fully agree with the formation of PS-S-tmbmz, and products corresponding to a higher % of sulfur also form. It is possible that, before and after the ligand binds to the solid, the thiol group oxidises to disulphide, but other oxidation products may also form. In fact it is known that, in oxidising conditions, thiolate compounds (RSH) may yield RSSR, RSO_2^- and RSO_3^- products. Depending on the nature of R, $RSCH_3$ (and the corresponding oxidation products may also form) [303]. Schemes 3.6 and 3.7 represent some of the products that may form.
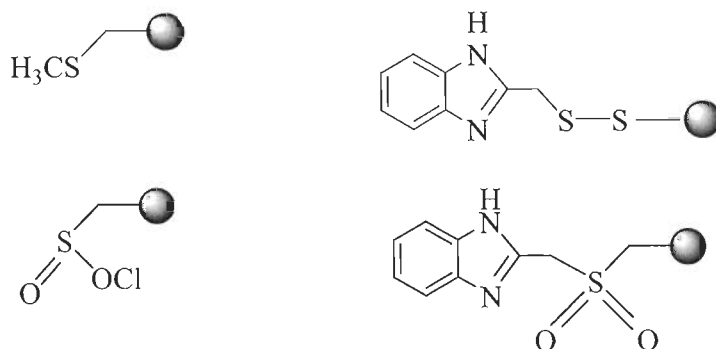
Scheme 3.6. Additional possible products of reaction of Htmbmz with chloromethylbenzene in the experimental conditions used. Some of these products originate a higher S/N ratio in the final catalyst than that of Htmbmz.
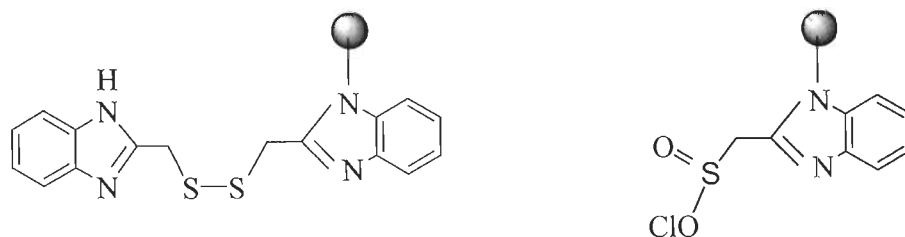
Scheme 3.7. Additional possible products of reaction of Htmbmz with chloromethylbenzene in the experimental conditions used.

If the disulfide forms in solution before the reaction of Htmbmz with chloromethylated polystyrene, or if the thiol group is oxidised further, then the NH group of benzimidazole may react with the –CH$_2$Cl group of chloromethylated polystyrene, forming products such as those included in Scheme 3.7. This method of anchoring has been applied by some of us to other ligands as well [77, 78, 184, 186]. Miller and Sherrington [87] have shown the covalent attachment of the imine nitrogen of 2-(2-pyridylimidazole) to polystyrene by the reactions of ligands and chloromethylated polystyrene in refluxing toluene. The corresponding non-polymer-bound complexes have also been isolated similarly.

It is not possible to characterise the exact nature of the prepared catalysts PS-[VO(ligand)$_n$] (**3.1**), or PS-[MoO$_2$(ligand)$_n$] (**3.2**) and PS-[Cu(ligand)$_n$] (**3.3**), but the stoichiometry of the (metal ion) : (tmbmz core) is close to 1 : 2. This is compatible with the elemental analyses, spectroscopic (IR and electronic) studies, field-emission scanning electron micrographs (FE-SEM), energy dispersive analyses by X-ray (EDAX) and thermo gravimetric patterns. What EPR further indicates is that for PS-[V^{IV}O(ligand)$_n$] and PS-[Cu(ligand)$_n$] the oxidovanadium(IV) and Cu(II) are in fact present in the solid catalysts and that the binding donors are N$_2$O$_2$. The O-donors may originate either from S=$\underline{O}$ or from DMF ligands or both, and it is not possible to sort out the exact nature of the binding mode(s) present.

3.3.8.5. Possible reaction steps

Peroxo-complexes may be able to transfer oxygen to aromatic hydrocarbons. However, alkanes are much less readily hydroxylated than aromatic hydrocarbons, and mixtures of alcohols and ketones are formed. The mechanism of oxygen transfer of peroxo-metal complexes to nucleophilic substrates has been a matter of considerable debate, and overall two main alternatives have been proposed. One proceeds through a simple bimolecular mechanism involving the nucleophile and the peroxo-metal complex; the other mechanism involves the formation of an intermediate resulting either from coordination of the substrate to the metal or form steps involving peroxy-olefin intermediates.

To get information on the reaction pathway and the intermediate species formed during oxidation of the substrates, we performed several spectroscopic studies with solutions of the non-polymer-bound complexes **3.4 - 3.6** (see above). As the non-polymer-bound complexes prepared are not good models of the PS-(ligand)$_n$–M species formed, these studies only give rather indirect information about the mechanisms of reactions promoted by these catalysts.

We now present three alternative reaction paths for the reaction promoted by the vanadium catalysts. In all cases the V^{IV}-complexes are oxidised to V^VO_2-complexes which then react with H_2O_2. When the H_2O_2 is consumed, the V^VO_2-complexes are reduced back to V^{IV}-complexes by the olefin. To apply these reaction pathways to the Cu^{II} (and Mo^{VI}) centers, the V=O and VO$_2$ cores can be substituted by Cu^{II} (or $Mo^{VI}O$ and $Mo^{VI}O_2$), and the initial and final oxidation steps ($V^{IV} \leftrightarrow V^V$) do not exist.

In one alternative (Scheme 3.8), similar to the mechanisms outlined in refs. [304] and [305] for the epoxidation of norbornene, no coordination of the olefin to vanadium occurs, but there is an attack of the olefin to a transient vanadyl diradical species (O=V^{IV}-O-O˙), forming a vanadium-peroxy-olefin intermediate. In the following steps, breakage of bond between the O atoms leads to the formation of the epoxide, this then yield the final products.

In a second alternative (Scheme 3.9) a peroxo (or oxohydroxoperoxo) coordinated species forms, and there is a nucleophilic attack of the olefin, yielding the epoxide and the initial V^VO_2-complex. This mechanism therefore corresponds to a simple bimolecular mechanism involving the reaction of the nucleophile and the peroxo-metal complex.

In a third alternative (Scheme 3.10) the V^V-oxoperoxocomplex forms, which upon coordination of the substrate and insertion of the bound alkene into one of the metal-peroxo bonds, followed by collapse of the resulting peroxometallocycle, yields the epoxide [304].
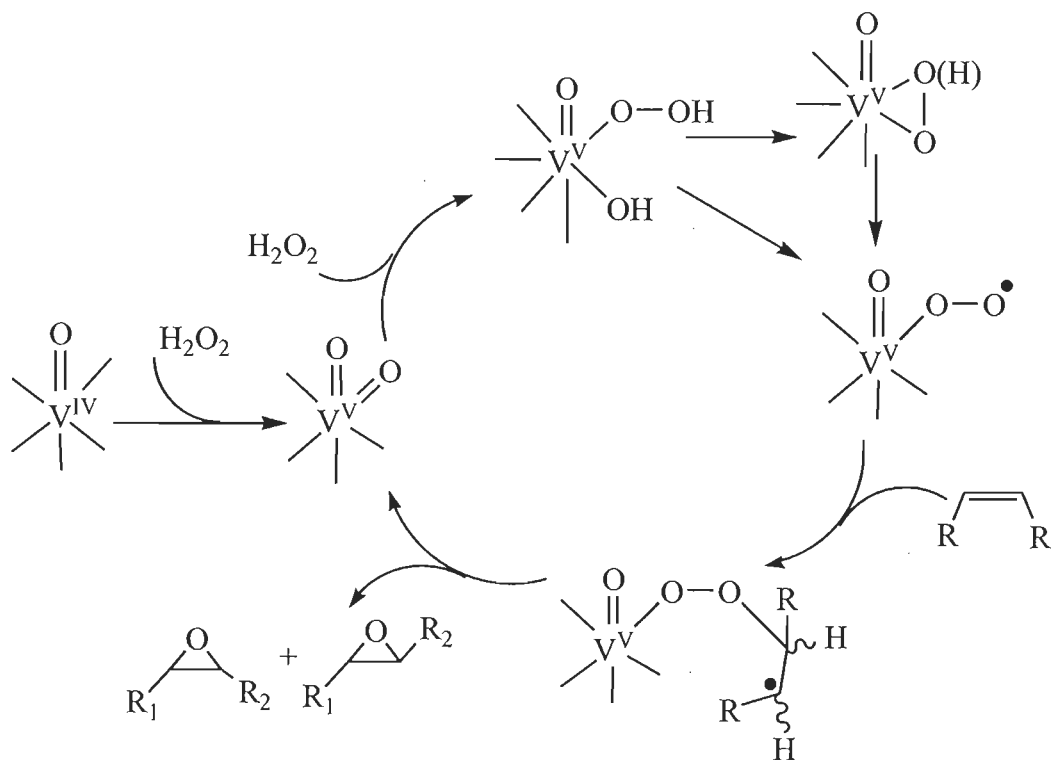
Scheme 3.8. Outline of one possible reaction pathway for the epoxidation of olefins involving a transient vanadyl diradical species and the formation of a vanadium-peroxy-olefin intermediate. The epoxides formed experience further oxidation (see text). The donor atoms of the V^{IV}- and V^{V}-intermediates are N and O atoms from tmbmz of the non-polymer-bound complexes or from the PS-ligand; solvent molecules may also coordinate.
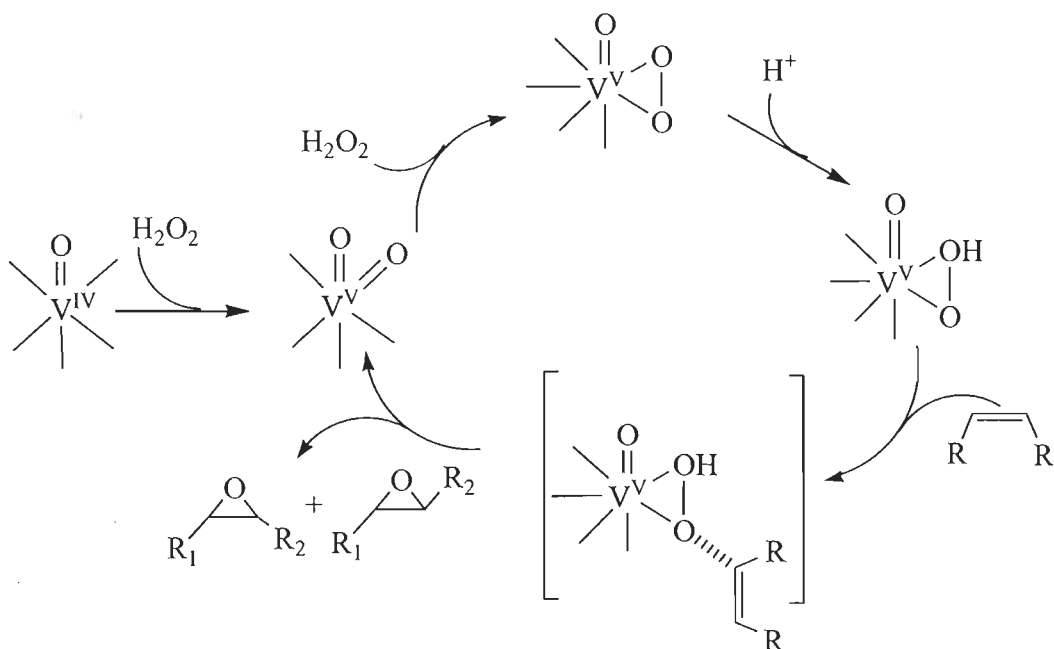
Scheme 3.9. Outline of a second possible reaction pathway for the epoxidation of olefins involving a simple bimolecular mechanism: the nucleophile and the peroxo-metal complex react.
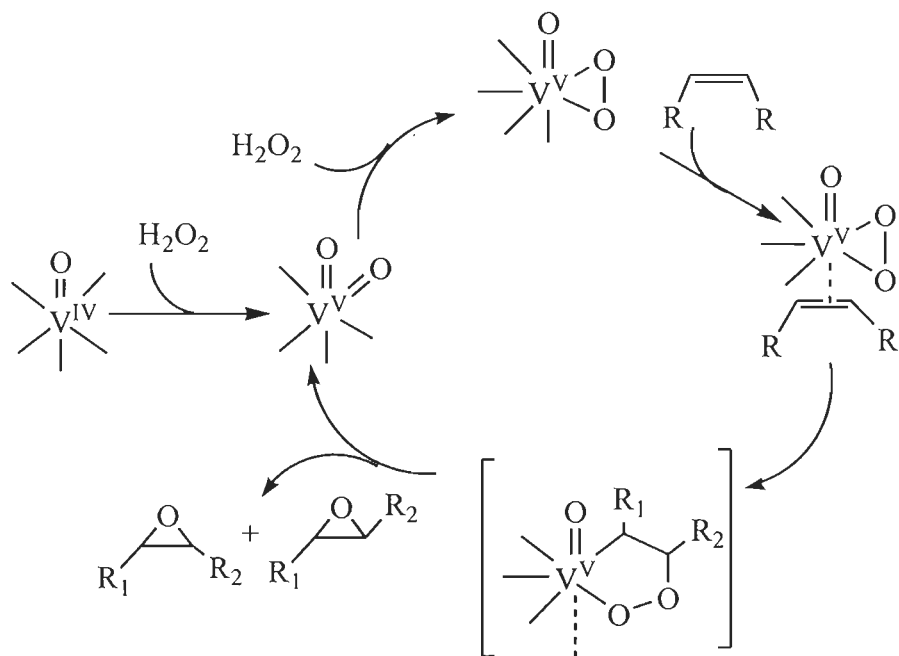
Scheme 3.10. Outline of a third possible reaction pathway for the epoxidation of olefins involving the formation of a peroxometallocycle.

As mentioned above, other secondary mechanisms also operate [305]. The formation of monohydroxylated products may be due to the acid-catalysed hydration of the olefin. Rearrangement of the epoxide to ketone, or secondary oxidation may explain the formations of (i) benzaldehyde from styrene, (ii) 2-cyhexene-1-one from cyclohexene and (iii) acetophenone from ethylbenzene.

To get information on the reaction pathway and the intermediate species formed during oxidation of the substrates, methanolic solutions of the non-polymer-bound complexes were treated with methanolic solutions of aqueous H_2O_2, and the progress of the reaction was monitored by electronic absorption spectroscopy and also by EPR (for $V^{IV}O$- and Cu^{II}-complexes).

Figure 3.12 presents the UV-Vis spectral changes observed during titration of $[V^{IV}O(tmbmz)_2)]$ with H_2O_2 in methanol. These and the EPR spectra clearly indicate the oxidation of the V^{IV}- to V^V-species. This is also consistent with the appearance of several ^{51}V NMR peaks (Fig. 3.19). Whatever the exact nature of the V^V-species formed (see above), oxoperoxocomplexes probably form, which upon addition of styrene leads to the substrate reaction. In the case of the similar system with [VO(sal-eta)]$_2$ [H$_2$sal-eta = Schiff base derived from salicylaldehyde and 2-aminoethanethiol], quite clear evidence was found for the coordination of styrene to vanadium [78]. In the present system no clear evidence for the binding of styrene to vanadium (IV) or vanadium(V) was found, so the reaction pathways involving the coordination of the substrates (e.g. Scheme 3.9) may be considered less plausible.

Figure 3.13 presents the UV-Vis spectral changes observed for the Cu^{II}-complex. At least three types of peroxo species, *viz.* side-on Cu^{II}-$(\mu$-η^2-peroxo)-Cu^{II}, bis(μ-oxo-Cu^{III}) and Cu^{II}-O-O-H (copper-hydroperoxide), have been reported in literature during catalytic action [306–308]. As copper complexes supported on polymers are expected to be monomeric, the formation of [(HOO)-Cu(ligand)] as intermediate species may be expected upon interaction with H_2O_2. These intermediates are expected to transfer the oxygen atoms to the substrates to give the products. However, the amount of hydroperoxide species is probably low and no clear change is detected in the EPR and UV-Vis spectra recorded that might be assigned to it (see above). Moreover, with the Cu^{II} complexes the formation of peroxo or hydroperoxo

species is not so favorable as with vanadium or molybdenum and the conversions are lower. The redox reactions involving Cu^{II}/Cu^{III} species are also not as easy as with the V^{IV}-/V^{V}-complexes.

For $[Cu^{II}(tmbmz)_2]$ (**3.6**) in DMF, we obtained evidence for the coordination of styrene to the Cu^{II} centre; this supports a reaction pathway with steps similar to those of the "cycle" of Scheme 3.10. However, a mechanism such as that outlined in the cycle of steps of Scheme 3.9 cannot be ruled out.

With MoO_2-complexes the formation of monoperoxo-complexes, e.g. $MoO(peroxo)(ligand)_n$ has been confirmed by many authors [e.g. 309]. The spectral changes observed in Fig. 3.14 as H_2O_2 is added are in fact compatible with the formation of an oxomonoperoxomolybdenum(VI) species. No further studies were done with this system to confirm the formation of intermediates, but we do not expect the steps outlined in Scheme 3.8 to be favorable, as a change in oxidation state of the Mo centre is involved.

The reaction pathways for the supported catalysts **3.1 - 3.3** probably occur by steps such as those outlined in Schemes 3.8 – 3.10. However, as the nature of the catalysts is not known with certainty and only EPR could be applied to give information on the binding modes (not possible for Mo^{VI}), we do not have much data to suggest intermediates or to further discuss the mechanisms operating.

The mechanism of the oxidation of alkanes and alcohols is normally considered consistent with single transfer steps [264]. For the vanadium complexes, the formation of an oxoperoxovanadium(V) is usually assumed. For hydroxylation of benzene either (i) a mechanism occurs in which the oxoperoxovanadium(V) undergoes intramolecular electron transfer to give a V^{IV}-$(O_2{}^{\bullet}$-$)$ biradical, which inserts into aromatic or aliphatic C-H bonds [310], or (ii) the reaction occurs via the radical anion of the vanadium(V) complex [311]. Other authors have also reported radical mechanisms involving alkylhydroperoxide intermediates for oxidation of alkanes, alkenes and arenes [312].

3.4. CONCLUSIONS

Polymer-anchored complexes: PS-$[VO(ligand)_n]$, PS-$[MoO_2(ligand)_n]$ and PS-$[Cu(ligand)_n]$ have been prepared from the reaction of Htmbmz and chloromethylated

polystyrene, followed by the reaction of the anchored ligand with the metal precursors. The nature of the tmbmz core is not fully retained upon anchoring to the polystyrene matrix, oxidation products of the thiolate group being formed. The anchored compounds were characterised by elemental analyses, spectroscopic (IR and electronic) studies, field-emission scanning electron micrograph (FE-SEM), energy dispersive analyses by X-ray (EDAX) and thermo gravimetric patterns, and EPR. EPR studies were especially useful to confirm that the $V^{IV}O$- and Cu^{II}-complexes are magnetically diluted and well dispersed in the polymer matrix, and to give evidence for the binding modes which predominantly involve N_2O_2 donors.

Catalytic potentials of these complexes have been tested for the oxidation of styrene, cyclohexene and ethylbenzene using 30 % H_2O_2 as an oxidant under optimised reaction conditions previously determined for the PS-[VO(ligand)$_n$]. Oxidation of styrene varied in the order: PS-[VO(tmbmz)$_2$] (81 %) > PS-[MoO$_2$(tmbmz)$_2$] (68 %) > PS-[Cu(tmbmz)$_2$] (57 %), the order of selectivity of the three main products being: benzaldehyde > 1-phenylethane-1,2-diol > styrene oxide. In the oxidation of cyclohexene, a maximum of 86 % conversion was obtained by PS-[VO(ligand)$_n$], followed by 66 % with PS-[MoO$_2$(ligand)$_n$] and 51 % with PS-[Cu(ligand)$_n$]; here the selectivity of products varied in the order: cyclohexane-1,2-diol > 2-cyclohexene-1-one > cyclohexeneoxide. At least four reaction products with the selectivity order: benzaldehyde > phenylacetic acid > acetophenone > 1-phenylethane-1,2-diol have been obtained during the oxidation of ethylbenzene. The net conversion of ethylbenzene obtained by the polymer-anchored catalysts is in the range 15 – 26 %, lower than for the oxidation of the alkenes. These catalysts do not leach during catalytic reactions and are recyclable up to three cycles with not much loss in their activities. It has been observed that non-polymer-bound complexes are also active catalysts, but their activities are generally lower than the corresponding anchored complexes; turn over frequency, stability, recycle ability and operational flexibility make the polymer-anchored catalysts better than the non-polymer-bound complexes.

Possible mechanisms are outlined. In all cases peroxo or peroxy-metal complexes form, and at least for the [Cu(tmbmz)$_2$] **3.6** and less clearly for [VO(tmbmz)$_2$] **3.4**, evidence was also obtained for the coordination of styrene.

*****

112

Chapter-4

Polymer-bound oxidovanadium(IV) and dioxidovanadium(V) complexes as catalyst for the oxidative desulfurization of model organosulfur compounds in diesel

4.1. INTRODUCTION

The removal of sulfur compounds from petroleum products has attracted attention of many researchers to fulfill the demand of environment friendly fuels. Sulfur compounds present in petroleum products are highly undesirable because they are not only harmful to health but also responsible for air pollution and acid rains. There are many ways to remove sulfur compounds from petroleum products. Hydrodesulfurization is one of the common methods to produce ultra low sulfur fuel but this process needs high temperature and pressure; such conditions, thus, require large consumption of hydrogen which reduces the life of the catalyst. The oxidative desulfurization is, therefore, another way to get ultra low sulfur fuel in mild reaction conditions like low temperature and ambient pressure. In oxidative desulfurization process, sulfur containing compounds are oxidised to sulfones followed by separation through extraction, distillation, decomposition [313–318] or adsorption on the alumina [319–325]. For oxidative desulfurization, several oxidants like H_2O_2, tert-butylhydroperoxide (TBHP) [313, 326–331] and organic acids have been reported [332–334]. But H_2O_2 is the commonly used as it is cheap, non-polluting and easily available commercial oxidant. The oxidation of organosulfur compounds such as sulfides, and dibenzothiophene (DBT) and their corresponding alkyl derivatives to sulfones [315, 329, 335–337] by H_2O_2 over various catalysts such as acetic acid [338–344], formic acid [345–346, 334], polyoxometalate [334, 347–349] and Ti-containing molecular sieves [313, 350] have been reported. The oxidation of organosulfur compounds has also been processed using various redox solid catalysts like Ti-containing zeolites (TS-1, Ti-beta) [313, 351–353], titanium-hexagonal mesoporous silica [354, 355], V- or Mo-containing molecular sieves [356, 357], solid bases such as hydrotalcites [315, 328] etc.

Oxidovanadium complexes have been used as catalyst for the oxidation of various organic compounds, epoxidation of alkenes and allyl alcohols, oxidative halogenations, and the oxidation of organic sulfides [358–366]. However, due to their homogeneous nature these catalysts are difficult to separate from the reaction mixture

and, thus, can not be recycled. Recently we have shown that grafting of vanadium complexes onto polymer support, not only improved their catalytic activities but catalysts became recoverable and recyclable also [76–78, 367]. In the present work, we report polymer-bound oxidovanadium(IV) and dioxidovanadium(V) complexes of polymer-bound ligand, PS-Hfsal-dmen (**4.I**, Scheme 4.1) for the oxidation of thiophene derivatives with sulfur > 500 ppm present in diesel. No catalytic desulfurization reaction using polymer-bound vanadium complexes as catalyst has been reported in the literature [138]. Polystyrene back bone provides extra stability to the catalysts and makes the catalytic reaction heterogeneous in nature. The corresponding neat complexes [VO(sal-dmen)(acac)] and [VO$_2$(sal-dmen)] with the ligand, Hsal-dmen (**4.II**) having similar donor atoms have also been prepared.

PS-Hfsal-dmen (**4.I**)   Hsal-dmen (**4.II**)   H$_2$fsal-dmen (**4.III**)
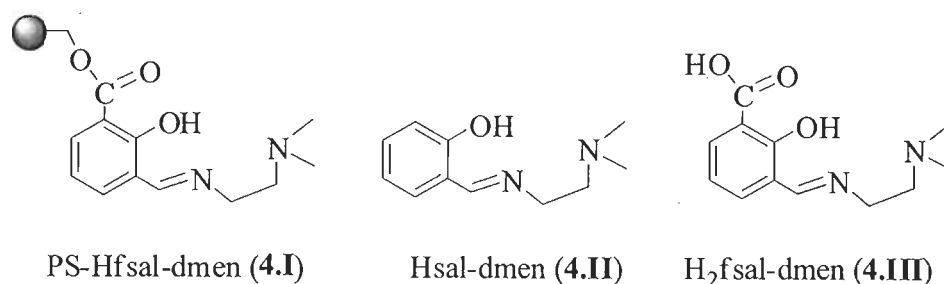
Scheme 4.1

4.2. EXPERIMENTAL

4.2.1. Materials and methods

Chloromethylated polystyrene [18.9 % Cl (4.3 mmol Cl per gram of resin)] cross-linked with 5 % divinylbenzene was obtained as a gift from Thermax Limited, Pune, India. Analytical reagent grade V$_2$O$_5$ (Loba Chemie, Mumbai, India), N,N-dimethylethylenediamine, thiophene, dibenzothiophene, thionaphthene, 2-methyl thiophene (Aldrich Chemicals Co., U.S.A), salicylaldehyde (Ranbaxy, India) were used as obtained. [VO(acac)$_2$] [233], 3-formylsalicylic acid [368], Hfsal-dmen [369] and Hsal-dmen [370] were prepared according to the methods reported in the literature.

Instrumentation and analyses details are reported in Chapter 2. A Thermax

Nicolet gas chromatograph fitted with a HP–1 capillary column (30 m × 0.25 μm × 0.25 μm) and FID detector was used to analyse the reaction products and their quantifications were made on the basis of the relative peak area of the respective product. The identity of the products was confirmed using a GC-MS model Perkin-Elmer, Clarus 500 and comparing the fragments of each product with the library available.

4.2.2. Syntheses of ligands and complexes

4.2.2.1. Polymer anchored ligand, PS-[Hfsal-dmen] (4.I)

Chloromethylated polystyrene (3.0 g) was allowed to swell in DMF (40 ml) for 2 h. A solution of H_2fsal-dmen (10.63 g, 45 mmol) in DMF (30 ml) was added to the above suspension followed by triethylamine (4.50 g) in ethylacetate (40 ml). The reaction mixture was heated at 90 °C for 20 h with slow mechanical stirring in an oil bath. After cooling to room temperature, the red resins were separated by filtration, washed thoroughly with hot DMF followed by hot methanol and dried in an air oven at 120 °C. Found: C, 74.03; H, 9.18; N, 6.96 %.

4.2.2.2. PS-[V^{IV}O(fsal-dmen)(acac)] (4.1)

Polymer-bound ligand PS-[Hfsal-dmen] (1.50 g) was allowed to swell in DMF (25 ml) for 2 h. A solution of [VO(acac)$_2$] (4.30 g, 20 mmol) in 20 ml DMF was added to the above suspension and the reaction mixture was heated at 90 °C in an oil bath for 15 h with slow mechanical stirring. After cooling to room temperature, the dark black polymer-bound complex obtained was separated by filtration, washed with hot DMF followed by hot methanol and dried at 120 °C in an air oven. Found: C, 71.88; H, 7.48; N, 4.23; V, 7.61 %.

4.2.2.3. PS-[V^{V}O$_2$(fsal-dmen)] (4.2)

Complex **4.1** (1.5 g) was suspended in 50 ml MeOH and air was bubbled for *ca.* 48 h. During this period the colour of the beads slowly changed to orange; these

were filtered off, washed with MeOH and dried at room temperature over silica gel. Found: C, 64.20; H, 7.30; N, 7.52; V, 9.38 %.

4.2.2.4. [VO^{IV}(sal-dmen)(acac)] (4.3)

A stirred solution of Hsal-dmen (0.96 g, 5 mmol) in methanol (10 ml) was treated with [VO(acac)$_2$] (1.33 g, 5 mmol) dissolved in methanol (20 ml) and the resulting reaction mixture was refluxed for 1 h after initial stirring of 1 h. The brown, X-ray-quality crystals formed upon slow evaporation were collected and dried under vacuum. Yield: 85 %. Found: C, 54.33; H, 6.39; N, 7.83; V, 14.21 %. Calcd. for C$_{16}$H$_{22}$N$_2$O$_4$V: C, 53.78; H, 6.21; N, 7.84; V, 14.26 %.

4.2.2.5. [V^{V}O$_2$(sal-dmen)] (4.4)

Complex **4.3** (0.27 g, 1 mmol) was dissolved in methanol. Air was bubbled through the solution slowly where it oxidised within 24 h to give yellow solution. The X-ray quality crystals of **4.4** formed upon slow evaporation of the solution were filtered and dried under vacuum. Yield: 70 %. Found: C, 48.16; H, 3.42; N, 12.07; V, 18.53 %. Calcd. For C$_{11}$H$_{15}$N$_2$O$_3$V: C, 48.18; H, 5.51; N, 10.22; V, 18.58 %. ^{51}V NMR (DMSO-d$_6$/ δ in ppm): −503 ppm (major signal) and –487 ppm (minor signal).

4.2.3. Catalytic reaction: Oxidation of organosulfur compounds

The oxidation of model organosulfur compounds was carried out in a 50 ml two-neck reaction flask fitted with a water condenser. The polymer-bound complex was allowed to swell in heptane for 2 h prior to use in each experiment. A solution of different organosulfur compounds such as thiophene (T), 2-methylthiophene (2-MT), dibenzothiophene (DBT) and benzothiophene (BT) with sulfur concentrations of 500 ppm was dissolved in 100 ml heptane. In a typical reaction, 10 ml of 500 ppm sulfur containing organosulfur compound, 30 % H$_2$O$_2$ (oxidant : substrate ratio of 3 : 1) and catalyst, PS-[V^{V}O$_2$(fsal-dmen)] (0.050 g) were taken in a reaction flask and stirred at 60 °C for 2 h. The progress of the reaction was monitored by withdrawing small

amount of the reaction mixture at every 10 min intervals and analysed quantitatively by gas chromatograph. The identities of the products were confirmed by GC-MS. Effect of various parameters such as temperature, amount of oxidant and catalyst were studied to obtain a suitable reaction condition for the best performance of the catalyst.

4.2.4. X-Ray crystal structure determination

Three-dimensional X-ray data for **4.3** and **4.4** were collected on a Bruker Kappa X8 Apex CCD diffractometer by the ϕ-ω scan method. Data was collected at low temperature. Reflections were measured from a hemisphere of data collected of frames each covering 0.3 degrees in ω. Of the 11502 in **4.4** and 75059 in **4.3** reflections measured, all of which were corrected for Lorentz and polarisation effects, and for absorption by semi-empirical methods based on symmetry-equivalent and repeated reflections, 1716 in **4.4** and 24423 in **4.3** independent reflections exceeded the significance level $|F|/\sigma(|F|) > 4.0$. Complex scattering factors were taken from the program package SHELXTL [371]. The structures were solved by direct methods and refined by full-matrix least-squares methods on F^2. The non-hydrogen atoms were refined with anisotropic thermal parameters in all cases. The hydrogen atoms were left to refine freely in the all cases in **4.4**, except for C9, and were included in calculated positions and refined by using a riding mode for all the atoms in **4.3**. For **4.3**, the absolute configuration has been established by refinement of the enantiomorph polarity parameter [$x = 0.557(13)$] [372]. The space group for **4.3** is P1, but there is pseudosymmetry [373] which emulates a centred unit cell in Pca2₁, but it is not supported by the diffraction pattern, which is consistent with the correct space group P1. A final difference Fourier map showed no residual density outside: 0.602, -0.591 e.Å^{-3} in **4.4** and 0.613, -0.584 e.Å^{-3} in **4.3**. Crystal data and details on data collection and refinement are summarised in Table 4.1.

Table 4.1. Crystal and structure refinement data for compounds **4.3** and **4.4**

	4.4	**4.3**
Formula	$C_{11}H_{15}N_2O_3V$	$C_{16}H_{22}N_2O_4V$
Mol.wt.	274.19	357.30
Space Group	$P2_1/n$	P1
Crystal System	Monoclinic	Triclinic
$a/\text{Å}$	6.341(4)	10.327(5)
$b/\text{Å}$	12.202(6)	12.750(5)
$c/\text{Å}$	15.727(9)	24.364(5)
$\alpha/\deg$		89.968(5)
$\beta/\deg$	98.03(3)	89.946(5)
$\gamma/\deg$		89.981(5)
$V/\text{Å}^3$	1204.9(11)	3340(2)
Z	4	8
T/K	100(2)	100(2)
λ, Å (Mo Kα)	0.71073	0.71073
$D_{calc}/\text{g cm}^{-3}$	1.511	1.421
μ/mm^{-1}	0.821	0.615
R_{int}	0.0586	0.0498
R_1[a]	0.0489	0.0476
wR_2 (all data)[b]	0.1359	0.1346

[a] $R_1 = \sum ||F_0| - |F_c|| / \sum |F_0|$. [b] $wR_2 = \{\sum[w(||F_0|^2 - |F_c|^2)^2]/\sum[w(F_0^4)]\}^{1/2}$

4.3. RESULTS AND DISCUSSION

4.3.1. Syntheses, reactivity and solid state characteristics

Ligand, Hfsal-dmen, obtained by the condensation of 3-formyl salicylic acid and N,N-dimethylethylenediamine, reacted with chloromethylated polystyrene (18.9 % Cl, 4.35 mmol Cl g^{-1} resin) cross linked with 5 % divinylbenzene in DMF in the presence of triethylamine and ethyl acetate to give polystyrene supported ligand, PS-Hfsal-dmen. In this process, the -COOH group of 3-formylsalicylic acid reacted with $-CH_2Cl$ group of polystyrene as shown in Scheme 4.2. The remaining chlorine content of 1.5 % (0.51 mmol Cl g^{-1} of resin) in PS-Hfsal-dmen suggested ca. 97 % loading of the ligand.
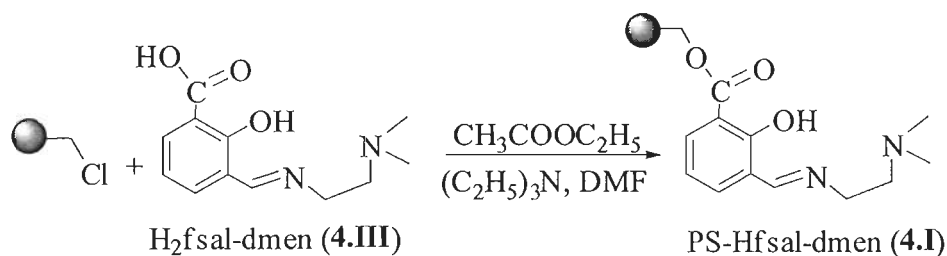
Scheme 4.2. Syntheses of PS-ligand

The polymer-bound ligand, PS-[Hfsal-dmen] on reaction with [VO(acac)$_2$] in DMF at ca. 90 °C gave polymer-bound complex, PS-[V^{IV}O(fsal-dmen)(acac)] **(4.1)**. Complex **4.1** on aerial oxidation in MeOH, gave the dioxidovanadium(V) complex, PS-[V^{V}O$_2$(fsal-dmen)] **(4.2)**. The whole synthetic procedures are presented in Scheme 4.3. Similarly, the reaction of [VO(acac)$_2$] with an equimolar amount of Hsal-dmen in refluxing methanol gave the oxidovanadium(IV) complex, [V^{IV}O(sal-dmen)(acac)] **(4.3)** which on aerial oxidation gave dioxidovanadium(V) complex, [V^{V}O$_2$(sal-dmen)] **(4.4)**.
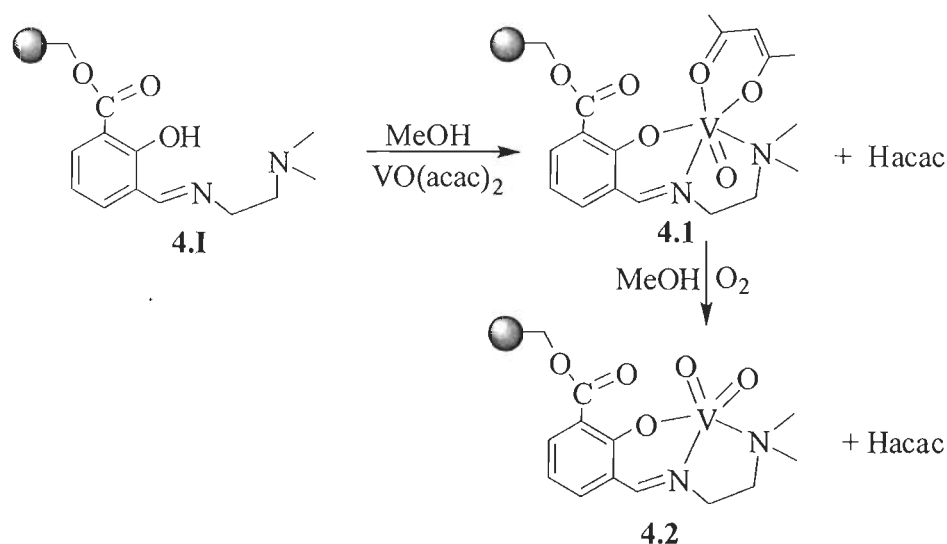
Scheme 4.3.

Table 4.2 provides data of metal and ligand loading in polymer-bound complexes, assuming the formation of PS-[Hfsal-dmen]. The obtained data show that metal to ligand ratio in polymer-bound complexes is close to 1 : 1.

Table 4.2. Ligand and metal loadings in polymer-bound complexes, and ligand-to-metal ratio data

Compound	Ligand loading (mmol g^{-1} of resin)	Metal ion loading[a] (mmol g^{-1} of resin)	Ligand : Metal ratio
PS-[Hfsal-dmen] **(4.I)**	2.4		
PS-[V^{IV}O(fsal-dmen)(acac)]	1.8	1.7	1 : 1.05
PS-[V^{V}O$_2$(fsal-dmen)]	1.6	1.4	1 : 1.14

[a] Metal ion loading = $\dfrac{\text{Observed metal \% } \times 10}{\text{Atomic weight of metal}}$

4.3.2. Description of structure of [V^{IV}O(sal-dmen)(acac)] (4.3)

In the study of heterochelates of coordination type [V^{V}OLL′] based on tridentate L (ONO [374, 375] or ONN, [273, 234]) and bidentate L′ (ON [375] or OO,

120

[374, 375]) donating ligands, the tridentate ligand L occupies three positions in the equatorial plane and the fourth position is occupied by either O or N atom of the other bidentate ligand L´.

In the complex **4.3**, the structure consists of eight independent vanadium monomers per asymmetric unit. The calculated Flack parameter indicated the presence of racemic twinning. The VO_4N_2 coordination sphere is a distorted octahedron in which vanadium atoms are displaced by: 0.2761 Å from the equatorial plane, mean deviation 0.0537(15) Å of N1, N2, O2 O2A for V1; 0.2951 Å, 0.0523(15) Å of N3 N4 O4 O3A for V2; 0.2968 Å, 0.0538(15) Å, of N5 N6 O6 O5A for V3; 0.2776 Å, 0.0546(15) Å of N7 N8 O8 O7A for V4; 0.2947 Å, 0.0545(15) Å of N9 N10 O10 O10A for V5; 0.2758 Å, 0.0495(15) Å of N11 N12 O12 O12A for V6; 0.2952 Å, 0.0543(15) Å of N13 N14 O14 O14A for V7; and 0.22757 Å, 0.0538(15) Å of N15 N16 O16 O15A for V8. The V=O distances of V1-O1, 1.604(3) Å, V2-O3, 1.613(3) Å, V3-O5, 1.609(3) Å, V4-O7, 1.604(3) Å, V5-O9, 1.611(3) Å, V6-O11, 1.604(3) Å, V7-O13, 1.612(3) Å and V8-O15, 1.607(3) Å are slightly longer than the range defined for other neutral VO^{3+} complexes of 1.55-1.60 Å [273, 216].The V-O_{phe} lengths (V1-O2, 1.956(3) Å, V2-O4, 1.955 Å, V3-O6, 1.960(3) Å, 1.957(3) Å, V4-O8, 1.957(3) Å, V5-O10, 1.956(3) Å, V6-O12, 1.958(3) Å, V7-O14, 1.960(3) Å and V8-O16, 1.955(3) Å) are longer than other similar compounds such as [VO(salhyb)(Q)], [VO(salhyp)(Q)] and [VO(salhyh)(Q)] [376], which are in the range of 1.85-1.87 Å, but enough similar than compounds with a nitrogen atom in trans with respect to oxygen atom of the phenolate [377, 275, 240]. The vanadium-imine nitrogen atom distances (V1-N1, V2-N3, V3-N5, V4-N7, V5-N9, V6-N11, V7-N13 and V8-N15, see Table 4.3) are in the range reported for the other similar compounds e.g. [VO(cat)(gsal)] [374], [VO(tBu₂-cat)(vsal)] [374], [VO(hshed)(shi)] [273], [VO(cat)(salimh)] [273], [VO(sal)(salimh)] [234], [VO(acac)(salimh)] [234], [VO(acac)(hshed)] [377], [VO(acac)(sal-aebmz)] [299], [VO(bha)(sal-aebmz)] [299] and [VO(acac)(salimRH)] [240].

Most V=O compounds observe a strong trans effect. The weakest bond of the ligand L′ should be trans to the vanadyl oxygen atom. The longer bond of the acac ligand is trans to the vanadyl oxygen atom, in the order of 2.2 Å (see Table 4.3). Although the carbon-carbon and carbon-oxygen distances of the acac ligand do not permit to differentiate the ketonic oxygen from the enolic oxygen one, the similarity of the our structure with [VO(acac)(salimh)] [234], suggest that the neutral carbonyl oxygen atom is in the axial position.
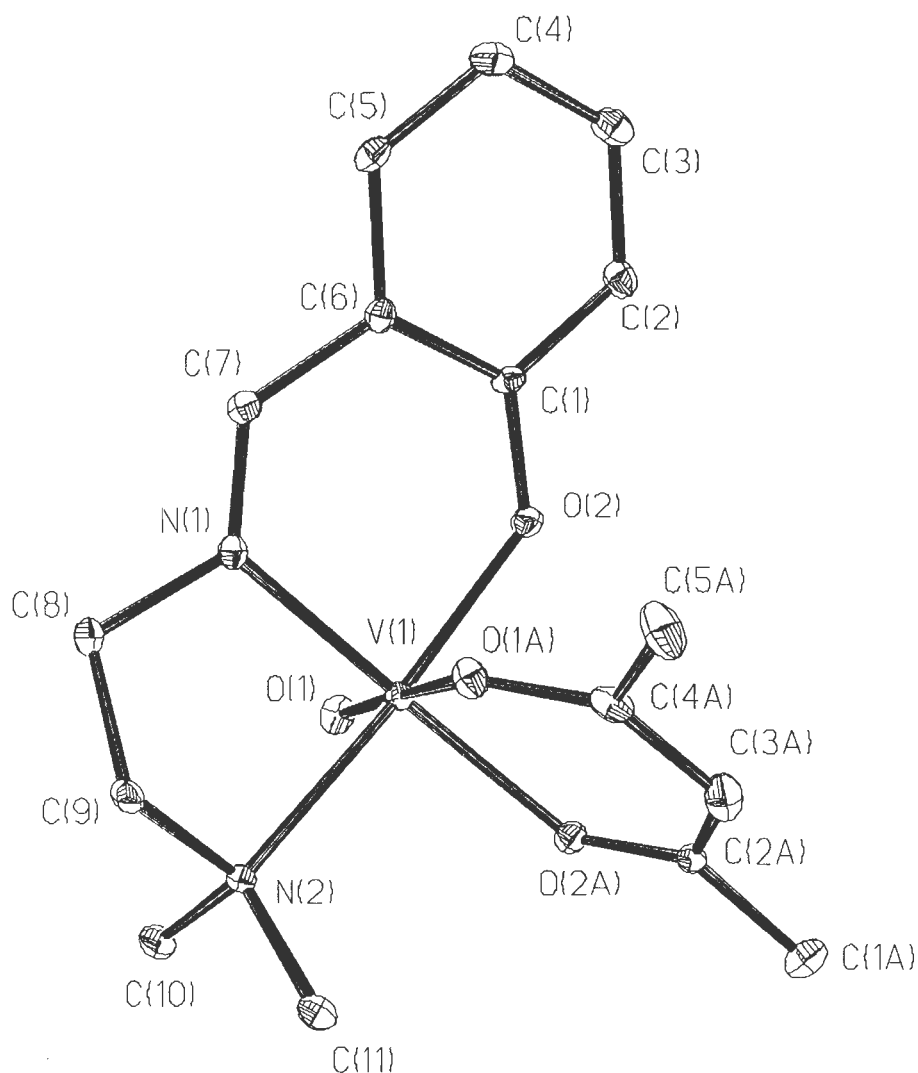
Fig. 4.1. ORTEP diagrams of [V^{IV}O(sal-dmen)(acac)] (**4.3**). All the non-hydrogen atoms are represented by their 30% probability ellipsoids.

4.3.3. Description of structure of [$V^V O_2$(sal-dmen)] (4.4)

In the unit cell we meet a discrete monomeric molecule. The vanadium(V) ion is five-coordinate, with a distorted square pyramidal environment. The metal ion lies 0.4782 Å above from the mean plane of the basal atoms, O1, O3, N1, N2 in the direction of the axial oxo ligand, O2. The τ value for this geometry is 0.22 indicating a significant distortion toward the trigonal bipyramidal form. The distances and angles (Table 4.4) are very similar to the structure published in the literature [378].
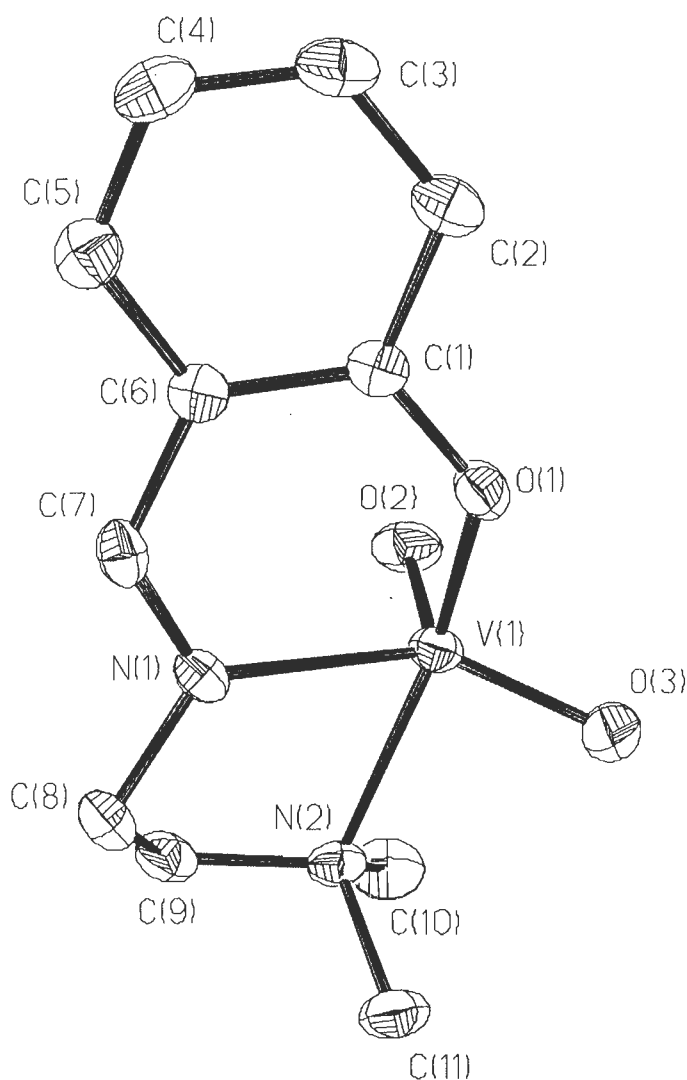
Fig. 4.2. ORTEP diagrams of [$V^V O_2$(sal-dmen)] **(4.4)**. All the non-hydrogen atoms are represented by their 30 % probability ellipsoids.

Table 4.3. Selected bond lengths and angles for [V^{IV}O(acac)(sal-dmen)] (**4.3**). Angles only for the first three polyhedrons in compound **4.3**.

4.3	Å	4.3	Å	4.3	(°)
V(1)-O(1)	1.604(3)	V(5)-O(9)	1.611(3)	O(1)-V(1)-O(2)	100.67(13)
V(1)-O(2)	1.956(3)	V(5)-O(10)	1.956(3)	O(1)-V(1)-O(2A)	99.57(13)
V(1)-O(2A)	1.991(3)	V(5)-O(10A)	2.001(3)	O(2)-V(1)-O(2A)	92.06(12)
V(1)-N(1)	2.063(3)	V(5)-N(9)	2.057(3)	O(1)-V(1)-N(1)	98.87(14)
V(1)-O(1A)	2.187(3)	V(5)-O(9A)	2.198(3)	O(2)-V(1)-N(1)	89.08(12)
V(1)-N(2)	2.223(3)	V(5)-N(10)	2.222(3)	O(2A)-V(1)-N(1)	160.98(12)
N(1)-C(7)	1.278(5)	N(9)-C(51)	1.279(5)	O(1)-V(1)-O(1A)	173.77(12)
N(1)-C(8)	1.471(5)	N(9)-C(52)	1.468(5)	O(2)-V(1)-O(1A)	84.75(11)
C(1)-O(2)	1.306(5)	O(10)-C(45)	1.299(5)	O(2A)-V(1)-O(1A)	83.18(11)
V(2)-O(3)	1.613(3)	V(6)-O(11)	1.604(3)	N(1)-V(1)-O(1A)	78.01(12)
V(2)-O(4)	1.955(3)	V(6)-O(12)	1.958(3)	O(1)-V(1)-N(2)	91.58(13)
V(2)-O(3A)	1.999(3)	V(6)-O(12A)	1.985(3)	O(2)-V(1)-N(2)	165.75(12)
V(2)-N(3)	2.057(3)	V(6)-N(11)	2.063(3)	O(2A)-V(1)-N(2)	93.04(12)
V(2)-O(4A)	2.200(3)	V(6)-O(11A)	2.181(3)	N(1)-V(1)-N(2)	81.82(12)
V(2)-N(4)	2.217(3)	V(6)-N(12)	2.218(3)	O(1A)-V(1)-N(2)	82.66(11)
N(3)-C(18)	1.284(5)	N(11)-C(62)	1.279(5)	O(3)-V(2)-O(4)	100.53(13)
N(3)-C(19)	1.466(4)	N(11)-C(63)	1.464(5)	O(3)-V(2)-O(3A)	100.75(13)
O(4)-C(12)	1.307(5)	O(12)-C(56)	1.313(4)	O(4)-V(2)-O(3A)	91.71(11)
V(3)-O(5)	1.609(3)	V(7)-O(13)	1.612(3)	O(3)-V(2)-N(3)	98.72(13)
V(3)-O(6)	1.960(3)	V(7)-O(14)	1.960(3)	O(4)-V(2)-N(3)	89.32(12)
V(3)-O(5A)	2.000(3)	V(7)-O(14A)	1.994(3)	O(3A)-V(2)-N(3)	159.97(12)
V(3)-N(5)	2.059(3)	V(7)-N(13)	2.061(3)	O(3)-V(2)-O(4A)	173.55(12)
V(3)-O(6A)	2.200(3)	V(7)-O(13A)	2.197(3)	O(4)-V(2)-O(4A)	84.38(11)
V(3)-N(6)	2.222(3)	V(7)-N(14)	2.224(3)	O(3A)-V(2)-O(4A)	83.16(11)
N(5)-C(29)	1.278(5)	N(13)-C(73)	1.281(5)	N(3)-V(2)-O(4A)	77.03(11)
N(5)-C(30)	1.465(5)	N(13)-C(74)	1.469(4)	O(3)-V(2)-N(4)	92.78(13)
O(6)-C(23)	1.298(5)	O(14)-C(67)	1.300(5)	O(4)-V(2)-N(4)	164.79(12)

124

V(4)-O(7)	1.604(3)	V(8)-O(15)	1.607(3)	O(3A)-V(2)-N(4)	93.00(12)
V(4)-O(8)	1.957(3)	V(8)-O(16)	1.955(3)	N(3)-V(2)-N(4)	81.37(12)
V(4)-O(7A)	1.989(3)	V(8)-O(15A)	1.990(3)	O(4A)-V(2)-N(4)	81.83(11)
V(4)-N(7)	2.063(3)	V(8)-N(15)	2.062(3)	O(5)-V(3)-O(6)	100.48(14)
V(4)-O(8A)	2.183(3)	V(8)-O(16A)	2.186(3)	O(5)-V(3)-O(5A)	100.83(13)
V(4)-N(8)	2.220(3)	V(8)-N(16) '	2.222(3)	O(6)-V(3)-O(5A)	91.97(12)
N(7)-C(40)	1.276(5)	N(15)-C(84)	1.279(5)	O(5)-V(3)-N(5)	98.82(13)
N(7)-C(41)	1.464(5)	N(15)-C(85)	1.463(5)	O(6)-V(3)-N(5)	89.04(12)
O(8)-C(34)	1.310(5)	O(16)-C(78)	1.313(5)	O(5A)-V(3)-N(5)	159.79(12)
				O(5)-V(3)-O(6A)	173.50(12)
				O(6)-V(3)-O(6A)	84.41(11)
				O(5A)-V(3)-O(6A)	83.17(10)
				N(5)-V(3)-O(6A)	76.84(11)
				O(5)-V(3)-N(6)	92.82(13)
				O(6)-V(3)-N(6)	164.77(12)
				O(5A)-V(3)-N(6)	92.80(12)
				N(5)-V(3)-N(6)	81.55(12)
				O(6A)-V(3)-N(6)	81.82(11)

Table 4.4. Selected bond lengths and angles for [V^VO_2(sal-dmen)] (**4.4**).

4.4	Å	4.4	(°)
V(1)-O(2)	1.604(2)	O(2)-V(1)-O(3)	109.75(12)
V(1)-O(3)	1.621(2)	O(2)-V(1)-O(1)	104.13(10)
V(1)-O(1)	1.911(2)	O(3)-V(1)-O(1)	98.28(11)
V(1)-N(1)	2.147(2)	O(2)-V(1)-N(1)	107.13(11)
V(1)-N(2)	2.185(2)	O(3)-V(1)-N(1)	141.05(11)
N(1)-C(7)	1.280(4)	O(1)-V(1)-N(1)	83.71(9)
N(1)-C(8)	1.460(4)	O(2)-V(1)-N(2)	95.63(11)
O(1)-C(1)	1.331(3)	O(2)-V(1)-N(2)	95.63(11)
		O(3)-V(1)-N(2)	88.66(11)
		O(1)-V(1)-N(2)	154.24(9)
		N(1)-V(1)-N(2)	75.60(9)

4.3.4. Field emission-scanning electron microscope (FE-SEM) and energy dispersive X-ray analyses (EDX) studies

The change in morphology of polymer beads after the loading of ligand and metal ion have been studies by field emission scanning electron micrographs (FE-SEM) and energy dispersive X-ray analyses (EDX) (Fig. 4.3). A considerable amount of N (ca. 8.7 %) and small amount of Cl (ca. 1.8 %), was determined on the surface of the beads containing bound ligand. The polymer-bound ligand, PS-Hfsal-dmen shows the smooth and flat surface (Fig. 4.3a). Up on metal incorporation, the polymer beads show slight roughening of the top layer on the surface; Fig. 4.3b and 4.3c. The presence of very low content of chlorine and relatively good content of nitrogen on the surface of the grafted complexes suggests the replacement of chlorine by carboxylic group. The presence of vanadium complex in the matrix was supported by the presence of 1.6 % and 1.2 % vanadium in PS-[$V^{IV}O$(fsal-dmen)(acac)] and PS-[V^VO_2(fsal-dmen)], respectively. Accurate information on the morphological changes in terms of exact orientation of ligand coordinated to the metal ion has not been possible due to low amount of the metal complex on polymer surface.
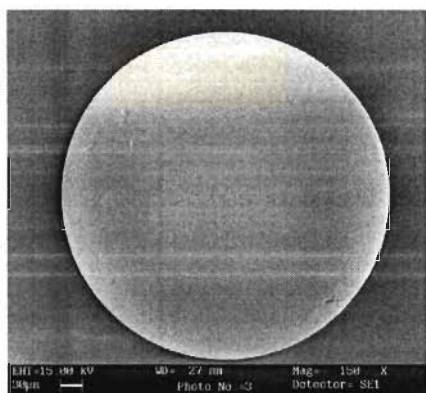
(a) PS-[Hfsal-dmen] (**4.I**)
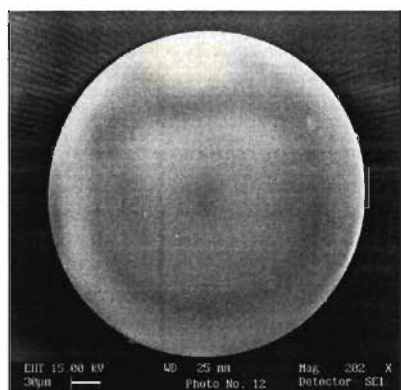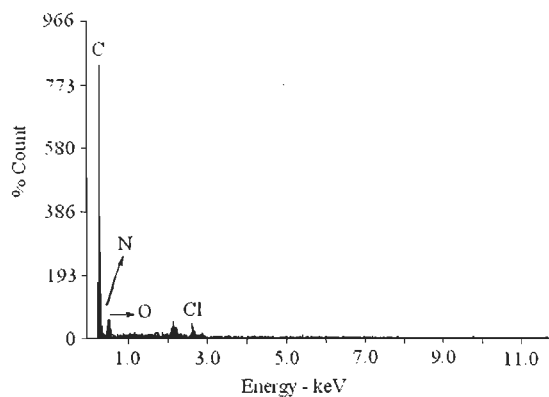
(b) PS-[V^{IV}O(fsal-dmen)(acac)] (**4.1**)
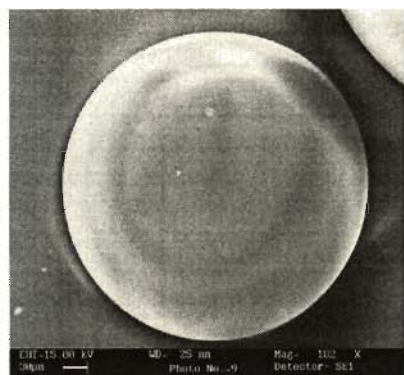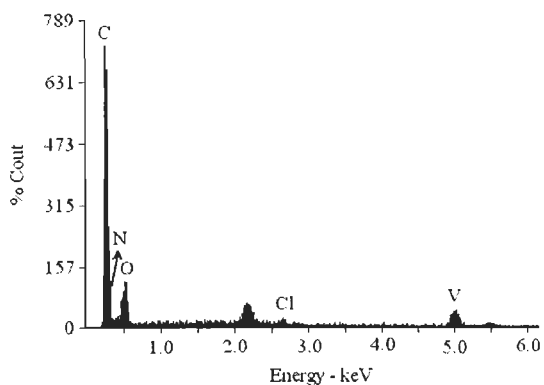
(c) PS-[V^{V}O$_2$(fsal-dmen)] (**4.2**)
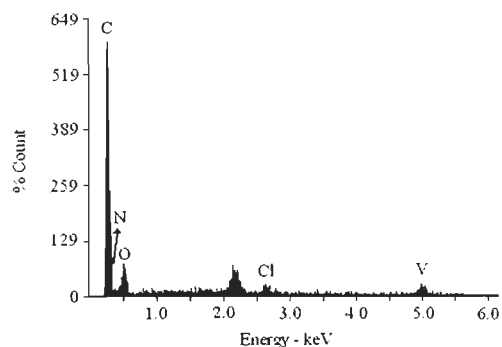
Fig. 4.3. FE-SEM and Energy dispersive X-ray analyses (EDX) profile of (a) PS-[Hfsal-dmen] (**4.I**) (b) PS-[V^{IV}O(fsal-dmen)(acac)] (**4.1**) and (c) PS-[^{V}VO$_2$(fsal-dmen)] (**4.2**).

127

4.3.5. TGA studies

The polymer-bound complexes PS-[V^{IV}O(fsal-dmen)(acac)] and PS-[V^{V}O$_2$(fsal-dmen)] are thermally stable up to ca. 175 °C. The complexes, thereafter, decompose in two steps. Quantitative measurement of weight loss at various stages was not possible due to their overlapping nature. However, the stability of final residues at ca. 700 °C suggests the formation of V$_2$O$_5$. Estimation of final residues was helpful in approximating the percentage of metal ions in the polymer-bound complexes.

4.3.6. IR spectral studies

The important IR bands for the neat and polymer-bound ligands and their vanadium complexes are given in Table 4.5. The chloromethylated polystyrene shows strong peaks at 1264 and 673 cm^{-1} [379] in the IR spectrum and absence of these peaks in PS-[Hfsal-dmen] suggests the covalent bonding of chloromethylated polystyrene with Hfsal-dmen. The polymer-bound ligand exhibits a sharp band at 1669 cm^{-1} due to the v(C=O) of the carboxylic group. Existence of this band suggests covalent bond formation between the ligand and the polymer through a carboxylic acid group. A band corresponding to v(C=N) at 1630 cm^{-1} in PS-[Hfsal-dmen] shifts to lower wave number thereby indicating the coordination of azomethine nitrogen to the metal ions. This observation suggests the coordination of the azomethine nitrogen atom to the metal ion. The presence of multiple bands of medium intensity covering the 2800 - 2900 cm^{-1} regions suggests the existence of –CH$_2$ group. In addition, PS-[V^{IV}O(fsal-dmen)(acac)] exhibits a medium intensity band at 974 cm^{-1} due to v(V=O) and this indicates the presence of vanadium at the centre. In dioxido complex PS-[V^{V}O$_2$(fsal-dmen)], the bands due to $v_{antisym}$(O=V=O) and v_{sym}(O=V=O) modes could not be resolved and observed only as a broad peak at 923 cm^{-1}. However, the corresponding neat complex exhibits two sharp bands at 924 and 952 cm^{-1} [236]. Neat oxidovanadium(IV) complex also exhibits spectral patterns very close to polymer-bound complex and is similar to those reported in the literature [380].

Table 4.5. IR spectral data of ligand and complexes

Compound	$\nu(C=O)$	$\nu(C=N)$	$\nu(V=O)$
PS-Hfsal-dmen	1669	1630	–
PS-[$V^{IV}O$(fsal-dmen)(acac)]	1667	1601	974
PS-[$V^{V}O_2$(fsal-dmen)]	1667	1629	923
[$V^{IV}O$(sal-dmen)(acac)]	–	1639	952
[$V^{V}O_2$(sal-dmen)]	–	1630	924, 952

4.3.7. Electronic spectral studies

The electronic spectra of polymer anchored and neat complexes are reproduced in Figs. 4.4 and 4.5, respectively. The spectrum of Hsal-dmen exhibits four bands at 401, 317, 255 and 216 nm. The bands at 255 and 216 nm are assignable to $\pi - \pi^*$ and $\phi - \phi^*$ transitions, respectively, while the first two bands seem split band of $n - \pi^*$ transition. The band at ca. 380 nm (in oxidovanadium(IV)) and 373 nm (in dioxidovanadium(V)) complexes has been assigned due to ligand to metal charge transfer (lmct) band. New band at 813 and 558 nm in neat [$V^{IV}O$(sal-dmen)] is assigned due to d – d transition which is not present in the polymer-bound complex due to its poor loading in the polymer matrix.. The electronic spectral patterns exhibited by the polymer-bound metal complexes are similar (Table 4.6) to those obtained for the corresponding non-polymer bound analogues, except low intensity of bands.

Table 4.6. Electronic spectral data of ligand and complexes

Compound	Solvent	λ_{max} (nm)
PS-[$V^{IV}O$(fsal-dmen)(acac)]	Nujol	395, 316, 257
PS-[$V^{V}O_2$(fsal-dmen)]	Nujol	389, 295, 254
Hsal-dmen	MeOH	401, 317, 255, 216
[$V^{IV}O$(sal-dmen)(acac)]	MeOH	813, 558, 380, 262, 221
[$V^{V}O_2$(sal-dmen)]	MeOH	373, 319, 259, 220
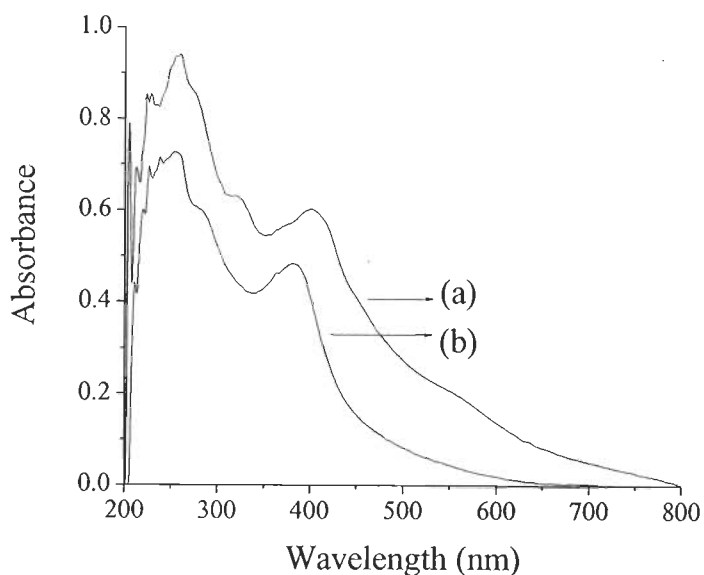
Fig. 4.4. Electronic spectra of (a) PS-[V^{IV}O(fsal-dmen)(acac)] and (b) PS-[V^{V}O$_2$(fsal-dmen)] recorded in Nujol.
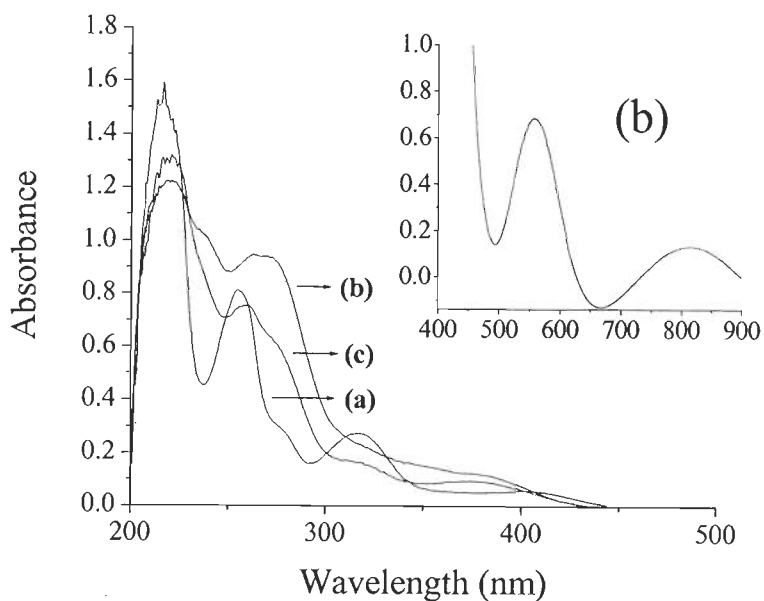
Fig. 4.5. Electronic spectra of (a) Hsal-dmen, (b) [V^{IV}O(sal-dmen)(acac)] and (c) [V^{V}O$_2$(sal-dmen)] recorded in MeOH.

130

4.3.8. EPR Spectral studies

EPR spectra of "frozen" (77 K) solutions of complex [VO(fsal-dmen)(acac)] (**5.3**) in MeOH and DMSO, and that of solid PS-[VO(fsal-dmen)(acac)] (**5.1**) at room temperature were recorded; Fig. 4.6 presents the EPR spectra. The spectrum of solid PS-[VO(fsal-dmen)(acac)] is characteristic of magnetically diluted $V^{IV}O$-complexes. The resolved EPR pattern indicates that the vanadium(IV) centers are well dispersed in the polymer matrix. All spectra are well resolved in both the parallel and perpendicular regions, the hyperfine features and spectrum being consistent with binding modes involving (O_{acac}, $O_{phenolate}$, N_{imine}, N_{py})$_{equatorial}$ and (O_{acac})$_{axial}$. Once a particular binding mode is assumed, the values of $A_{\parallel}$ can be estimated using the additivity relationship proposed by Wurthrich and Chasteen [237, 238], with estimated accuracy of $\pm 3 \times 10^{-4}$ cm^{-1}. However, for the potential donor groups under consideration, their predicted contributions to the parallel hyperfine coupling constant are rather similar {O_{acac}, ~41.7; $O_{phenolate}$ ~38.9; N_{imine} ~41.6; N_{amine} ~40.1, O_{DMSO} ~41.9; O_{MeOH} ~45.5, all A∥ contributions in cm^{-1} × 10^4} and hence it is not possible to distinguish between the several plausible binding modes. The Spin Hamiltonian parameters obtained are given in Table 4.7.

The EPR spectrum of non-polymer bound complex [$V^{IV}O$(sal-dmen)(acac)] in methanol exhibits the presence of two species, indicating the partial interaction of methanol with complex. In DMSO, both the species convert into one and exhibits EPR patterns due to coordinated DMSO. This implies the substitution of one of the equatorial donor atoms by an O atom of the solvent.

4.3.9. ^{51}V NMR studies

The ^{51}V chemical shift values for the V^V-complexes are included in the Experimental section. For complex **5.4**, one major signal at δ = −503 ppm and a minor one at − 487 ppm were obtained in DMSO-d$_6$. These chemical shifts are within the values expected for dioxidovanadium(V) complexes containing a O/N donor set [257]. Upon addition of methanol to a 4 mM solution of **4** in DMSO, both the

resonances collapse and give rise to a single band at −543 ppm, which is identical to what obtained when **4** was recorded in MeOH only. The signal at −543 ppm is, therefore, assigned to $[V^VO_2(sal\text{-}dmen)(MeOH)]$, −503 ppm due to $[V^VO_2(sal\text{-}dmen)(DMSO)]$ and the minor signal at − 487 ppm due to $[V^VO_2(sal\text{-}dmen)(H_2O)]$.

Table 4.7. Spin Hamiltonian parameters obtained from the experimental EPR spectra recorded.

Complex	Solvent	$g_{\parallel}$	$A_{\parallel}$ $(\times 10^4 cm^{-1})$	$A_{\perp}$ $(\times 10^4 cm^{-1})$	$g_{\perp}$
PS-$[V^{IV}O(fsal\text{-}dmen)(acac)]$	Solid	1.949	169.6	63.5	1.978
$[V^{IV}O(sal\text{-}dmen)(acac)]$	MeOH	1.952	164.0	59.0	1.981
		1.951	161.2	55.9	1.979
	DMSO	1.950	163.1	57.0	1.980
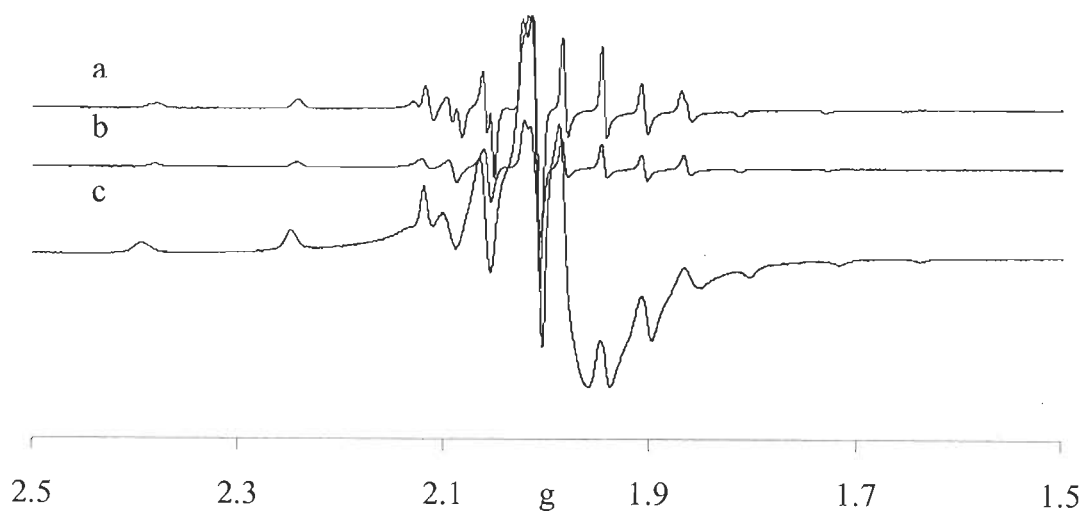
Fig. 4.6. First derivative EPR spectra of frozen solutions of $[V^{IV}O(sal\text{-}dmen)(acac)]$ (4m M) (**a**) in MeOH; (**b**) in DMSO. First derivative EPR spectra (**c**) of solid sample of PS-$[V^{IV}_{.}O(fsal\text{-}dmen)(acac)]$ at room temperature.

4.3.10. Catalytic activity: Catalytic desulfurization of organosulfur compounds

The catalytic potential of polymer-bound complex, PS-[V^VO_2(fsal-dmen)] was checked for selective oxidation of different organosulfur compounds like thiophene (T), benzothiophene (BT), 2-methylthiophene (MT), and dibenzothiophene (DBT) with the concentration of 500 ppm sulfur and all substrates gave the corresponding sulfones; Scheme 4.4. The products were identified by gas chromatography and further confirmed by GC-MS spectroscopy. Various parameters like temperature of the reaction mixture, amount of catalyst and oxidant have been optimised while considering thiophene (T) as a representative substrate.
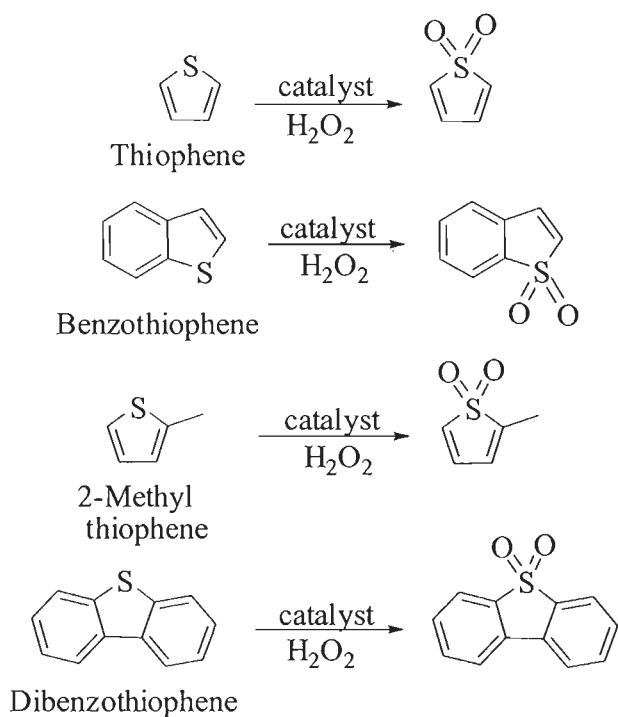
Scheme 4.4.

The oxidation of organosulfur compounds depends on the amount of oxidant, H_2O_2 used during the reaction. Reactions were carried out at three different oxidant to substrate ratios of 2 : 1, 3 : 1 and 4 : 1 using thiophene (S concentration 500 ppm) and catalyst (0.050 g) at 60 °C. As illustrated in Fig. 4.7, a maximum of 83.3 %

desulfurization has been achieved within 2 h of reaction time at a H_2O_2 to S molar ratio of ca. 2 : 1. Increasing this ratio to ca. 3 : 1 led to a desulfurization of ca. 99.8 % while ca. 4 : 1 molar ratio showed no further improvement in desulfurization.
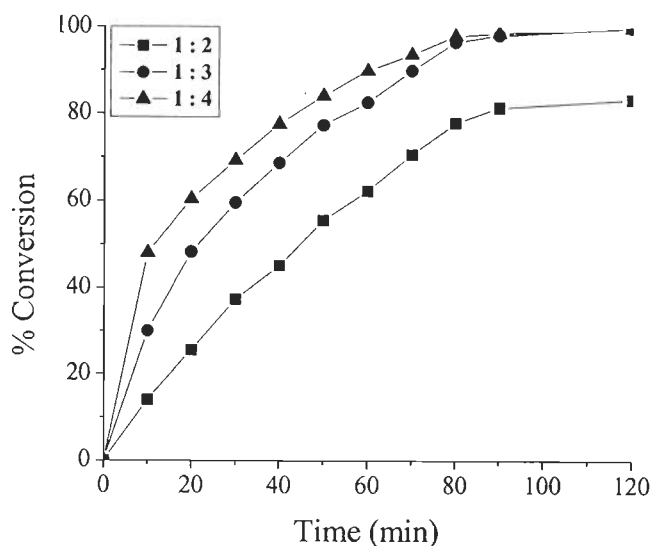
Fig. 4.7. Effect of H_2O_2 : sulfur ratio as a function of time on the desulfurization of thiophene. Reaction conditions: Catalyst PS-[V^VO_2(fsal-dmen)] (0.050 g) and thiophene (S: 500 ppm) in n-heptane at 60 °C.

In another experiment, three different catalyst loadings *viz.* 0.025 g, 0.050 g and 0.075 g were considered at a S concentration to H_2O_2 ratio of 1 : 3 under the above reaction conditions, and the results are presented in Fig. 4.8. As seen in the figure, 0.025 g of catalyst gave only 82 % desulfurization while 0.050 g and 0.075 g of catalyst loadings have shown a comparable desulfurization of 99.8 and 99.7 %, respectively. Thus, 0.050 g of catalyst was considered to be adequate to carry out the reaction for maximum oxidation. The temperature of the reaction mixture has also influenced on the performance of the catalyst. As shown in Fig. 4.9, running the reaction at 60 °C gave a much better yield of the reaction products than at room temperature while reaction at 80 °C gave only comparable desulfurization.
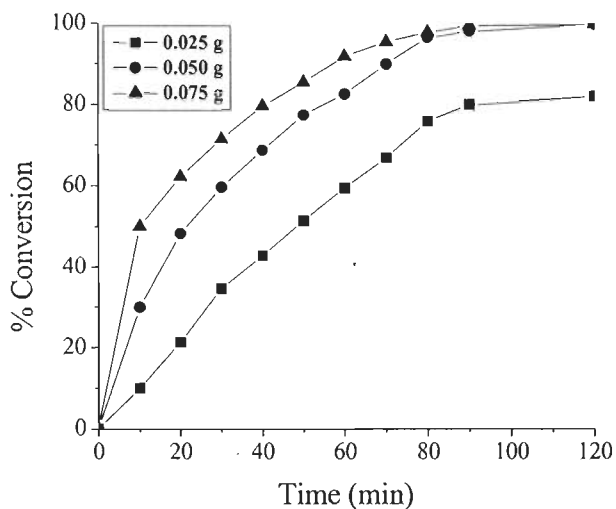
Fig. 4.8. Effect of the amount of catalyst PS-[V^VO_2(fsal-dmen)] on the desulfurization of thiophene as function of time. Reaction conditions: Thiophene (S: 500 ppm), H_2O_2 (0.76 g, 6.78 mmol) in n-heptane at 60 °C.
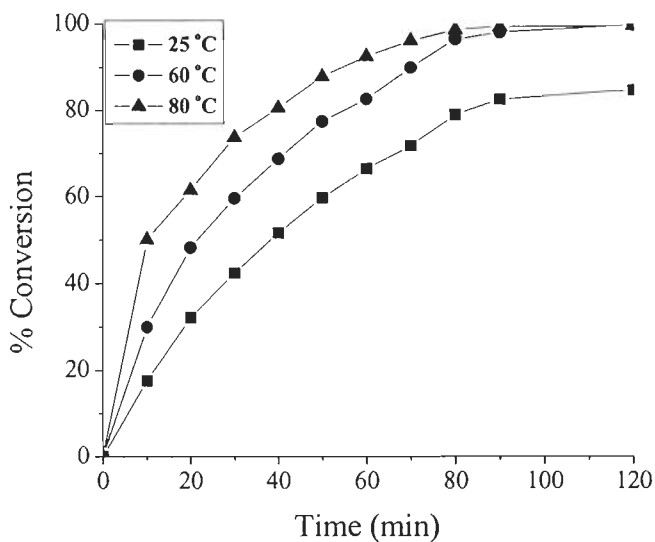
Fig. 4.9. Effect of temperature on the desulfurization of thiophene. Reaction conditions: Thiophene (S: 500 ppm), H_2O_2 (0.76 g, 6.78 mmol) and catalyst PS-[V^VO_2(fsal-dmen)] (0.050 g).

Thus, the optimised reaction conditions concluded for the maximum desulfurization of thiophene are: S (500 ppm) in n-heptane, catalyst PS-[VO$_2$(fsal-dmen)] (0.050 g), H$_2$O$_2$ (6.78 mmol) and temperature (60 °C). Under the optimised reaction conditions we have also tested the catalytic activity of the polymer-bound complex PS-[V^{IV}O(fsal-dmen)(acac)] (**4.1**), and the progress of the desulfurization of organosulfur compounds as a function of time is presented in Table 4.8.

Table 4.8. Desulfurization percentage and reaction products using anchored oxido- and dioxido-vanadium catalysts. Reaction conditions: substrate (equivalent to 500 ppm of S) in n-heptane, (S: H$_2$O$_2$ = 1: 3 molar ratio), catalyst (0.050 g) and temperature (60 °C).

Catalyst	Sulfur containing compounds	Sulfur content (in ppm)		Sulfur removal (%)
		Initial concentration	After desulfurization	
4.1	Thiophene	500	65.5	86.9
4.1	Benzothiophene	500	63	87.4
4.1	Dibenzothiophene	500	60.5	87.9
4.1	2-Methylthiophene	500	57.5	88.5
4.2	Thiophene	500	9.5	98.1
4.2	Benzothiophene	500	8.5	98.3
4.2	Dibenzothiophene	500	8	98.4
4.2	2-Methylthiophene	500	6	98.8
4.3	Thiophene	500	148.5	70.3
4.3	Benzothiophene	500	144.5	71.1
4.3	Dibenzothiophene	500	141.5	71.7
4.3	2-Methylthiophene	500	140.5	71.9
4.4	Thiophene	500	113	77.4
4.4	Benzothiophene	500	109.5	78.1
4.4	Dibenzothiophene	500	111.5	77.7
4.4	2-Methylthiophene	500	108	78.4

4.3.11. Reactivity of non-polymer bound complexes with H_2O_2

Solutions of $[V^{IV}O(sal–dmen)(acac)]$ **(4.3)** in methanol are sensitive towards addition of H_2O_2, as monitored by electronic absorption spectroscopy, yielding oxoperoxo species. Fig. 4.10 presents the spectral changes observed for **4.3**. Thus, the progressive addition of a dilute H_2O_2 solution in methanol to a solution of $[V^{IV}O(sal–dmen)(acac)]$ **(4.3)** in methanol results first in flattening of the band appearing at 813 nm; upon further addition of one drop portions of the H_2O_2 solution this band disappears. The intensity of the 538 nm band slowly decreases and disappears. Similarly, the bands at 322 and 239 nm show decrease in intensity, while the intensity of the 259 and 215 nm bands increase. These changes indicate the interaction of $[V^{IV}O(sal–dmen)(acac)]$ with H_2O_2 in methanol. The disappearance of d–d bands is in accordance with the oxidation of the $V^{IV}O$-complex to an oxoperoxovanadium(V) species.
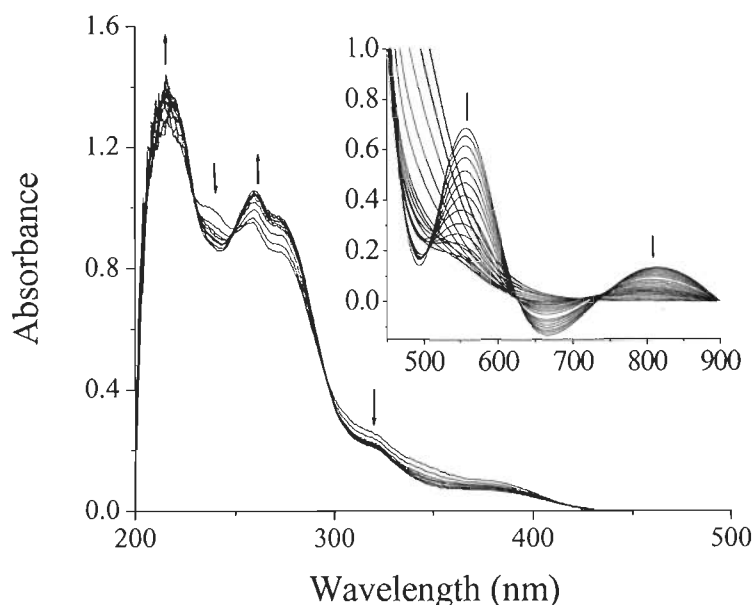
Fig. 4.10. UV-Vis spectral changes observed during titration of [VO(sal–dmen)(acac)] **4.3** with H_2O_2. The spectra were recorded after successive additions of one drop portions of H_2O_2 (6.6×10^{-4} mmol of 30 % H_2O_2 dissolved in 10 ml of methanol) to 50

ml of ca. 10^{-3} M solution of **4.3** in methanol.

The spectral changes during a similar titration of **4.4** with H_2O_2 (diluted in methanol) in methanol is shown in Fig. 4.11. With low amounts of H_2O_2 added no appreciable changes in band positions were observed, but further additions of H_2O_2 yielded a final spectrum which is very similar to that obtained in the titration of $[V^{IV}O$ (sal-dmen)(acac)] **(4.3)** with H_2O_2, thus demonstrating that the same oxoperoxovanadium(V) species form upon addition of H_2O_2 to the methanolic solutions of either **4.3** or **4.4**.
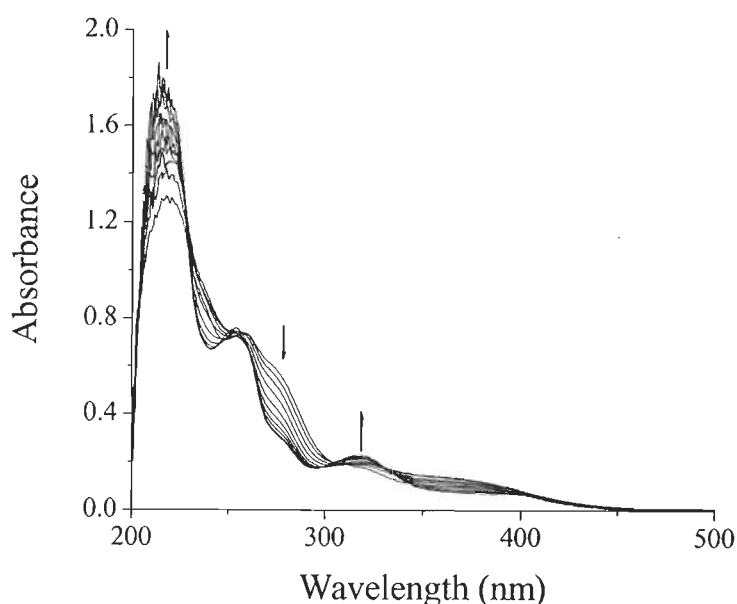
Fig. 4.11. Spectral changes observed during titration of $[V^VO_2(sal–dmen)]$ **(4.4)** with H_2O_2. The spectra were recorded after successive additions of one drop portions of H_2O_2 (6.6×10^{-4} mmol of 30 % H_2O_2 dissolved in 10 ml of methanol) to 50 ml of ca. 10^{-4} M solution of **4.4** in methanol.

4.4. CONCLUSIONS

Ligand H_2fsal-dmen **(4.II)** derived from 3-formylsalicylic acid and N,N'-dimethyletylenediamine has been covalently bonded to chloromethylated polystyrene cross-linked with 5 % divinylbenzene. The polymer-anchored ligand PS-[Hfsal-dmen]

(4.I) on reaction with $[V^{IV}O(acac)_2]$ gives the complex PS-$[V^{IV}O(fsal–dmen)(acac)]$ (4.1), which upon oxidation yielded the dioxidovanadium(V), PS-$[V^{V}O_2(fsal–dmen)]$ (4.2). The corresponding non-polymer bound complexes $[V^{IV}O(sal–dmen)(acac)]$ (4.3) and $[V^{V}O_2(sal–dmen)]$ (4.4) have also been prepared and characterised. The anchored compounds were characterised by elemental analyses, spectroscopic (IR and electronic) studies, field-emission scanning electron micrograph (FE-SEM), energy dispersive analyses by X-ray (EDX) and thermo gravimetric patterns. The structures of neat complexes (4.3) and (4.4) have also been confirmed by single X-ray crystallography.

Complexes 4.1 and 4.2 have been used as catalyst for the oxidative desulfurization of model organosulfur compounds like thiophene (T), dibenzothiophene (DBT), benzothiophene (BT), 2-methyl thiophene (MT) and diesel. The sulfur in model organosulfur compounds and diesel has been oxidised to the corresponding sulfones in the presence of H_2O_2. The polymer-bound heterogeneous catalysts are free from leaching during catalytic action and are recyclable.

<div align="center">

*****

</div>

Chapter-5

Polymer-bound oxidovanadium(IV) and dioxidovanadium(IV) complexes: Syntheses, characterisation and catalytic application for the hydroamination of styrene and vinyl pyridine

5.1. INTRODUCTION

Addition of an organic N-H bond to olefins to give nitrogen-containing molecules, called hydroamination (Scheme 5.1), normally proceeds through Markovnikov and/or anti-Markovnikov way of addition on the basis of regioselectivity. Transition metal catalysed hydroamination of olefins has attracted much attention in the past decades due to the ubiquity of the amine functionality in natural products, biological systems, pharmaceuticals and fine chemicals [191, 381-385].
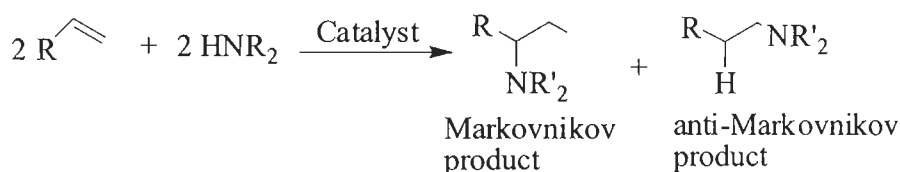
Scheme 5.1. Hydroamination of olefins producing the Markovnikov- or anti-Markovnikov-type product.

Additions of amines to unsaturated carbon–carbon multiple bonds may proceed either through intermolecular or intramolecular hydroamination depending on whether the secondary amine is present on the olefin itself at an appropriate position or not. The direct intramolecular hydroamination of unsaturated amines offers an efficient, atom-economical and straightforward route to nitrogen-containing molecules [191, 385, 386]. Various approaches catalysed by alkali metals [387, 388], transition metals [389-392], organo-lanthanide complexes [393, 394] and Brønsted acid [395, 396] have been extensively studied for this seemingly simple but challenging transformation. Efficient platinum (II) [397, 398], gold (I) [399, 400], copper (II) [401], iron (III) [402], and other metal salts [403, 404] catalysed hydroaminations of amides and carbamates have also been reported.

Vanadium complexes are generally efficient oxidation catalysts and they are, therefore, prospective catalyts for oxidative amination [78] as well as hydroamination. It has been recently demonstrated that the polymer-bound oxidovanadium(IV) complex PS-

[V^{IV}O(sal-cys)·DMF] (H$_2$sal-cys = Schiff base derived from salicylaldehyde and L-cysteine) is effective catalyst for the oxidative amination of styrene with secondary amines like diethylamine, imidazole and benzimidazole in mild basic conditions [78]. However, no hydroamination using vanadium complexes as catalysts has been reported so far in the literature. We, therefore, decided to prepare oxido- and dioxido-vanadium complexes and use them as catalysts for this purpose. In this work we report the preparation of the Schiff base derived from 3-formylsalicylic acid and 2-(2-aminoethyl)pyridine (Hfsal-aepy, **5.I**) [405], of the corresponding polymer-bound ligand **5.II** (PS-Hfsal-aepy; Scheme 5.2), of the oxidovanadium(IV) and dioxidovanadium(V) complexes and test their catalytic ability for the hydroamination of styrene and vinyl pyridine with amines such as aniline and diethylamine. The polystyrene backbone provides extra stability to the catalyst and makes the catalytic reaction heterogeneous in nature. The neat complexes [V^{IV}O(sal-aepy)(acac)] and [V^{V}O$_2$(sal-aepy)] with the ligand **5.III**, have also been prepared and we compared their catalytic performance with the corresponding polymer-bound analogues.

Hfsal-aepy (**5.I**)   PS-Hfsal-aepy (**5.II**)   Hsal-aepy (**5.III**)
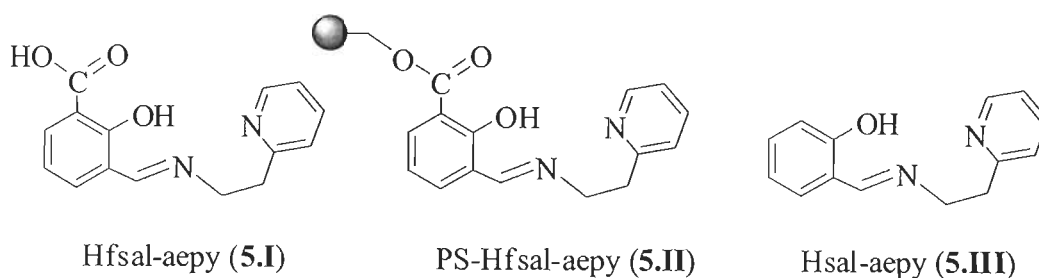
Scheme 5.2

5.2. EXPERIMENTAL

5.2.1. Materials and methods

Chloromethylated polystyrene [18.9 % Cl (5.3 mmol Cl per gram of resin)] cross-linked with 5 % divinylbenzene was obtained as a gift from Thermax Limited, Pune, India. Analytical reagent grade V$_2$O$_5$ (Loba Chemie, Mumbai, India), 2-(2-aminoethyl)pyridine, styrene, vinyl pyridine (Acros Organics. New Jersey, U.S.A), salicylaldehyde (Ranbaxy, India) were used as obtained. Aniline, diethyl amine, toluene

and other chemicals were used as obtained. [$V^{IV}O(acac)_2$] [233], 3-formylsalicylic acid [368], and ligands (Hfsal-aepy) (**5.I**) [405] and (Hsal-aepy) (**5.III**) [406] were prepared according to the methods reported in the literature.

Instrumentation and analyses details are reported in Chapters 2 and 4.

5.2.2. Syntheses of ligands and complexes

5.2.2.1. Polymer anchored ligand, PS-[Hfsal-aepy] (5.II)

Chloromethylated polystyrene (3.0 g) was allowed to swell in DMF (40 ml) for 2 h. A solution of Hfsal-aepy (12.16 g, 45 mmol) in DMF (30 ml) was added to the above suspension followed by triethylamine (4.50 g) in ethylacetate (40 ml). The reaction mixture was heated at 90 °C for 20 h with slow mechanical stirring in an oil bath. After cooling to room temperature, the red resins were separated by filtration, washed thoroughly with hot DMF followed by hot methanol and dried in an air oven at 120 °C. Found: C, 74.24; H, 10.53; N, 5.99 %.

5.2.2.2. PS-[$V^{IV}O$(fsal-aepy)(acac)] (5.1)

The polymer-anchored ligand PS-[Hfsal-aepy] (1.50 g) was allowed to swell in DMF (25 ml) for 2 h. A solution of [$V^{IV}O(acac)_2$] (5.30 g, 20 mmol) in 20 ml DMF was added to the above suspension and the reaction mixture was heated at 90 °C in an oil bath for 15 h with slow mechanical stirring. After cooling to room temperature, the dark black polymer-anchored complex obtained was separated by filtration, washed with hot DMF followed by hot methanol and dried at 120 °C in an air oven. Found: C, 62.69; H, 10.66; N, 4.29; V, 7.13 %.

5.2.2.3. PS-[$V^{V}O_2$(fsal-aepy)] (5.2)

Complex **5.1** (1.5 g) was suspended in 50 ml MeOH along with 30 % aqueous H_2O_2 (1.11 g, 1.0 ml) and air was bubbled for *ca.* 48 h. During this period the colour of the beads slowly changed to orange. The beads were filtered off, washed with MeOH and

dried at room temperature over silica gel. Found: C, 67.21; H, 8.79; N, 3.55; V, 6.09 %, ^{51}V NMR (solid suspended in DMSO-d$_6$, δ/ppm): −511 (broad).

5.2.2.4. [V^{IV}O(sal-aepy)(acac)] (5.3)

A stirred solution of Hsal-aepy (1.13 g, 5 mmol) in acetonitrile (25 ml) was treated with [V^{IV}O(acac)$_2$] (1.33 g, 5 mmol) dissolved in acetonitrile (25 ml) and the resulting reaction mixture stirred for 3 h. The brown solid which separated was filtered off, washed with acetonitrile and dried *in vacuo* over silica gel. The brown crystals obtained upon slow evaporation were collected and dried under vacuum. Yield: 70%. Found: C, 58.43; H, 5.18; N, 7.19; V, 12.99 %.Calcd. for C$_{19}$H$_{20}$N$_2$O$_4$V: C, 58.32; H, 5.15; N, 7.16; V, 13.02 %. One of the crystals was used for single crystal X-ray analyses.

5.2.2.5. [V^{V}O$_2$(sal-aepy)] (5.4)

Complex **5.3** (0.391 g, 1 mmol) was dissolved in 20 ml of methanol and after addition of aqueous 30 % H$_2$O$_2$ (0.2 ml), the solution was aerially oxidised for several hours. After reducing the volume of solvent, the yellow solid of **5.4** was obtained, which was filtered and dried at 80 °C in air oven. Yield: 80 %. Found: C, 54.53; H, 4.21; N, 9.04; V, 16.50 %. Calcd. for C$_{14}$H$_{13}$N$_2$O$_3$V: C, 54.56; H, 4.25; N, 9.09;V, 16.53. ^{1}H NMR (DMSO-d$_6$) δ = 6.7 − 8.51 (m, 7 H, aromatic), 8.33 (s, 1H, Ar–C=N), -CH$_2$ 3.32, 3.22(t, 2H each, -CH$_2$-), ^{51}V NMR (DMSO-d$_6$, δ/ppm): −515 and −492. ^{13}C NMR (DMSO-d$_6$, δ/ppm) gives nine signals corresponding to the 14 carbon atoms *viz.* 157.7, 149.7, 149.2, 137, 135, 124, 122, 38, 35 and the assignment of the peaks was made with the help of the Chem Draw® software, and all of them matching within ± 2 % accuracy with the predicted values.

5.2.3. X-Ray crystal structure determination

The X-ray structure details are same as reported in Chapter 4. Crystal data and details on data collection and refinement are summarised in Table 5.1.

Table 5.1. Crystal and structure refinement data for compound **5.3**

	5.3
Formula	$C_{19}H_{20}VN_2O_4$
Mol. wt.	391.31
Crystal system	Orthorhombic
Space group	P2(1)/n
Temperature /K	293(2)
Wavelength /Å	0.71073
a /Å	20.070(4)
b /Å	10.750(2)
c /Å	8.5203(17)
$\alpha/°$	90.00
$\beta/°$	90.00
$\gamma/°$	90.00
V/ Å^3	1838.3(6)
Z	1
Density/Mgm^{-3}	1.414
Abs. Coeff. /mm^{-1}	0.566
F(000)	812
Total no. of reflections	3931
Reflections, $I > 2\sigma(I)$	3602
Max. $2\theta/°$	26.88
Ranges (h, k, l)	-25 <= h <=25 -13 <= k <=13 -10 <= l <= 10
Complete to 2θ (%)	99.1%
Refinement method	Full-matrix least-squares on F^2
Goof (F^2)	2.133
R indices [$I > 2\sigma(I)$]	0.0281
R indices (all data)	0.0337

5.2.4. Catalytic reactions: Hydroamination of styrene and vinyl pyridine

The hydroamination of styrene and vinyl pyridine was carried out in a 50 ml two-neck reaction flask fitted with a water condenser. The polymer-anchored complex was allowed to swell in toluene for 2 h prior to use in each experiment. In a typical reaction, 10 mmol of styrene (1.04 g) or vinyl pyridine (1.05 g) and 20 mmol of amine (1.86 g aniline or 2.92 g diethylamine) were mixed in 15 ml toluene. The catalyst, PS-[V^{IV}O(fsal-aepy)(acac)] (0.050 g) was added to the above reaction mixture and stirred at 90 °C for 1 h. The progress of the reaction was monitored by withdrawing small aliquots of the reaction mixture at every five minute intervals and analysed quantitatively by gas chromatograph. The identities of the products were confirmed by GC-MS. The effect of various parameters such as temperature, amount of amine and catalyst were studied to obtain suitable reaction conditions for the best performance of the catalyst.

5.2.5. Characterisation of Hydroaminated Products

5.2.5.1. Products of reaction of Styrene with Diethylamine

(i) **N,N-diethyl-2-phenylethanamine:** ^{1}H NMR (DMSO-d$_6$, δ/ppm): 7.47–7.26 (m, 5 H, aromatic), 4.13 (q, 1 H, -CH-), 3.89 (d, 3 H, -CH$_3$), 3.51 (q, 4 H, -CH$_2$-), 0.99 (t, 6 H, CH$_3$).

(ii) **N,N-diethyl-1-phenylethanamine:** ^{1}H NMR (DMSO-d$_6$, δ/ppm): 7.48–7.26 (m, 5 H, aromatic), 2.70, 2.73 (t, 2 H each, -CH$_2$-), 3.03 (q, 4 H, -CH$_2$-), 0.99 (t, 6 H, -CH$_3$).

5.2.5.2. Products of reaction of Styrene with Aniline

(i) **N-phenethylaniline:** ^{1}H NMR (DMSO-d$_6$, δ/ppm): 6.68–7.56 (m, 10 H, aromatic), 5.17 (s, 1 H, -NH), 3.51, 3.13(t, 2 H each, -CH$_2$-).

(ii) **N-(1-phenylethyl)aniline:** ^{1}H NMR (DMSO-d$_6$, δ/ppm): 6.47–7.56 (m, 10 H, aromatic), 5.01 (s, 1 H, -NH-), 4.05 (q, 4 H,-CH-), 0.94 (d, 1 H, CH$_3$).

5.2.5.3. Products of reaction of Vinyl pyridine with Diethylamine

(i)   **N,N-diethyl-2-(pyridin-4-yl)ethanamine:** ^{1}H NMR (DMSO-d_6, δ/ppm): 8.65–7.26 (m, 5 H, aromatic), 3.05 (q, 4 H, -CH$_2$-), 2.68, 2.70 (t, 2 H each, -CH$_2$-), 0.99 (t, 6 H, -CH$_3$).

(ii) **N,N-diethyl-1-(pyridin-4-yl)ethanamine:** ^{1}H NMR (DMSO-d_6, δ/ppm): 8.60–7.37 (m, 5 H, aromatic), 4.10 (q, 1 H, -CH-), 2.43 (q, 4 H, -CH$_2$-), 1.31 (q, 1 H, -CH-), 0.97 (t, 6 H, -CH$_3$).

5.2.5.4. Products of reaction of Vinyl pyridine with Aniline

(i)   **N-(2-(pyridin-3-yl)ethyl)aniline:** ^{1}H NMR (DMSO-d_6, δ/ppm): 8.45–6.6 (m, 9 H, aromatic), 5.56 (s, 1 H, -NH), 3.40, 2.82(t, 2 H each, -CH$_2$-).

(ii) **N-(1-(pyridin-3-yl)ethyl)aniline:** ^{1}H NMR (DMSO-d_6, δ/ppm): 8.62–6.85 (m, 9 H, aromatic), 4.10 (q, 1 H, -CH-), 4.01 (s, 1 H, -NH-), 0.97 (d, 1 H, -CH$_3$).

5.3. RESULTS AND DISCUSSION

5.3.1. Syntheses, reactivity and solid state characteristics

Ligand, Hfsal-aepy (**5.I**), obtained by the condensation of 3-formylsalicylic acid and 2-(2-aminoethyl)pyridine, reacted with chloromethylated polystyrene (18.9 % Cl, 5.35 mmol Cl g^{-1} resin) cross linked with 5 % divinylbenzene in DMF in the presence of triethylamine and ethyl acetate to give polystyrene supported ligand, PS-[Hfsal-aepy]. In this process, the –COOH group of 3-formylsalicylic acid reacted with the –CH$_2$Cl group of polystyrene as shown in Scheme 5.3. The remaining chlorine content of 1.7 % (0.42 mmol Cl g^{-1} of resin) in PS-[Hfsal-aepy] suggests ca. 97 % loading of the ligand.

Hfsal-aepy (**5.I**)   PS-[Hfsal-aepy] (**5.II**)
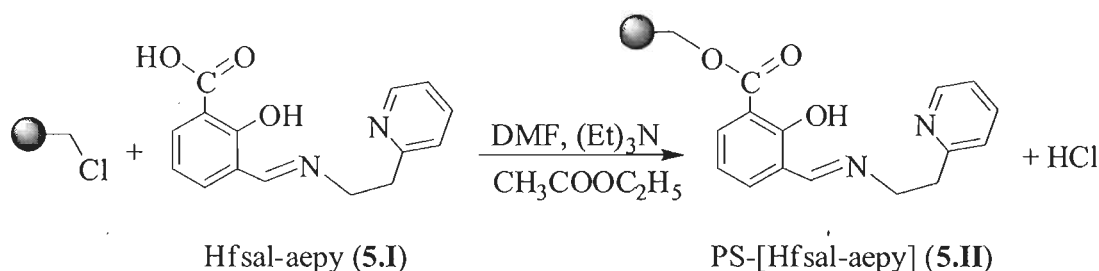
Scheme 5.3

The polymer-bound complex, PS-[V^{IV}O(fsal-aepy)(acac)] **5.1** was synthesised by reacting the polymer-bound ligand, PS-[Hfsal-aepy] with [V^{IV}O(acac)$_2$] in DMF at ca. 90 °C. Complex **5.1** on aerial oxidation in MeOH, gave the dioxidovanadium(V) complex, PS-[V^{V}O$_2$(fsal-aepy)] **5.2**. The whole synthetic procedures are presented in Scheme 5.4. Similarly, the reaction of [VO(acac)$_2$] with an equimolar amount of **5.III** in acetonitrile at room temperature yielded the oxidovanadium(IV) complex [V^{IV}O(sal-aepy)(acac)] (**5.3**), while [V^{V}O$_2$(sal-aepy)] (**5.4**) was obtained by aerobic oxidation of **5.3** in solvent in the presence of a small amount of H$_2$O$_2$. Table 5.2 provides data of metal and ligand loading in polymer-bound complexes, assuming the formation of PS-[Hfsal-aepy]. The obtained data show that the metal to ligand ratio in polymer-bound complexes is close to 1 : 1.

PS-[Hfsal-aepy](**5.II**)   PS-[VO(fsal-aepy)(acac)] (**5.1**)

PS-[VO(fsal-aepy)(acac)] (**5.1**)   PS-[VO$_2$(fsal-aepy)] (**5.2**)
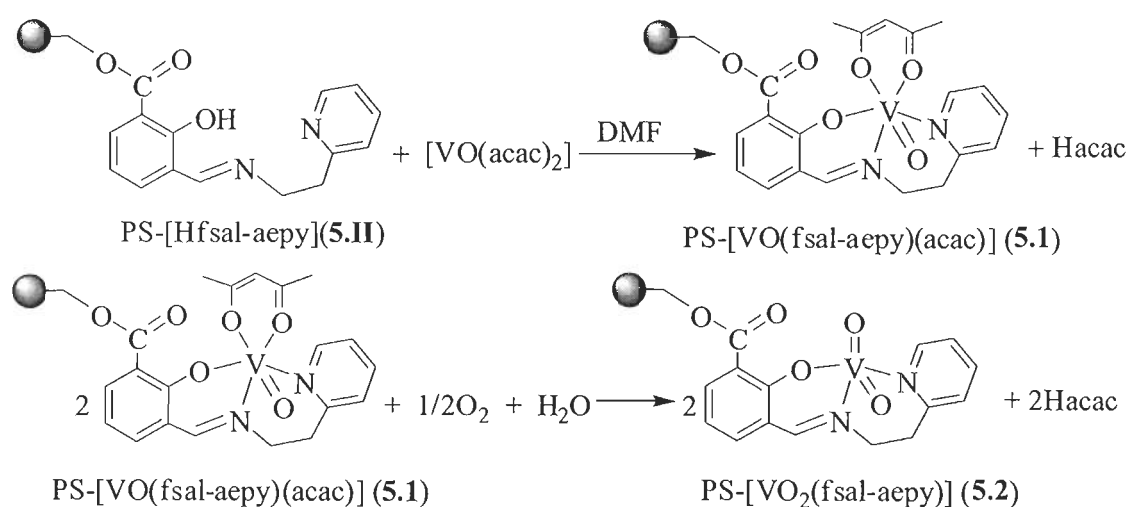
Scheme 5.4

Table 5.2. Ligand and metal loadings in polymer-bound complexes, and ligand-to-metal ratio data

Compound	Ligand loading (mmol g^{-1} of resin)	Metal ion loading[a] (mmol g^{-1} of resin)	Ligand : Metal ratio
PS-[Hfsal-aepy]	2.14	-	-
PS-[V^{IV}O(fsal-aepy)(acac)]	1.53	1.39	1 : 1.09
PS-[V^{V}O$_2$(fsal-aepy)]	1.26	1.19	1 : 1.06

[a] Metal ion loading = $\dfrac{\text{Observed metal \%} \times 10}{\text{Atomic weight of metal}}$

5.3.2. Field emission-scanning electron microscope (FE-SEM) and energy dispersive X-ray analyses (EDX) studies

Field emission scanning electron micrographs (FE-SEM) of pure chloromethylated polystyrene, polymer-bound ligand, PS-[Hfsal-aepy] and complexes were recorded taking single bead of each to understand the morphological changes occurring at various levels of syntheses. A light roughening of the top layer of bead having polymer-anchored ligand as compared to the relatively smooth and flat surface of the neat polystyrene bead suggests the change of nature of bead upon covalent bonding. Images of beads with metal complex show further roughening of the top layer which is possibly due to interaction of metal ions with ligand to adapt to the fixed geometry of the complex. Some of these images are reproduced in Fig. 5.1. Accurate information on the morphological changes in terms of exact orientation of ligand coordinated to the metal ion has not been possible due to the low amount of the metal complex bound to the polymer surface. However, pure polymer beads show mainly two components carbon (80.7 %) and chlorine (18.3 %) on the surface, as evaluated semi-quantitatively by energy dispersive X-ray analyses. A considerable amount of N (ca. 4.5 %) and small amount of Cl (ca. 1.8 %), was determined on the surface of the beads containing bound ligand. The polystyrene beads of immobilised metal complexes PS-[V^{IV}O(fsal-aepy)(acac)] and PS-[V^{V}O$_2$(fsal-aepy)] show metal content along with nitrogen, suggesting the formation of metal complex with the anchored ligand at various sites. The Energy dispersive X-ray analyses (EDX) profiles of two representative samples are presented in Fig. 5.1.

5.3.3. TGA studies

The polymer-anchored complexes PS–[V^{IV}O(fsal-aepy)(acac)] and PS–[V^{V}O$_2$(fsal-aepy)] are thermally stable up to ca. 175 °C under an oxygen atmosphere and thereafter they decompose exothermically in multiple steps. Quantitative measurement of weight loss at various steps was not possible due to their overlapping nature. However, the stability of final residues of both complexes at ca. 700 °C suggests the covalent bonding of these complexes to polymer support and the

formation of V_2O_5. Estimation of final residues was helpful in approximating the percentage of metal ions in the polymer-anchored complexes.

(a)

PS-[Hfsal-aepy] **(5.II)**

(b)

PS-[V^{IV}O(fsal-aepy)(acac)] **(5.1)**
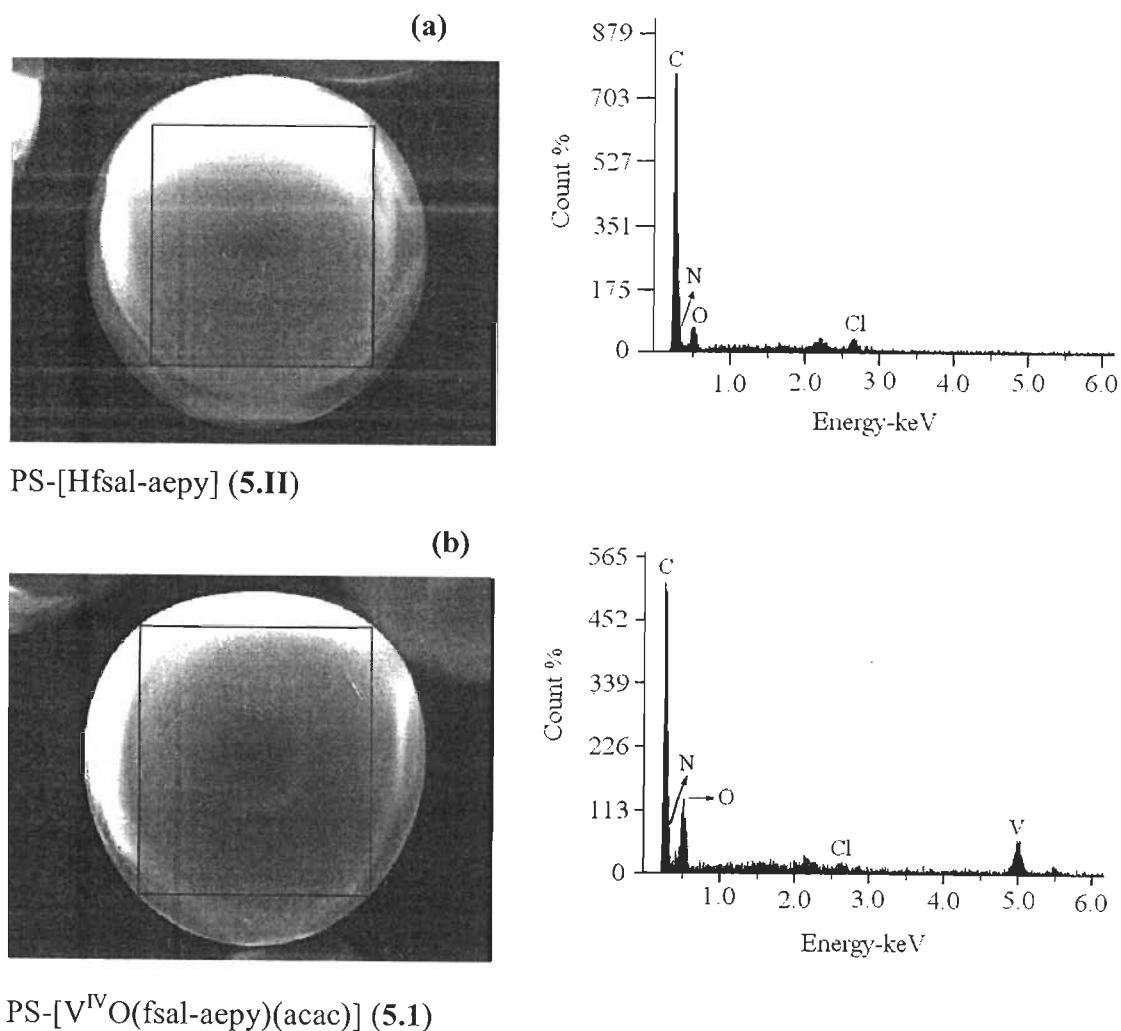
Fig. 5.1. FE-SEM (left) and EDX (right) profiles of (a) PS-[Hfsal-aepy] **(5.II)** and (b) PS-[V^{IV}O(fsal-aepy)(acac)] **(5.1)**.

5.3.4. Structure Description of [V^{IV}O(sal-aepy)(acac)] (5.3)

The molecular structure of [V^{IV}O(sal-aepy)(acac)] **5.3** together with the atom-numbering scheme is shown in Fig. 5.2; Table 5.3 provides selected bond lengths and bond angles. The geometry of the six-coordinated mononuclear complex can be

described as distorted octahedral; the axial sites of the octahedron are defined by the doubly bonded oxygen and the oxygen (O2) of the bidentate acac⁻ ligand, and the remaining coordinating atoms approximately form a plane.Bonding parameters are in the usual range [234, 273, 299, 374, 375]; the bond length to the function *trans* to the oxido group is somewhat elongated (V–O4 = 1.6091(12) Å vs V–O2 = 2.1129(11 Å)), as a consequence of the trans influence. Although the carbon-carbon and carbon-oxygen distances of the acac⁻ ligand do not permit to differentiate the ketonic oxygen from the enolic one, the similarity of the structure with [V^{IV}O(acac)(salimh)] [234] suggests that the neutral carbonyl oxygen atom is in the axial position.
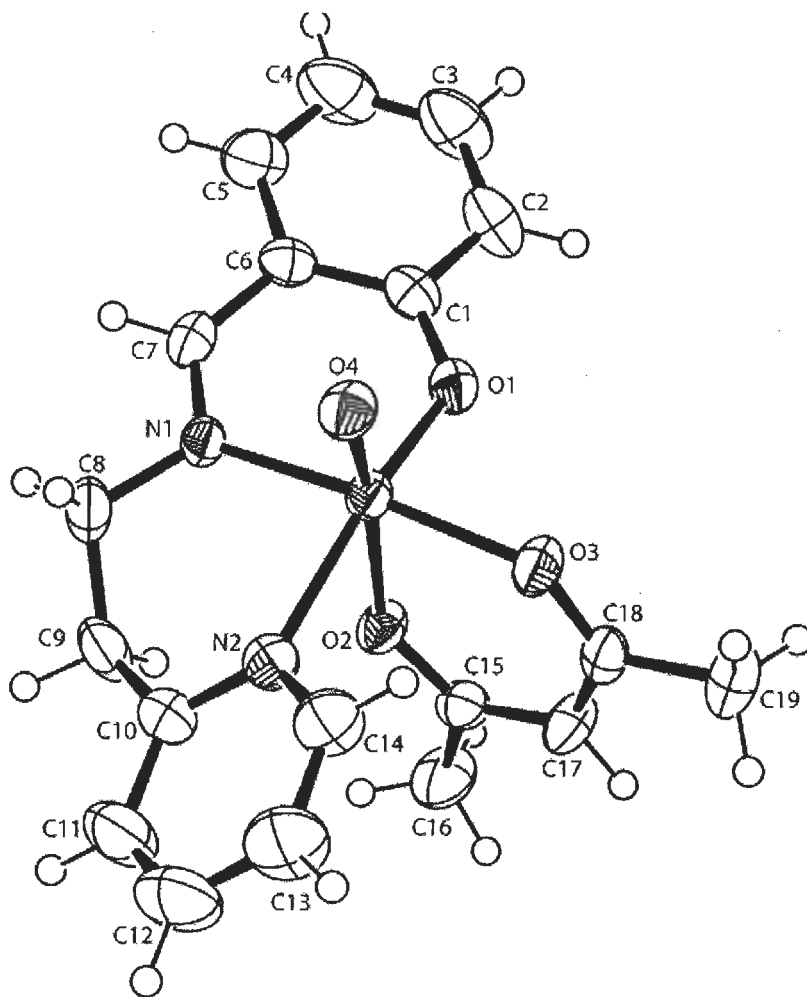
Fig. 5.2. ORTEP plot (at 30% probability level) of [V^{IV}O(sal-aepy)(acac)] (**5.3**).

Table 5.3. Selected bond lengths (Å) and bond angles (°) for complex **5.3**.

Bond lengths (Å)		Bond angles (°)	
V(1)- O(4)	1.6091(12)	O(4)-V(1)-O(1)	104.63(6)
V(1)- O(1)	1.9439 (11)	O(4)-V(1)-O(3)	94.94(6)
V(1)- O(3)	2.0003 (12)	O(1)-V(1)-O(3)	89.40(5)
V(1)- N(1)	2.0729 (14)	O(4)-V(1)-N(1)	94.76(6)
V(1)- O(2)	2.1129 (11)	O(1)-V(1)-N(1)	87.88(5)
V(1)- N(2)	2.1936 (14)	O(3)-V(1)-N(1)	170.30(5)
O(1)- C(1)	1.311(2)	O(4)-V(1)-O(2)	169.76(6)
O(2)- C(15)	1.2569(18)	O(1)-V(1)-O(2)	85.58(5)
O(3)- C(18)	1.273(2)	O(3)-V(1)-O(2)	84.10(5)
N(1)- C(7)	1.291(2)	N(1)-V(1)-O(2)	86.41(5)
N(1)- C(8)	1.460(2)	O(4)-V(1)-N(2)	91.80(6)
N(2)- C(10)	1.337(2)	O(1)-V(1)-N(2)	163.56(5)
N(2)- C(14)	1.341(2)	O(3)-V(1)-N(2)	90.03(5)
C(9)- C(10)	1.492(2)	N(1)-V(1)-N(2)	89.95(6)
C(9)- C(8)	1.513(3)	O(2)-V(1)-N(2)	78.02(5)
C(6)- C(5)	1.402(2)	C(1)-O(1)-V(1)	130.19(11)
C(6)- C (1)	1.410(2)	C(15)-O(2)-V(1)	130.12(11)
C(6)- C(7)	1.426(2)	C(18)-O(3)-V(1)	131.96(12)
C(1)- C(2)	1.410(2)	C(7)-N(1)-C(8)	116.94(15)
C(2)- C(3)	1.359(3)	C(7)-N(1)-V(1)	123.36(12)
C(2)- H(2)	0.9300	C(8)-N(1)-V(1)	118.60(11)
C(3)- C(4)	1.381(3)	C(10)-N(2)-C(14)	118.27(16)
C(3)- H(3)	0.9300	C(10)-N(2)-V(1)	124.98(12)
C(5)- C(4)	1.365(3)	C(14)-N(2)-V(1)	116.40(12)

5.3.5. IR spectral studies

The chloromethylated polystyrene shows strong peaks at 1264 and 673 cm^{-1} [379] in the IR spectrum and absence of these peaks in PS-[Hfsal-aepy] suggests the covalent bonding of chloromethylated polystyrene with Hfsal-aepy. The polymer-anchored ligand exhibits a sharp band at 1670 cm^{-1} due to the v(C=O). Existence of this band suggests covalent bond formation between the ligand and the polymer through an ester group. A band corresponding to v(C=N) at 1630 cm^{-1} in PS-[Hfsal-aepy] shifts to lower wave numbers thereby indicating the coordination of azomethine nitrogen to the metal ions. The presence of multiple bands of medium intensity covering the 2900-2800 cm^{-1} regions is consistent with the presence of –CH$_2$ groups. In addition, PS-[V^{IV}O(fsal-aepy)(acac)] exhibits a medium intensity band at 981 cm^{-1} due to v(V=O), indicating the existence of V=O bonds. Similarly the dioxido complex PS-[V^{V}O$_2$(fsal-aepy)] exhibits two such bands at 958 and 931 cm^{-1} corresponding to $v_{antisym}$(O=V=O) and v_{sym}(O=V=O) modes, respectively [236]. Non-polymer bound vanadium complexes also exhibit spectral patterns very close to polymer-anchored analogues, also similar to those reported in the literature [380].

Table 5.4. IR spectral data of ligand and complexes

Compound	v(C=O)	v(C=N)	v(V=O)
PS-Hfsal-aepy	1670	1630	-
PS-[V^{IV}O(fsal-aepy)(acac)]	1668	1600	981
PS-[V^{V}O$_2$(fsal-aepy)]	1674	1603	958, 931
Hsal-aepy	-	1632	-
[V^{IV}O(sal-aepy)(acac)]	-	1596	934
[V^{V}O$_2$(sal-aepy)]	-	1601	964, 919

5.3.6. Electronic spectral studies

The electronic spectral profiles of non-polymer bound and polymer-bound complexes are presented in Fig. **5.**3a and **5.**3b, respectively and the corresponding

data are presented in Table 5.5. The spectrum of Hsal-aepy exhibits three bands at 217, 255 and 318 nm. These bands are assigned to $\varphi. -\varphi^*$, $\pi- \pi^*$ and $n - \pi^*$ transitions, respectively. All three bands are also observed in the complexes with only slight variations. A new band appearing at 380 nm is possibly due to ligand to metal charge (lmct) transition. The electronic spectral patterns exhibited by the polymer-bound ligand and metal complexes are similar (Table 5.5) to those obtained for the corresponding non-polymer bound analogues, except the low intensity of bands. The lower energy (less intense) bands appearing at 534 and 770 nm due to d – d transitions in complex **5.3** could not be located in the corresponding polymer-bound complex due to its poor loading and extinction coefficient in the polymer matrix. However, a weak shoulder band due to ligand-to-metal charge transfer (lmct) transition could be located in the expected region.
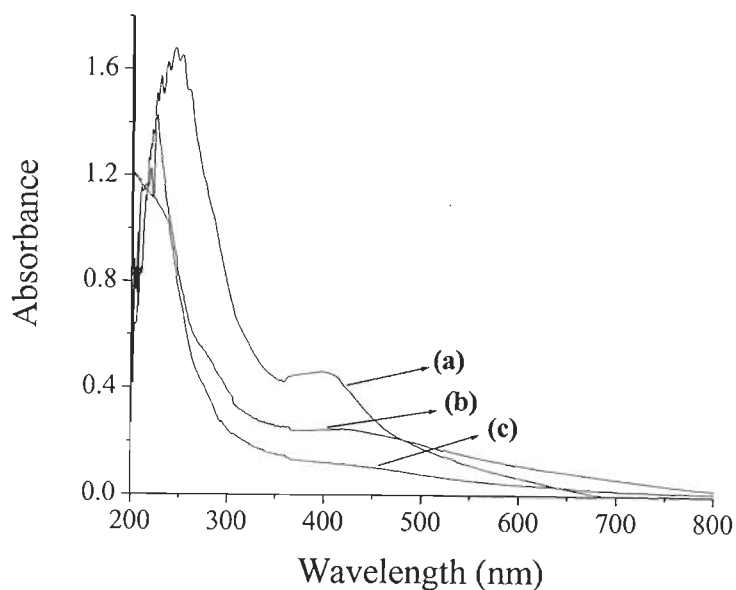
Fig. 5.3 (a). Electronic spectra of (a) PS-[Hfsal-aepy], (b) PS-[V^{IV}O(fsal-aepy)(acac)] and (c) PS-[V^VO$_2$(fsal-aepy)] recorded with the solids dispersed in Nujol.
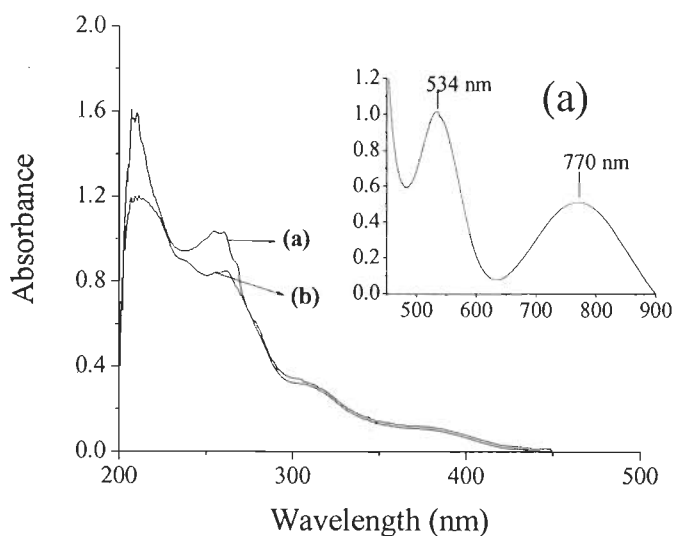
Fig. 5.3 (b). Electronic spectra of (a) [V^{IV}O(sal-aepy)(acac)], and (b) [V^{V}O$_2$(sal-aepy)] recorded in MeOH.

Table 5.5. Electronic spectral data of ligand and complexes

Compound	Solvent	λ_{max} (nm)
PS-Hfsal-aepy	Nujol	245, 260, 399
PS-[V^{IV}O(fsal-aepy)(acac)]	Nujol	226, 286, 423
PS-[V^{V}O$_2$(fsal-aepy)]	Nujol	229, 277, 421
Hsal-aepy	MeOH	217, 255.5, 318.5
[V^{IV}O(sal-aepy)(acac)]	MeOH	206, 260, 318, 380, 534, 770
[V^{V}O$_2$(sal-aepy)]	MeOH	211, 261, 311, 380

5.3.7 ^{51}V NMR studies

The ^{51}V chemical shift values for the V^V-complexes are included in the Experimental section. The line widths at half height are typically around 200 Hz. It is interesting to emphasise that we could measure a good signal for complex PS-[V^{V}O$_2$(fsal-aepy)] **5.2** suspended in DMSO, which presents a resonance at $\delta = -511$ ppm (broad) and a minor peak at -491 ppm. For complex **5.4** in DMSO-d$_6$ a

resonance was obtained at $\delta = -517$ and a minor one at -492 ppm. These chemical shifts are within the values expected for dioxidovanadium(V) complexes containing a O/N donor set [257]. The resonance at -491 ppm gains intensity with time in DMSO (24 h), and we assign this resonance at -491 ppm to $[V^VO_2(sal\text{-}aepy)(DMSO)]$.

Upon addition of methanol to a 4 mM solution of **5.4** in DMSO, both the -517 and -491 ppm resonances give rise to a single one at -542 ppm, identical to what is obtained when **5.4** is dissolved directly in MeOH only. The signal at -542 ppm is therefore assigned to $[V^VO_2(sal\text{-}aepy)(MeOH)]$ (**CI** in Scheme 5.5).
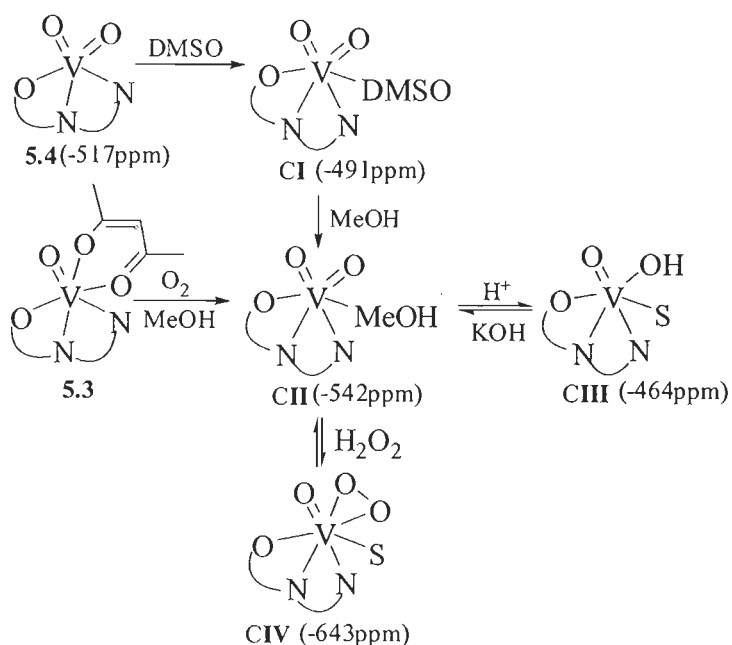
Scheme 5.5. General outline of speciation of vanadium species in solution

In the present study we have reinvestigated complex **5.4** in solution, trying to establish speciation using ^{51}V NMR spectroscopy. Addition of 3 equiv of HCl or $HClO_4$ to a methanolic solution of **5.4** results in a reduction in intensity of the $\delta = -542$ ppm peak, while a new broader signal at $\delta = -464$ ppm slowly gains intensity (see Fig. **5.4**). The colour of the solution turns to red and the pH $\sim 2.5\text{-}3.0$. We explain the changes observed by the protonation of oxo group, this generating an oxohydroxo species **CIII** (see Scheme 5.5).

155

Upon addition of 3 equiv. aqueous 30 % solution of H_2O_2 to the methanolic solution of **5.4** (ca. 4 mM) yields a resonance at −643 ppm, which we assign as due to $[V^VO(O_2)_2^-]$. Leaving the NMR tube open for 24 h, only the resonance at −542 ppm is recorded, indicating the reversibility of the process [258, 260].
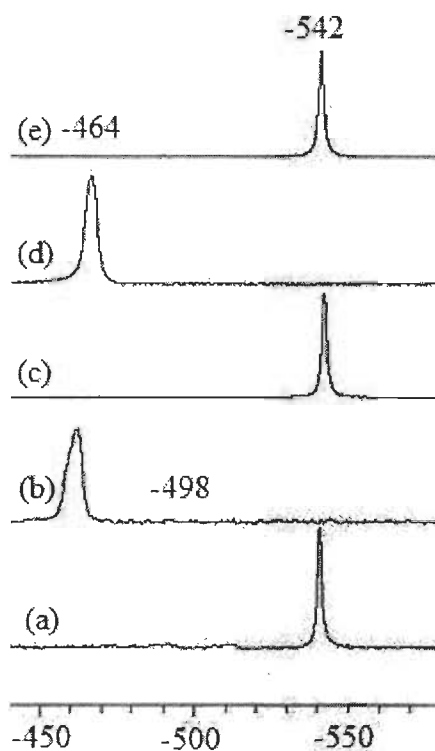
Fig. 5.4. ^{51}V NMR spectra of methanolic solutions of complex **5.4** (ca. 4 mM): (a) after preparation of the solution, (b) solution of (a) after addition of 3 equiv. HCl, (c) solution of (c) after 24 h leaving the tube open. (d) solution of (a) after addition of 3 equiv. $HClO_4$, (e) solution of (d) after 24 h leaving the tube open.

5.3.8. EPR Spectral studies

EPR spectra of "frozen" (77 K) solutions (in MeOH and DMSO) of complex **5.3** were recorded, and of solid **5.1** at room temperature. The EPR spectra are

depicted in Fig. 5.5. The spectrum of solid **5.1** is characteristic of magnetically diluted $V^{IV}O$-complexes. The resolved EPR pattern indicates that the vanadium(IV) centers are well dispersed in the polymer matrix. All spectra are well resolved in both the parallel and perpendicular regions, the hyperfine features and spectrum being consistent with binding modes involving (O_{acac}, $O_{phenolate}$, N_{imine}, N_{py})$_{equatorial}$(O_{acac})$_{axial}$. Once a particular binding mode is assumed, the values of $A_∥$ can be estimated using the additivity relationship proposed by Wurthrich [237] and Chasteen, [238] with estimated accuracy of ± $3×10^{-4}$ cm^{-1}. However, for the potential donor groups under consideration their predicted contributions to the parallel hyperfine coupling constant are rather similar {O_{acac}, ~41.7; $O_{phenolate}$ ~38.9; N_{imine} ~41.6; N_{py} ~40.7, O_{DMSO} ~41.9; O_{MeOH} ~45.5, all $A_∥$ contributions in cm^{-1} × 10^4 } [238, 407-409], so it is not possible to distinguish between the several plausible binding modes. Globally, by comparing the spectra of **5.3** in MeOH and DMSO indicates that the binding modes of **5.1** and **5.3** are same in solution, and probably also in the solid state. The spectra were simulated [235] and the spin Hamiltonian parameters obtained are included in Table 5.6.

Table 5.6 Spin Hamiltonian parameters obtained from the experimental EPR spectra recorded.

Complex	Solvent	$G_∥$	$A_∥$ ($×10^4$cm^{-1})	$A_⊥$ ($×10^4$cm^{-1})	$g_⊥$
PS-[$V^{IV}O$(fsal-aepy)(acac)]	Solid	1.945	167.6	59.3	1.979
	DMSO	1.946	168.8	58.4	1.980
[$V^{IV}O$(sal-aepy)(acac)]	MeOH	1.951	164.0	63.4	1.982
	DMSO	1.953	163.5	56.3	1.981
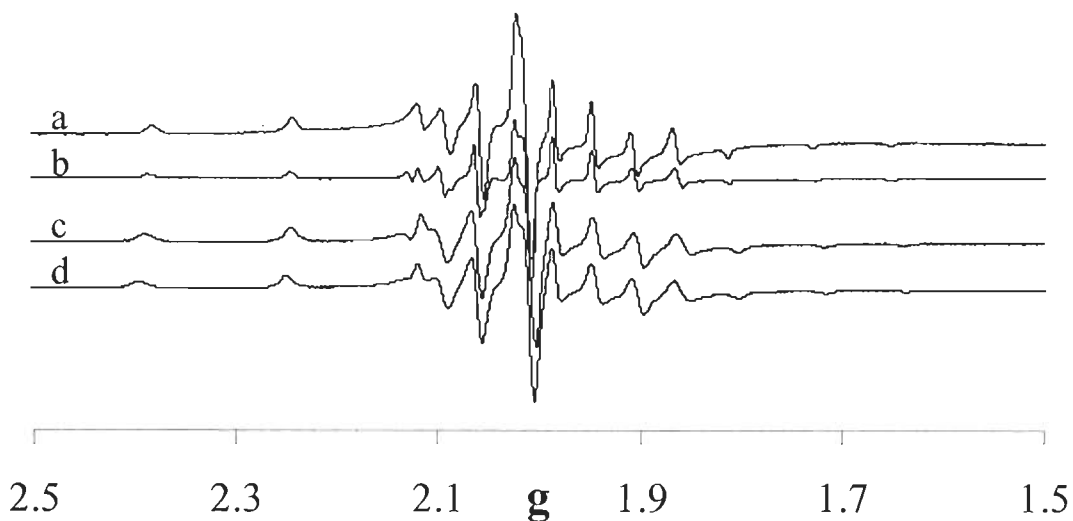
Fig. 5.5. First derivative EPR spectra of frozen solutions of [V^{IV}O(sal-aepy)(acac)] **(a)** in DMSO; **(b)** in MeOH. First derivative EPR spectra of **(c)** solid sample of PS-[V^{IV}O(fsal-aepy)(acac)] at room temperature and **(d)** PS-[VO(fsal-aepy)(acac)] at 77 K after swelling in DMSO.

As mentioned the EPR spectra of both complexes in DMSO are in good agreement with an O$_2$N$_2$ binding mode and in the case of **5.3** with the maintenance of the binding mode after its dissolution either in MeOH or DMSO. However, the coordination of solvent cannot be ruled out, but this implies the substitution of one of the equatorial donor atoms by an O-atom of the solvent.

5.3.9. Catalytic activity: Catalytic hydroamination of styrene and vinyl pyridine

Hydroamination of styrene and vinyl pyridine catalysed by polymer-anchored complexes, PS-[V^{IV}O(fsal-aepy)(acac)] and PS-[V^{V}O$_2$(fsal-aepy)] gave the corresponding enamines, Scheme 5.6, and the products were analysed by gas chromatography. The Markovnikov and anti-Markovnikov products have further been separated by column liquid chromatography and their identity confirmed by ^{1}H NMR and GC/MS spectroscopy. Various parameters such as temperature of reaction

mixture, amount of catalyst or amines have been optimised by taking styrene and aniline as representative substrates.
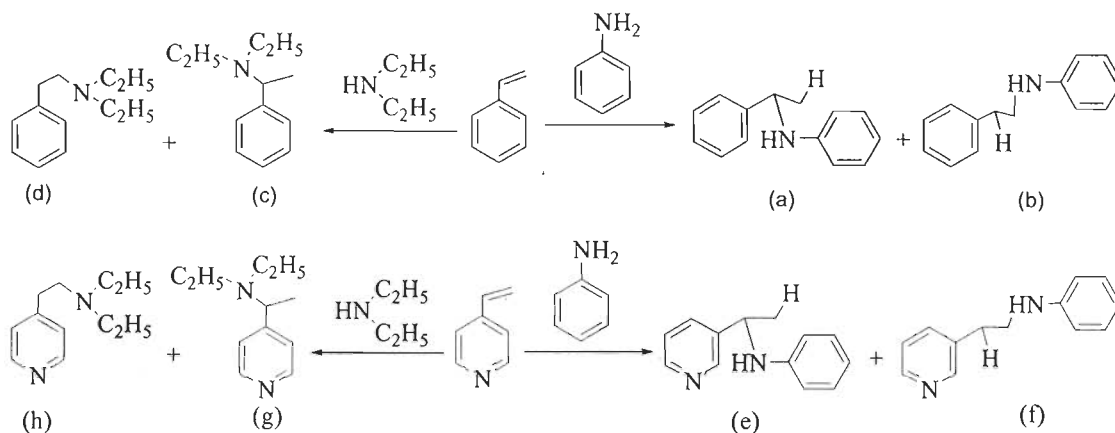
Scheme 5.6. (a) N-(1-phenylethyl)aniline, (b) N-phenethylaniline, (c) N,N-diethyl-1-phenylethanamine, (d) N,N-diethyl-2-phenylethanamine, (e) N-(1-(pyridin-3-yl)ethyl)aniline, (f) N-(2-(pyridin-3-yl)ethyl)aniline, (g) N,N-diethyl-1-(pyridin-4-yl)ethanamine, (h) N,N-diethyl-2-(pyridin-4-yl)ethanamine.

The reactions were carried out at different styrene to aniline molar ratios of 1 : 1, 1 : 2 and 1 : 3 using a fixed amount of styrene (1.04 g, 10 mmol), catalyst precursors (0.050 g) in 15 ml of toluene at 90 °C. Samples were periodically analysed up to 2 h. As illustrated in Fig. 5.6, a maximum of 64.4 % conversion has been achieved after 2 h of reaction time at a styrene to amine molar ratio of 1 : 1. Increasing this ratio to 1 : 2 led to a conversion of ca. 75.8 % while 1 : 3 molar ratio showed a maximum of ca. 80.1 % conversion.

In another experiment, three different catalyst loadings *viz.* 0.025 g, 0.050 g and 0.075 g were considered at a styrene to amine ratio of 1 : 2 under the above reaction conditions, and the results are presented in Fig. 5.7. As seen in the figure, 0.025 g of catalyst gave only 69.4 % conversion while 0.050 g and 0.075 g of catalyst loadings have shown a comparable conversion of 75.8 and 80.5 %, respectively. Thus, 0.050 g of catalyst was considered to be adequate to carry out the reaction for maximum hydroamination. The temperature of the reaction mixture has also influenced the performance of the catalyst. As shown in Fig. 5.8, running the reaction

at 90 °C gave a much better yield of the reaction products than at 70 or 80 °C. At 100 °C the conversion is somewhat higher than at 90 °C, but the latter temperature may be considered the most adequate to carry out further catalytic reactions.
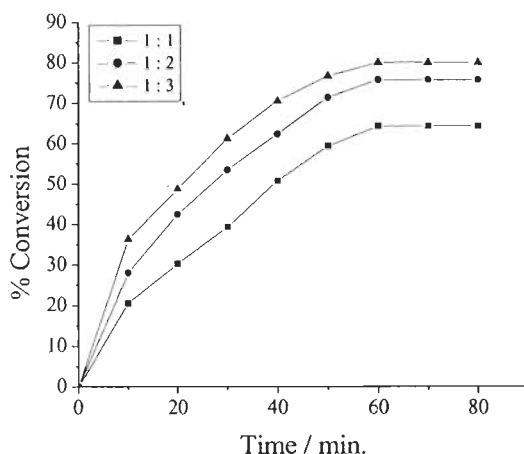
Fig. 5.6. Effect of the styrene to aniline ratio on the hydroamination of styrene with aniline. Reaction conditions: styrene (1.04 g, 10 mmol), PS-[V^{V}O$_2$(fsal-aepy)] (0.050 g) in 15 ml of toluene at 90 °C.
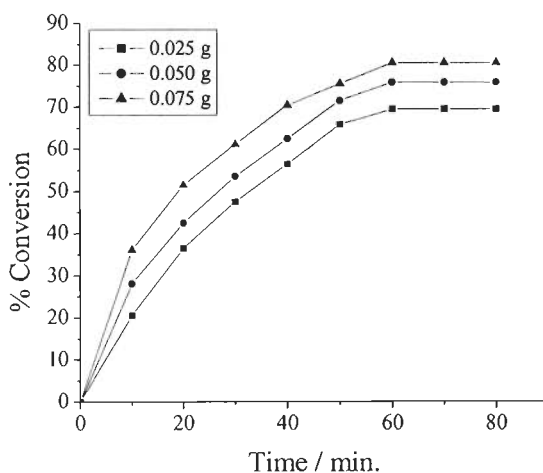
Fig. 5.7. Effect of the amount of catalyst PS-[V^{V}O$_2$(fsal-aepy)] on the hydroamination of styrene with aniline. Reaction conditions: styrene (1.04 g, 10 mmol), aniline (0.186 g, 20 mmol), in 15 ml of toluene at 90 °C.
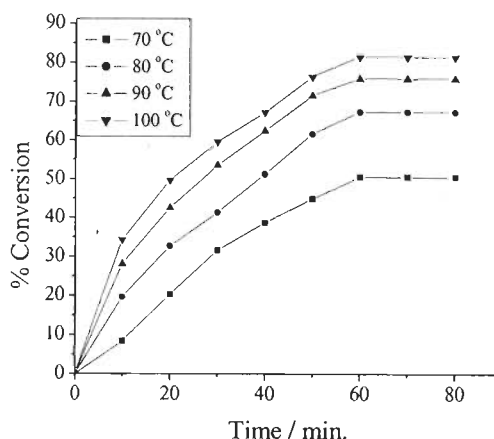
Fig. 5.8. Effect of temperature on the hydroamination of styrene with aniline. Reaction conditions: styrene (1.04 g, 10 mmol), aniline (0.186 g, 20 mmol), PS-[$V^{V}O_2$(fsal-aepy)] (0.050 g) in 15 ml of toluene.

Thus, the optimised reaction conditions concluded for the hydroamination of styrene with aniline are: styrene (1.04 g, 10 mmol), catalyst PS-[$V^{V}O_2$(fsal-aepy)] (0.050 g), toluene (15 ml) and temperature (90 °C), Under these conditions the hydroamination of styrene, catalysed by **5.2**, with aniline and diethylamine (20 mmol each) has also been carried out. It is clear from Table 5.7 that aniline gave a maximum of 75.8 % conversion while diethylamine gave only 59.6 %. Similarly, hydroamination of vinyl pyridine, catalysed by **5.2**, with aniline and diethyl amine has been carried out under the above optimised reaction conditions and gave 92.2 % conversion with aniline and 70.6 % with diethyl amine.

Table 5.7 presents data on hydroamination, turn over frequency (TOF) of the catalyst, and selectivity of the Markovnikov and anti-Markovnikov products obtained. The selectivity of N-phenethylaniline, N,N-diethyl-2-phenylethanamine, N-(2-(pyridin-3-yl)ethyl)aniline and N,N-diethyl-2-(pyridin-4-yl)ethanamine, i.e. the yield of the anti-Markovnikov products (c.f. Scheme 5.6), are higher than those of N-(1-phenylethyl)aniline, N,N-diethyl-1-phenylethanamine, N-(1-(pyridin-3-yl)ethyl)

aniline, and N,N-diethyl-1-(pyridin-4-yl)ethanamine, i.e. the Markovnikov products. This can be rationalised taking into account the steric hindrance imposed by the amine, which decreases the formation of the Markovnikov products.

The catalytic activity of the neat complex **5.3**, a close analogue of **5.1** in terms of coordination environment, was also tested for the hydroamination of styrene using approximately the same "concentration" as used for **5.1**. Its performance for various hydroaminated products after 2 h of reaction is also presented in Table 5.7. It is clear from the table that the neat complex exhibits slightly lower conversion than the anchored analogue for all reactions. The improvement in the catalytic activity of the anchored complex may be due to uniform distribution of metal centers on the polymer matrix, and/or an increased availability of styrene molecules which may adsorb on the polymer, close to the catalyst. The ester group on the α-position of nitrogen has no influence on the catalytic reaction as it is bound to the polymer.

The selectivity of the Markovnikov hydroaminated products is slightly higher for the non-anchored complex than for the polymer bound one. However, this effect is rather marginal and may be due to additional steric hindrance posed by polymeric support to anchored catalyst which might further restrict the Markovnikov product formation. The calculated turn-over frequencies for all the reactions with anchored catalysts are higher than those carried out using their non-polymer bound counterparts. Further, their stability and recycle ability make them better catalyst over the neat analogues.

The recyclability of the polymer anchored complexes PS-[V^{IV}O(fsal-aepy)(acac)] **(5.1)** and PS-[V^{V}O2(fsal-aepy)] **(5.2)** was checked up to the three cycles after washing the catalysts with acetonitrile and drying at ca. 100 °C after use. In the third cycle, the hydroamination of styrene with aniline catalysed by **5.1** gave a maximum of 64.1 % conversion while with diethylamine 45.3 % conversion has been obtained. Similarly, the hydroamination of vinyl pyridine with aniline and diethyl amine in the third cycle gave 78.2 % and 57.6 % conversion, respectively. Complex

5.2 has comparable results even up to third cycle of hydroamination. In the third cycle, styrene gave 74.2 % conversion with aniline and 54.9 % with diethylamine. Similarly vinyl pyridine gave 87.6 % conversion with aniline and 65.4 % with diethyl amine in the third cycle. Thus, these complexes have very good recycle ability.

Table 5.7. Conversion percentage and reaction products using neat and anchored catalysts

Catalyst	Olefin	Amine	% Conv.	TOF (h^{-1})	% Selectivity	
					Markovnikov product	anti-Markovnikov product
5.1	Styrene	Aniline	65.7	47.0	21.8	78.2
5.1		Diethylamine	47.7	34.1	27.4	72.6
5.1	Vinylpyridine	Aniline	82.0	58.6	17.8	82.2
5.1		Diethylamine	60.4	43.2	11.6	88.4
5.2	Styrene	Aniline	75.8	65.2	14.5	85.5
5.2		Diethylamine	59.6	49.9	28.5	71.5
5.2	Vinylpyridine	Aniline	92.2	77.3	18.9	81.1
5.2		Diethylamine	70.6	59.2	23.2	76.8
5.3	Styrene	Aniline	52.5	20.7	33.3	66.7
5.3		Diethylamine	31.3	12.3	35.5	64.5
5.3	Vinylpyridine	Aniline	69.4	27.3	30.3	69.7
5.3		Diethylamine	45.6	35.9	24.3	75.7
5.4	Styrene	Aniline	66.1	22.4	26.5	73.5
5.4		Diethylamine	42.4	13.2	34.4	65.6
5.4	Vinylpyridine	Aniline	88.3	27.4	31.8	68.2
5.4		Diethylamine	63.5	19.7	25.4	74.6

5.3.10. Reaction mechanism

Two basic approaches have been employed to catalytically effect aminations and involve either alkene/alkyne or amine activation routes. When carrying out

catalytic reactions with Pt-, Pd-, Rh-, and Ru- etc. -based catalysts, Müller and Beller[191] suggested that a possible route for oxidative amination is through intermediate complex formation. In the present study both approaches have been employed to catalytically affect aminations and involve either styrene/vinylpyridine or aniline/diethylamine activation routes (Scheme 5.7). We have used styrene and diethylalamine as the model reaction substrates with complex **5.3** and **5.4**.

5.3.11. Possible routes to hydroamination catalysed by [VO(sal-aepy)(acac)] (5.3)

Our catalytic system is based on either an oxidovanadium- (IV) or a dioxidovanadium(V) complex. Previously [78] experimental evidence has been obtained for the binding of styrene with a $V^{IV}O$-complex. We now further explore this possibility by studying the interaction with neat vanadium complex [$V^{IV}O$(sal-aepy)(acac)] **(5.3)** with styrene and/or diethylamine by spectroscopic techniques *viz.* UV/Vis absorption, ^{51}V NMR and EPR.

We have monitored the changes, by UV-Vis absorption spectroscopy, by treating [$V^{IV}O$(sal-aepy)(acac)] **5.3** with styrene in methanol. Thus, the addition of one drop of a 0.5 M styrene solution in methanol (complex **5.3** : styrene molar ratio of ca. 1 : 10) to 5 ml of ca. 10^{-4} molar solutions of **5.3** in methanol, resulted in the spectral changes with time shown in Fig. 5.9. Upon addition of styrene two new bands show up at 281 and 292 nm, while the band at 263 nm slowly shifts to 244 nm with increase in intensity. The position and optical densities of the bands due to d - d transitions remain approximately constant; therefore, the interaction of styrene with **5.3** does not change the oxidation state of vanadium, but it does make some changes in the coordination geometry around the vanadium centre. Probably the styrene molecule interacts with vanadium via a side-on pi bond.
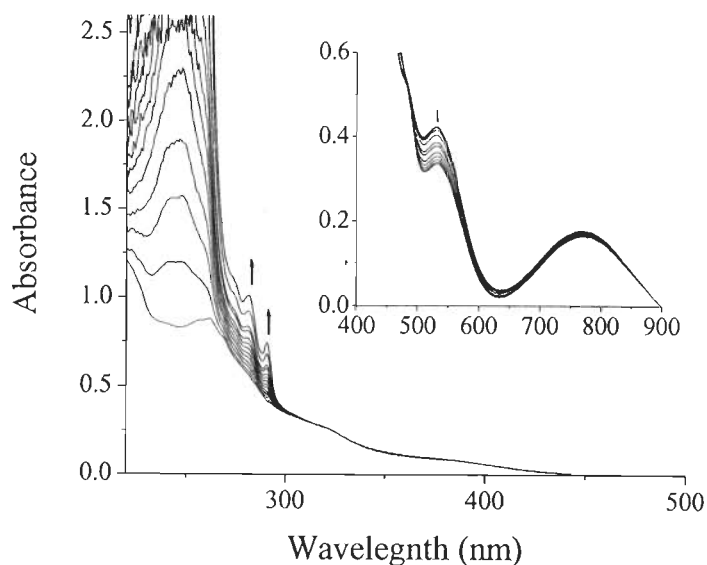
Fig. 5.9. Reaction of [$V^{IV}O$(sal-aepy)(acac)] **(5.3)** with styrene. The spectra were recorded at a interval of 2 min. after adding 1 drop of styrene solution to ca. 5 ml of 10^{-4} M solution of **5.3** in methanol (complex **5.3** : styrene molar ratio of ca. 1 : 10).

EPR spectra have been recorded in order to find evidence for the intermediate species formed during the catalytic cycle. The neat complex [$V^{IV}O$(sal-aepy)(acac)] **5.3** was dissolved in MeOH (4 mM), different amounts of styrene were added, samples were taken and frozen and the spectra recorded (Fig. 5.10). After addition of ca. 10 equiv. of styrene, the spin Hamiltonian parameters obtained are: $g_\parallel = 1.949$, $g_\perp = 1.979$, $A_\parallel = 162.80 \times 10^{-4}$ cm^{-1}, $A_\perp = 58.10 \times 10^{-4}$ cm^{-1}. This spectrum slightly differs from the complex in the absence of styrene. These results give some indication of the interaction of styrene with the metal complex detected by EPR. This interaction is weak and it is not clear from EPR if there is a coordination of styrene to the V^{IV}-center. DFT calculations indicate that [$V^{IV}O$(L)(alkene)] (L = salan type ligand) complexes may form, but the V^{IV}-alkene interaction is side-on and rather weak.

Similarly, we have monitored by UV-Vis the changes observed upon treating [$V^{IV}O$(sal-aepy)(acac)] **5.3** with diethylamine in methanol. The addition of one drop of 0.5 M diethylamine solution in methanol (complex **5.3**/diethylaminr molar ratio of

165

ca. 1 : 10) to 5 ml of ca. 10^{-4} molar solutions of **5.3** in methanol resulted in the spectral changes with time as shown in Fig. 5.11. Upon addition of diethylamine there are spectral changes: the band at 238 nm disappears while bands at 212, 261 and 304 nm gain intensity.
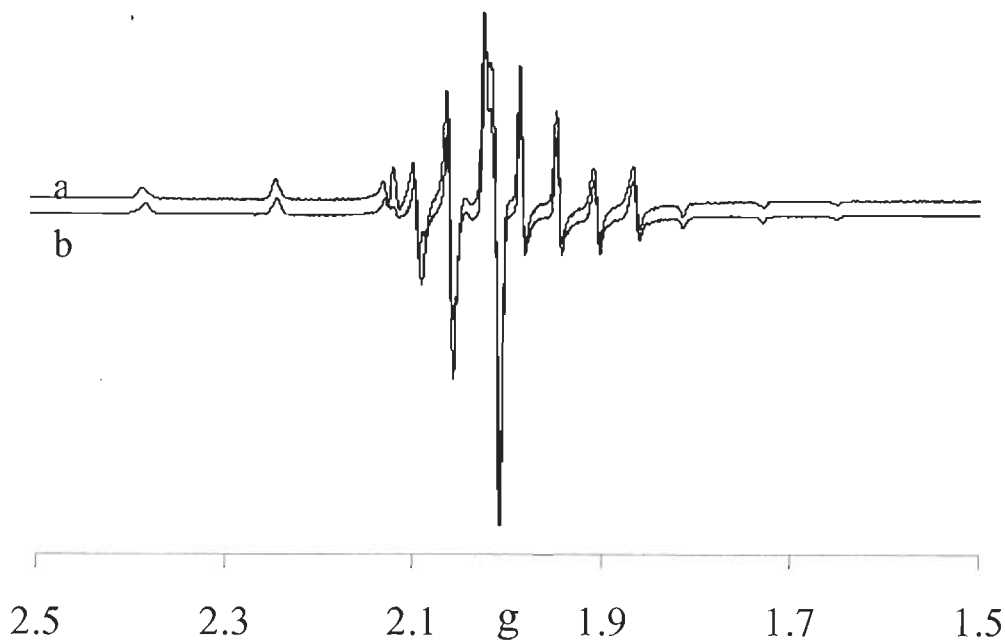
Fig. 5.10. EPR spectra of frozen methanolic solutions, ca. 4 mM of [$V^{IV}O$(sal-aepy)(acac)] **(5.3)** (a) before and (b) after addition of 10 equiv. styrene dissolved in MeOH. Styrene : complex molar ratio = 10.

The interaction of dietylamine with the $V^{IV}O$-centre is clearly supported by the EPR results (Fig. 5.12). Upon addition of diethylamine to a 4 mM solution of **5.3** in MeOH, an entirely different EPR spectra is obtained, the spin Hamiltonian parameters for the new species formed being: $g_{\parallel} = 1.957$, $g_{\perp} = 1.977$, $A_{\parallel} = 159.9 \times 10^{-4}$ cm^{-1}, $A_{\perp} = 53.5 \times 10^{-4}$ cm^{-1}. These results clearly indicate a change in the binding mode, certainly involving the coordination of the N-atom of diethylamine to the metal complex. A tentative outline of the global mechanistic steps of hydroamination process with complex **5.3** is given in Scheme 5.7.
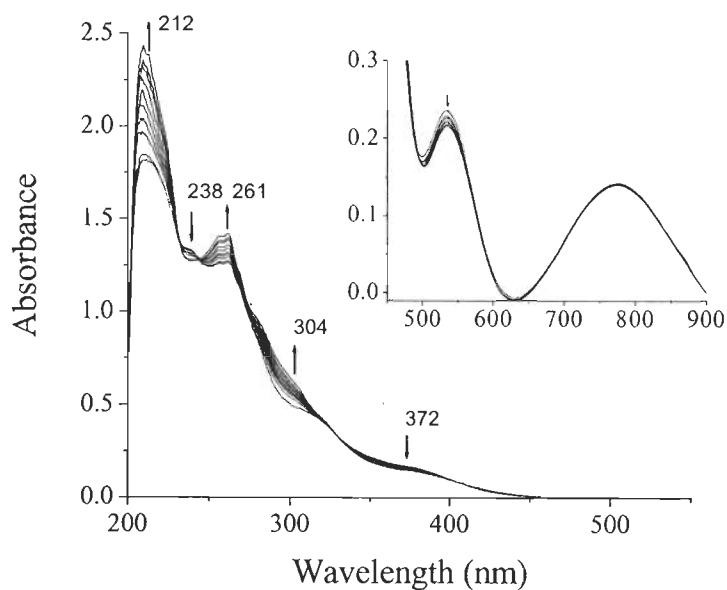
Fig. 5.11. Addition of [V^{IV}O(sal-aepy)(acac)] with diethylamine. The spectra were recorded at a interval of 2 min. after adding 1 drop of diethylamine to ca. 5ml of a 10^{-4} M solution of [V^{IV}O(sal-aepy)(acac)] in methanol.
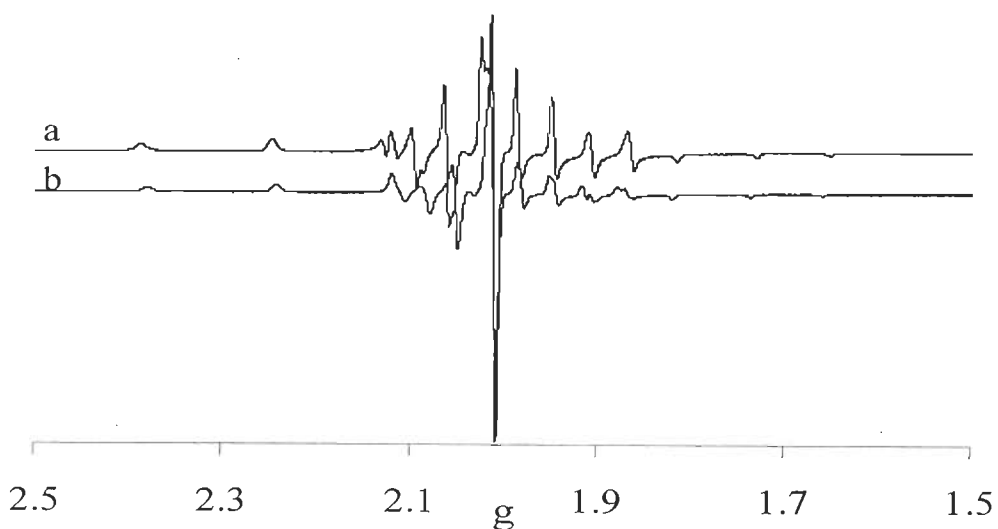
Fig. 5.12a. First derivative EPR spectra of [V^{IV}O(sal-aepy)(acac)] **(5.3)** frozen solutions: (a) the neat complex (4 mM) in MeOH; (b) solution of (a) after additions of equiv. diethylamine dissolved in MeOH up to 8 equiv. (spectrum shown in b).
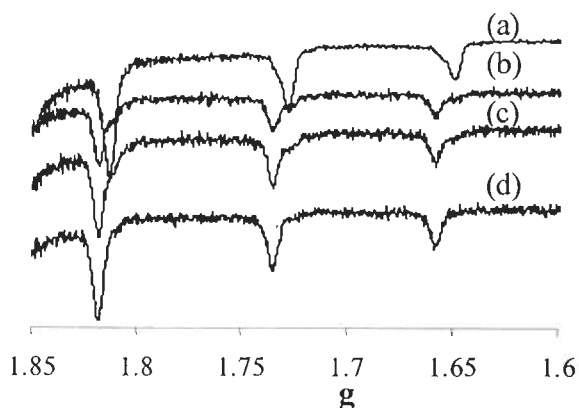
Fig. 5.12b. High field region of the EPR spectra of frozen solutions of [V^{IV}O(sal-aepy)(acac)] **(5.3)**: (a) the neat complex (ca. 4 mM) in MeOH; (b–d) the same solution after successive additions of diethylamine dissolved in MeOH up to 8 equiv.
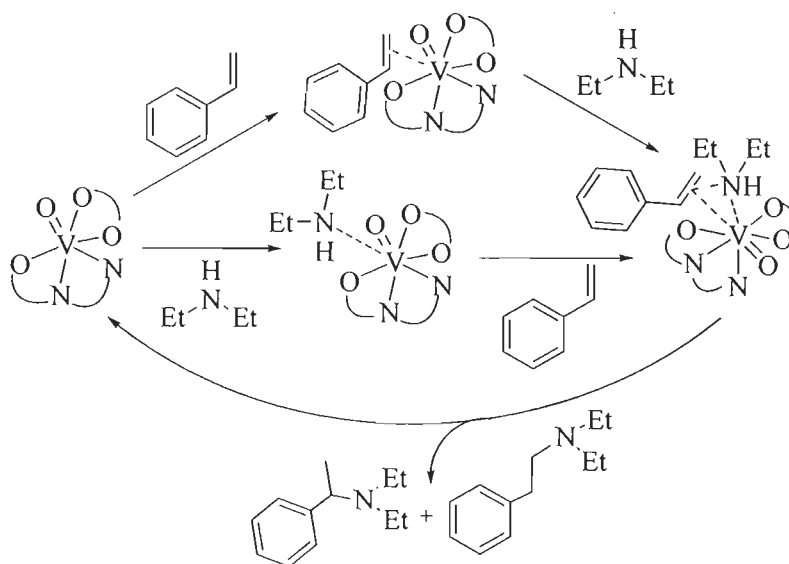
Scheme 5.7. Outline of the catalytic hydroamination processes of [V^{IV}O(sal-aepy)(acac)] **(5.3)** (4 mM) in MeOH, showing the proposed intermediates formed. O__O ≡ acac$^-$; O__N__N ≡ sal-aepy ligand.

5.3.12. Possible routes to Hydroamination catalysed by [V^{V}O$_2$(sal-aepy)] (5.4)

To better understand the hydroamination of styrene catalysed by **5.2** and **5.4**,

we considered [V^VO_2(sal-aepy)] (**5.4**) and diethylamine as a model system and used ^{51}V NMR spectroscopy. The ^{51}V NMR spectrum of [V^VO_2(sal-aepy)] (**5.4**) dissolved in MeOH is shown in Fig. 5.13(a) as well as after stepwise additions of styrene. Upon addition of styrene (3 additions, *viz.* 2, 5 and 10 equiv) to **5.4**, a downfield shift is observed (Fig. 5.13), and no further change is seen upon further addition of styrene. It appears that styrene binds to V^V forming [V^VO_2(sal-aepy)(styrene)] complexes with δ = −538 ppm. The addition of diethylamine to the solution of spectrum of Fig. 5.13(c) does not change further the ^{51}V NMR spectra observed. Similar experiments but adding diethylamine (Fig. 5.14) yield a complex, probably [V^VO_2(sal-aepy)(HNEt$_2$)] with δ = −539 ppm. Addition of styrene to the solution of spectrum of Fig. 5.14(c) does not change significantly the ^{51}V NMR spectra observed.

These ^{51}V NMR studies indicate the formation of intermediates species that may be relevant for the mechanism of hydroamination and Scheme 5.8 suggests plausible outlines of the reaction indicating the possible intermediates formed.
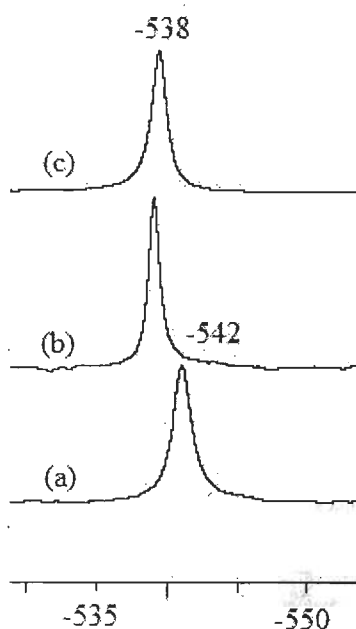
Fig. 5.13. ^{51}V NMR spectra for solutions (ca. 4 mM) of [V^VO_2(sal-aepy)] (**5.4**): (a) in MeOH, and (b-c) after stepwise additions of styrene up to 10 equivalent.
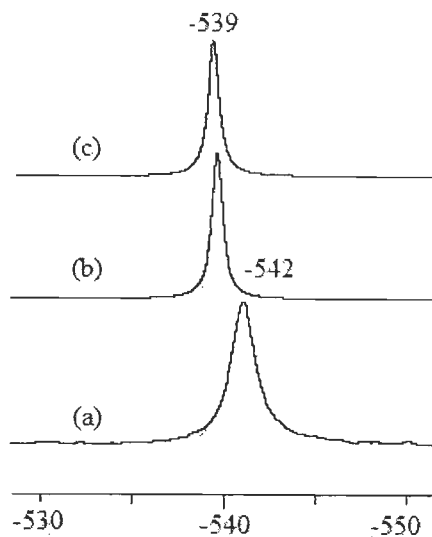
Fig. 5.14. ^{51}V NMR spectra for solutions (ca. 4 mM) of $[V^VO_2(sal-aepy)]$ **(5.4)**: (a) in MeOH, and (b-c) after stepwise additions (*viz.* 2, 5 and 10 equiv) of diethylamine up to a total of 8 equivalent.
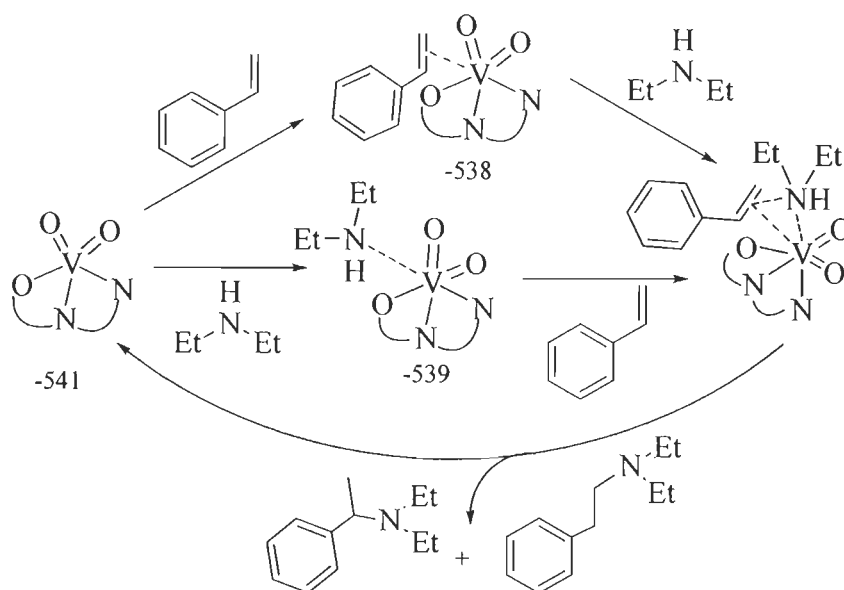
Scheme 5.8. Plausible outline of the hydroamination process catalysed by $[V^VO_2(sal-aepy)]$ **(5.4)**, showing the intermediates that may form.

The activation of styrene is accomplished by $V^{IV}O$- or V^VO_2- catalysts, which render coordinated styrene more susceptible to attack by exogenous amine nucleophiles. It is possible that a template effect also operates. Styrene binds to vanadium which then couples with the amine to give another intermediate complex involving the bound product followed by cleavage of the M–C bond. Depending on the carbon atom of styrene where the attack of the amine takes place, the addition proceeds either obeying the Markovnikov rule or opposite to the Markovnikov′ rule is obtained. The regioselectivity favors the product that corresponds to the least steric hindrance for the intermediate amino-styrene addition product, in this case the anti-Markovnikov′ rule product.Intermediate amino-styrene complexes can then react in different ways, leading to hydroamination [410].

Another possible route could be the amine activation by the metal to generate highly nucleophilic amido species, which are then able to directly attack the styrene. One of the possible amine activation route uses N-H addition to electron-rich, metal centers. So far, N-H activation via addition of amines to vanadium complexes has not been investigated. The formation of amido complexes directly from amines has only seldom been observed and confirmed reports of oxidative additions of R_2N-H to coordinatively unsaturated metal centers are rare [411-415].

5.4. CONCLUSIONS

The polymer anchored oxidovanadium(IV) and dioxidovanadium(V) complexes of the ligand derived from 3-formylsalicylic acid and 2-(2-aminoethyl)pyridine have been synthesised and characterised. The corresponding neat $V^{IV}O$- and V^VO_2-complexes **5.3** and **5.4**, respectively, were synthesised and characterised. Complex [$V^{IV}O$(sal-aepy)(acac)] (**5.3**) was characterised by single crystal X-ray diffraction, showing that it is a six-coordinated mononuclear V^{IV}-complex with the O-atoms of the acac⁻ ligand bound in an equatorial/axial fashion.

The polymer-anchored and corresponding non- polymer-anchored complexes

were used with success as catalyst for the hydromination of styrene and vinyl pyridine with amines such as aniline and diethylamine. The reaction conditions were optimised to obtain maximum conversion. Under the optimised conditions a mixture of two types of aminated products was obtained in good yield, the anti-Markovnikov products being favored over the Markovnikov products. The polymer-anchored gave better conversions and TOFs than their corresponding non-supported counterparts. Moreover, the polymer-anchored catalysts are recyclable.

The formation of possible intermediates during the catalytic reaction has been established using the neat complexes, styrene and diethylamine as a model system. Upon addition of either styrene, diethylamine or both to solutions of **5.3** in MeOH, by EPR and UV-Vis it was shown that the changes observed in the spectra are compatible with the formation of species involving the binding of either the alkene or the amine to the V^{IV}-centre. Similarly, upon addition of either styrene, diethylamine or both to solutions of **5.4** in MeOH, by ^{51}V NMR spectroscopy it was also shown that new peaks are detected, compatible with the formation of species involving the binding of either the alkene or the amine to the V^{V}-centre.

*****

References

1. B.H. Davis, in G. Ertl, H. Knözinger and J. Weitkamp (Eds.), "Handbook of Heterogeneous Catalysis", Vol. 1, VCH, Weinheim, 1997.

2. I. Horiuti and M. Polanyi, "Exchange reactions of hydrogen on metallic catalysts", *Trans. Faraday Soc.*, 1934, **30**, 1164 – 1172.

3. H.S. Taylor, "A theory of the catalytic surface", *Proc. R. Soc. A.*, 1925, **108**, 105 – 111.

4. A.J. van Peski, "Synthetic oil by catalytic polymerization of cracked gasoline hydrocarbons", 1937, US Pat. 2067030 19370105.

5. F. Schick and E. Emilius, "Catalytic cracking of heavy hydrocarbons", 1937, US Pat. 2097989 19371102.

6. E.J. Houdry, W.F. Burt, A.E. Pew Jr. and W.A. Peters Jr., "Catalytic processing of petroleum hydrocarbons by the Houdry process", *Oil Gas J.*, 1938, **37**, 40 – 43.

7. E.B. Andrews, "Cobalt-molybdenum desulfurization catalyst", *Proc. Chem. Eng. Group Soc. Chem. Ind.*, 1963, 1396 – 1400.

8. W.J. Hendriks, J.C. Vlugter and H.I. Waterman, "Catalytic desulfurization of crude oil", *Brennstoff-Chemie*, 1961, **42**, 1 – 11.

9. W.J. Hendriks, J.C. Vlugter and H.I. Watermann, "Preparation of concentrates of sulfur compounds from a Middle East gas oil and their catalytic desulfurization", *Brennstoff-Chemie*, 1961, **42**, 278 – 283.

10. W.J. Hendriks, J.C. Vlugter and H.I. Watermann, "Catalytic desulfurization and composition of light oils obtained by catalytic cracking", *Brennstoff-Chemie*, 1961, **42**, 145 – 149.

11. F.A. Cotton, G. Wilkinson, C.A. Murillo and M. Bochmann, "Advanced Inorganic Chemistry", John Wiley & Sons, Inc. 6th Edition, 1999, p.1270.

12. D.R. Armstrong, R. Fortune and P.G. Perkins, "A molecular orbital investigation of the wacker process for the oxidation of ethylene to acetaldehyde", *J. Catal.*, 1976, **45**, 339 – 348.

13. B.R. James and M. Kastner, "Reactions of ethylene with rhodium(III) chloride, Catalytic oxidation of ethylene to acetaldehyde in aqueous hydrochloric acid solutions containing pentachloroaquorhodate(III)", *Canadian J. Chem.*, 1972, **50**, 1698 – 1707.

14. P.B. Weisz and V.J. Frilette, "Intracrystalline and molecular-shape-selective catalysis by zeolite salts", *J. Phy. Chem.*, 1960, **64**, 382 – 383.

15. P.B. Weisz, W.O. Haag and P.G. Rodewald, "Catalytic production of high-grade fuel (gasoline) from biomass compounds by shape-selective catalysis", *Science*, 1979, **206**, 57 – 58.

16. M. Boudart, "Catalysis by supported metals", *Adv. Catal.*, 1969, **20**, 153 – 166.

17. S.H. Oh and C.C. Eickel, "Influence of metal particle size and support on the catalytic properties of supported rhodium: carbon monoxide-oxygen and carbon monoxide-nitric oxide reactions", *J. Catal.*, 1991, **128**, 526 – 536.

18. K.I. Jagel and F.G. Dwyer, "Hydro-carbon monoxide oxidation catalysts for vehicle exhaust emission control", *Proc. – Am. Petro. Inst., Div. Refining*, 1971, **51**, 169 – 185.

19. G.H. Meguerian and C.R. Lang, "Nitric oxide/nitrogen dioxide reduction catalysts for vehicle emission control", *Proc. – Am. Petro. Inst., Div. Refining*, 1971, **51**, 186 – 206.

20. O. Norbert, "DESONOX Process for Flue Gas Cleaning", *Catal. Today*, 1993, **16**, 247 – 261.

21. J.A. Sullivan, J. Cunningham, M.A. Morris and K. Keneavey, "Conditions in which Cu-ZSM-5 out performs supported vanadia catalysts in SCR of NO, by NH$_3$", *Appl. Catal. B: Environ.*, 1995, **7**, 137 – 151.

22. J. James and R.H.R. Julian, "The development of supported vanadia catalysts for the combined catalytic removal of the oxides of nitrogen and of chlorinated hydrocarbons from flue gases", *Catal. Today*, 1997, **35**, 97 – 105.

23. S. Blumrich and B. Engler, "The DESONOX/REDOX-process for flue gas cleaning. A flue gas purification process for the simultaneous removal of NO, and SO$_2$ resp. CO and UHC", *Catal. Today*, 1993, **17**, 301 – 310.

24. "The 12 Principle of Green Chemistry", United States Environmental Protection Agency". http://www.epa.gov/greenchemistry/pubs/principles.html. Retrieved on 2006-07-31.

25. For detail see: A.V. Ramaswamy, "Catalysis and theoretical concepts in Catalysis: Principles and Applications", Edited by: B. Viswanathan, S. Sivasanker and A.V. Ramaswamy, Narosa Publishing House, New Delhi, 2002, p.206.

26. I. Chorkendorff and J.W. Niemantsverdriet, "Concept of Modern Catalysis and Kinetics", Wiley-VCH GmbH & Co. KGaA, Weinheim, Germany, 2003.

27. G.H. Mahdavinia, S. Rostamizadeh, A.M. Amani and Z. Emdadi, "Ultrasound-promoted greener synthesis of aryl-14-H dibenzo[a,j]xanthenes catalyzed by $NH_4H_2PO_4/SiO_2$ in water", *Ultrason. Sonochem.*, 2009, **16**, 7 – 10.

28. H. Naeimi and M. Moradian, "Alumina-supported metal(II) Schiff base complexes as heterogeneous catalysts in the high-regioselective cleavage of epoxides to halohydrins by using elemental halogen", *Polyhedron*, 2008, **27**, 3639 – 3645.

29. G.S. Mishra and A. Kumar, "Liquid phase oxidation of n-octane catalyzed by silica gel supported vanadium (VO^{2+}) complex using molecular oxygen", *React. Kinet. Cata. Lett.*, 2003, **80**, 223 – 231.

30. M.J.L. Kishore, G.S. Mishra and A. Kumar, "Synthesis of hetero binuclear macrocyclic CoV complex bonded to chemically modified alumina support for oxidation of cyclohexane using oxygen", *J. Mol. Catal. A: Chem.*, 2005, **230**, 35 – 42.

31. S.L. Jain, J.K. Joseph, F.E. Kühn and O. Reiser, "An Efficient Synthesis of Poly(ethylene glycol)-Supported Iron(II) Porphyrin using a Click Reaction and its Application for the Catalytic Olefination of Aldehydes", *Adv. Synth. Catal.*, 2009, **351**, 230 – 234.

32. R. Wang, B. Gao and W. Jiao, "A novel method for immobilization of Co tetraphenylporphyrins on P(4VP-co-St)/SiO_2: Efficient catalysts for aerobic oxidation of ethylbenzenes", *Appl. Surf. Sci.*, 2009, **255**, 4109 – 4113.

33. C.T. Kresge, M.F. Leonowicz, W.J. Roth, J.C. Vartuli and J.S. Beck, "Ordered mesoporous molecular sieves synthesized by a liquid-crystal template mechanism", *Nature*, 1992, **359**, 710 – 712.

34. M. Masteri-Farahani, F. Farzaneh and M. Ghandi, "Synthesis of tetradentate N_4 Schiff base dioxomolybdenum(VI) complex within MCM-41 as selective catalyst for epoxidation of olefins", *Catal. Commun.*, 2007, **8**, 6 – 10.

35. S. Singhal, S.L. Jain and B. Sain, "Alumina-supported molybdenum(VI) oxide: An efficient and recyclable heterogeneous catalyst for regioselective ring opening of epoxides with thiols, acetic anhydride, and alcohols under solvent-free conditions", *Chem. Lett.*, 2008, **37**, 620 – 621.

36. S. Sahoo, P. Kumar, F. Lefebvre and S.B. Halligudi, "Synthesis of chiral sulfoxides by enantioselective sulfide oxidation and subsequent oxidative kinetic resolution using immobilized Ti–binol complex", *J. Catal.*, 2009, **262**, 111 – 118.

37. S. Sahoo, P. Kumar, F. Lefebvre and S.B. Halligudi, "Enantioselective hydrogenation of olefins by chiral iridium phosphorothioite complex covalently anchored on mesoporous silica", *J. Catal.*, 2008, **254**, 91 – 100.

38. G. Liu, Y. Gao, X. Lu, M. Liu, F. Zhang and H. Li, "Microwave-assisted catalytic allylation of aldehydes promoted by a mesoporous silica-supported BINOL ligand in solid media", *Chem. Commun.*, 2008, **27**, 3184 – 3186.

39. A.R. McDonald, C. Müller, D. Vogt, G.P.M. van Klink and G. van Koten, "BINAP-Ru and -Rh catalysts covalently immobilised on silica and their repeated application in asymmetric hydrogenation", *Green Chem.*, 2008, **10**, 424 – 432.

40. B.V. Romanovskii, R.E. Mardaleishvili, V.Yu. Zakharov and O.M. Zakharova, "Adsorption and catalytic properties of transition metal phthalocyanines in a zeolite matrix", *Vestnik Moskovskogo Universiteta, Seriya 2: Khimiya*, 1977, **18**, 240.

41. W. Zhang, J.L. Loebach, S.R. Wilson and E.N. Jacobson, "Enantioselective epoxidation of unfunctionalized olefins catalyzed by salen manganese complexes", *J. Am. Chem. Soc.*, 1990, **112**, 2801 – 2803.

42. M.L. Kantam, B.P.C. Rao, B.M. Choudary and B. Sreedhar, "Selective transfer hydrogenation of carbonyl compounds by ruthenium nanoclusters supported on alkali-exchanged zeolite beta", *Adv. Synth. Catal.*, 2006, **348**, 1970 – 1976.

43. M.L. Kantam, B.P.C. Rao, B.M. Choudary and R.S. Reddy, "A mild and efficient method for N-arylation of nitrogen heterocycles with aryl halides catalyzed by Cu(II)-NaY zeolite", *Synlett*, 2006, **14**, 2195 – 2198.

44. M.L. Kantam, B.P.C. Rao, B.M. Choudary, K.K. Rao, B. Sreedhar, Y. Iwasawa and T. Sasaki, "Synthesis of nanocrystalline zeolite beta in supercritical fluids, characterization and catalytic activity", *J. Mol. Catal. A: Chem.*, 2006, **252**, 76 – 84.

45. M.R. Maurya, A.K. Chandrakar and S. Chand, "Oxidation of phenol, styrene and methyl phenyl sulfide with H_2O_2 catalysed by dioxovanadium(V) and copper(II) complexes of 2-aminomethylbenzimidazole-based ligand encapsulated in zeolite-Y", *J. Mol. Catal. A: Chem.*, 2007, **263**, 227 – 237.

46. M.R. Maurya, A.K. Chandrakar and S. Chand, "Oxovanadium(IV) and copper(II) complexes of 1,2-diaminocyclohexane based ligand encapsulated in zeolite-Y for the catalytic oxidation of styrene, cyclohexene and cyclohexane", *J. Mol. Catal. A: Chem.*, 2007, **270**, 225 – 235.

47. M.R. Maurya, A.K. Chandrakar and S. Chand, "Zeolite-Y encapsulated metal complexes of oxovanadium(VI), copper(II) and nickel(II) as catalyst for the oxidation of styrene, cyclohexane and methyl phenyl sulfide", *J. Mol. Catal. A: Chem.*, 2007, **274**, 192 – 201.

48. M.R. Maurya, A.K. Chandrakar and S. Chand, "Oxidation of methyl phenyl sulfide, diphenyl sulfide and styrene by oxovanadium(IV) and copper(II) complexes of NS donor ligand encapsulated in zeolite-Y", *J. Mol. Catal. A: Chem.*, 2007, **278**, 12 – 21.

49. D.P. Serrano, R.A. Garćia and D. Otero, "Friedel–Crafts acylation of anisole over hybrid zeolitic-mesostructured materials", *App. Catal. A: Gen.*, 2009, **359**, 69 – 78.

50. P. Chutia, S. Kato, T. Kojima and S. Satokawa, "Synthesis and characterization of Co(II) and Cu(II) supported complexes of 2-pyrazinecarboxylic acid for cyclohexene oxidation", *Polyhedron*, 2009, **28**, 370 – 380.

51. M. Salavati-Niasari, M. Shakouri-Arani and Fatemeh Davar, "Flexible ligand synthesis, characterization and catalytic oxidation of cyclohexane with host (nanocavity of zeolite-Y)/guest (Mn(II), Co(II), Ni(II) and Cu(II) complexes of tetrahydro-salophen) nanocomposite materials", *Micropor. Mesopor. Mater.*, 2008, **116**, 77 – 85.

52. M. Salavati-Niasari and S. Abdolmohammadi, "Host (nanocavity of zeolite-Y)/guest (12- and 14-membered azamacrocyclic Ni(II) complexes) nanocatalyst: Synthesis, characterization and catalytic oxidation of cyclohexene with molecular oxygen", *J. Incl. Phenom. Macrocycl. Chem.*, 2008, **60**, 145 – 152.

53. P. Seneci, "Solid-Phase Synthesis and Combinatorial Techniques"; John Wiley: New York, 2001.

54. K. Burgess, "Solid-Phase Organic Synthesis"; John Wiley: NewYork, 2000.

55. A.D. Pomogailo, "Catalysis by Polymer-Immobilized Metal Complexes", Gordon and Breach: Australia, 1998.

56. D. Seebach, R.E. Marti and T. Hintermann, "Polymer- and dendrimer-bound Ti-TADDOLates in catalytic (and stoichiometric) enantioselective reactions. Are pentacoordinate cationic Ti complexes the catalytically active species", *Helv. Chim. Acta*, 1996, **79**, 1710 – 1740.

57. B. Hinzen and S.V. Ley, "Polymer supported perruthenate: A new oxidant for clean organic synthesis", *J. Chem. Soc., Perkin Trans. 1*, 1997, **13**, 1907 – 1908.

58. R. Arshady, G.W. Kenner and A. Ledwith, "The introduction of chloromethyl groups into styrene-based polymers, 1. Synthesis of 4-chloromethylstyrene and 4-methoxymethylstyrene and their copolymerizations with styrene", *Makromol. Chem.*, 1976, **177**, 2911 – 2918.

59. R.B. Merrifield, "Solid phase peptide synthesis: The synthesis of a tetrapeptide", *J. Am. Chem. Soc.*, 1963, **85**, 2149 – 2154.

60. S. Mohanraj and W.T. Ford, "Phase-transfer-catalyzed chlorination of poly(p-methylstyrene)", *Macromolecules*, 1986, **19**, 2470 – 2472.

61. N. Ise and I. Tabushi, "An Introduction to speciality Polymers", edited by: Cambridge University Press, Cambridge, 1980.

62. D. Hudson, "Matrix assisted synthetic transformations: A mosaic of diverse contributions. II", *J. Comb. Chem.*, 1999, **1**, 403 – 457.

63. D.J. Gravert and K.D. Janda, "Organic synthesis on soluble polymer supports: Liquid-phase methodologies", *Chem. Rev.*, 1997, **97**, 489 – 509.

64. A.R. Vaino and K.D. Janda, "Solid-phase organic synthesis: A critical understanding of the resin", *J. Comb. Chem.*, 2000, **2**, 579 – 596.

65. S. Itsuno, I. Moue and K. Ito, "Preparation of crosslinked polystyrene beads including oligo(oxyethylene) chain as crosslinking agent and their use as phase-transfer catalysts", *Polym. Bull.*, 1989, **21**, 365 – 370.

66. M. Renil and M. Meldal, "POEPOP and POEPS: Inert polyethylene glycol cross-linked polymer-supports for solid synthesis", *Tetrahedron Lett.*, 1996, **37**, 6185 – 6188.

67. S. Tangestaninejad, V. Mirkhani, M. Moghadam and G. Grivani, "Readily prepared heterogeneous molybdenum-based catalysts as highly recoverable, reusable and active catalysts for alkene epoxidation", *Catal. Commun.*, 2007, **8**, 839 – 844.

68. C. Chen, L. Hong, B. Zhanga and R. Wang, "Catalytic asymmetric addition of alkynylzinc reagents to ketones using polymer-supported chiral Schiff-base amino alcohols", *Tetrahedron: Asym.*, 2008, **19**, 191 – 196.

69. W. Trakarnpruk and W. Kanjina, "Preparation, characterization and oxidation catalysis of polymer-supported ruthenium and cobalt complexes", *Ind. Eng. Chem. Res.*, 2008, **47**, 964 – 968.

70. M.R. Maurya and S. Sikarwar, "Oxovanadium(IV) complex of β-alanine derived ligand immobilized on polystyrene for the oxidation of various organic substrates", *Catal. Commun.*, 2007, **8**, 2017 – 2024.

71. A. Syamal and M.M. Singh, "Syntheses of polystyrene-supported chelating resin containing the Schiff base derived from 3-formylsalicylic acid and o-hydroxybenzylamine and its copper(II), nickel(II), iron(III), zinc(II) cadmium(II), zirconium(IV), molybdenum(V and VI) and uranium(VI) complexes", *Indian J. Chem.*, 1992, **31A**, 110 – 115.

72. A. Syamal, M.M. Singh and D. Kumar, "Syntheses and characterization of a chelating resin containing ONNO donor quadridentate Schiff base and its coordination complexes with copper(II), nickel(II), cobalt(II), iron(III), zinc(II), cadmium(II), molybdenum(VI) and uranium(VI)", *React. Funct. Polym.*, 1999, **39**, 27 – 35.

73. A. Syamal and M.M. Singh, "Novel polystyrene-anchored Fe(III), Co(II), Ni(II), Cu(II), Zn(II), Cd(II), Mo(VI) and U(VI) complexes of the chelating resin containing an ON donor bidentate Schiff base", *Indian J. Chem.*, 1993, **32A**, 431 – 434.

74. R. Ando, T. Yagyu and M. Maeda, "Characterization of oxovanadium(IV)-Schiff-base complexes and those bound on resin, and their use in sulfide oxidation", *Inorg. Chim. Acta*, 2004, **357**, 2237 – 2244.

75. X.-Q. Yu, J.-S. Huang, W.-Y. Yu and C.-M. Che, "Polymer-supported ruthenium porphyrins: Versatile and robust epoxidation catalysts with unusual selectivity", *J. Am. Chem. Soc.*, 2000, **122**, 5337 – 5342.

76. M.R. Maurya, M. Kumar, A. Kumar and J.C. Pessoa, "Oxidation of *p*-chlorotoluene and cyclohexene catalysed by polymer-anchored

oxovanadium(IV) and copper(II) complexes of amino acid derived tridentate ligands", *Dalton Trans.*, 2008, 4220 – 4232.

77. M.R. Maurya, U. Kumar and P. Manikandan, "Synthesis and characterisation of polymer-anchored oxidovanadium(IV) complexes and their use for the oxidation of styrene and cumene", *Eur. J. Inorg. Chem.*, 2007, 2303 – 2314.

78. M.R. Maurya, U. Kumar, I. Correia, P. Adão and J.C. Pessoa, "A Polymer-bound oxidovanadium(IV) complex prepared from an L-cysteine-derived ligand for the oxidative amination of styrene", *Eur. J. Inorg. Chem.*, 2008, 577 – 587.

79. M.M. Miller, D.C. Sherrington and S. Simpson, "Alkene epoxidations catalyzed by molybdenum(VI) supported on imidazole-containing polymers. Part 3. Epoxidation of oct-1-ene and propene", *J. Chem. Soc. Perkin Trans.*, 1994, **2**, 2091 – 2096.

80. D.C. Sherrington and S. Simpson, "Polymer-supported Mo alkene epoxidation catalysts", *React. Polym.*, 1993, **19**, 13 – 25.

81. L. Canali, D.C. Sherrington and H. Deleuze, "Synthesis of resins with pendently-bound chiral manganese-salen complexes and use as heterogeneous asymmetric alkene epoxidation catalysts", *React. Funct. Polym.*, 1999, **40**, 155 – 168.

82. L. Canali, E. Cowan, C.L. Gibson, D.C. Sherrington and H. Deleuze, "Remarkable matrix effect in polymer-supported Jacobsen's alkene epoxidation catalysts", *Chem. Commun.*, 1998, **23**, 2561 – 2562.

83. L. Canali, E. Cowan, H. Deleuze, C.L. Gibson and D.C. Sherrington, "Polystyrene and polymethacrylate resin-supported Jacobsen's alkene epoxidation catalyst", *J. Chem. Soc. Perkin 1*, 2000, **13**, 2055 – 2066.

84. M.R. Maurya and S. Sikarwar, "Oxidation of phenol and hydroquinone catalysed by copper(II) and oxovanadium(IV) complexes of N,N'-bis(salicyledene)diethylenetriamine (H_2saldien) covalently bonded to chloromethylated polystyrene", *J. Mol. Catal. A: Chem.*, 2006, **263**, 175 – 185.

85. G.R. Krishnan and K. Sreekumar, "Ring opening of epoxides catalysed by poly(amidoamine) dendrimer supported on crosslinked polystyrene", *Polymer*, 2008, **49**, 5233 – 5240.

86. M.R. Maurya, M. Kumar and S. Sikarwar, "Polymer-anchored oxoperoxo complexes of vanadium(V), molybdenum(VI) and tungsten(VI) as catalyst for

the oxidation of phenol and styrene using hydrogen peroxide as oxidant", *React. Funct. Polym.*, 2006, **66**, 808 – 818.

87.   M.M. Miller and D.C. Sherrington, "Alkene epoxidations catalyzed by Mo(VI) supported on imidazole-containing polymers. I. Synthesis, characterization, and activity of catalysts in the epoxidation of cyclohexene", *J. Catal.*, 1995, **152**, 368 – 376

88.   M.R. Maurya, S. Sikarwar and S.B. Halligudi, "Bis(2-[α-hydroxyethyl]benzimidazolato)copper(II) anchored onto chloromethylated polystyrene for the biomimetic oxidative coupling of 2-aminophenol to 2-aminophenoxazine-3-one", *J. Mol. Catal. A: Chem.*, 2005, **236**, 132 – 138.

89.   M.R. Maurya, S. Sikarwar, T. Joseph, P. Manikandan and S.B. Halligudi, "Synthesis, characterization and catalytic potential of polymer-anchored copper(II), oxovanadium(IV) and dioxomolybdenum(VI) complexes of 2-(α-hydroxymethyl)benzimidazole", *React. Funct. Polym.*, 2005, **63**, 71 – 83.

90.   M.R. Maurya, M. Kumar and S. Sikarwar, "Polymer-anchored oxoperoxo complexes of vanadium(V), molybdenum(VI) and tungsten(VI) as catalyst for the oxidation of phenol and styrene using peroxide as oxidant", *React. & Funct. Polym.*, 2006, **66**, 808 – 818.

91.   M.R. Maurya, M. Kumar and U. Kumar, "Polymer-anchored oxovanadium(IV) complexes of 2-(2'–hydroxyphenyl)benzimidazole as catalyst for the liquid phase oxidation of organic substrates", *J. Mol. Catal. A: chem.*, 2007, **273**, 133 – 143.

92.   K.C. Gupta and A.K. Sutar, "Catalytic activity of polymer anchored N,N'-bis (o-hydroxy acetophenone) ethylene diamine Schiff base complexes of Fe(III), Cu(II) and Zn(II) ions in oxidation of phenol", *React. Funct. Polym.*, 2008, **68**, 12 – 26.

93.   K.C. Gupta and A.K. Sutar, "Polymer supported catalysts for oxidation of phenol and cyclohexene using hydrogen peroxide as oxidant", *J. Mol. Catal. A: Chem.*, 2008, **280**, 173 – 185.

94.   K.C. Gupta and A.K. Sutar, "Synthesis of polymer-supported metal-ion complexes and evaluation of their catalytic activities", *J. Appl. Polym. Sci.*, 2008, **108**, 3927 – 3941.

95.   A. Syamal and M.M. Singh, "Synthesis of polystyrene-supported chelating resin containing an oxygen-nitrogen donor bidentate Schiff base and its nickel(II), cobalt(II), copper(II), iron(III), zinc(II), molybdenum(VI) and uranium(VI) complexes", *Indian J. Chem.*, 1994, **33A**, 58 – 62.

96. A. Syamal and M.M. Singh, "Synthesis and characterization of polystyrene-supported chelating resin containing an ON donor bidentate Schiff base and its copper(II), nickel(II), cobalt(II), iron(III), zinc(II), molybdenum(VI) and uranium(VI) complexes", *React. Polym.,* 1994, **24**, 27 – 34.

97. A. Syamal and M.M. Singh, "Novel polystyrene-anchored copper(II), nickel(II), cobalt(II), iron(III), zinc(II), cadmium(II), molybdenum(VI) and uranium(VI) complexes of the chelating resin containing thiosemicarbazone", *Indian J. Chem.,* 1993, **32A**, 861 – 867.

98. K.S. Devaky and V.N.R. Pillai, "Selective conversion of chloromethyl and bromomethyl groups to aminomethyl groups in multifunctional crosslinked polystyrenes", *Eur. Polym. J.,* 1988, **24**, 209 – 213.

99. G. Grivani, S. Tangestaninejad, M.H. Habibi and V. Mirkhani, "Epoxidation of alkenes by a highly reusable and efficient polymer-supported molybdenum carbonyl catalyst", *Catal. Commun.,* 2005, **6**, 375 – 378.

100. F. Minutolo, D. Pini and P. Salvadori, "Polymer-bound chiral (salen) Mn (III) complex as heterogeneous catalyst in rapid and clean enantioselective epoxidation of unfunctionalised olefins", *Tetrahedron Lett.,* 1996, **37**, 3375 – 3378.

101. D. Kumar, P.K. Gupta and A. Syamal, "Syntheses, magnetic and spectral studies on polystyrene supported coordination compounds of bidentate and tetradentate Schiff bases", *J. Chem. Sci.,* 2005, **117**, 247 – 253.

102. D. Kumar, A. Syamal and A.K. Singh, "Syntheses and characterization of coordination compounds of monobasic bidentate (NS donor) Schiff bases derived from aldehydopolystyrene and 2-aminoethanethiol or 2-aminothiophenol", *J. Indian Chem. Soc.,* 2004, **81**, 911 – 916.

103. D. Kumar, A. Syamal and L.K. Sharma, "Synthesis and characterization of polystyrene-anchored tridentate Schiff base and its complexes with di-, tri-, tetra- and hexavalent metal ions", *Oriental J. Chem.,* 2003, **19**, 577 – 582.

104. D. Kumar, A. Syamal and P.K. Gupta, "Syntheses, magnetic and spectral studies of the coordination compounds of polystyrene-anchored dibasic tridentate Schiff base", *J. Indian Chem. Soc.,* 2003, **80**, 3 – 6.

105. D. Kumar, A. Syamal and A.K. Singh, "Synthesis and characterization of manganese(II), cobalt(II), nickel(II), copper(II), zinc(II), cadmium(II), iron(III), zirconium(IV), dioxomolybdenum(VI) and dioxouranium(VI) coordination compounds of polystyrene-supported tridentate dibasic Schiff

base derived from semicarbazide and 3-formylsalicylic acid", *Indian J. Chem.*, 2003, **42A**, 280 – 286.

106. D. Kumar, P.K. Gupta and A. Syamal, "Synthesis and characterization of polystyrene supported coordination compounds of dibasic tridentate Schiff base", *Indian J. Chem.*, 2002, **41A**, 2494 – 2499.

107. D. Kumar, A. Syamal, L.K. Sharma, Jaipal, P.K. Gupta and A.K. Singh, "Syntheses and characterization of new functionalized polymers", *J. Polym. Mater.*, 2002, **19**, 315 – 319.

108. D. Kumar, A. Syamal, Jaipal and P.K. Gupta, "Polystyrene supported coordination compounds of an unsymmetrical quadridentate Schiff base", *Oriental J. Chem.*, 2005, **21**, 89 – 94.

109. D.R. Patel, M.K. Dalal and R.N. Ram, "Preparation, characterization and catalytic activity of polymer supported Ru(III) complexes", *J. Mol. Catal. A: Chem.*, 1996, **109**, 141 – 148.

110. V.B. Valodkar, G.L. Tembe, M. Ravindranathan and H.S. Rama, "Catalytic epoxidation of olefins by polymer-anchored amino acid ruthenium complexes", *React. Funct. Polym.*, 2003, **56**, 1 – 15.

111. V.B. Valodkar, G.L. Tembe, M. Ravindranathan, R.N. Ram and H.S. Rama, "Catalytic oxidation by polymer-supported copper(II)-L-valine complexes", *J. Mol. Catal. A: Chem.*, 2004, **208**, 21 – 32.

112. V.B. Valodkar, G.L. Tembe, M. Ravindranathan, R.N. Ram and H.S. Rama, "A study of synthesis, characterization and catalytic hydrogenation by polymer-anchored Pd(II)-amino acid complexes", *J. Mol. Catal. A: Chem.*, 2003, **202**, 47 – 64.

113. J. John, M.K. Dalal and R.N. Ram, "Polymer anchored palladium(II)-diaminopropane complexes: synthesis and catalytic behavior", *J. Mol. Catal. A: Chem.*, 1999, **137**, 183 – 191.

114. K. Gauli, R.N. Ram and H.P. Soni, "Oxidation of toluene using polymer anchored Ni(II) complex as catalyst", *J. Mol. Catal. A: Chem.*, 2005, **242**, 161 – 167.

115. K.C. Gupta and A.K. Sutar, "Polymer anchored Schiff base complexes of transition metal ions and their catalytic activities in oxidation of phenol", *J Mol. Catal. A: Chem.*, 2007, **272**, 64 – 74.

116. T.E. Muller, K.C. Hultzsch, M. Yus, F. Foubelo and M. Tada, "Hydroamination: direct addition of amines to alkenes and alkynes", *Chem. Rev.*, 2008, **108**, 3795 – 3892.

117. J. Bourgeois, I. Dion, P.H. Cebrowski, F. Loiseau, A.-C. Bedard and A.M. Beauchemin, "The tandem cope-type hydroamination / [2, 3]-rearrangement sequence: a strategy to favor the formation of intermolecular hydroamination products and enable difficult cyclizations", *J. Am. Chem. Soc.*, 2009, **131**, 874 – 875.

118. C. Munro-Leighton, S.A. Delp, N.M. Alsop, E.D. Blue and T.B. Gunnoe, "Anti-Markovnikov hydroamination and hydrothiolation of electron deficient vinylarenes catalyzed by well-defined monomeric copper(I) amido and thiolate complexes", *Chem. Commun.*, 2008, **1**, 111 – 113.

119. L. Fadini and A. Togni, "Asymmetric hydroamination of acrylonitrile derivatives catalyzed by Ni(II)-complexes", *Tetrahedron: Asym.*, 2008, **19**, 2555 – 2562.

120. G.V. Shanbhag, S.M. Kumbar and S.B. Halligudi, "Chemoselective synthesis of β-amino acid derivatives by hydroamination of activated olefins using AlSBA-15 catalyst prepared by post-synthetic treatment", *J. Mol. Catal. A: Chem.*, 2008, **284**, 16 – 23.

121. B. Lian, T.P. Spaniol, P. Horrillo-Martínez, K.C. Hultzsch and J. Okuda "Imido and amido titanium complexes that contain a [OSSO]-type bis(phenolato) ligand: Synthesis, structures, and hydroamination catalysis", *Eur. J. Inorg. Chem.*, 2009, **3**, 429 – 434.

122. V.A. Lee, M. Sajitz and L.L. Schafer, "The direct synthesis of unsymmetrical vicinal diamines from terminal alkynes: a tandem sequential approach for the synthesis of imidazolidinones", *Synthesis,* 2009, 97 – 104.

123. K. Komura, R. Hongo, J. Tsutsui and Y. Sugi, "Na-Y Zeolite as a highly active catalyst for the hydroamination of α, β-unsaturated compounds with aromatic amines", *Catal. Lett.,* 2009, **128**, 203 – 209.

124. C. Kwak, J.J. Lee, J.S. Bae, K. Choi and S.H. Moon, "Hydrodesulfurization of DBT, 4-MDBT, and 4,6-DMDBT on fluorinated CoMoS/Al$_2$O$_3$ catalysts", *Appl. Catal. A: Gen.,* 2000, **200**, 233 – 242.

125. H. Nikolaj, M. Brorson and T. Henrik, "Activities of unsupported second transition series metal sulfides for hydrodesulfurization of sterically hindered 4,6-Dimethyldibenzothiophene and of unsubstituted dibenzothiophene", *Catal. Lett.,* 2000, **65**, 169 – 174.

126. A. Attar and W.H. Corcoran, "Desulfurization of organic sulfur compounds by selective oxidation. 1. Regenerable and noregenerable oxygen carriers", *Ind. Eng. Chenz. Prod. Res. Dev.*, 1978, **17**, 102 – 109.

127. A. Ishihara, D. Wang, F. Dumeignil, H. Amano, E.W. Qian and T. Kabe, "Oxidative desulfurization and denitrogenation of a light gas oil using an oxidation/adsorption continuous flow process", *Appl. Catal. A: Gen.*, 2005, **279**, 279 – 287.

128. D. Wang, E.W. Qian, H. Amano, K. Okata, A. Ishihara and T. Kabe, "Oxidative desulfurization of fuel oil. Part I. Oxidation of dibenzothiophenes using tert-butyl hydroperoxide", *Appl. Catal. A: Gen.*, 2003, **253**, 91 – 99.

129. A. Chica, A. Corma and M.E. Domine, "Catalytic Oxidative desulfurization (ODS) of diesel fuel on a continuous fixed-bed reactor", *J. Catal.*, 2006, **242**, 299 – 308.

130. S. Otsuki, T. Nonaka, N. Takashima, W. Qian, A. Ishihara, T. Imai and T. Kabe, "Oxidative desulfurization of light gas oil and vacuum gas oil by oxidation and solvent extraction", *Energy Fuels*, 2000, **14**, 1232 –1239.

131. J.T. Sampanthar, H. Xiao, J. Dou, T.Y. Nah, X. Rong and W.P. Kwan, "A novel oxidative desulfurization process to remove refractory sulfur compounds from diesel fuel", *Appl. Catal. B: Environ.*, 2006, **63**, 85 – 93.

132. A. Chica, G. Gatti, B. Moden, L. Marchese and E. Iglesia, "Selective catalytic oxidation of organosulfur compounds with tert-butyl hydroperoxide", *Chem. Eur. J.*, 2006, **12**, 1960 – 1967.

133. J.L. G-Gutierrez, G.A. Fuentes, M.E. H-Teran, F. Murrieta, J. Navarrete and F. J-Cruz, "Ultra-deep oxidative desulfurization of diesel fuel with H_2O_2 catalyzed under mild conditions by polymolybdates supported on Al_2O_3", *Appl. Catal. A: Gen.*, 2006, **305**, 15 – 20.

134. J.M. C-Martin, M.C. C-Sanchez and J.L.G. Fierro, "Highly efficient deep desulfurization of fuels by chemical oxidation", *Green Chem.*, 2004, **6**, 557 – 562.

135. H.Y. Lü, J. Gao, Z. Jiang, Y. Yang, B. Song and C. Li "Oxidative desulfurization of dibenzothiophene with molecular oxygen using emulsion catalysis", *Chem. Commun.*, 2007, 150 – 152.

136. H.Y. Lü, J.B. Gao, Z.X. Jiang, F. Jing, Y.X. Yang, G. Wang and C. Li, "Ultra-deep desulfurization of diesel by selective oxidation with

$[C_{18}H_{37}N(CH_3)_3]_4[H_2NaPW_{10}O_{36}]$ catalyst assembled in emulsion droplets", *J. Catal.*, 2006, **239**, 369 – 375.

137. J.M. Campos-Martin, M.C. Capel-Sanchez and J.L.G. Fierro, "Highly efficient deep desulfurization of fuels by chemical oxidation", *Green Chem.*, 2004, **6**, 557 – 562.

138. C. Komintarachat and W. Trakarnpruk, "Oxidative desulfurization using polyoxometalates", *Ind. Eng. Chem. Res.*, 2006, **45**, 1853 – 1856.

139. S.S. Cheng and T.F. Yen, "Use of ionic liquids as phase-transfer catalysis for deep oxygenative desulfurization", *Energy Fuels*, 2008, **22**, 1400 – 1401.

140. P.S. Tam, J.R. Kittrell and J.W. Eldridge, "Desulfurization of fuel oil by oxidation and extraction. 1. Enhancement of extraction oil yield", *Ind. Eng. Chem. Res.*, 1990, **29**, 321 – 324.

141. F.R. Zaykina, A.Yu Zaykin, G.S. Yagudin and M.I. Fahruddinov, "Specific approaches to radiation processing of high-sulfuric oil", *Radiat. Phys. Chem.*, 2004, **71**, 467 – 470.

142. A. Ishihara, D.H. Wang, F. Dumeignil, H. Amano, W.E. Qian and T. Kabe, "Oxidative desulfurization and denitrogenation of a light gas oil using an oxidation/adsorption continuous flow process" *Appl. Catal. A: Gen.*, 2005, **279**, 279 – 287.

143. N.Y. Chan, T.Y. Lin and T.F.Yen, "Superoxides: Alternative Oxidants for the Oxidative Desulfurization Process", *Energy Fuels*, 2008, **22**, 3326 – 3328.

144. Sh. Haji and C. Erkey, "Removal of dibenzothiophene from model diesel by adsorption on carbon aerogels for fuel cell applications", *Ind. Eng. Chem. Res.*, 2003, **42**, 6933 – 6937.

145. D. Jayne, Y. Zhang, Sh. Haji and C. Erkey, "Dynamics of removal of organosulfur compounds from diesel by adsorption on carbon aerogels for fuel cell applications", *Int. J. Hydrogen Energy*, 2005, **30**, 1287 – 1293.

146. L. Ma and R.T. Yang, "Selective adsorption of sulfur compounds: Isotherms, heats, and relationship between adsorption from vapor and liquid solution", *Ind. Eng. Chem. Res.*, 2007, **46**, 2760 – 2768.

147. L. Ma and R.T. Yang, "Heats of adsorption from liquid solutions and from pure vapor phase: adsorption of thiophenic compounds on Na-Y and 13X zeolites", *Ind. Eng. Chem. Res.*, 2007, **46**, 4874 – 4882.

148. G. Yu, Sh. Lu, H. Chen and Z. Zhu, "Diesel fuel desulfurization with hydrogen peroxide promoted by formic acid and catalyzed by activated carbon", *Carbon*, 2005, **43**, 2285 – 2294.

149. C.O. Ania, J.B. Parra, A. Arenillas, F. Rubiera, T.J. Bandosz and J.J. Pis, "On the mechanism of reactive adsorption of dibenzothiophene on organic waste derived carbons", *Appl. Surf. Sci.*, 2007, **253**, 5899 – 5903.

150. C.O. Ania and T.J. Bandosz, "Metal-loaded polystyrene-based activated carbons as dibenzothiophene removal media via reactive adsorption", *Carbon*, 2006, **44**, 2404 – 2412.

151. J.L. Garcia-Gutierrez, G.A. Fuentes, M.E. Hernandez-Teran, F. Murrieta, J. Navarrete and F. Jimenez-Cruz, "Ultra-deep oxidative desulfurization of diesel fuel with H_2O_2 catalyzed under mild conditions by polymolybdates supported on Al_2O_3", *Appl. Catal. A: Gen.*, 2006, **305**, 15 – 20.

152. L.C. Caero, F. Jorge, A. Navarro and A. Gutierrez-Alejandre, "Oxidative desulfurization of synthetic diesel using supported catalysts Part II. Effect of oxidant and nitrogen compounds on extraction–oxidation process", *Catal. Today*, 2006, **116**, 562 – 568.

153. B. Zapata, F. Pedraza and M.A. Valenzuela, "Catalyst screening for oxidative desulfurization using hydrogen peroxide", *Catal. Today*, 2005, **106**, 219 – 221.

154. V.B. Valodkar, G.L. Tembe, M. Ravindranathan and H.S. Rama, "Catalytic oxidation of alkanes and alkenes by polymer-anchored amino acids–ruthenium complexes", *J. Mol. Catal. A: Chem.*, 2004, **223**, 31 – 38.

155. N.T.S. Phan, D.H. Brown and P. Styring, "A polymer-supported salen-type palladium complex as a catalyst for the Suzuki–Miyaura cross-coupling reaction", *Tetrahedron Lett.*, 2004, **45**, 7915 – 7919.

156. X.-Y. Yuan, H.-Y. Li, P. Hodge, M. Kilner, C.T. Tastard and Z.-P. Zhang, "An easy synthesis of robust polymer-supported chiral 1,1'-bi-(2-naphthol) (BINOLs): application to the catalysis of the oxidation of prochiral thioethers to chiral sulfoxides", *Tetrahedron: Asym.*, 2006, **17**, 2401 – 2407.

157. S. Kobayashi, K. Kusakabe and H. Ishitani, "Chiral catalyst optimization using both solid-phase and liquid-phase methods in asymmetric Aza Diels-Alder reactions", *Org. Lett.*, 2000, **2**, 1225 – 1227.

158. D.A. Annis and E.N. Jacobsen, "Polymer-supported chiral Co(salen) complexes: Synthetic applications and mechanistic investigations in the

hydrolytic kinetic resolution of terminal epoxides", *J. Am. Chem. Soc.,* 1999, **121**, 4147 – 4154.

159.   D.C. Sherrington, "Polymer-supported metal complex alkene epoxidation catalysts", *Catal. Today*, 2000, **57**, 87 – 104.

160.   L. Canali, E. Cowan, C.L. Gibson, D.C. Sherrington and H. Deleuze, "Remarkable matrix effect in polymer-supported Jacobsen's alkene epoxidation catalysts", *Chem. Commun.*, 1998, **23**, 2561 – 2562.

161.   M.D. Angelino and P.E. Laibinis, "Polymer-supported SALEN complexes for heterogeneous asymmetric synthesis: Stability and selectivity", *J. Polym. Sci., Part A: Polym. Chem.*, 1999, **37**, 3888 – 3898.

162.   T.S. Reger and K.D. Janda, "Polymer-supported (Salen)Mn Catalysts for asymmetric epoxidation: A comparison between soluble and insoluble matrices", *J. Am. Chem. Soc.,* 2000, **122**, 6929 – 6934.

163.   C.E. Song, E.J. Roh, B.M Yu, D.Y. Chi, S.C. Kim and K.-J. Lee, "Heterogeneous asymmetric epoxidation of alkenes catalyzed by a polymer-bound (pyrrolidine salen) manganese(III) complex", *Chem. Commun.*, 2000, 615 – 616.

164.   F. Minutolo, D. Pini, A. Petri and P. Salvadori, "Heterogeneous asymmetric epoxidation of unfunctionalized olefins catalyzed by polymer-bound (salen) manganese complexes", *Tetrahedron: Asym.,* 1996, **7**, 2293 – 2302.

165.   B.B. De, B.B. Lohray, S. Sivaram and P.K. Dhal, "Synthesis of catalytically active polymer-bound transition metal complexes for selective epoxidation of olefins", *Macromolecules*, 1994, **27**, 1291 – 1296.

166.   B.B. De, B.B. Lohray, S. Sivaram and P.K. Dhal, "Enantioselective epoxidation of olefins catalyzed by polymer-bound optically active Mn(III)-Salen complex", *Tetrahedron: Asym.,* 1995, **6**, 2105 – 2108.

167.   E. Breysse, C. Pinel and M. Lemaire, "Use of heterogenized dialdimine ligands in asymmetric transfer hydrogenation", *Tetrahedron: Asym.,* 1998, **9**, 897 – 900.

168.   K. Smith and C.-H. Liu, "Asymmetric epoxidation using a singly-bound supported Katsuki-type (salen)Mn complex", *Chem. Commun.*, 2002, **8**, 886 – 887.

169.   R.I. Kureshy, N.H. Khan, S.H.R. Abdi and P. Iyer, "Synthesis of catalytically active polymer-bound Mn(III) salen complexes for enantioselective

epoxidation of styrene derivatives", *React. Funct. Polym.,* 1997, **34,** 153 – 160.

170.   H. Zhang, Y. Zhang and C. Li, "Asymmetric epoxidation of unfunctionalized olefins catalyzed by Mn(salen) axially immobilized onto insoluble polymers", *Tetrahedron: Asym.,* 2005, **16,** 2417 – 2423.

171.   G. Grivani, S. Tangestaninejad, M.H. Habibi, V. Mirkhani and M. Moghadam, "Epoxidation of alkenes by a readily prepared and highly active and heterogeneous molybdenum- based catalyst", *Appl. Catal. A: Gen.,* 2006, **299,** 131 – 136.

172.   S. Tangestaninejad, M.H. Habibi, V. Mirkhani and G. Grivani, "Simple preparation of some reusable and efficient polymer-supported tungsten carbonyl catalysts and clean epoxidation of cis-cyclooctene in the presence of H$_2$O$_2$", *J. Mol. Catal. A: Chem.,* 2006, **255,** 249 – 253.

173.   M. Moghadam, S. Tangestaninejad, M.H. Habibi and V. Mirkhani, "A convenient preparation of polymer-supported manganese porphyrin and its use as hydrocarbon monooxygenation catalyst", *J. Mol. Catal. A: Chem.,* 2004, **217,** 9 – 12.

174.   S. Tangestaninejad, M. Moghadam, V. Mirkhani and H. Kargar, "Efficient and selective hydrocarbon oxidation with sodium periodate under ultrasonic irradiation catalyzed by polystyrene-bound Mn (TPyP)", *Ultrason. Sonochem.,* 2006, **13,** 32 – 36.

175.   M. Moghadam, S. Tangestaninejad, V. Mirkhani, I. Mohammadpoor-Baltork and H. Kargar, "Mild and efficient oxidation of alcohols with sodium periodate catalyzed by polystyrene-bound Mn(III)porphyrin", *Bioorg. Med. Chem.,* 2005, **13,** 2901 – 2905.

176.   S. Tangestaninejad and V. Mirkhani, "Polystyrene-bound manganese(III) porphyrin as a heterogeneous catalyst for alkene epoxidation", *J. Chem. Res. (S),* 1998, **12,** 788 – 789.

177.   M. Moghadam, S. Tangestaninejad, V. Mirkhani, H. Kargar and H. Komeili-Isfahani, "Polystyrene-bound imidazole as a heterogeneous axial ligand for Mn(TPP)Cl and its use as hydrocarbon monooxygenation catalyst in the alkene epoxidation and alkane hydroxylation with sodium periodate under various reaction conditions", *Catal. Commun.,* 2005, **6,** 688 – 693.

178.   V. Mirkhani, M. Moghadam, S. Tangestaninejad and H. Kargar, "Mn(Br$_8$TPP)Cl supported on polystyrene-bound imidazole: An efficient and reusable catalyst for biomimetic alkene epoxidation and alkane hydroxylation

with sodium periodate under various reaction conditions", *Appl. Catal. A: Gen.*, 2006, **303**, 221 – 229.

179. E. Brule and Y.R. de Miguel, "Supported manganese porphyrin catalysts as P450 enzyme mimics for alkene epoxidation", *Tetrahedron Lett.*, 2002, **43**, 8555 – 8558.

180. E. Brule, K.K Hii and Y.R. de Miguel, "Polymer-supported manganese porphyrin catalysts-peptide-linker promoted chemoselectivity", *Org. Biomol. Chem.*, 2005, **3**, 1971 – 1976.

181. R.R. Srivastava and S.E. Collibee, "Application of polymer-supported triphenyl phosphine in the palladium-catalyzed cyanation reaction under microwave conditions", *Tetrahedron Lett.*, 2004, **45**, 8895 – 8897.

182. K. Inada and N. Miyaura, "The cross-coupling reaction of arylboronic acids with chloropyridines and electron-deficient chloroarenes catalyzed by a polymer-bound palladium complex", *Tetrahedron*, 2000, **56**, 8661 – 8664.

183. N.E. Leadbeater and M. Marco, "Preparation of polymer-supported ligands and metal complexes for use in catalysis", *Chem. Rev.*, 2002, **102**, 3217 – 3274.

184. M.R. Maurya, U. Kumar and P. Manikandan, "Polymer supported vanadium and molybdenum complexes as potential catalysts for the oxidation and oxidative bromination of organic substrates", *Dalton Trans.*, 2006, 3561 – 3575.

185. M.R. Maurya, M. Kumar and A. Arya, "Model dioxovanadium(V) complexes through direct immobilization on polymer support, their characterization and catalytic activities", *Catal. Commun.*, 2008, **10**, 187 – 191.

186. M.R. Maurya, S. Sikarwar and P Manikandan, "Oxovanadium(IV) complex of 2-(α-hydroxyethyl)benzimidazole covalently bonded to chloromethylated polystyrene for oxidation of benzoin", *Appl. Catal. A: Gen.*, 2006, **315**, 74 – 82.

187. M.P. Weberski Jr., C.C. McLauchlan and C.G. Hamaker, "Synthesis and X-ray structural characterization of M(3,5-^{t}Bu$_2$-salophen) (M = Cu, V=O)", *Polyhedron*, 2006, **25**, 119 – 123.

188. C.C. McLauchlan and K.J. McDonald, "Chloro[hydrotris(pyrazol-1-yl)borato]oxo-(1*H*-pyrazole)vanadium(IV)", *Acta Cryst.*, 2005, **E61**, m2379 – m2381.

189. C.C. McLauchlan and K.J. McDonald, "Cocrystallization of dichloro(N,N-dimethylformamide)[hydrotris(pyrazol-1-yl)borato]vanadium(III) with its partially oxidized analog chloro(N,N-dimethylformamide)[hydrotris(pyrazol-1-yl)borato]oxovanadium(IV)", *Acta Cryst.*, 2006, **E62**, m588 – m590.

190. S.L. Jain and B. Sain, "An efficient approach for immobilizingthe oxo-vanadium schiff base onto polymer supports using staudinger ligation", *Adv. Synth. Catal.*, 2008, **350**, 1479 – 1483.

191. T.E. Müller and M. Beller, "Metal initiated amination of alkenes and alkynes", *Chem. Rev.*, 1998, **98**, 675 – 703.

192. H. Trauthwein, A. Tillack and M. Beller, "New rhodium-catalyzed amination reactions", *Chem. Comm.*, 1999, 2029 – 2030.

193. M. Kawatsura and J.F. Hartwig, "Palladium-catalyzed intermolecular hydroamination of vinylarenes using arylamines", *J. Am. Chem. Soc.*, 2000, **122**, 9546 – 9547.

194. U. Nettekoven and J.F. Hartwig, "A new pathway for hydroamination. Mechanism of palladium-catalyzed addition of anilines to vinylarenes", *J. Am. Chem. Soc.*, 2002, **124**, 166 – 1167.

195. M.R. Gagne, S.P. Nolan and T.J. Marks, "Organolanthanide-centered hydroamination/cyclization of aminoolefins. Expedient oxidative access to catalytic cycles", *Organometallics*, 1990, **9**, 1716 – 1718.

196. S. Tian, V.M. Arredondo, C.L. Stern and T.J. Marks, "Constrained geometry organolanthanide catalysts. Synthesis, structural characterization, and enhanced aminoalkene hydroamination/cyclization activity", *Organometallics*, 1999, **18**, 2568 – 2570.

197. J.T. Hartwig, "Development of catalysts for the hydroamination of olefins", *Pure Appl. Chem.*, 2004, **76**, 507 – 516.

198. T. Kondo, T. Okada and T. Mitsudo, "Ruthenium-catalyzed intramolecular oxidative amination of aminoalkenes enables rapid synthesis of cyclic amines", *J. Am. Chem. Soc.*, 2002, **124**, 186 – 187.

199. J.A. Jordan-Hore, C.C.C. Johansson, M. Gulias, E.M. Beck and M.J. Gaunt, "Oxidative Pd(II)-catalyzed C-H bond amination to carbazole at ambient temperature", *J. Am. Chem. Soc.*, 2008, **130**, 16184 – 16186.

200. J.L. Brice, J.E. Harang, V.I. Timokhin, N.R. Anastasi and S. Stahl, "Aerobic oxidative amination of unactivated alkenes catalyzed by palladium", *J. Am. Chem. Soc.*, 2005, **127**, 2868 – 2869.

201. V.N. Srinivasarao, S.K. Talluri, G. Shyla and S.A rumugam, "Enantionaselective synthesis of (–)-cytoazone and (+)-*epi*-cytoxazone via Rh-catalyzed diastereoselective oxidative C–H aminations", *Tetrahedron Lett.*, 2007, **48**, 65 – 68.

202. R.F. Shannon, L.B. Jodie and S.S. Shannon, "Effective intramolecular oxidative amination of olefins through dioxygen-coupled palladium catalyst", *Angew. Chem. Int. Ed.*, 2002, **41**, 164 – 166.

203. V.V. Goryunenko, A.V. Gulevskaya and F. Pozharskii, "Purines, pyrimidines, and related fused systems 21. Oxidative amination of 3-chloro-6,8-dimethylpyrimido[4,5-*c*]pyridazine-5,7,(6*H*,8*H*)-dione", *Russ. Chem. Bull., Int. Ed.*, 2004, **53**, 846 – 852.

204. A. Tillack, H. Trauthwein, C.G. Hartung, M. Eichberger, S. Pitter, A. Jansen and M. Beller, "Rhodium-catalyzed amination of aromatic olefins [1]", *Monatsh. Chem.*, 2000, **131**, 1327 – 1334.

205. M. Beller, H. Trauthwein, M. Eichberger, C. Breindl and T.E. Müller, "Anti-Markonikov reactions, 6. Rhodium-catalyzed amination of vinylpyridines: Hydroamination versus oxidative amination", *Eur. J. Inorg. Chem.*, 1999, 1121 – 1132.

206. M. Beller, H. Trauthwein, M. Eichberger, C. Breindl, J. Herwig, T.E. Müller and O.R. Thiel, "Anti-Markovnikov functionalizations of unsaturated compounds, Part 5. The first rhodium-catalyzed anti-Markovnikov hydroamination: Studies on hydroamination and oxidative amination of aromatic olefins", *Chem. Eur. J.*, 1999, **5**, 1306 – 1319.

207. M. Beller, H. Trauthwein, M. Eichberger, C. Breindl, T.E. Müller and A. Zapf, "New cationic rhodium–amine complexes and their implication in the catalytic anti-Markovnikov oxidative amination of styrenes", *J. Organomet. Chem.*, 1998, **566**, 277 – 285.

208. F. Ragaini, T. Longo and S. Cenini, "Addition of ethyl urethane to olefins: A new approach to synthesis of aliphatic carbamates", *J. Mol. Catal. A: Chem.*, 1996, **110**, L171 – L175.

209. J.-J. Brunet, D. Neibecker and K. Philippot, "Rhodium-mediated 100% regioselective oxidative hydroamination of α-olefins", *Tetrahedron Lett.*, 1993, **34**, 3877 – 3880.

210. T. Hosokawa, M. Takano, Y. Kuroki and S.-I. Murahashi, "Palladium(II)-catalyzed amidation of alkenes", *Tetrahedron Lett.*, 1992, **33**, 6643 – 6646.

211. J.J. Bozell and L.S. Hegedus, "Palladium-assisted functionalization of olefins: A new amination of electron-deficient olefins", *J. Org. Chem.*, 1981, **46**, 2561 – 2563.

212. J.G. Matthew and B.S. Jonathan, "Derailing the Wacker oxidation: Development of a palladium-catalyzed amidation reaction", *Org. Lett.*, 2001, **3**, 25 – 28.

213. M. Weyand, H.J. Hecht, M. Kiess, M.F. Liaud, H. Vilter and D. Schomburg, "X-ray structure determination of a vanadium-dependent haloperoxidase from Ascophyllum nodosum at 2.0 A resolution", *J. Mol. Biol.*, 1999, **293**, 595 – 611.

214. J.N. Carter-Franklin, J.D. Parrish, R.A. Tchirret-Guth, R.D. Little and A. Butler, "Vanadium haloperoxidase-catalyzed bromination and cyclization of terpenes", *J. Am. Chem. Soc.*, 2003, **125**, 3688 – 3689.

215. D. Rehder, G. Santoni, G.M. Licini, C. Schulzke and B. Meier, "The medicinal and catalytic potential of model complexes of vanadate-dependent haloperoxidases", *Coord. Chem. Rev.*, 2003, **237**, 53 – 63.

216. G. Asgedom, A. Sreedhara, J. Kivikoski, J. Valkonen, E. Kolehmainen and C.P. Rao, "Alkoxo bound monooxo- and dioxovanadium(V) complexes: synthesis, characterization, X-ray crystal structures, and solution reactivity studies", *Inorg. Chem.*, 1996, **35**, 5674 – 5683.

217. C.P. Rao and A. Sreedhara, "Biomimetic and biointeraction studies of vanadium: role of oxovanadium complexes", *J. Inorg. Biochem.*, 1997, **67**, 393.

218. J.C. Pessoa, S. Marcao, I. Correia, G. Goncalves, A. Dornyei, T. Kiss, T. Jakusch, I. Tomaz, M.M.C.A. Castro and C.F.G.C. Geraldes et al., "Vanadium(IV and V) complexes of reduced Schiff bases derived from the reaction of aromatic o-hydroxyaldehydes and diamines containing carboxyl groups", *Eur. J. Inorg. Chem.*, 2006, 3595 – 3606.

219. N.A. Illa´n-Cabeza, M.N. Moreno-Carretero and J.C. Pessoa, "Preparation and characterisation of oxovanadium(IV) complexes derived from 2,6-diformyl-4-methylphenol and L-His and L-Ala. Spectroscopic study of the system $V^{IV}O^{2+}$ + BDF–His", *Inorg. Chim. Acta,* 2005, **358**, 2246 – 2254.

220. A. Butler, "Mechanistic considerations of the vanadium haloperoxidases", *Coord. Chem. Rev.,* 1999, **187**, 17 – 35.

221. G.J. Colpas, B.J. Hamstra, J.W. Kampf and V.L. Pecoraro, "Functional models for vanadium haloperoxidase: reactivity and mechanism of halide oxidation", *J. Am. Chem. Soc.,* 1996, **118**, 3469 – 3478.

222. B.J. Hamstra, G.J. Colpas and V.L. Pecoraro, "Reactivity of dioxovanadium(V) complexes with hydrogen peroxide: Implications for vanadium haloperoxidase", *Inorg. Chem.,* 1998, **37**, 949 – 955.

223. D. Rehder, *Bioinorganic Vanadium Chemistry*, John Wiley & Sons, New York, 2008.

224. P.P. Knops-Gerrits, D.D. Vos, F. Thibault-Starzyk and P.A. Jacobs, "Zeolite-encapsulated Mn(II) complexes as catalysts for selective alkene oxidation", *Nature,* 1994, **369**, 543 – 546.

225. G.S. Mishra and A. Kumar, "Preparation of heterogeneous vanadium (VO^{2+}) catalyst for selective hydroxylation of cyclohexane by molecular oxygen", *Catal. Lett.,* 2002, **81**, 113 – 117.

226. T. Joseph, D. Srinivas, C.S. Gopinath and S.B. Halligudi, "Spectroscopic and Catalytic Activity Studies of VO(Saloph) Complexes Encapsulated in Zeolite-Y and Al-MCM-41 Molecular Sieves", *Catal. Lett.,* 2002, **83**, 209 – 214.

227. P.A. Awasarkar, S. Gopinathan and C. Gopinathan, "Organooxytitanium and organotin derivatives of dibasic tetradentate chelating disulfides", *Synth. React. Inorg. Met. Org. Chem.,* 1985, **15**, 133 – 147.

228. R.H. Groeneman, L.R. MacGillivray and J.L. Atwood, "One-dimensional coordination polymers based upon bridging terephthalate ions", *Inorg. Chem.,* 1999, **38**, 208 – 209.

229. D.A. Annis and E.N. Jacobson, "Polymer-supported chiral Co(salen) complexes: Synthetic applications and mechanistic investigations in the hydrolytic kinetic resolution of terminal epoxides", *J. Am. Chem. Soc.,* 1999, **121**, 4147 – 4154.

230. J.K. Karjalainen, O.E.O. Harmi and D.C. Sherrington, "Highly efficient heterogeneous polymer-supported Sharpless alkene epoxidation catalysts", *Tetrahedron: Asym.,* 1998, **9**, 1563 – 1575.

231. L. Canali and D.C. Sherrington, "Utilisation of homogeneous and supported chiral metal(salen) complexes in asymmetric catalysis", *Chem. Soc. Rev.,* 1999, **28**, 85 – 93.

232. D.C. Sherrington, "Polymer-supported metal complex alkene epoxidation catalysts", *Catal. Today,* 2000, **57**, 87 – 104.

233. R.A., Rowe and M.M. Jones, "Vanadium(IV) oxy(acetylacetonate)", *Inorg. Synth.,* 1957, **5**, 113 – 116.

234. C.R. Cornman, J. Kampf, M.S. Lah and V.L. Pecoraro, "Modeling vanadium bromoperoxidase: Synthesis, structure, and spectral properties of vanadium(IV) complexes with coordinated imidazole", *Inorg. Chem.,* 1992, **31**, 2035 – 2043.

235. A. Rockenbauer and L. Korecz, "Automatic computer simulations of ESR spectra", *Appl. Magn. Reson.,* 1996, **10**, 29 – 43.

236. M.R. Maurya, "Development of the coordination chemistry of vanadium through bis(acetylacetonato)oxovanadium(IV): Synthesis, reactivity and structural aspects", *Coord. Chem. Rev.,* 2003, **237**, 163 – 181.

237. K. Wuethrich, "E.S.R. (electron spin resonance) investigation of VO^{2+} complex compounds in aqueous solution. II", *Helv. Chim. Acta,* 1965, **48**, 1012 – 1017.

238. N.D. Chasteen, in: J. Reuben (Ed.), *Biological Magnetic Resonance,* Plenum, New York, 1981, 53.

239. E. Garribba, G. Micera and D. Sanna, *6th International Vanadium Symposium,* Lisbon, 2008, Book of Abstracts, O30.

240. T.S. Smith II, C.A. Root, J.W. Kampf, P.G. Rasmussen and V.L. Pecoraro, "Reevaluation of the additivity relationship for vanadyl−imidazole complexes: correlation of the epr hyperfine constant with ring orientation", *J. Am. Chem. Soc.,* 2000, **122**, 767 – 775.

241. K. Nakajima, M. Kojima and J. Fujita, "Asymmetric oxidation of sulfides to sulfoxides by organic hydroperoxides with optically active Schiff base-oxovanadium(IV) catalysts", *Chem. Lett.,* 1986, **9**, 1483 – 1486.

242. C. Bolm and F. Bienewald, "Asymmetric sulfide oxidation with vanadium catalysts and H_2O_2", *Angew Chem. Int. Ed. Engl.,* 1996, **34**, 2640 – 2642.

243.   K. Nakajima, K. Kojima, M. Kojima and J. Fujita, "Preparation and characterization of optically active Schiff base-oxovanadium(IV) and - oxovanadium(V) complexes and catalytic properties of these complexes on asymmetric oxidation of sulfides into sulfoxides with organic hydroperoxides", *Bull. Chem. Soc. Jpn.,* 1990, **63**, 2620 – 2630.

244.   J. Skarzewski, E. Ostrycharz, and R. Siedlecka, "Vanadium catalyzed enantioselective oxidation of sulfides: easy transformation of bis(arylthio)alkanes into C2 symmetric chiral sulfoxides", *Tetrahedron: Asym.,* 1999, **10**, 3457 – 3461.

245.   A.H. Vetter and A. Berkessel, "Schiff-base ligands carrying two elements of chirality: matched-mismatched effects in the vanadium-catalyzed sulfoxidation of thioethers with hydrogen peroxide", *Tetrahedron Lett.,* 1998, **39**, 1741 – 1744.

246.   B. Pelotier, M.S. Anson, I.B. Campbell, S.J.F. Macdonald, G. Priem and R. F.W. Jackson, " Enantioselective sulfide oxidation with H_2O_2: A solid phase and array approach for the optimization of chiral Schiff base-vanadium catalysts", *Synlett,* 2002, 1055 – 1060.

247.   M. Palucki, P. Hanson and E.N. Jacobsen, "Asymmetric oxidation of sulfides with hydrogen peroxide catalyzed by (salen)Mn(III) complexes", *Tetrahedron Lett.,* 1992, **33**, 7111 – 7114.

248.   K. Noda, N. Hosoya, R. Irie, Y. Yamashita and T. Katsuki, "Catalytic asymmetric oxidation of sulfides using (salen)manganese(III) complex as a catalyst", *Tetrahedron,* 1994, **50**, 9609 – 9618.

249.   S. Colonna, A. Manfredi, M. Spadoni, L. Casella and M. Gulloti, "Asymmetric oxidation of sulphides to sulphoxides catalysed by titanium complexes of *N*-salicylidene-L-amino acids", *J. Chem. Soc., Perkin Trans. I,* 1987, 71 – 73.

250.   C. Sasaki, K. Nakajima, M. Kojima and J. Fujita, "Preparation and characterization of optically active quadridentate Schiff base-titanium(IV) complexes and the catalytic properties of these complexes on asymmetric oxidation of methyl phenyl sulfide with organic hydroperoxides", *Bull. Chem. Soc. Jpn.,* 1991, **64**, 1318 – 1324.

251.   R.A. Sheldon and J.K. Kochi, Metal Catalyzed Oxidations of Organic Compounds, Academic Press, New York, 1981.

252.   B.M. Trost, I. Fleming and S.V. Ley (Eds.), Comprehensive Organic Synthesis, vol. 7, Pergamon, Oxford, 1991, p. 251.

253. I. Flament and M. Stoll, "Pyrazines. I. Synthesis of 3-alkyl-2-methylpyrazines by condensation of ethylenediamine with 2,3-dioxoalkanes", *Helv. Chim. Acta,* 1967, **50**, 1754 – 1758.

254. H. Wynberg and H.J. Kooreman, "The mechanism of the hinsberg thiophene ring synthesis", *J. Am. Chem. Soc.,* 1965, **87**, 1739 – 1742.

255. W.W. Paudler and J.M. Barton, "The synthesis of 1,2,4-triazine", *J. Org. Chem.,* 1966, **31**, 1720 – 1722.

256. G.B. Gill, in: G. Pattenden (Ed.), Comprehensive Organic Synthesis, Vol. 3, Pergamon Press, New York, 1991, pp. 821 – 838.

257. D. Rehder, C. Weidemann, A. Duch and W. Priebsch, "Vanadium-51 shielding in vanadium(V) complexes: a reference scale for vanadium binding sites in biomolecules", *Inorg. Chem.,* 1988, **27**, 584 – 587.

258. V. Conte, F. D. Furia and S. Moro, "Studies directed toward the prediction of the oxidative reactivity of vanadium peroxo complexes in water. Correlations between the nature of the ligands and ^{51}V-NMR chemical shifts", *J. Mol. Catal.,* 1995, **104**, 159 – 169.

259. D.C. Crans, A.D Keramidas, H. Hoover-Litty, O.P. Anderson, M.M. Miller, L.M. Lemoine, S. Pleastic-Williams, M. Vandenberg, A.J. Rossomando and L.J. Sweet, "Synthesis, structure and biological activity of a new insulinomimetic peroxovanadium compound: Bisperoxovanadium imidazole monoanion", *J. Am. Chem. Soc.,* 1997, **119**, 5447 – 5448.

260. J.S. Jaswal and A.S. Tracey, "Reactions of mono- and diperoxovanadates with peptides containing functionalized side chains", *J. Am. Chem. Soc.,* 1993, **115**, 5600 – 5607.

261. K.P. Bryliakov, N.N. Karpyshev, S.A. Fominsky, A.G. Tolstikov and E.P. Talsi, "^{51}V and ^{13}C NMR spectroscopic study of the peroxovanadium intermediates in vanadium catalyzed enantioselective oxidation of sulfides", *J. Mol. Catal.,* 2001, **171**, 73 – 80.

262. V. Conte, F.D. Furia and S. Moro, "The ^{51}V-NMR investigation on the formation of peroxo vanadium complexes in aqueous solution: some novel observations", *J. Mol. Catal.,* 1994, **94**, 323 – 333.

263. J.S. Jaswal and A.S. Tracey, "Formation and decomposition of peroxovanadium(V) complexes in aqueous solution", *Inorg. Chem.,* 1991, **30**, 3718 – 3722.

264. A. Butler, M.J. Clague and G.E. Maister, "Vanadium peroxide complexes", *Chem. Rev.,* 1994, **94**, 625 – 638.

265. O. Bortolini, F. Di Furia and G. Modena, "Metal catalysis in oxidation by peroxides. Part 15. Steric effects in the oxidation of organic sulfides with vanadium(V) and molybdenum(VI) peroxy complexes", *J. Mol. Catal.,* 1982, **16**, 61 – 68.

266. M.J. Clague, N.L. Keder and A. Butler, "Biomimics of vanadium bromeperoxidase: vanadium (V)-schiff base catalyzed oxidation of bromide by hydrogen peroxide", *Inorg. Chem.,* 1993, **32**, 4754 – 4761.

267. A. Butler and M.J. Clague, in: H.H. Thorp and V.L. Pecoraro (Eds.), Mechanistic Bioinorganic Chemistry, Adv. Chem. Ser., 1995, **246**, 329.

268. A. Butler and A.H. Baldwin, in: P. Sadler, H.A.O. Hill and A. Thompson (Eds.), Structure and Bonding, 1997, **89**, 109.

269. V. Conte, F. Di Furia and S. Moro, "The versatile chemistry of peroxo complexes of vanadium, molybdenum and tungsten as oxidants of organic compounds", *J. Phys. Org. Chem.,* 1996, **9**, 329 – 336.

270. O. Bortolini, M. Carraro, V. Conte and S. Moro, "Histidine-containing bisperoxovanadium(V) compounds. Insight into the solution structure by an ESI-MS and ^{51}V-NMR comparative study", *Eur. J. Inorg. Chem.,* 1999, **9**, 1489 – 1495.

271. G. Santoni, G. Licini and D. Rehder, "Catalysis of oxo transfer to prochiral sulfides by oxovanadium(V) compounds that model the active center of haloperoxidases", *Chem. Eur. J.,* 2003, **9**, 4700 – 4708.

272. C.J. Schneider, J.E. Penner-Hahn and V.L. Pecoraro, "Elucidating the protonation site of vanadium peroxide complexes and the implications for biomimetic catalysis", *J. Am. Chem. Soc.,* 2008, **130**, 2712 – 2713.

273. C.R. Cornman, G.J. Colpas, J.D. Hoeschele, J. Kampf and V.L. Pecoraro, "Implications for the spectroscopic assignment of vanadium biomolecules: structural and spectroscopic characterization of monooxovanadium(V) complexes containing catecholate and hydroximate based noninnocent ligands", *J. Am. Chem. Soc.,* 1992, **114**, 9925 – 9953.

274. C.R. Cornman, J. Kampf and V.L. Pecoraro, "Gold(III) glycyl-L-histidine dipeptide complexes. Preparation and X-ray structures of monomeric and cyclic tetrameric species", *Inorg. Chem.,* 1992, **31**, 1983 – 1985.

275. G. Zampella, P. Fantucci, V.L. Pecoraro and L. De Gioia, "Reactivity of Peroxo Forms of the Vanadium Haloperoxidase Cofactor. A DFT Investigation", *J. Am. Chem. Soc.*, 2005, **127**, 953 – 960.

276. T.S. Smith II and V.L. Pecoraro, "Oxidation of organic sulfides by vanadium haloperoxidase model complexes", *Inorg. Chem.*, 2002, **41**, 6754 – 6760.

277. R.I. de la Rosa, M.J. Clague and A. Butler, "A functional mimic of vanadium bromoperoxidase", *J. Am. Chem. Soc.*, 1992, **114**, 760 – 761.

278. D. C. Sherrington, in: B. K. Hodnett, A. P. Keybett, J. H. Clark and K. Smith (Eds.), Supported Reagents and Catalysts in Chemistry, Royal Society of Chemistry, Cambridge, 1998, pp. 220.

279. B. Meunier, "Metalloporphyrins as versatile catalysts for oxidation reactions and oxidative DNA cleavage", *Chem Rev.*, 1992, **92**, 1411 – 1456.

280. D.E. De Vos, M. Dams, B.F. Sels and P.A. Jacobs, "Ordered Mesoporous and Microporous Molecular Sieves Functionalized with Transition Metal Complexes as Catalysts for Selective Organic Transformations", *Chem. Rev.*, 2000, **102**, 3615 – 3640.

281. K.J. Balkus Jr. and A.G. Gabrielov, "Zeolite encapsulated metal complexes", *J. Incl. Phenom. Mol. Recog. Chem.*, 1995, **21**, 159 – 184.

282. K.J. Balkus Jr., A.A. Welch and B.E. Gnade, "The encapsulation of rhodium(III) phthalocyanines in zeolites X and Y", *J. Incl. Phenom. Mol. Recogn. Chem.*, 1991, **10**, 141 – 151.

283. C.R. Jacob, S.P. Varkey and P. Ratnasamy, "Zeolite-encapsulated copper (X₂-salen) complexes", *Appl. Catal. A: Gen.*, 1998, **168**, 353 – 364.

284. M.R. Maurya, S.J.J. Titinchi and S. Chand, "Spectroscopic and catalytic activity study of N,N'-bis(salicylidene)propane-1,3-diamine copper(II) encapsulated in zeolite-Y", *Appl. Catal. A: Gen.*, 2002, **228**, 177 – 187.

285. K. Srinivasan, P. Michaud and J.K. Kochi, "Epoxidation of olefins with cationic (salen)manganese(III) complexes. The modulation of catalytic activity by substituents", *J. Am. Chem. Soc.*, 1986, **108**, 2309 – 2320.

286. R. Irie, Y. Ito and T. Katsuki, "Donor ligand effect in asymmetric epoxidation of unfunctionalized olefins with chiral salen complexes", *Synlett*, 1991, **4**, 265 – 266.

287. S.B. Kumar, S.P. Mirajkar, G.C.G. Pais, P. Kumar and R. Kumar, "Epoxidation of styrene over a titanium silicate molecular sieve TS-1 using dilute H_2O_2 as oxidizing agent", *J. Catal.,* 1995, **156**, 163 – 166.

288. J.S. Reddy, U.R. Khire, P. Ratnasamy and R.B. Mitra, "Cleavage of the carbon–carbon double bond over zeolites using hydrogen peroxide", *J. Chem. Soc. Chem. Commun.,* 1992, 1234 – 1235.

289. L.I. Matienko and L.A. Mosolova, "Selective oxidation of ethylbenzene by dioxygen. The effect of chelate center on catalysis by bicyclic nickel complexes", *Russ. Chem. Bull.,* 1999, **48**, 55 – 60.

290. R. Alcantara, L. Canoira, P.G. Joao, J.-M. Santos and I. Vazquez, "Ethylbenzene oxidation with air catalysed by bis(acetylacetonate)nickel(II) and tetra-n-butylammonium tetrafluoroborate", *Appl. Catal. A: Gen.,* 2000, **203**, 259 – 268.

291. Z. Lei and Y. Wang, "Oxidation of alkylbenzenes catalyzed by iron(II,III)-1,10-phenanthroline and 2,2'-bipyridine complexes", *Chin. Chem. Lett.,* 1993, **4**, 21 – 22.

292. S. Evans and J.R. Lindsay Smith, "The oxidation of ethylbenzene by dioxygen catalysed by supported iron porphyrins derived from iron(III) tetrakis(pentafluorophenyl)porphyrin", *J. Chem. Soc., Perkin Trans. 2,* 2001, 174 – 180.

293. T. Maeda, A.K. Pee and D. Haa, JP 7.196573, 1995; Chem. Abs. 256345, 1995.

294. Y. Ishii, T. Iwahama, S. Sakaguchi, K. Nakayama and Y. Nishiyama, "Alkane oxidation with molecular oxygen using a new efficient catalytic system: n-hydroxyphthalimide (NHPI) combined with Co(acac)n (n = 2 or 3)", *J. Org. Chem.,* 1996, **61**, 4520 – 4526.

295. G.J.-J. Chen, J.W. McDonald and W.E. Newton, "Synthesis of molybdenum(IV) and molybdenum(V) complexes using oxo abstraction by phosphines. Mechanistic implications", *Inorg. Chem.,* 1976, **15**, 2612 – 2615.

296. P. Carr, B. Pigott, S.F. Wong and R.N. Sheppard, "Molybdenum-95 NMR spectra of bis(benzimidazol-2-ylmethanethiolato)dioxomolybdenum and x-ray crystal structure of bis(benzimidazol-2-ylmethanethiolato)bis(DMF)dioxo bis(μ-oxo)dimolybdenum", *Inorg. Chim. Acta,* 1986, **123**, 5 – 8.

297. A. Syamal and O.P. Singhal, "Syntheses and characterization of new dioxouranium(VI) complexes with tridentate sulfur donor ligands", *J. Inorg. Nucl. Chem.*, 1981, **43**, 2821 – 2825.

298. A. Syamal and M.R. Maurya, "Coordination chemistry of Schiff base complexes of molybdenum", *Coord. Chem. Rev.*, 1989, **95**, 183 – 238.

299. M.R. Maurya, A. Kumar, M. Ebel and D. Rehder, "Synthesis, characterization, reactivity and catalytic potential of model vanadium(IV, V) complexes with benzimidazole-derived ONN donor ligands", *Inorg. Chem.*, 2006, **45**, 5924 – 5937.

300. A. Zsigmond, A. Horvath and F. Notheisz, "Effect of substituents on the Mn(III) salen catalyzed oxidation of styrene", *J. Mol. Catal. A: Chem.*, 2001, **171**, 95 – 102.

301. V. Hulea and E. Dumitriu, "Styrene oxidation with H_2O_2 over Ti-containing molecular sieves with MFI, BEA and MCM-41 topologies", *Appl. Catal. A. Gen.*, 2004, **277**, 99 – 106.

302. U. Sakagushi and A.W. Addison, "Spectroscopic and redox studies of some copper(II) complexes with biomimetic donor atoms: Implications for protein copper centres", *J. Chem. Soc. Dalton Trans.*, 1979, 600 – 608.

303. G. Capozi and G. Modena, in: S. Patai (ed.), The Chemistry of the Thiol Group, John Wiley & Sons, London, 1974, Part 2, pp. 785-839 and refs. therein.

304. H. Mimoun, M. Mignard, P. Brechot and L. Saussine, "Selective epoxidation of olefins by oxo[N-(2-oxidophenyl)salicylidenaminato]vanadium(V) alkylperoxides. On the mechanism of the Halcon epoxidation process", *J. Am. Chem. Soc.*, 1986, **108**, 3711 – 3718.

305. N.K. Kala Raj, A.V. Ramaswamy and P. Manikandan, "Oxidation of norbornene over vanadium-substituted phosphomolybdic acid catalysts and spectroscopic investigations", *J. Mol. Catal. A: Chem.*, 2005, **227**, 37 – 45.

306. E.I. Solomon, P. Chen, M. Metz, S.-K. Lee and A.E. Palner, "Oxygen binding, activation, and reduction to water by copper proteins", *Angew. Chem. Int. Ed.*, 2001, **40**, 4570 – 4590.

307. J.P. Klinman, "Mechanisms Whereby Mononuclear Copper Proteins Functionalize Organic Substrates", *Chem. Rev.*, 1996, **96**, 2541 – 2561.

308. K.D. Karlin, J.C. Hayes, Y. Gultneh, R.W. Cruse, J.W. McKown, J.P. Hutchinson and J. Zubieta, "Copper-mediated hydroxylation of an arene: model system for the action of copper monooxygenases. Structures of a binuclear copper(I) complex and its oxygenated product", *J. Am. Chem. Soc.*, 1984, **106**, 2121 – 2128.

309. A.J. Burke, "Chiral oxoperoxomolybdenum(VI) complexes for enantioselective olefin epoxidation: Some mechanistic and stereochemical reflections", *Coord. Chem. Rev.*, 2008, **252**, 170 – 175 and refs. therein.

310. H. Mimoun, L. Saussine, E. Daire, M. Postel, J. Fisher and R. Weiss, "Vanadium(V) peroxy complexes. New versatile biomimetic reagents for epoxidation of olefins and hydroxylation of alkanes and aromatic hydrocarbons", *J. Am. Chem. Soc.*, 1983, **105**, 3101 – 3110.

311. M. Bonchio, V. Conte, F. di Furia and G. Modena, "Metal catalysis in oxidation by peroxides. 31. The hydroxylation of benzene by $VO(O_2)(PIC)(H_2O)_2$: mechanistic and synthetic aspects", *J. Org. Chem.*, 1989, **54**, 4368 – 4371.

312. G.B. Shul'pin, D. Attanasio and L. Suber, "Efficient hydrogen peroxide oxidation of alkanes and arenes to alkyl peroxides and phenols catalyzed by the system vanadate-pyrazine-2-carboxylic acid", *J. Catal.*, 1993, **142**, 147 – 152.

313. V. Hulea, F. Fajula and J. Bousquet, "Mild oxidation with H_2O_2 over Ti-containing molecular sieves-a very efficient method for removing aromatic sulfur compounds from fuels", *J. Catal.*, 2001, **198**, 179 – 186.

314. A.V. Anisimov, E.V. Fedorova, A.Z. Lesnugin, V.M. Senyavin, L.A. Aslanov, V.B. Rybakov and A.V. Tarakanova, "Vanadium peroxocomplexes as oxidation catalysts of sulfur organic compounds by hydrogen peroxide in bi-phase systems", *Catal. Today*, 2003, **78**, 319 – 325.

315. J. Palomeque, J.M. Clacens and F. Figueras, "Oxidation of dibenzothiophene by hydrogen peroxide catalyzed by solid bases", *J. Catal.*, 2002, **211**, 103 – 108.

316. K. Yazu, Y. Yamamoto, T. Furuya, K. Miki and K. Ukegawa, "Oxidation of dibenzothiophenes in an organic biphasic system and its application to oxidative desulfurization of light oil", *Energy Fuels*, 2001, **15**, 1535 – 1536.

317. S. Djangkung, S. Murti, H. Yang, K. Choi, Y. Kora and I. Mochida, "Influences of nitrogen species on the hydrodesulfurization reactivity of a gas

oil over sulfide catalysts of variable activity", *Appl. Catal. A: Gen.*, 2003, **252**, 331 – 346.

318.   Y. Shiraishi, T. Naito and T. Hirai, "Vanadosilicate molecular sieve as a catalyst for oxidative desulfurization of light oil", *Ind. Eng. Chem. Res.*, 2003, **42**, 6034 – 6039.

319.   S. Kazuhiko and A. Koichi, "Oxidative desulfurization of fuel oil", 2004, JP 2004196927.

320.   H. Masataka, K. Nobuyasu, K. Tatsuya, K. Naoto and Y. Tomohiro, "Method for oxidative desulfurization of liquid petroleum product and oxidative desulfurization plant", 2003, JP 2003193066.

321.   C.C. Avelino, M.E. Domine and M.S. Cristina, "Oxidative desulfurization of gasoline, kerosene and diesel fractions, comprises liquid phase oxidation in absence of solvent and in presence of molecular sieve catalyst", 2003, ES2192969.

322.   G.X. Yu, S.X. Lu, H. Chen and Z. Zhu, "Oxidative desulfurization of diesel fuels with hydrogen peroxide in the presence of activated carbon and formic acid", *Energy Fuels*, 2005, **19**, 447 – 452.

323.   L.F. Verduzco, E.T. García and R.G. Quintana, "Desulfurization of diesel by oxidation/extraction scheme: influence of the extraction solvent", *Catal. Today*, 2004, **98**, 289 – 294.

324.   S. Muratua, K. Mirata, K. Kidena and M. Nomura, "A novel oxidative desulfurization system for diesel fuels with molecular oxygen in the presence of cobalt catalysts and aldehydes", *Energy Fuels*, 2004, **18**, 116 – 121.

325.   F. Zannikios, E. Lois and S. Stournas, "Desulfurization of petroleum fractions by oxidation and solvent extraction", *Fuel process Techno.*, 1995, **42**, 35 – 45.

326.   L.C. Caero, J. Forge, A. Navarro and A. Gutierrez-Alejandre, "Oxidative desulfurization of synthetic diesel using supported catalysts", *Catal. Today*, 2006, **116**, 562 – 568.

327.   L.F. Ramı́rez-Verduzco, E. Torres-Garcı́a, R. Go′mez-Quintana, V. Gonza′lez-Peña and F. Murrieta-Guevara, "Desulfurization of diesel by oxidation/extraction scheme: influence of the extraction solvent", *Catal. Today*, 2004, **98**, 289 – 294.

328. E. Dumitriu, C. Guimon, A. Cordoneanu, S. Casenave, T. Hulea, C. Chelaru, H. Martinez and V. Hulea, "Heterogeneous sulfoxidation of thioethers by hydrogen peroxide over layered double hydroxides as catalysts", *Catal. Today*, 2001, **66**, 529 – 534.

329. F. Figueras, J. Palomeque, S. Loridant, C. Fe`che, N. Essayem and G. Gelbard, "Influence of the coordination on the catalytic properties of supported W catalysts", *J. Catal.*, 2004, **226**, 25 – 31.

330. E. Torres-Garcı́a, G. Canizal, L.F. Ramı́rez-Verduzco, F. Murrieta-Guevara and J.A. Ascencio, "Influence of surface phenomena in oxidative desulfurization with WO_x/ZrO_2 catalysts", *Appl. Phys. A*, 2004, **79**, 2037 – 2040.

331. D. Wang, E.W. Qian, H. Amano, K. Okata, A. Ishihara and T. Kabe, "Oxidative desulfurization of fuel oil. Part I. Oxidation of dibenzothiophenes using tert-butyl hydroperoxide", *Appl. Catal. A: Gen.*, 2003, **253**, 91 – 99.

332. J. March, Advanced Organic Chemistry: Reactions, Mechanisms and Structure, Wiley-Interscience, New York, 1992.

333. L.F. Ramı́rez-Verduzco, F. Murrieta-Guevara, J.L. Garcı́a-Gutie´rrez, R. Saint Martin-Castanõn, M. del C Martinez-Guerrero, M. del C Montiel-Pacheco and R. Mata-Dı́az, "Desulfurization of middle distillates by oxidation and extraction process", *Petro. Sci. Techno.*, 2004, **22**, 129 – 139.

334. M. Te, C. Fairbridge and Z. Ring, "Oxidation reactivities of dibenzothiophenes in polyoxometalate/H_2O_2 and formic acid/H_2O_2 systems", *Appl. Catal. A: Gen.*, 2001, **219**, 267 – 280.

335. R.S. Drago and D.S. Burns, "Molybdate and tungstate doped porous carbons as hydrogen peroxide activation catalysts for sulfide oxidations", *J. Catal.*, 1997, **166**, 377 – 379.

336. E. Dumitriu, C. Guimon, A. Cordoneanu, S. Casenave, T. Hulea, C. Chelaru, H. Martinez and V. Hulea, "Heterogeneous sulfoxidation of thioethers by hydrogen peroxide over layered double hydroxides as catalysts", *Catal. Today*, 2001, **66**, 529 – 534.

337. B.M. Choudary, C.R.V. Reddy, B.V. Prakash, M.L. Kantam, and B. Sreedhar, "The first example of direct oxidation of sulfides to sulfones by an osmate molecular oxygen system", *Chem. Commun.*, 2003, 754 – 755.

338. F. Zannikos, E. Lois and S. Stournas, "Desulfurization of petroleum fractions by oxidation and solvent extraction", *Fuel Processing Techno.*, 1995, **42**, 35 – 45.

339. S.E. Bonde, W. Gore, G.E. Dolbear and E.R. Skov, "Selective oxidation and extraction of sulfur-containing compounds to economically achieve ultra-low proposed diesel fuel sulfur requirements", *Prepr.—Am. Chem.Soc., Div. Petro. Chem.*, 2000, **45**, 364 – 366.

340. W. Gore, S.E. Bonde, G.E. Dolbear and E.R. Skov, U.S. 20020035306 (2002).

341. G.E. Dolbear and E.R. Skov, "Selective oxidation as a route to petroleum desulfurization", *Prepr.—Am. Chem. Soc., Div. Petro. Chem.*, 2000, **45**, 375 – 378.

342. S.E. Bonde, W. Gore and G.E. Dolbear, "DMSO extraction of sulfones from selectively oxidized fuels", *Prepr.—Am. Chem. Soc., Div. Petro. Chem.*, 1999, **44**, 199 – 201.

343. A. Kh. Sharipov, Z.A. Suleimanova and I.S. Faizrakhmanov, "Foam-emulsion oxidation of petroleum sulfur compounds to sulfones", *Neftekhimiya*, 1994, **34**, 459 – 466.

344. Y. Shiraishi, K. Tachibana, T. Hirai and I. Komasawa, "Desulfurization and denitrogenation process for light oils based on chemical oxidation followed by liquid–liquid extraction", *Ind. Eng. Chem. Res.*, 2002, **41**, 4362 – 4375.

345. S. Otsuki, T. Nonaka, N. Takashima, W. Qian, A. Ishihara, T. Imai and T. Kabe, "Oxidative desulfurization of light gas oil and vacuum gas oil by oxidation and solvent extraction", *Energy Fuels*, 2000, **14**, 1232 – 1239.

346. T. Aida and D. Yamamoto, "Oxidative desulfurization of liquid fuels", *Prepr.—Am. Chem. Soc., Div. Fuel Chem.*, 1994, **39**, 623 – 626.

347. F.M. Collins, A.R. Lucy and S. Christopher, "Oxidative desulfurization of oils via hydrogen peroxide and heteropolyanion catalysis", *J. Mol. Catal. A: Chem.*, 1997, **117**, 397 – 403.

348. K. Yazu, Y. Yamamoto, T. Furuya, K. Miki and K. Ukegawa, "Oxidation of dibenzothiophenes in an organic biphasic system and its application to oxidative desulfurization of light oil", *Energy Fuels*, 2001, **15**, 1535 – 1536.

349. K. Yadzu, K. Miki, K. Ukegaw and N. Yamamoto, "Oxidative desulfurization method of fuel oil", JP 2001354978A 20011225 (2001).

350. Y. Shiraishi, T. Hirai and I. Komosawa, "Oxidative desulfurization process for light oil using titanium silicate molecular sieve catalysts", *J. Chem. Eng. Jpn.*, 2002, **35**, 1305 – 1311.

351. V. Hulea, P. Moreau and F. Di Renzo, "Thioether oxidation by hydrogen peroxide using titanium-containing zeolites as catalysts", *J. Mol. Catal. A: Chem.*, 1996, **111**, 325 – 332.

352. V. Hulea and P. Moreau, "The solvent effect in the sulfoxidation of thioethers by hydrogen peroxide using Ti-containing zeolites as catalysts", *J. Mol. Catal. A: Chem.*, 1996, **113**, 499 – 505.

353. R.S. Reddy, J.S. Reddy, R. Kumar and P. Kumar, "Sulfoxidation of thioethers using titanium silicate molecular sieve catalysts", *J. Chem. Soc. Chem. Commun.*, 1992, 84 – 85.

354. M. Ziolek, "Catalytic liquid-phase oxidation in heterogeneous system as green chemistry goal-advantages and disadvantages of MCM-41 used as catalyst", *Catal. Today*, 2004, **90**, 145 – 150.

355. N.N. Trukhan, A.Y. Derevyankin, A.N. Shmakov, E.A. Paukshtis, O.A. Kholdeeva and V.N. Romannikov, "Alkene and thioether oxidations with H_2O_2 over Ti- and V-containing mesoporous mesophase catalysts", *Micropor. Mesopor. Mater.*, 2001, **44–45**, 603 – 608.

356. Y. Shiraishi, T. Naito and T. Hirai, "Vanadosilicate molecular sieve as a catalyst for oxidative desulfurization of light oil", *Ind. Eng. Chem. Res.*, 2003, **42**, 6034 – 6039.

357. P.S. Raghavan, V. Ramaswamy, T.T. Upadhya, A. Sudalai, A.V. Ramaswamy and S.J. Sivasanker, "Selective catalytic oxidation of thioethers to sulfoxides over Mo-silicalite-1 (MoS-1) molecular sieves", *J. Mol. Catal. A: Chem.*, 1997, **122**, 75 – 80.

358. R. Hiatt, in: R.L. Augustine, D.J. Trekker (Eds.), Oxidation, vol. 2, Marcel Dekker, New York, 1971 (Chapter 3).

359. G.A. Tolstikov, V.P. Yurev and U.M. Dzhemilev, "Metal-catalysed Oxidation of Organic Compounds by Hydroperoxides", *Russ. Chem. Rev.*, 1975, **44**, 319 – 332.

360. R.A. Sheldon and J.K. Kochi, "Metal-catalyzed oxidations of organic compounds in the liquid phase: a mechanistic approach", *Adv. Catal.*, 1976, **25**, 272 – 413.

361. J.E. Lyons, Aspects of Homogeneous Catalysis vol. 3, in: R. Ugo (Ed.), D. Reidel Publishing Company, Dordrecht, Holland, Boston, USA, 1977, p. 1.

362. K.B. Sharpless and T.R. Verhoeven, "Metal-catalyzed, highly selective oxygenations of olefins and acetylenes with tert-butyl hydroperoxide. Practical considerations and mechanisms", *Aldrichim. Acta*, 1979 **12**, 63 – 74.

363. R.A. Sheldon, "Synthetic and mechanistic aspects of metal-catalyzed epoxidations with hydroperoxides", *J. Mol. Catal.*, 1980, **7**, 107 – 126.

364. J. Sobczak and J.J. Ziolkovski, "The catalytic epoxidation of olefins with organic hydroperoxides", *J. Mol. Catal.*, 1981, **13**, 11 – 42.

365. R.A. Sheldon and J.K. Kochi, Metal-catalyzed Oxidation of Organic Compounds, Academic Press, New York, 1981.

366. C.J. Chang, J.A. Labinger and H.B. Gray, "Aerobic epoxidation of olefins catalyzed by electronegative vanadyl salen complexes", *Inorg. Chem.*, 1997, **36**, 5927 – 5930.

367. M.R. Maurya, A. Arya, A. Kumar and J.C. Pessoa, "Polystyrene bound oxidovanadium(IV) and dioxidovanadium(V) complexes of histamine derived ligand for the oxidation of methyl phenyl sulfide, diphenyl sulfide and benzoin", *Dalton Trans.*, 2009, 2185 – 2195.

368. J.C. Duff and E.J. Bills, "Reactions between hexamethylenetetramine and phenolic compounds. I. A new method for the preparation of 3- and 5-aldehydosalicylic acids", *J. Chem. Soc.*, 1923, 1987.

369. T. Floriana, P. Luminita and A. Marius, "A synthetic approach towards homotrinuclear complexes: design of Mn(II), Ni(II) and Cu(II) trinuclear complexes using two new unsymmetrical tetradentate ligands derived from 3-formylsalicylic acid", *Synth. React. Inorg. Metal-Org. Chem.*, 1998, **28**, 13 – 22.

370. R. Karmakar, C.R. Choudhury, D.L. Hughes, G.P.A. Yap, M.S. El Fallah, C. Desplanches, J.P. Sutter and S. Mitra, "Two new end-to-end single dicyanamide bridged Cu(II) complexes with schiff base ligands: Structural, electrochemical and magnetic properties", *Inorg. Chim. Acta*, 2006, **359**, 1184–1192.

371. G.M. Sheldrick, *SHELXL-97: An Integrated System for Solving and Refining Crystal Structures from Diffraction Data (Revision 4.1)*; University of Göttingen, Germany, 1997.

372. G. Bernardinelli and H.D. Flack, "Least-squares absolute-structure refinement. Practical experience and ancillary calculations", *Acta Cryst., Sect. A: Found. Crystallogr.*, 1985, **A41**, 500 – 511.

373. A. Guzei Ilea, J. Roberts and D.A. Saulys, "Pseudosymmetry in pyridinium tetrachloro(oxo)pyridineniobate(V) pyridine solvate", *Acta. Cryst., Sect. C,* 2002, **58**, m141– m143.

374. B. Baruan, S. Das and A. Chakravorty, "A Family of Vanadate Esters of Monoionized and Diionized Aromatic 1,2-Diols: Synthesis, Structure, and Redox Activity", *Inorg. Chem.*, 2002, **41**, 4502 – 4508.

375. S.P. Rath, T. Ghosh and S. Mondal, "Synthesis, structure and metal redox of alkoxide bound oxovanadium(V) complexes incorporating N-salicylidene/N-naphthalidene-α-amino alcohols", *Polyhedron,* 1997, **16**, 4179 – 4186.

376. S. Nica, M. Rudolph, H. Görls and W. Plass, "Structural characterization and electrochemical behavior of oxovanadium(V) complexes with N-salicylidenehydrazides", *Inorg. Chim. Acta*, 2007, **360**, 1743 – 1752.

377. X. Li, M.S. Lah and V.L. Pecoraro, "Vanadium complexes of the tridentate Schiff base ligand N-salicylidene-N'-(2-hydroxyethyl)ethylenediamine: acid-base and redox conversion between vanadium(IV) and vanadium(V) imino phenolates", *Inorg. Chem.*, 1988, **27**, 4657 – 4664.

378. M.-J. Xie, Y.S. -Ping, L.-D Zheng, J.-Z. Hui and C. Peng, "{2-[2-(N,N'-Dimethylamino)ethyliminomethyl]phenolato-κ3N,N',O}dioxovanadium(V)", *Acta Cryst., Sect.* E, 2004, **E60**, m1382 – m1383.

379. P. Arroyo, S. Gil, A. Munoz, P. Palanca, J. Sanchis and V. Sanz, "Polymer-supported molybdenyl thioglycolate as oxygen atom transfer reagent", *J. Mol. Catal. A: Chem.,* 2000, **160**, 403 – 408.

380. A. Syamal and K.S. Kale, "Magnetic and spectral properties of oxovanadium(IV) complexes of ONO donor tridentate, dibasic Schiff bases derived from salicylaldehyde or substituted salicylaldehyde and o-hydroxybenzylamine", *Inorg. Chem.,* 1979, **18**, 992 – 995.

381. P.J. Walsh, F.J. Hollander and R.G. Bergman, "Generation, alkyne cycloaddition, arene carbon-hydrogen activation, nitrogen-hydrogen activation and dative ligand trapping reactions of the first monomeric imidozirconocene (Cp$_2$Zr:NR) complexes", *J. Am. Chem. Soc.*, 1988, **110**, 8729 – 8731.

382. J.S. Johnson and R.G. Bergman, "Imidotitanium complexes as hydroamination catalysts: Substantially enhanced reactivity from an unexpected cyclopentadienide/amide ligand exchange", *J. Am. Chem. Soc.*, 2001, **123**, 2923 – 2924.

383. Y. Li and T.J. Marks, "Organolanthanide-catalyzed intramolecular hydroamination/cyclization of aminoalkynes", *J. Am. Chem. Soc.*, 1996, **118**, 9295 – 9306.

384. M. Beller, H. Trauthwein, M. Eichberger, C. Breindl and T.E. Müller, "Anti-Markovnikov reactions. Part 6. Rhodium-catalyzed amination of vinylpyridines. Hydroamination versus oxidative amination", *Eur. J. Inorg. Chem.*, 1999, 1121 – 1132.

385. M. Nobis and B. Driessen-Holscher, "Recent developments in transition metal catalyzed intermolecular hydroamination reactions - a breakthrough?", *Angew. Chem., Int. Ed.*, 2001, **40**, 3983 – 3985.

386. S. Hong and T.J. Marks, "Organolanthanide-catalyzed hydroamination", *Accounts Chem. Res.*, 2004, **37**, 673 – 686.

387. C.G. Hartung, C. Breindl, A. Tillack and M. Beller, "A Base-catalyzed domino-isomerization-hydroamination reaction-a new synthetic route to amphetamines", *Tetrahedron*, 2000, **56**, 5157 – 5162.

388. R.J. Schlott, J.C. Falk and L.W. Narducy, "Lithium amide catalyzed amine-olefin addition reactions", *J. Org. Chem.*, 1972, **37**, 4243 – 4245.

389. C. Brouwer and C. He, "Efficient gold-catalyzed hydroamination of 1,3-dienes", *Angew Chem. Int. Ed.*, 2006, **45**, 1744 – 1747.

390. K. Komeyama, T. Morimoto and K. Takaki, "A simple and efficient iron-catalyzed intramolecular hydroamination of un-activated olefins", *Angew. Chem. Int. Ed.*, 2006, **45**, 2938 – 2941.

391. R. Lira and J.P. Wolfe, "Palladium-catalyzed synthesis of N-aryl-2-benzylindolines via tandem arylation of 2-allylaniline: Control of selectivity through in situ catalyst modification", *J. Am. Chem. Soc.*, 2004, **126**, 13906 – 13907.

392. M. Utsunomiya, R. Kuwano, M. Kawatswa and J.F. Hartwig, "Rhodium-catalyzed anti-Markovnikov hydroamination of vinylarenes", *J. Am. Chem. Soc.*, 2003, **125**, 5608 – 5609.

393. B.D. Stubbert, C.L. Stern and T.J. Marks, "Synthesis and catalytic characteristics of novel constrained-geometry organoactinide catalysts. The first example of actinide-mediated intramolecular hydroamination", *Organometallics*, 2003, **22**, 4836 – 4838.

394. M.A. Giardello, V.P. Conticello, L. Brard, M.R. Gagne and T.J. Marks, "Chiral organolanthanides designed for asymmetric catalysis. A kinetic and mechanistic study of enantioselective olefin hydroamination/cyclization and hydrogenation by C1-symmetric $Me_2Si(Me_4C_5)(C_5H_3R^*)ln$ complexes where R^* = chiral auxiliary", *J. Am. Chem. Soc.*, 1994, **116**, 10241 – 10254.

395. C.M. Haskins and D.W. Knight, "Sulfonamides as novel terminators of cationic cyclisations", *Chem. Commun.*, 2002, 2724 – 2725.

396. L.L. Anderson, J. Arnold and R.G. Bergman, "Proton-catalyzed hydroamination and hydroarylation reactions of anilines and alkenes: a dramatic effect of counteranions on reaction efficiency", *J. Am. Chem. Soc.*, 2005, **127**, 14542 – 14543.

397. H. Qian and R.A. Widenhoefer, "Platinum-catalyzed intermolecular hydroamination of vinyl arenes with carboxamides", *Org. Lett.*, 2005, 7, 2635 – 2638.

398. D. Karshtedt, A.T. Bell and T.D. Tilley, "Platinum-based catalysts for the hydroamination of olefins with sulfonamides and weakly basic anilines", *J. Am. Chem. Soc.*, 2005, **127**, 12640 – 12646.

399. J. Zhang, C.-G. Yang and C. He, "Gold(I)-catalyzed intra- and intermolecular hydroamination of unactivated olefins", *J. Am. Chem. Soc.*, 2006, **128**, 1798 – 1799.

400. C. Brouwer and C. He, "Efficient gold-catalyzed hydroamination of 1,3-Dienes", *Angew. Chem., Int. Ed.*, 2006, **45**, 1744 – 1747.

401. J.G. Taylor, N. Whittall and K.K. Hii, "Copper-catalyzed intermolecular hydroamination of alkenes", *Org. Lett.*, 2006, **8**, 3561 – 3564.

402. J. Michaux, V. Terrasson, S. Marque, J. Wehbe, D. Prim and J.-M. Campagne, "Intermolecular $FeCl_3$-catalyzed hydroamination of styrenes", *Eur. J. Org. Chem.*, 2007, 2601 – 2603.

403. J.-M. Huang, C.-M. Wong, F.-X. Xu and T.-P. Loh, "$InBr_3$-catalyzed intermolecular hydroamination of unactivated alkenes", *Tetrahedron Lett.*, 2007, **48**, 3375 – 3377.

404. H. Qin, N. Yamagiwa, S. Matsunaga and M. Shibasaki, "Bismuth-catalyzed intermolecular hydroamination of 1,3-dienes with carbamates, sulfonamides, and carboxamides", *J. Am. Chem. Soc.*, 2006, **128**, 1611 – 1614.

405. A. Manus, I. Ramade, E. Codjovi, O. Guillou, O. Kahn and J.C. Trombe, "Crystal structure and magnetic properties of [Ln₂Cu₄] hexanuclear clusters (where Ln = trivalent lanthanide). Mechanism of the gadolinium(III)-copper(II) magnetic interaction", *J. Am. Chem. Soc.*, 1993, **115**, 1822 – 1829.

406. S.S. Tandon, S. Chander and L.K. Thompson; "Ligating properties of tridentate Schiff base ligands, 2-[[(2-pyridinylmethyl)imino]methyl]phenol (HSALIMP) and 2-[[[2-(2-pyridinyl)ethyl]imino]methyl]phenol (HSALIEP) with zinc(II), cadmium(II), nickel(II) and manganese(III) ions. X-ray crystal structures of the [Zn(SALIEP)(NO₃)]₂ dimer, [Mn(SALIEP)₂](ClO₄), and [Zn(AMP)₂(NO₃)₂]", *Inorg. Chim. Acta*, 2000, **300–302**, 683 – 692.

407. E. Garriba, G. Micera and D. Sanna, "The solution structure of bis(acetylacetonato)oxovanadium(IV)", *Inorg. Chim. Acta,* 2006, **359**, 4470 – 4476.

408. N. Butenko, I. Tomaz, O. Nouri, E. Escribano, V. Moreno, S. Gama, V. Ribeiro, J.P. Telo, J.C. Pesssoa and I. Cavaco, "DNA cleavage activity of $V^{IV}O(acac)_2$ and derivatives", *J. Inorg. Biochem.*, 2009, **103**, 622 – 632.

409. P. Adão, J.C. Pessoa, R.T. Henriques, M.L. Kuznetsov, F. Avecilla, M.R. Maurya, U. Kumar and I. Correia, "Synthesis, characterization and application of vanadium-salan complexes in oxygen transfer reactions", *Inorg. Chem.*, 2009, **48**, 3542 – 3561.

410. L.S. Hegedus, In: B.M. Trost and I. Fleming, *Compr. Org. Synth.,* vol. 4, Pergamon Press, Oxford, 1991, pp. 551 – 569.

411. M.S. Driver and J.F. Hartwig, "General N–H activation of primary alkylamines by a late transition-metal complex", *J. Am. Chem. Soc.*, 1996, **118**, 4206 – 4207.

412. A.L. Casalnuovo, J.C. Calabrese and D. Milstein, "N-H Activation. 1. Oxidative addition of ammonia to Iridium(1). Isolation, structural characterization, and reactivity of amidoiridium hydrides", *Inorg. Chem.*, 1987, **26**, 971 – 973.

413. M.D. Fryzuk and C.D. Montgomery, "Amides of the platinum group metals", *Coord. Chem. Rev.*, 1989, **95**, 1 – 40.

414. M. Schulz and D. Milstein, "N–H*vis*. C–H activation; a major ligand size effect", *J. Chem. Soc., Chem. Commun.*, 1993, 318 – 319.

415. R.A. Widenhoefer and S.L. Buchwald, "Halide and amine influence in the equilibrium formation of palladium tris(o-tolyl)phosphine mono(amine) complexes from Palladium Aryl Halide Dimers", *Organometallics,* 1996, **15**, 2755 – 2763.

*****

Summary & Conclusion

Most of the catalytic processes widely engaged in the manufacture of bulk as well as fine chemicals, are homogeneous in nature. Homogeneous catalysts also face the problem of separation from the substrate and products, and very often decompose or polymerize during catalytic action. Present thesis highlighted the importance of polymer-supported complexes in the development of industrial processes. With easy recovery and reusable properties such catalysts have provided better process selectivity and easy separation of the product(s) from the reaction mixture. As literature cited only limited reports on the catalytic aspects of polymer-anchored vanadium complexes, polystyrene-supported oxovanadium(IV) complexes, PS-[VO(sal-his)(acac)], PS-[VO$_2$(sal-his)] (PS = polystyrene support, Hsal-his = Schiff base derived from salicylaldehyde and histamine), PS-[VO(ligand)$_2$], PS-[MoO$_2$(ligand)$_2$], PS-[Cu(ligand)$_2$] (ligand = thiomethyl benzimidazole), PS-[VO(fsal-aepy)(acac)], PS-[VO$_2$(fsal-aepy)] (H$_2$fsal-aepy = Schiff base derived from 3-formylsalicylic acid and 2-(2-aminoethyl)pyridine), PS-[VO(fsal-dmen)(acac)] and PS-[VO$_2$(fsal-dmen)] (H$_2$fsal-dmen = Schiff base derived from 3-formylsalicylic acid and N,N'-dimethylethylene diamine), have been prepared to explore their catalytic properties. Complexes PS-[MoO$_2$(ligand)$_2$], PS-[Cu(ligand)$_2$] (ligand = thiomethyl benzimidazole) have also been prepared. These complexes have been characterized by elemental analyses, spectral (FT-IR, electronic, ^{1}H NMR, ^{51}V NMR and EPR) studies, field emission scanning electron micrographs (FE-SEM-EDX) and thermal analysis patterns. The respective non-polymer-supported (neat) complexes have also been prepared and characterized. The formulations of the polymer-anchored complexes have been inferred on the basis of respective neat complexes and conclusions drawn from the various characterization studies.

Catalytic abilities of these polymer-anchored complexes have also been explored considering various organic substrates. Complexes PS-[VO(sal-his)(acac)] and PS–[VO$_2$(sal–his)] have been used as catalyst for the oxidation of methyl phenyl sulfide, diphenyl sulfide and benzoin with 30% H$_2$O$_2$ as oxidant. Methyl phenyl sulfide on oxidation give 93.8% conversion with 63.7% selectivity towards methyl

phenyl sulfoxide and 36.3% towards methyl phenyl sulfone has been achieved and diphenyl sulfide gave 83.4% conversion where selectivity of reaction products varied in the order: diphenyl sulfoxide (71.8%) > diphenyl sulfone (28.2%). A maximum of 91.2% conversion of benzoin has been achieved within 6 h, and the selectivity of reaction products are: methylbenzoate (37.0%) > benzil (30.5%) > benzaldehyde-dimethylacetal (22.5%) > benzoic acid (8.1%). The PS–bound complex, PS–[VO(sal–his)(acac)] exhibits very comparable catalytic potential.

Oxidation of styrene catalyzed by PS-[VO(ligand)$_2$], PS-[MoO$_2$(ligand)$_2$] and PS-[Cu(ligand)$_2$] (ligand = tmbmz derived ligand) gave three reaction products namely, styrene oxide, benzaldehyde and 1-phenylethane-1,2-diol using H$_2$O$_2$ as an oxidant and conversion varied in the order: PS-[VO(tmbmz)$_2$] (81 %) > PS-[MoO$_2$(tmbmz)$_2$] (68 %) > PS-[Cu(tmbmz)$_2$] (57 %). In the oxidation of cyclohexene, a maximum of 86 % conversion was obtained by PS-[VO(ligand)$_n$], followed by 66 % with PS-[MoO$_2$(ligand)$_n$] and 51 % with PS-[Cu(ligand)$_n$]; here the selectivity of products varied in the order: cyclohexane-1,2-diol > 2-cyclohexene-1-one > cyclohexeneoxide. Oxidation of ethylbenzene by H$_2$O$_2$ gave benzaldehyde, phenyl acetic acid, styrene and 1-phenylethane-1,2-diol. The products formed are independent of catalysts and follow the order: benzaldehyde > phenyl acetic acid > acetophenone > 1-phenylethane-1,2-diol. A good performance of these catalysts is possibly due to the formation of peroxo species easily in presence of H$_2$O$_2$ as well as ease in transferring oxygen from the intermediate peroxo species to the substrate.

Polymer-anchored complex, PS-[VO$_2$(fsal-dmen)] have been used for the oxidative desulfurization reaction. The catalytic oxidative desulfurization of model organo-sulfur compounds like thiophene (T), dibenzothiophene (DBT), benzothiophene (BT), 2-methyl thiophene (MT) with the concentration of 500 ppm sulfur and diesel has been carried out in presence of 30 % H$_2$O$_2$. The sulfur in model organosulfur compounds and diesel has been oxidized to the corresponding sulfones in presence of H$_2$O$_2$. The catalytic activities of these complexes have also been compared with the corresponding free complexes and it has been observed that some of the free complexes have comparable catalytic activities. However, the recycle

ability and easy separation of the catalysts from the reaction mixture make polymer-anchored complexes better catalysts over neat ones. Besides, these complexes are stable and do not leach during catalytic actions in solution. The formation of possible intermediates during catalytic actions has also been explored.

Complex, PS-[VO$_2$(fsal-aepy)] catalyzed the hydroamination of styrene and vinyl pyridine with amines like aniline and diethylaminne in mild conditions and 76 % of hydroaminated products has been obtained. Similarly hydroamination of vinyl pyridine catalyzed by PS-[VO$_2$(fsal-aepy)], with aniline and diethyl amine has been carried out under above optimized reaction condition and give 90.2 % conversion with aniline and 67.6 % conversion with diethyl amine. The formation of possible intermediates during the catalytic reaction has been established using the neat complexes, styrene and diethylamine as a model system.

Thus, synthesis and characterization of polymer-supported vanadium complexes and their catalytic potentials presented in the thesis contribute considerably to the existing knowledge. It is hoped that these catalysts may find industrial applications in near future.

*****